DISS. ETH 18281

"Click-to-Chelate": An Efficient Strategy for the Development of Organometallic Technetium and Rhenium Compounds for Potential Application in Radiopharmacy

A dissertation submitted to

ETH ZURICH

for the degree of

DOCTOR OF SCIENCES

presented by

HARRIET SARAH ROSE STRUTHERS

MChem, University of Oxford

born 27.05.83

British citizen

accepted on the recommendation of

Prof. Dr. Roger Schibli, examiner

Prof. Dr. P. August Schubiger, co-examiner

2009

Thank you!

I am very grateful to so many people who have made the last three and a half years so enjoyable, and to everyone who contributed to my thesis. I especially want to thank Judith, who taught me how to radiolabel; Alain; Alexander; Christian; Walti, who organized a bike so I could get to work; Monica, for looking after my computer; and Professor Schubiger, for agreeing to co-referee my thesis. I learnt many things in my first year at PSI from Marie-Line and Todor, and am very grateful to both of them for taking time out from their own work to teach me. I thank Simone for the good time we had in the year we spent sharing the same lab and for agreeing that the *schaum* is more important than the coffee… but most importantly, for her friendship over the last three years. I am very grateful to Cristina for all her advice, many helpful discussions, and for always being able and willing to answer the questions which proved I was a chemist and not a pharmacist! I owe a big, big thank you to Tom as well, for all his help in the lab. My thanks also go to Bernhard Spingler from the University of Zurich and Adelheid Hagenbach from the Free University in Berlin, for solving my crystal structures; Jason Holland from the Memorial Sloan-Kettering Cancer Center, for running DFT calculations for me; Anja Stoffel and Leonardo Scapozza from the University of Geneva, for showing me the PK-LDH assay and providing me with hTK1; and David Viertl, Marek Kosinski and Franz Buchegger from the University Hospital in Lausanne, for helping me perform cell uptake experiments. By far my biggest and most important thank you, however, is to Roger, who made this thesis possible and taught me so much. It was a privilege to be part of the Schibli group and for all the opportunities it gave me, I will always be incredibly grateful.

Contents

Summary

Radiopharmaceuticals provide a unique opportunity for the target-specific delivery of radionuclides to image, treat and monitor numerous diseases. The rapidly increasing number of new targets requires the development of innovative and efficient strategies to conjugate radionuclides to molecules of biomedical interest. Since many radionuclides with suitable decay characteristics for diagnostic applications, and the majority of radionuclides with suitable decay characteristics for therapeutic applications, are transition metals or have metallic character, the development of new conjugation strategies is a challenge for both bioinorganic and coordination chemistry. Technetium-99m, a metastable isotope of the group 7 element technetium, remains the most widely used radionuclide in diagnostic nuclear medicine, as a result of its near-perfect decay characteristics (γ-emission, 140 keV, $T_{1/2}$ = 6 hours) and ready availability at low cost from a commercial $^{99}Mo/^{99m}Tc$ generator. This work focuses on the development of strategies to incorporate technetium-99m into biologically relevant molecules, primarily using the complex $[^{99m}Tc(CO)_3(H_2O)_3]^+$ as a radiolabelling precursor.

The outstanding characteristics of click chemistry and, in particular, the copper catalyzed azide-alkyne cycloaddition, which forms exclusively 1,4-bifunctionalized triazoles in high yields and under mild reaction conditions, provide an ideal platform for the functionalization of a range of biomolecules. During the course of this work, it could be shown that click chemistry can be employed for both the formation of efficient chelating systems (primarily for the *fac*-$M(CO)_3$ core; M = ^{99m}Tc, Re) and simultaneous conjugation of the chelating system to a biomolecule in a single, high-yielding step. This led us to call this strategy "click-to-chelate". Experimental evidence and DFT calculations suggested that the most efficient triazole-containing chelating systems coordinate to the metal through N3 of the heterocycle. Chelators of this type are derived from the reaction of a suitable bidentate alkyne with any azide-containing biomolecule. By varying the alkyne component of the reaction, a range of polydentate 1,2,3-triazole-containing chelating systems, which combine different donor groups and structures, can be readily synthesized. Several new triazole-containing chelating systems were prepared in this way. Model $Re(CO)_3$ complexes were synthesized and fully characterized. For three complexes, x-ray crystallography confirmed the expected

tridentate coordination of the ligands through N3 of the triazole and two donor groups, which were originally part of the alkyne. Radiolabelling of the ligand systems with the $[^{99m}Tc(CO)_3(H_2O)_3]^+$ precursor identified which ligands were the most suitable tridentate chelators for radiopharmaceutical purposes. Furthermore, a one-pot procedure was developed, which avoids isolation and purification of the triazole-containing ligands before labelling. This facilitates the rapid preparation of radiolabelled compounds, and provides a basis for the production of combinatorial libraries of labelled compounds for preliminary *in vitro* screening and assessment. Complexes with different structures, overall charges and lipophilicities can be synthesized from a common precursor to allow qualitative structure-activity relationships to be deduced in a matter of hours.

The modular approach was applied to the synthesis of two series of technetium-labelled thymidine derivatives. A technetium-99m labelled thymidine analogue capable of being phosphorylated by human thymidine kinase 1 (hTK1) would be of considerable practical interest, since hTK1 has proven to be a suitable target for the non-invasive imaging of tumour proliferation. In the first series of compounds, thymidine was functionalized with an azide at the N3 position. The reactions with various alkynes were radiolabelled *in situ* to provide a series of organometallic thymidine derivatives with different structures and overall charges. Incubation of the complexes with hTK1 revealed that all of the compounds maintained substrate activity towards the enzyme, providing the first examples of hTK1 substrates labelled with a metal complex. Using the same strategy, but with commercially available 3′-azido-3′-deoxythymidine (AZT) as the azide component, the first organometallic hTK1 substrates in which thymidine is modified at the C3′ position were also identified. For the N3-functionalized compounds phosphorylation rates ranged from 9-18% of the value for thymidine, and for the C3′-functionalized compounds from 13-28%. Neutral and cationic complexes were more readily phosphorylated than an anionic complex when the metal chelate was at the N3 position, whereas an anionic complex was as favourable as neutral complexes when thymidine was functionalized at the C3′ position, and in this case cationic complexes were considerably poorer substrates.

Replacement of a CO ligand in the *fac*-$\{M(CO)_3\}^+$ core with an isolobal nitrosyl ligand gives the dicationic organometallic core *fac*-$\{M(CO)_2(NO)\}^{2+}$. In a further part of this

work, the substitution reactions and labelling of biomolecules with the dicarbonyl-nitrosyl precursor $[Re(CO)_2(NO)Br_3]^-$ were investigated and compared with analogous reactions of the tricarbonyl precursor $[Re(CO)_3Br_3]^{2-}$. This approach enables isostructural complexes to be synthesized and the influence of the overall charge to be investigated without having to account for the structural differences of the metal chelates. Thymidine was used as a model biomolecule and was functionalized at the N3 position with an iminodiacetic acid chelating system; spacers of different length were introduced between the chelating system and thymidine part of the molecule. For all of the ligands, $Re(CO)_2(NO)$ and $Re(CO)_3$ complexes were prepared and fully characterized. The crystal structure of one of the $Re(CO)_2(NO)$ labelled thymidine analogues was also solved. Incubation of the complexes with hTK1 revealed that all were substrates for the enzyme and could be phosphorylated in the presence of ATP. Despite differing overall charges, the isostructural complexes had similar rates of phosphorylation (20-40% of the value for thymidine depending on the spacer length), suggesting that the structure of the metal chelate is more important than the overall charge of the derivative in the search for the best TK1 substrates. Cell internalization studies were performed with several $^{99m}Tc(CO)_3$-labelled thymidine derivatives to further assess the potential of the compounds as proliferation markers. No uptake was observed, suggesting that the introduction of a technetium chelate modifies the native nucleoside structure too dramatically for it to be recognized by nucleoside transporters and actively transported into cells.

While no thymidine derivatives with potential as proliferation markers have been synthesized up to now, we could show that the click chemistry strategy is an efficient platform for the functionalization of biomolecules with metal chelating systems. The same strategy can be applied not only in other areas of radiopharmacy, for example, for the synthesis of chelating systems for different cores of technetium, rhenium and other metals, but can be transferred to other areas of bioinorganic and bioorganometallic chemistry where the site-specific conjugation of metal chelates to biologically relevant molecules is an important contemporary topic.

Zusammenfassung

Radiopharmazeutika eröffnen die einzigartige Möglichkeit, Radionuklide an spezifische Zielorte zu bringen, um Krankheiten sichtbar zu machen, zu behandeln und die Behandlung zu verfolgen. Die Entdeckung immer neuer krankheitsrelevanter Zielstrukturen erfordert die Entwicklung neuartiger und effizienter Strategien, um die Bindung der Radionukliden an biomedizinisch interessante Moleküle zu verbessern. Viele Radionuklide mit geeigneten Zerfallseigenschaften für diagnostische Anwendungen und die Mehrheit der für die Therapie geeigneten Radionuklide gehören zu den Übergangsmetallen oder haben metallischen Charakter. Dies stellt eine Herausforderung für die bioanorganische Chemie und Koordinationschemie dar. Technetium-99m, ein Isotop des 7. Nebengruppenelemtents Technetium, ist aufgrund seiner nahezu optimalen Zerfallseigenschaften (γ-Emission, 140 keV, $T_{1/2}$ = 6 Stunden) und der raschen und günstigen Verfügbarkeit durch kommerzielle $^{99}Mo/^{99m}Tc$-Generatoren das am meisten verwendete Radionuklid in der diagnostischen Nuklearmedizin. Die vorliegende Arbeit befasst sich mit der Entwicklung von Strategien für den Einbau von Technetium-99m in biologisch relevante Molekülen. Dabei wird primär der $[^{99m}Tc(CO)_3(H_2O)_3]^+$-Komplex als Vorläufermolekül für die Radiomarkierungen verwendet.

Die einzigartigen Eigenschaften der Click-Chemie, im Speziellen der durch Kupfer katalysierten Azid-Alkin-Cycloaddition, welche ausschliesslich 1,4-bifunktionaliserte Triazole in hohen Ausbeuten unter milden Reaktionsbedingungen produziert, bieten ideale Voraussetzungen für die Funktionalisierung von Biomolekülen. Allerdings war bis zum Zeitpunkt dieser Dissertation noch keine Arbeiten bekannt, bei denen Click-Chemie zur Bildung eines effizienten Chelatorsystems bei gleichzeitiger Kopplung an ein Biomolekül eingesetzt wurde. Es konnte im Verlauf dieser Arbeit gezeigt werden, dass die Click-Reaktion die Bildung effizienter Chelatorsysteme für die organometallische *fac*-$M(CO)_3$-Einheit in einem einzigen nahezu quantitativen Schritt ermöglicht. Dieser Umstand bewog uns, den Ansatz „click-to-chelate“ zu nennen. Sowohl experimentelle Daten als auch DFT-Berechnungen liessen vermuten, dass das Tc(I)/Re(I)-Zentrum über das N3-Atom des Heterocyclus koordiniert. Solche Chelatoren wurden durch die Reaktion eines geeigneten bidentaten Alkins mit einem

Azid-funktionalisierten Biomolekül erhalten. Durch Variation der Alkin-komponente konnte leicht eine Vielzahl von polydentaten 1,2,3-Triazol-enthaltenden Chelatorsystemen mit verschiedenen Donorgruppen und Strukturen synthetisiert werden. Es wurden Modellkomplexe mit $Re(CO)_3$ synthetisiert und vollständig charakterisiert. Die Röntgenstrukturanalyse dreier Komplexe bestätigte die erwartete tridentate Koordination der Liganden über das N3-Atom des Triazols und zwei Donorgruppen, welche ursprünglich dem Alkin entstammten. Die für radiopharmazeutische Zwecke am besten geeigneten tridentaten Chelatoren wurden durch Radiomarkierung der Ligandensysteme mit $[^{99m}Tc(CO)_3(H_2O)_3]^+$ ermittelt. Weiterhin wurde eine Eintopfreaktion entwickelt, welche es erlaubte, die Triazol-enthaltenden Liganden ohne Abtrennung und Reinigung zu markieren. So könnten rasch und einfach kombinatorische Bibliotheken mit radiomarkierten Molekülen für *in vitro*-Untersuchungen aufgebaut und Komplexe verschiedener Struktur, Gesamtladung und Lipophilie ausgehend von einem gemeinsamen Vorläufermolekül synthetisiert werden. Dies ermöglicht qualitative Struktur-Aktivitäts-Beziehungen innerhalb weniger Stunden herzuleiten.

Dieser modulare oder kombinatorische Ansatz wurde mittels zweier Serien Technetium-markierter Thymidinderivate überprüft. Thymidinkinase 1 (hTK1) ist eine geeignete Zielstruktur, um die Tumorproliferation durch nicht-invasives Imaging sichtbar zu machen. Es ist daher von grossem Interesse, Thymidinanaloga, welche von hTK1 phosphoryliert werden, mit Technetium-99m zu markieren. Die erste Serie von Thymidinderivate wurde an der Position N3 der Base mit einem Azid funktionalisiert. Die Reaktionen mit verschiedenen Alkinen wurden *in situ* radiomarkiert und ergaben eine Reihe organometallischer ^{99m}Tc-Thymidinderivate mit verschiedener Struktur und Gesamtladung. Die Komplexe wurden anschliessend mit hTK1 inkubiert, und es zeigte sich, dass alle Verbindungen Substrate des Enzyms waren. Mit der gleichen Methode, jedoch mit kommerziellem 3′-Azido-3′-deoxythymidin (AZT) als Azid-enthaltende Komponente, wurden auch die ersten organometallischen hTK1-Substrate, bei welchen Thymidin an der Position C3′ modifiziert wurde, identifiziert. In *in vitro*-Tests wurde die Phosphorylierungsrate der organometallischen Komplexe durch hTK1 gemessen und mit Thymidin verglichen. Für die an der Position N3 funktionalisierten Verbindungen betrug die Phosphorylierungsrate 9-18% des Wertes für Thymidin, für

die an der Position C3′ funktionalisierten Verbindungen 13-28%. Die Resultate zeigten, dass neutrale und kationische Komplexe effizienter phosphoryliert wurden als ein anionischer Komplex, wenn sich der Metallchelator an der Position N3 befand. Bei dem an der Position C3′ funktionalisierten Thymidin war der anionische Komplex gleich gute Substrate wie die neutralen Komplexe, kationischen Komplexe dagegen signifikant schlechtere Substrate.

In einem weiteren Teil der Dissertation wurden Substitutionsreaktionen und Markierung von Biomolekülen mit dem gemischten Dicarbonyl-Nitrosyl Vorläufer des Rhenium(I), $[Re(CO)_2(NO)]^{2+}$als Alternative zur $[Re(CO)_3]^+$-Einheit untersucht. Dies erlaubte den Einfluss der Gesamtladung zu untersuchen, ohne strukturelle Unterschiede der Metallchelatoren berücksichtigen zu müssen. Thymidin wurde an der Position N3 mit einem Iminodiessigsäure-Chelatorsystem funktionalisiert. Ausserdem wurden Spacer unterschiedlicher Länge zwischen Chelatorsystem und Thymidin in das Molekül eingefügt. Mit alle Liganden wurden die entsprechenden $Re(CO)_2(NO)$- und $Re(CO)_3$-Komplexe gebildet und vollständig charakterisiert. Weiterhin wurde die Kristallstruktur eines mit $Re(CO)_2(NO)$-markierten Thymidinderivats aufgeklärt. Durch Inkubation der Komplexe mit hTK1 wurde gezeigt, dass alle Verbindungen ihre Substrateigenschaften gegenüber dem Enzym behielten und in Gegenwart von ATP phosphoryliert wurden. Die isostrukturellen Komplexe wiesen trotz unterschiedlicher Gesamtladungen ähnliche Phosphorylierungsraten auf, welche abhängig von der jeweiligen Spacerlänge zwischen 20 und 40% des Wertes für Thymidin betrugen. Aufgrund dieser Resultate kann angenommen werden, dass die Struktur des Metallkomplexes ein wichtigeres Kriterium für die Entwicklung von hTK1-Substraten darstellt als deren Gesamtladung. Um die Eignung der Verbindungen als Proliferationsmarker zu testen, wurden mit mehreren $^{99m}Tc(CO)_3$-markierten Thymidinderivaten Zellinternalisierungsstudien durchgeführt. Da keine Aufnahme in die Zellen beobachtet wurde, muss angenommen werden, dass das Einfügen eines Technetium-Komplexes die ursprüngliche Struktur des Nukleosidderivats so stark verändert, dass es von den Nukleosidtransportern nicht mehr erkannt und aktiv in die Zellen transportiert wird.

Obwohl schlussendlich kein als Proliferationsmarker geeignetes Thymidinderivat gefunden werden konnte, war es uns möglich mittels der Funktionalisierung von Thymidin die Tauglichkeit der „click-to-chelate“-Strategie aufzuzeigen. Es ist dabei zu

bedenken, dass die Methode nicht nur in der Radiopharmazie angewandt werden kann, sondern auch auf andere Bereiche der bioanorganischen und bioorganometallischen Chemie, wo die ortsspezifische Konjugation von Metallchelatoren an biologisch relevante Moleküle von grosser Bedeutung ist, übertragen werden kann.

Abbreviations

ADP	adenosine diphosphate
ATP	adenosine triphosphate
AZT	3′-azido-3′-deoxythymdine
BBN	bombesin
BFU	1-(2′-deoxy-2′-fluoro-β-D-arabinofuranosyl)-bromouracil
BNCT	boron neutron capture therapy
Boc	*tertiary*-butoxycarbonyl
CuAAC	copper catalyzed azide-alkyne cycloaddition
Cys	cysteine
DFT	density functional theory
DNA	deoxyribonucleic acid
dT	thymidine
DTT	dithiothreitol
dTTP	thymidine triphosphate
dUrd	deoxyuridine
ESI	electrospray ionization
FDG	fluorodeoxyglucose
FdUrd	5-fluorodeoxyuridine
FLT	3′-fluoro-3′-deoxythymdine
FMAU	1-(2′-deoxy-2′-fluoro-β-D-arabinofuranosyl)-thymidine
GRP	gastrin releasing peptide
hCNT	human concentrative nucleoside transporter
hENT	human equilibrative nucleoside transporter
HEPES	4-(2-hydroxyethyl)-1-piperazineethanesulfonic acid

HIV	human immunodeficiency virus
HPLC	high performance liquid chromatography
HSV1-TK	herpes simplex virus 1 thymidine kinase
hTK1	human thymidine kinase type 1
HYNIC	hydrazinonicotinamide
IDA	iminodiacetic acid
IdUrd	5-iododeoxyuridine
IR	infrared
LDH	lactate dehydrogenase
MS	mass spectroscopy
NADH	reduced nicotinamide adenine dinucleotide
NBMPR	nitrobenzylmercaptopurine ribonucleoside
NMR	nuclear magnetic resonance
NT	nucleoside transporter
PBS	phosphate buffered saline
PEP	phosphoenolpyruvate
PET	positron emission tomography
PK	pyruvate kinase
SPECT	single photon emission computed tomography
SPPS	solid phase peptide synthesis
TBDMS	*tertiary*-butyldimethylsilyl
TK2	mitochondrial thymidine kinase type 2
TLC	thin-layer chromatography
Tris	tris(hydroxymethyl)aminomethane
UV	ultraviolet

Introduction

1.1 Technetium-labelled radiopharmaceuticals

Target-specific radiopharmaceuticals are those whose pharmacokinetic profiles are determined primarily by receptor binding or biological interactions rather than by the physicochemical properties of the compound. Rational design of such compounds requires a thorough investigation of the molecular target, as well as the targeting molecule and its metabolism. To minimise detrimental changes in size, conformation and target affinity, the radiolabelling site and the choice of radionuclide are crucial. Technetium-99m has near-perfect decay characteristics (γ-emission, 140 keV, $T_{1/2}$ = 6 hours) for applications in diagnostic nuclear medicine using single photon emission computed tomography. Furthermore, unlike most positron emitting isotopes it is readily available at low cost from a $^{99}Mo/^{99m}Tc$ generator. As a result of the lanthanide contraction, the properties of technetium and rhenium are very similar. The close relationship is especially valuable in a radiopharmaceutical context because rhenium has two accessible nuclides with suitable decay characteristics for therapeutic applications. In principle, labelling techniques developed with technetium-99m can be conferred to the preparation of their rhenium analogues. However, whereas non-metal radionuclides can be covalently attached to the target molecule, stable incorporation of a radiometal such as technetium or rhenium into a biomolecule requires an appropriate bifunctional chelating agent and an efficient strategy to assemble the desired bioconjugate.

1.1.1 Technetium

Technetium is the lowest atomic number element with no stable isotopes. Of more than twenty known isotopes, only three are long-lived, and only technetium-99 (a β^- emitter without any accompanying γ-radiation, half-life 2.12 x 10^5 years) can be obtained in weighable amounts. As is typical of transition metals, technetium has extensive and diverse coordination and redox chemistry. Many complexes of technetium are known, with oxidation states ranging from -1 to 7, coordination geometries between 4 and 9, and with a variety of different ligand systems and coordinating groups. Investigation of the coordination chemistry of technetium continues to be primarily driven by the use of its metastable isomer technetium-99m in nuclear medicine.

Technetium-99m is the most widely used radionuclide in diagnostic nuclear medicine. The half-life of 6 hours is sufficiently long to allow pharmaceutical preparation, accumulation in the target tissue, and external measurement, without exposing the patient to high levels of radiation for a prolonged period. The 140 keV γ-radiation which is emitted with 89% abundance, is ideal for imaging purposes, but is low enough that the effect on healthy tissue is minimal. In addition to its superior decay properties, technetium-99m is readily available from a commercial $^{99}Mo/^{99m}Tc$ generator at comparatively low cost. In the generator system, $[^{99}MoO_4]^{2-}$ is adsorbed at the top of an alumina ion exchange column, where it decays continuously to $[^{99m}TcO_4]^-$. Monoanionic $[^{99m}TcO_4]^-$ can then be preferentially eluted at regular intervals with a physiological sodium chloride solution. Technetium-99m labelled compounds prepared from generator-eluted pertechnetate account for around 80% of clinically relevant radiopharmaceuticals.

1.1.2 Labelling cores and bifunctional chelators

The synthesis of technetium labelled compounds most commonly follows a post-labelling approach. This involves selection of an appropriate bifunctional chelator, coupling the metal chelator to the target biomolecule, followed by radiolabelling with a suitable technetium-99m precursor. Bifunctional chelators are selected for their ability to stabilize the metal in a given oxidation state and to be labelled efficiently, in high yield, and ideally at low ligand concentration. Stabilizing the metal in the desired oxidation state is essential, to avoid redox reactions and transchelation *in vivo*. Labelling at low ligand concentration is necessary to avoid receptor saturation and/or potential side effects of the modified biomolecule, and is a prerequisite in the development of technetium-biomolecule conjugates which do not require HPLC purification, for example, for clinical use. The structures of the most commonly used technetium labelling cores are shown in Figure 1.

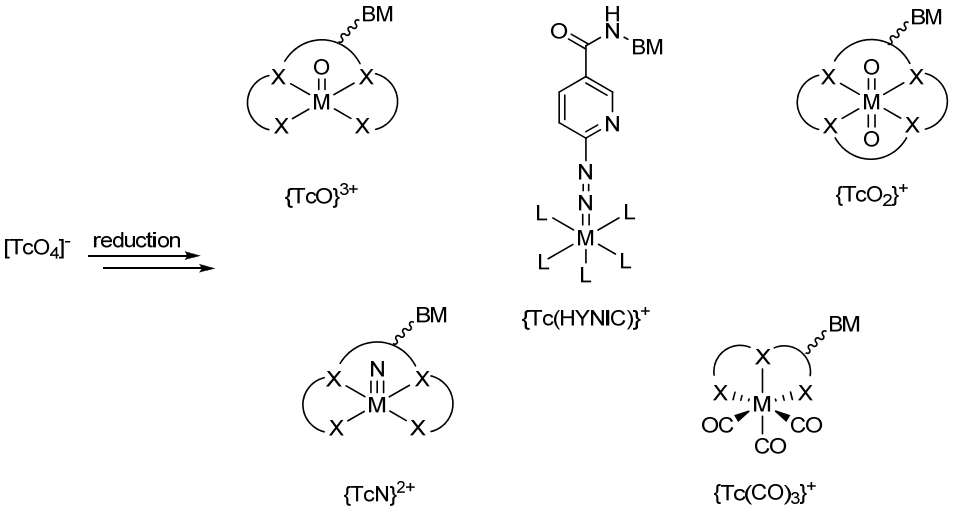

Figure 1. Technetium-99m cores commonly used to label biomolecules. M = ^{99m}Tc, BM = biomolcule, X = O, N, S, P etc. and L = co-ligand, such as tricine, glucoheptonate or a phosphine.

The majority of target-specific compounds labelled with technetium incorporate the $\{TcO\}^{3+}$ core, which can easily be prepared in aqueous solution by reduction of $[^{99m}TcO_4]^-$ with $SnCl_2$, and forms stable square pyramidal complexes with a range of donor ligands. The coordination chemistry of technetium complexes of this type, and of their non-radioactive rhenium analogues is established and well characterized.[1,2] Thorough investigation over the last 30 years has shown that the most suitable ligand systems incorporate combinations of nitrogen, phosphorous and sulphur donor atoms, and include tripeptide and tetrapeptide sequences such as Gly-Gly-Cys.[3,4] Coupling strategies normally involve coupling a free amine or carboxylic acid in the chelator to an appropriate group in the target molecule. Bifunctional chelating systems are not exclusively tetradentate, but the disadvantages of mixed ligand denticity approaches (for example, the "3+1" approach) include decreased *in vivo* stability as a result of ligand exchange reactions of the monodentate ligand.

After reduction of $[^{99m}TcO_4]^-$ with $SnCl_2$, labelling of bifunctional chelating system-targeting molecule conjugates with the $\{TcO\}^{3+}$ core is typically accomplished by a ligand exchange reaction of labile ligands such as glucarate, glucoheptonate or mannitol. An alternative approach is to react the intermediate complex with a hydrazinonicotinamide (HYNIC) coupled biomolecule, to form a particularly robust $\{Tc(NNHR)\}^+$ core, which is further stabilized by one or more pharmacokinetic

modifying co-ligands.[5] This approach has proven to be flexible enough for the modification of a range of biomolecules, and has the advantage that the biological properties of the radioconjugate can be modified by altering the co-ligands which stabilize the metal centre, rather than the bifunctional chelate. However, significant limitations are the co-ligand dependent formation of multiple species in solution, as well as potentially low *in vivo* stability.[6] The Re and ^{99}Tc analogues of technetium-99m labelled HYNIC conjugates have also proved difficult to characterize, which complicates analysis of the technetium-99m labelled compounds and their biological interactions.

Other cores of technetium which have been used to a lesser extent in the development of target-specific technetium-99m radiopharmaceuticals include the $\{TcN\}^{2+}$ core, which is isoelectronic with the $\{TcO\}^{3+}$ core, and the $\{TcO_2\}^{+}$ core. The $\{TcN\}^{2+}$ core was originally developed as a labelling precursor with the aim of obtaining cationic complexes in the +5 oxidation state, which are otherwise not well known.[7] More recently, the $\{TcN\}^{2+}$ core has been used to label small peptides and benzodiazepine receptor ligands. Cysteine was used as a bidentate chelator to couple the biomolecule to the metal centre, which is stabilized by a novel tridentate phosphine-containing ligand to give a pseudo-octahedral structure. The $\{TcO_2\}^{+}$ core forms octahedral complexes with linear or macrocyclic tetraamines such as cyclam.[8] Antibodies and smaller peptides have been functionalized and labelled with the $\{TcO_2\}^{+}$ core in this way, but preparation of the labelled conjugates suffered from a comparatively low radiolabelling efficiency. Water soluble dithiophosphines have also been shown to form complexes with the $\{TcO_2\}^{+}$ core, which are stable *in vitro* and *in vivo*.[9] In this case the ligand backbone is functionalized with a pendent carboxylic acid, to allow conjugation to a targeting molecule.

1.1.3 The $\{Tc(CO)_3\}^{+}$ and $\{Tc(CO)_2(NO)\}^{2+}$ cores

The precursors *fac*-$[M(CO)_3(H_2O)_3]^{+}$ (M = ^{99m}Tc, ^{99}Tc, Re) can all be prepared under fully aqueous conditions at atmospheric pressure in high yields and with excellent (radio)chemical purity.[10,11] For radiopharmaceutical purposes the synthesis of the

technetium-99m precursor was improved to avoid using carbon monoxide and instead employing potassium boronocarbonate as both a reducing agent and *in situ* source of CO. A kit formulation of *fac*-$[^{99m}Tc(CO)_3(H_2O)_3]^+$, which requires only the addition of generator eluted $[^{99m}TcO_4]^-$, is commercially available under the trade name Isolink.

As a labelling precursor $[^{99m}Tc(CO)_3(H_2O)_3]^+$ has many advantages over more established technetium cores. The tightly bound CO ligands are resistant to ligand exchange, whereas the labile water molecules can be replaced by almost any type of chelator. The low-spin d^6 complexes which are formed have a very high kinetic stability, so that the metal centre is protected from further ligand exchange or re-oxidation, which are common problems for complexes of the $\{TcO\}^{3+}$ core. The basic chemistry and reactions of the $[^{99m}Tc(CO)_3(H_2O)_3]^+$ precursor with a large range of potential ligand systems have been widely investigated with a view to the rational design of bifunctional chelators for incorporation into small biomolecules.[12-15] While, in principle, numerous combinations of donor atoms and ligand system backbones are possible, amino acids, aromatic amines and thioethers have been found to form the most stable metal chelates.

The impact of ligand denticity on the pharmacokinetics of $^{99m}Tc(CO)_3$-labelled complexes has also been investigated.[16] Tridentate ligands are also advantageous in this respect, as complexes with bidentate chelators, which retain an exchangeable water ligand, show significant aggregation with plasma proteins *in vitro* and *in vivo*. The drawback of functionalization of a biomolecule with a tridentate chelating system, however, is the more complex synthetic strategy, particularly the need for protecting group chemistry to avoid cross reactivity between the functional groups of the chelator and/or between the chelator and the biomolecule. Examples of typical bifunctional chelating ligands for the $\{M(CO)_3\}^+$ core are shown in Figure 2. Substitutionally inert complexes are formed in combination with mono-, bi- and tridentate ligands. However, the requirement in radiopharmaceutical preparations to label at a low ligand concentration to avoid receptor saturation by unlabelled ligand and the need for a reasonable reaction rate favour the formation of complexes with tridentate chelating systems.

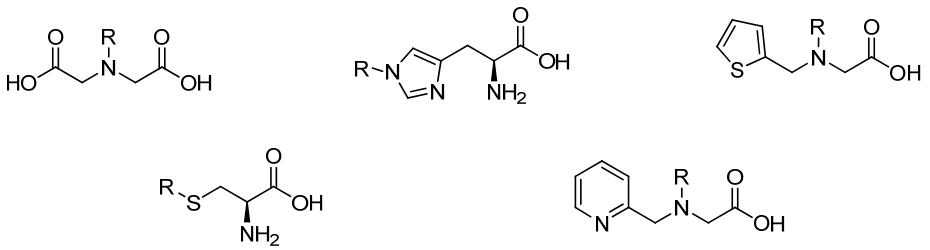

Figure 2. Bifunctional chelators for the $M(CO)_3$ core (M = ^{99m}Tc, Tc, Re). R = NH_2, CO_2H etc. or a biomolecule.

The favourable properties of the $[^{99m}Tc(CO)_3(H_2O)_3]^+$ precursor, most notably its straightforward preparation and the formation of well-defined and kinetically stable complexes, encouraged the development of other low oxidation state organometallic cores of technetium as potential radiolabelling precursors. A prominent example arises from the replacement of a carbonyl ligand by an isolobal nitrosyl ligand to give the $\{M(CO)_2(NO)\}^{2+}$ core (M = Tc, Re). The mixed carbonyl-nitrosyl core has an additional positive charge, and the precursor is therefore likely to have a greater affinity for anionic chelating systems and exhibit different preferences for the donor atoms and groups commonly used in tridentate chelating systems. It is also known that the presence of a nitrosyl group can have a considerable effect on transition metal centres and their coordination spheres, particularly the substitution lability of ligands *trans* to the nitrosyl group.[17] Initially it was hoped that complexes with bidentate chelators would show a reduced tendency to aggregate with plasma proteins *in vivo* compared with analogous $^{99m}Tc(CO)_3$-labelled compounds and, therefore, enable a more straight-forward functionalization strategy.

The chemistry of mixed carbonyl-nitrosyl complexes of rhenium in organic solvents is established,[18,19] but only more recently has the aqueous chemistry been investigated. For example, the water exchange reactions of $[Re(CO)_2(NO)(H_2O)_3]^{2+}$, the reactions of $[Re(CO)_2(NO)Br_3]NEt_4$ in aqueous solution with potential bifunctional chelating agents, and a synthetic route to the corresponding technetium-99m precursor *fac*-$[^{99m}Tc(CO)_2(NO)(H_2O)_3]^{2+}$ directly from generator-eluted pertechnetate have all been explored.[20-23] A comparative study of the ligand exchange reactions of $[Re(CO)_3Br_3][NEt_4]_2$ and $[Re(CO)_2(NO)Br_3]NEt_4$ with a series of potential chelating systems revealed that stable complexes are formed with ligands containing carboxylic

acids and aromatic and aliphatic amines.[24] A surprising result of this investigation was the dissociation of a carbonyl ligand leading to complexes of the form [Re(CO)(NO)L] when the mixed carbonyl-nitrosyl precursor was reacted with ligands with four coordinating groups. In contrast, the tricarbonyl precursor gives complexes which are invariably only tridentately coordinated, even when a greater number of donor groups is available. Although the survey of ligands was small, the presence of at least two carboxylic acid groups has been suggested as a prerequisite for this behavior.

1.1.4 The $\{TcO_3\}^+$ core

There has recently been a renewed interest in the $\{TcO_3\}^+$ core as a potential labelling precursor.[25] The $\{TcO_3\}^+$ core is smaller than the $\{Tc(CO)_3\}^+$ core, and might therefore be expected to have less effect on receptor binding properties when incorporated into small receptor targeting molecules. Unlike their rhenium analogues, very few Tc(VII) complexes incorporating the $\{TcO_3\}^+$ core are known. This is due in part to the more facile reduction of Tc(VII) than Re(VII), but also to the difficulties associated with handling the potentially useful but volatile and water-sensitive precursor Tc_2O_7. A number of complexes of the general formula $[TcO_3XL]$ (X = Cl, Br; L = bpy, phen) were reported by Davison *et al.*, but the insolubility in organic solvents and rapid hydrolysis back to $[TcO_4]^-$ in water, precluded thorough characterization.[26] Alberto's group have very recently reported an alternative strategy for the synthesis of these types of compounds as well as $[TcO_3L]$ complexes with tridentate ligands, which show improved water stability, through the formation of a mixed anhydride with a strong Lewis acid and subsequent ligand exchange.[25] They hope that this new approach will pave the way for an aqueous preparation of the corresponding $[^{99m}TcO_3L]$ complexes.

One of the most intriguing features of the trioxo core is the two potential functionalization strategies which it offers. By analogy to labelling with the tricarbonyl core, a tridentate bifunctional chelator could be used to both stabilize the metal centre, and provide a point of attachment to a biological targeting molecule. Alternatively, a novel approach being investigated by the Alberto group incorporates an alkene into a

biologically relevant molecule and makes use of the known reaction of $[TcO_3XL]$ compounds with alkenes to give the corresponding diolate complexes (Scheme 1).

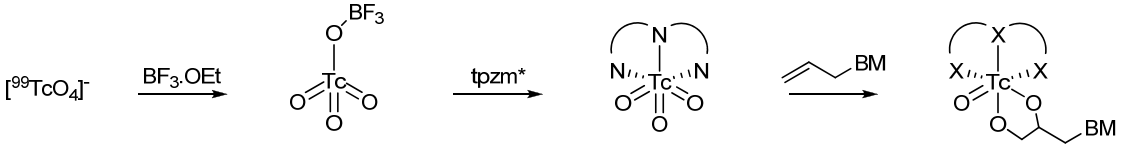

Scheme 1. Reaction of $[TcO_3L]$ complexes with an alkene-functionalized biomolecule.

1.1.5 Functionalization strategies

There are many strategies for the incorporation of bifunctional chelators for various technetium cores into biomolecules. A widely used approach is conjugation of a bifunctional chelating agent to an amine or thiol in the biomolecule using, for example, an activated ester, isothiocyanate or maleimide.[27] This of course relies first on the incorporation of an appropriate conjugating group into the bifunctional chelator, and second on selective reacitivty with an amine or thiol in the target biomolecule. As a result, multi-step syntheses are common and protection and deprotection strategies are invariably necessary, to avoid cross reactivity between functional groups in the chelator and the biomolecule. A typical example is provided by the *N*τ-functionalization of histidine, which is known to be an excellent tridentate ligand system for the $M(CO)_3$ core. Functionalization of the *N*τ nitrogen of the imidazole ring requires a six-step synthetic procedure, after which the ligand system must be coupled to a biomolecule and deprotected before labelling.[28]

An alternative approach involves the construction of a chelating system by direct functionalization of an appropriate group in the biomolecule, although again, multi-step syntheses and protecting group chemistry are common. Celen *et al.* functionalized thymidine with a *N*-(2-mercaptoethyl)-2-(2-mercaptoethylamino)acetamide (MAMA) chelating system for the $\{TcO\}^{3+}$ core in this way.[29] The synthesis involved alkylation of thymidine followed by refluxing in acetonitrile to install the chelating system. The thiol groups of the chelator were protected and had to be deprotected before radiolabelling. Whichever approach is used, construction of a chelating system-

biomolecule conjugate is invariably time-consuming and crucially, the biomolecule must be able to withstand all of the reaction conditions associated with the conjugation or functionalization strategy. A further disadvantage is that such procedures are normally designed for a specific target and lack versatility. However, one elegant strategy which has proven amenable to the synthesis and radiolabelling of a series of compounds, is the single amino acid chelate approach, which focuses on the facile incorporation of a tridentate chelator for the $M(CO)_3$ core into peptides.[30,31] The rationale for such an approach is the potential for synthesis of combinatorial libraries of peptide radiopharmaceuticals from which the optimal agents for a specific target can be selected.

The most versatile strategy for the synthesis of chelator-peptide conjugates is solid phase synthesis, as it allows the preparation of a series of analogues in parallel and is the most efficient way to identify optimal combinations of the site of functionalization, spacer length and the nature of the metal chelate. Several groups have incorporated chelating systems for the $\{TcO\}^{3+}$ core at the N-terminus end of a targeting peptide as part of its synthesis.[32,33] The disadvantage of this approach is that the site of functionalization cannot be readily modified. In this respect, chelating systems based on natural amino acids such as Gly-Gly-Cys are more flexible, but do not provide optimally stable coordination environments. An improved strategy was reported by Blower *et al.* and involves incorporation of a HYNIC functionalized lysine analogue, which can be introduced at any point in the peptide.[34]

Valliant and co-workers have further improved this strategy so that reference Re and/or ^{99}Tc complexes can be prepared in parallel to the unlabelled ligand, and purification steps are minimized. Their single amino acid chelate approach also relies on a functionalized lysine derivative in which the side chain has been reacted with two equivalents of 2-picolinaldehyde (or 2-quinolinaldehyde) to provide a suitable tridentate κ*N*,κ*N*,κ*N* chelator for the $\{M(CO)_3\}^+$ core as illustrated in Scheme 2.[30,31] The advantage of this particular chelator is that it requires no additional protecting groups, and thus no additional deprotection steps, either before or after the peptide has been cleaved from the resin. Most recently, this approach was applied to the synthesis of a series of $M(CO)_3$ labelled *β*-breaker peptides designed to target *β*-amyloid plaques.[35] *In*

vitro testing of the $Re(CO)_3$ labelled conjugates identified two promising compounds, the $^{99m}Tc(CO)_3$ analogues of which were prepared for further screening.

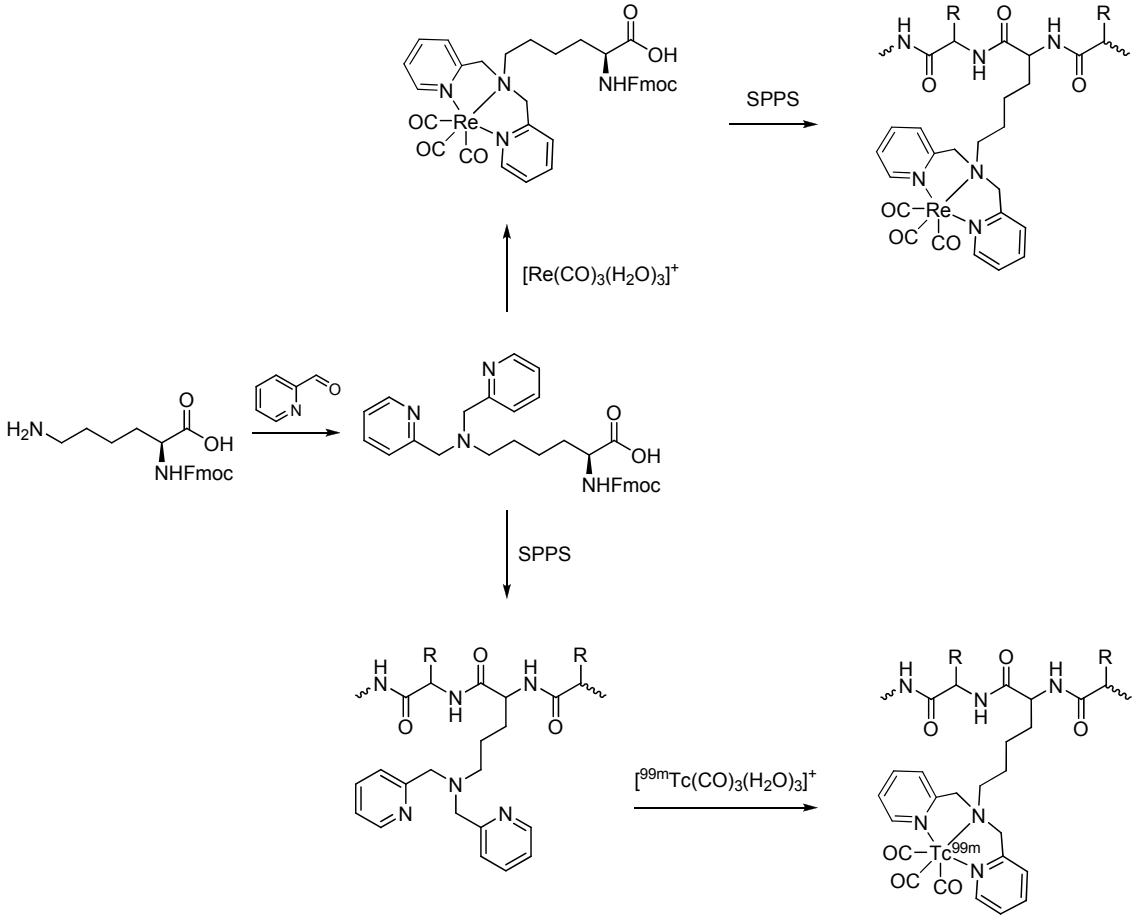

Scheme 2. The single amino acid chelate strategy.

1.2 Click chemistry

The term "click chemistry" was first introduced by Sharpless and co-workers in 2001.[36,37] It describes a modular approach to organic synthesis, rapidly creating molecular diversity using only a small number of near-perfect reactions (Figure 3). Click reactions are defined by a stringent set of criteria, which are what ultimately make the reactions so valuable. A click reaction must be efficient and selective, but at the same time wide in scope, giving consistently high yields with a variety of starting materials. It must be easy to perform, be insensitive to oxygen or water, and use only

readily available reagents. Reaction work-up and product isolation must be simple, ideally without requiring chromatographic purification. Reactions which meet the click chemistry criteria do so by having a high thermodynamic driving force. Such processes tend to proceed rapidly to completion and be highly selective for a single product. Click reactions are further characterized by the formation of carbon-heteroatom bonds, and therefore rely on the use of preformed carbon-carbon bonds. The most useful reagents in this sense are olefins and acetylenes, which can easily be functionalized by addition or oxidation.

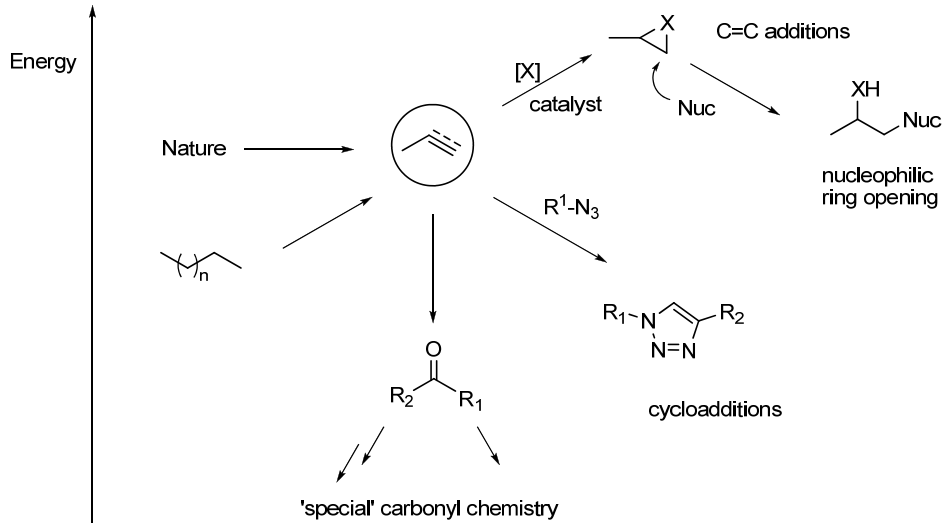

Figure 3. Click Chemistry: Energetically highly favourable linking reactions. Unsaturated compounds provide the carbon framework. New groups are attached through carbon-heteroatom bonds. Modified from Kolb, H. et al. *Drug Discovery Today* **2003**, *8*, 1128-1137.

1.2.1 The Cu catalyzed azide-alkyne cycloaddition

The synthesis of 1,2,3-triazoles by the 1,3-dipolar cycloaddition of azides and alkynes is known as the Huisgen cyclization.[38] Although the reaction was first reported decades ago, the formation of mixtures of 1,4- and 1,5-substituted isomers meant it did not find widespread application (Scheme 3). In 2002, the Sharpless and Meldal groups independently reported the Cu(I)-catalyzed version of the cycloaddition, which leads to a dramatic improvement in both rate and regioselectivity, efficiently providing 1,4-disubstituted 1,2,3-triazoles under mild reaction conditions.[39,40] As the premier example

of a click reaction, the copper catalyzed azide-alkyne cycloaddition (CuAAC) is characterized by its efficiency, selectivity, the mild reaction conditions, the straightforward purification of the products and, as a result, its enormous scope. Additionally, alkynes and azides are easy to install and among the least reactive groups in organic chemistry, which eliminates the need for protecting group chemistry. The reaction proceeds as efficiently in water as in organic solvents and, with complete conversion and selectivity, requires minimal purification. The 1,2,3-triazole itself is also astonishingly stable and essentially inert to oxidation, reduction and hydrolysis. Not surprisingly, the reaction has found a multitude of wide-ranging applications in synthesis, medicinal chemistry, molecular biology, and materials science.

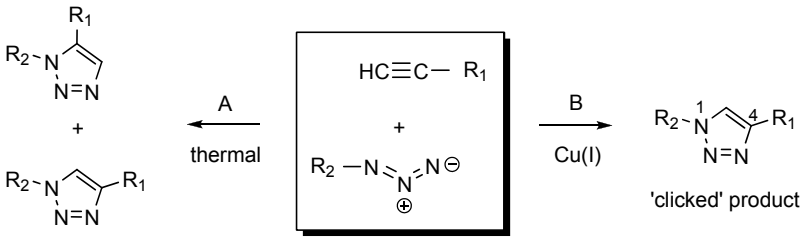

Scheme 3. (A) Husigen cycloaddition of terminal alkynes and azides under thermal reaction conditions yields a mixture of the 1,4-functionalized and 1,5-functionalized isomers. (B) The Cu(I)-catalyzed reaction results in exclusive formation of 1,4-disubstituted-1,2,3-triazoles. R_1 and R_2 can be any chemical/biochemical component.

Click chemistry was originally envisaged as a tool for drug discovery and many reports on the use of the CuAAC reaction focus on the development of novel combinatorial libraries coupling two drug-like fragments in high yield and under mild conditions.[37] The Sharpless group used this approach to prepare a library of 85 human α-1,3-fucosyltransferase inhibitors, and were able to identify a nanomolar inhibitor that displays excellent selectivity.[41] Similarly, Meldal and Tornøe produced and screened solid phase combinatorial libraries to identify nanomolar inhibitors of a cysteine protease.[42] They exploit the fact that the 1,2,3-triazole is an excellent biologically stable mimic of an amide bond, with a similar size and polarity, but which is resistant to proteolytic hydrolysis.[43] The number and variety of applications of the CuAAC reaction that have been reported since its introduction is immense. Examples include the modification of natural products and drugs with property modifying groups or fluorophore or biotin tags, the synthesis of macrocyclic compounds, the modification of

DNA and nucleotides, the synthesis of dendrimers and polymers, conjugation of carbohydrates, and the modification of surfaces and nanoparticles. The reaction in these contexts has been very recently reviewed.[44]

1.2.2 Click chelators

Initially the use of the CuAAC in inorganic and bioinorganic chemistry reflected other applications of triazole formation, namely as a way of selectively connecting two components in high yield and with high purity, although despite the broad applicability, and insensitive and robust nature of the reaction, comparatively few examples were reported. The first, and when our own work started, only metal ligands synthesized using the CuAAC reaction and in which the triazole is one of the coordinating groups were polytriazolylamines reported in 2004 as Cu(I) stabilizing ligands for applications in catalysis.[45] The ligands are reported to coordinate to the metal through N3 of the triazole, although none of the complexes were structurally characterized. In fact the coordinative properties of triazoles and their metal complexes have been known for some time, yet only relatively recently have 1,2,3-triazoles synthesized using click chemistry been more widely explored as ligands for transition metals.[46] The structures of several polydentate ligands which were synthesized using click chemistry are shown in Figure 4.

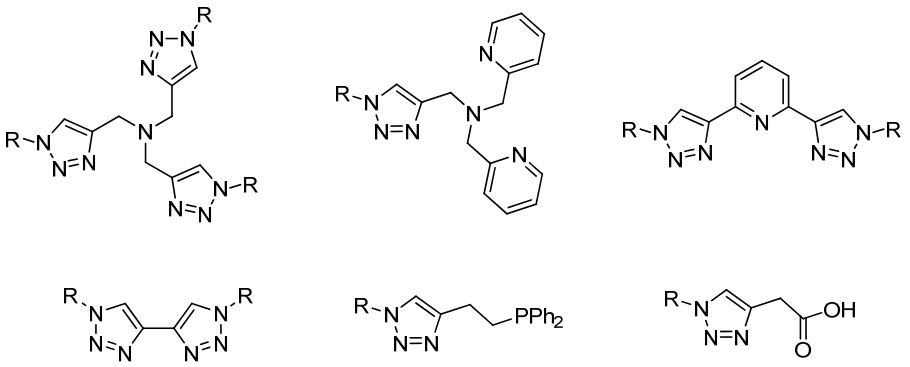

Figure 4. Metal chelators synthesized using the CuAAC reaction.[45,47-52]

Transition metal catalyzed cross-coupling reactions are widely used in organic synthesis and it is well documented that the ligands used to stabilize the transition metal can have

a significant impact on the outcome of such reactions. By analogy to the triazole-containing Cu(I) stabilizing ligands, Zhang *et al.* have shown that the CuAAC reaction can be used to prepare bidentate triazole-phosphine ligands for palladium, and that the complexes are effective catalysts for Suzuki coupling reactions.[47] The triazole of the bidentate ligands is again expected to coordinate through N3, and spectroscopic characterization supports this assumption. Recognizing the scope of this approach, and particularly the ease with which the CuAAC facilitates tuning the properties of the ligand, triazole-phosphine containing compounds have also been explored as ligands for rhodium and ruthenium complexes for use in catalysis.[53] As monodentate ligands for platinum and palladium complexes, x-ray structure analysis has shown that 1,2,3-triazoles synthesized using click chemistry coordinate to the metal through N3 of the triazole.[54] A series of platinum complexes with bidentate triazole-amine and triazole-carboxylic acid containing chelating systems have also been described and one of the complexes is reported to exhibit selective cytotoxicity towards breast cancer cell lines.[48] Structural characterization of the complexes showed that the ligands coordinate through N3 of the triazole and the amine/carboxylate to form five-membered chelate rings with the metal.

Another class of ligands which has begun to receive attention are the triazole analogues of the widely used bipyridine and terpyridine ligand systems. Complexes of the ligands have been reported with copper, rhenium, ruthenium and iron among others.[49-51] Monkowius and co-workers crystallized copper, rhenium and ruthenium complexes in combination with the novel bi-1,2,3-triazole ligands, to show that the ligands coordinate through N3 of the triazole.[49] While the complexes are structurally similar to their bipyridine and terpyridine analogues, preliminary investigations suggest that similarities in the optical properties of the complexes do not exist.[49,50] Several groups have, however, identified nitrogen-rich polydentate ligands containing combinations of triazoles and pyridine, which coordinate zinc and show the potential to be used as metal responsive fluorophores.[52,55,56] The complexes synthesized by Zhu *et al.* are interesting because they have prepared derivatives in which the ligands coordinate to the metal through N3 of the triazole and which have been structurally characterized, but also derivatives in which coordination to the metal through N3 of the triazole would be sterically difficult, but yet still show increased fluorescence on coordination of Zn^{2+},

and in these cases they suggest that coordination to the metal is through N2 of the triazole.[52]

1.3 Human thymidine kinase 1

Human Thymidine Kinase 1 (hTK1) is one of four mammalian deoxyribonucleoside kinases, which catalyze the first and rate determining steps in the salvage pathway synthesis of nucleotides. More specifically, hTK1 is a cytosolic kinase which catalyzes the γ-phosphate transfer from ATP to the 5′-hydroxyl group of the endogenous deoxyribonucleosides thymidine (dT) and 2′-deoxyuridine (dUrd), to form thymidine-5′-monophosphate and 2′-deoxyuridine-5′-monophosphate, respectively.[57] Unlike the activity of the other nucleoside kinases, hTK1 is subject to strict cell cycle regulation.[58] The enzyme is only transcribed during the S-phase of the cell cycle, and it contains regulatory information that promotes its degradation after mitosis. As a tightly S-phase-correlated enzyme, hTK1 is present only in proliferating cells. It appears to be widely distributed and expressed in all neoplastic cells, but is virtually absent in all non-proliferating normal cells, making it an ideal target for proliferation markers.

It is well documented that hTK1 is among the most selective of the nucleoside kinases, and is particularly sensitive to changes in the structure of the natural substrates dT and dUrd.[59] Among non-natural nucleoside analogues, which retain activity towards hTK1, the C3′-modified derivatives 3′-azido-3′-deoxythymidine (AZT), 3′-fluoro-3′-deoxythymidine (FLT) and 2′3′-didehydro-3′-deoxythymidine (d4T) are prominent, as they exhibit potent anti-viral activity. Phosphorylation by hTK1 is the first step in their activation as human immunodeficiency virus reverse transcriptase inhibitors.[60] Eriksson *et al.* have shown that minor modification of the structures of dT and dUrd at the 5-position is possible. For example, 5-halo and 5-ethyl substitutions are tolerated, but substitution with bulkier groups such as 5-propenyl or 5-(2-chloroethyl) are not.[61] Interestingly, herpes simplex virus 1 thymidine kinase (HSV1-TK) shows a much broader substrate specificity than human thymidine kinase. Some of the most active agents against herpes simplex virus 1 are C5-modified thymidine derivatives, such as bromovinyldeoxyuridine, which are phosphorylated by HSV1-TK, but are not substrates

for hTK1. More recently, Tjarks and co-workers have shown that hTK1 is also amenable to modification at the N3-position. Functionalization with a series of bulky carborane derivatives, tethered from N3 of the pyrimidine base with varying spacer length, does not prevent phosphorylation of the nucleoside analogue.[62-64] The experimental results of structure-activity relationships have all since been rationalized by the determination of the 3-D structure of hTK1 (Figure 5),[65] which confirms that this enzyme has a much smaller binding site than other nucleoside kinases.

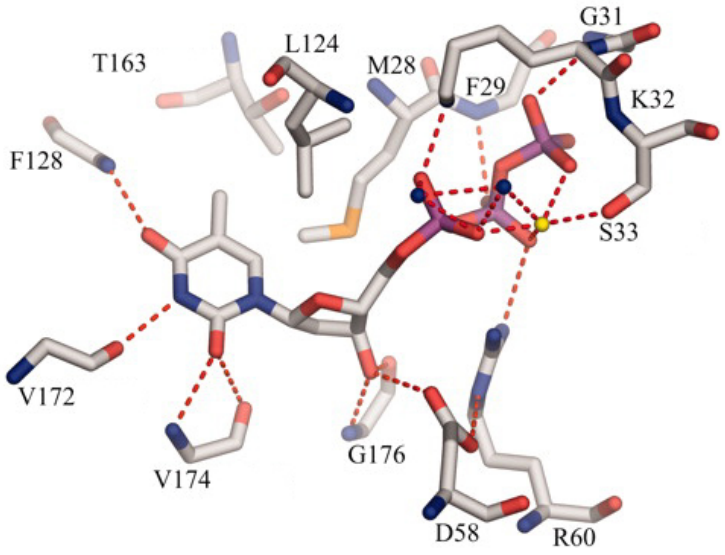

Figure 5. Binding interactions of dTTP in the active site of hTK1: The hydrogen bond donors and acceptors of the base all form hydrogen bonds to main chain atoms. O2 and N3 bond to main chain atoms of the lasso loop, and O4 bonds to main chain nitrogen of the α/β-domain. The methyl group at the C5 position lies in a hydrophobic pocket directed toward the β-carbon of a Thr and surrounded by Met, Leu, and Tyr. The 3′-oxygen atom of the deoxyribose is hydrogen bonded to the amino group of a conserved Gly in the lasso domain and to the side chain of the conserved Asp in the flexible loop of the α/β-domain. Modified from Welin, M. *et al. Proc. Natl. Acad. Sci. U.S.A.* **2004**, *101*, 17970-17975.

Determination of the structures of different nucleoside kinases were fundamental in further understanding the role of the enzymes as providers of precursors for DNA replication, repair and maintenance, as well as their medical and biotechnological relevance as catalysts for the phosphorylation of several nucleoside analogue prodrugs. hTK1 is most likely unique in its origin; structural characterization reveals a tetramer, with a completely different overall monomer structure to other nucleoside kinases,

which are dimeric and share much greater sequence homology.[66] hTK1 was co-crystallized with the feedback inhibitor thymidine triphosphate (dTTP) in its active site, which lies between an α/β-domain and a smaller zinc containing lasso domain.[65] In keeping with a general mechanism of feedback inhibition of dNKs, the base and deoxyribose occupy the nucleoside binding site, whereas the phosphate groups bind backward to the phosphate binding site.[67] The hTK1 substrate selectivity can be readily accounted for by analysis of the interactions between the nucleoside and the active site of the enzyme as shown in Figure 6. The high specificity for 2′-deoxyribonucleosides is consistent with an interaction between the 2′-carbon and glycine and tyrosine residues in the active site. Similarly, the low steric tolerance at the 5-position of the base is consistent with a small hydrophobic pocket. This enables ethyl or halide substitution of the methyl group of thymidine, but analogues with bulkier or more polar groups at this position lose their ability to be phosphorylated. Modification at the N3 position has proved possible with both small (for example, propargyl) and much more spatially demanding substituents such as carboranes. It has been suggested that N3 substituents can occupy the space between the two domains of the hTK1 monomer.[65] Similarly, tolerance of C3′ modification could be a result of the comparatively open nature of the C3′/C4′ environment and the proximity of the C3′ substituent to the surface of the enzyme.

1.3.1 Thymidine analogues

Nucleoside analogues of medical importance can be divided into two groups. In the first group are non-toxic prodrugs which exhibit anti-tumour or anti-viral activity after phosphorylation to active triphosphates by nucleoside and nucleotide kinases. These therapeutic compounds mimic physiological nucleosides in terms of uptake and metabolism, and are incorporated into newly synthesized DNA, resulting in synthesis inhibition, chain termination and cell death. The majority of these compounds are phosphorylated to their monophosphate analogues by cytoplasmic deoxycitidine kinase, which has a much broader specificity than hTK1 and is capable of phosphorylating both pyrimidine and purine nucleoside analogues.[68] The second group of medically relevant nucleoside analogues contains (radio)labelled thymidine analogues for both imaging

and therapeutic purposes, which aim to target the high hTK1 activity in proliferating cells. Despite the narrow substrate specificity of hTK1, a number of thymidine analogues have been successfully developed in this context.

[^{18}F]Fluorodeoxyglucose (FDG) is the most widely used agent for imaging tumours, as its retention is a function of glucose metabolism governed by hexokinase. Because the mechanism of FDG uptake is only indirectly related to cell division, it is not an ideal tracer for monitoring proliferation. In addition, since many types of cells use glucose, FDG is not selective for tumours, and increased uptake is also seen in inflammatory tissue.[69] Radiolabelled thymidine analogues offer a more selective measure of cell proliferation. Although carbon-11 labelled thymidine can be used for tumour imaging, the short half life of carbon-11, rapid *in vivo* degradation of thymidine, and relatively slow incorporation into DNA, limit image quality and complicate the calculation of proliferation rates. To overcome these problems, a number of thymidine analogues, which incorporate radionuclides with longer half-lives and/or are resistant to degradation, have been synthesized and investigated. Prominent examples include 1-(2′-deoxy-2′-fluoro-β-D-arabinofuranosyl)-[^{11}C-methyl]thymidine (^{11}C-FMAU), ^{18}F-FLT and 1-(2′-deoxy-2′-fluoro-β-D-arabinofuranosyl)-[^{76}Br]bromouracil (^{76}Br-BFU), the structures of which are shown in Figure 6. These analogues show the same nucleoside transport and phosphorylation as thymidine, but substitution of hydrogen at the 2′ position of the ribose in ^{11}C-FMAU and ^{76}Br-BFU, makes these derivatives considerably more resistant to degradation. In principle, the ideal tracer to monitor cell proliferation should be rapidly incorporated into DNA. Lu *et al.* have shown that this is the case for both ^{11}C-FMAU and ^{76}Br-BFU.[70] The uptake of ^{18}F-FLT is also very high in proliferating cells and it gives excellent images of several malignancy types. However, unlike ^{11}C-FMAU and ^{76}Br-BFU, ^{18}F-FLT cannot be incorporated into DNA, and instead, sufficient accumulation of radioactivity is a result of its internalization into cells and phosphorylation by hTK1, which lead to intracellular trapping.[70,71]

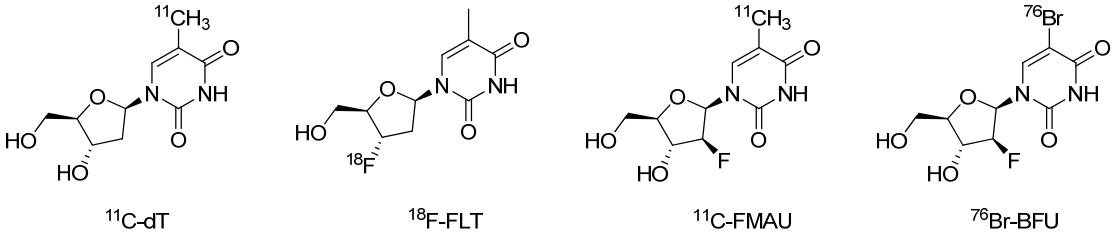

Figure 6. Thymidine analogues for PET imaging.

As potential agents for boron neutron capture therapy (BNCT), thymidine derivatives incorporating carboranes have been extensively investigated.[72] BNCT is a two component system for the treatment of cancer that is based on the reaction of thermal neutrons with ^{10}B, to produce high linear energy transfer $^{4}He^{2+}$ and $^{7}Li^{3+}$ particles. The short range of these particles means that, provided the ^{10}B-containing compound is taken up selectively by tumour cells, irradiation with thermal neutrons will kill the tumour cells but cause minimal damage to healthy adjacent cells. A large number of natural and unnatural nucleosides modified with various boron-containing groups at different positions of either the base or the sugar have been synthesized and biologically evaluated for use in BNCT.[73-75] Carboranes, which are attractive because they contain a comparatively large number of boron atoms, were first incorporated into deoxyuridine at the C5 position,[76-78] and it was reported in some cases that the compounds were phosphorylated *in vitro*.[78-80] This is surprising given the low tolerance of hTK1 to modification at the C5 position, and that a series of C5 functionalized derivatives reported by the Tjarks group showed no phosphorylation in enzymatic reactions with hTK1.[62] It has been suggested that the phosphorylation may have been catalyzed by mitochondrial thymidine kinase (TK2), since the roles of hTK1 and TK2 were not independently investigated and TK2 is known to phosphorylate C5 functionalized dUrd derivatives.[61,62] Tjarks' group have had much more success with carborane-nucleoside analogues in which thymidine is functionalized at the N3 position (Figure 7). Since their first report on thymidine derivatives functionalized at this position, several series of compounds have been synthesized and evaluated as substrates for hTK1 and TK2 and thus their potential for use in targeted BNCT. It was shown with the first series of compounds that the N3 functionalized derivatives are good substrates for hTK1 but not TK2.[62] Later derivatives investigated the influence of spacer length, incorporation of hydrophilic groups to address the low water solubility, and the use of negatively

charged *nido-m*-carboranes rather than *closo-o*-carboranes.[63,64] Astonishingly, phosphorylation rates of up to 90% of the value for thymidine were achievable when spacer length and the charge of the carborane group were optimized.[64]

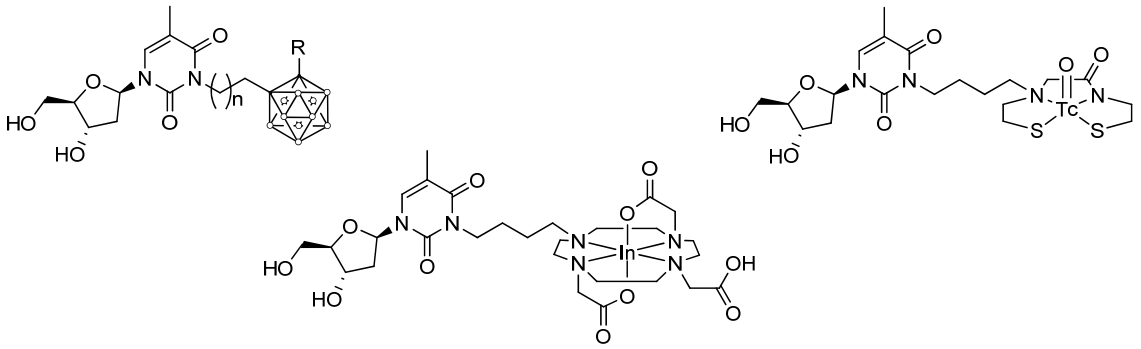

Figure 7. N3-functionalized thymidine derivatives for potential applications in imaging and therapy.[29,81,82]

In light of the pioneering work of the Tjarks group and their identification of the N3 position of thymidine as being able to tolerate substantial modification, other groups began to investigate thymidine derivatives functionalized at this position with radiometal complexes. Radiometal labelled thymidine derivatives are attractive for applications in both imaging, and as potential therapeutic agents. Neumeier *et al.* report the synthesis and preparation of thymidine functionalized with a macrocyclic chelator, which was radiolabelled with gallium-68 and with indium-111.[82] Surprisingly, however, the ^{111}In-labelled compound showed no activity towards hTK1. Although in principle a neutral complex is formed with ^{111}In, the authors suggest that partial residual charges may exist in solution, which disturb either the interaction between the complex and the active site of the enzyme, or the interaction of the phosphate donor with the enzyme. Similarly, a technetium labelled derivative in which thymidine is functionalized at the N3 position with a tetradentate N_2S_2-chelator for the $\{^{99m}TcO\}^{3+}$ core has been reported, but showed no affinity for hTK1 *in vitro*.[29] Another active area of research into radiolabelled nucleoside analogues, is in the preparation of reporter probes to monitor gene therapy, most commonly in combination with HSV1-TK. A technetium labelled thymidine analogue would also be interesting and useful in this context as a result of its favourable decay properties and availability. In one series of compounds thymidine was modified with a technetium chelate at the C5′ position and tested for inhibition of HSV1-TK.[83] Although no inhibition of the viral enzyme was

observed, the compounds did show selective inhibition of hTK1, but these compounds were not pursued as potential proliferation markers. Subsequently, other groups have also reported technetium-99m and/or rhenium labelled thymidine derivatives, where thymidine has been functionalized at either the C5′ position or the C2′ position, but their biological activity was not evaluated.[84]

1.4 Nucleoside transporters

Nucleoside transporters are divided into two types, the equilibrative nucleoside transporters hENTs, which facilitate diffusion in accordance with the concentration gradient of the nucleoside analogue, and concentrative nucleoside transporters hCNTs, which transport nucleosides against their concentration gradients by coupling the transport to Na^+ transport. The most widely and abundantly expressed nucleoside transporter is the equilibrative nucleoside transporter hENT1, which is thought to play the most important role in the transport of nucleosides and most nucleoside analogues across plasma membranes. hENT2 is also a plasma membrane protein, but has a more limited tissue distribution, is less abundantly expressed, and most cells which express this transporter also co-express hENT1.[85] Both transporters have broad permeant selectivities and can transport both purine and pyrimidine nucleosides, but are distinguished by their sensitivity to nitrobenzylmercaptopurine ribonucleoside (NBMPR), which inhibits the activity of hENT1 but not hENT2. hCNTs are much less widely distributed and the subtypes are more selective in terms of the nucleosides they transport, differentiating for example between purine and pyrimidine based nucleosides and their analogues.[86]

It has been suggested that the hENT1 transporter is more sensitive to modification of the ribose than of the nucleobase, and it is known that AZT, for example, is not actively transported by hENT1.[87] That AZT permeates cell membranes primarily by non-facilitated diffusion and not using a nucleoside transport system, was first reported by Zimmerman *et al.* in 1987, long before the classification of the different types and subtypes of nucleoside transporter.[88] In similar experiments, Kong *et al.* compared the transport of AZT with the transport of FLT, another C3′-modified thymidine analogue.[89]

They showed that unlike the uptake of AZT, the uptake of FLT by HL-60 cells is dependent on nucleoside transport proteins, since it can be inhibited by NBMPR. In light of the importance of AZT and FLT as anti-viral drugs and of [^{18}F]FLT as a proliferation marker, the mechanisms of their uptake and the correlation of uptake and transporter expression have been further investigated to assess the roles of the individual nucleoside transporters.[87,90] It has been shown that AZT is recognized by hENT2 and some concentrative nucleoside transporters, but that their restricted expression in comparison to hENT1 limits the roles these transporters play in the internalization of the dT analogue. Similarly, it has been shown that although FLT is recognized by hENT2, hCNT1 and hCNT3, its uptake correlates primarily with hENT1 expression. One reason for the low sensitivity of [^{18}F]FLT PET, however, is that nucleoside transporter levels vary considerably between individuals.[91,92] Given that nucleoside transporter deficient cells are typically highly resistant to nucleoside analogue drugs, it has very recently been suggested that [^{18}F]FLT might be a useful predictor of chemotherapeutic resistance.[90]

1.5 Aim of the project

The primary aim of this thesis was to investigate novel strategies to facilitate labelling of biologically relevant molecules with technetium and rhenium. This involved the design and synthesis of suitable chelating systems for different cores of technetium and rhenium and their incorporation into biologically relevant molecules. Thymidine was chosen as a model biomolecule to evaluate the different strategies, since radiometal-labelled thymidine derivatives are potential markers of cell proliferation as a result of the overexpression of hTK1 in a variety of cancers. All of the rhenium and technetium labelled thymidine analogues synthesized were tested for their ability to be phosphorylated by hTK1.

In the first part of the project click chemistry was employed in the synthesis of suitable chelating systems for the $M(CO)_3$ core (M = ^{99m}Tc, Re). The copper catalyzed azide-alkyne cycloaddition was used to synthesize histidine-like chelating systems, which were incorporated into a variety of biologically relevant molecules and labelled with

rhenium and technetium-99m (Chapter 2). Subsequently, a variety of alkyne building blocks were synthesized and reacted a model azide to give a series of triaziole-containing chelating systems, which impart different physicochemical characteristics on their $M(CO)_3$ labelled complexes (Chapter 3). To assess the potential of the approach in facilitating the rapid synthesis and radiolabelling of a number of derivatives for preliminary *in vitro* screening, the alkyne building blocks were reacted with azide-functionalized thymidine derivatives and labelled with the $M(CO)_3$ core (Chapter 4).

The second part of the project was to evaluate the substitution reactions and labelling of biomolecules with the $Re(CO)_2(NO)$ core. Whereas in the first part of the project the properties of a series of thymidine conjugates were varied by modifying the metal chelating system, in the second part of the project, labelling with the $\{Re(CO)_2(NO)\}^{2+}$ and $\{Re(CO)_3\}^{+}$ cores enabled the preparation of isostructural but differently charged thymidine derivatives (Chapter 5). Previous investigations of the ligand exchange reactions of the precursor $[Re(CO)_2(NO)Br_3]^-$ core established the surprising lability of one of the carbonyl ligands in the presence of tetradentate chelating systems. The coordinative behaviour of a potentially tetradentate ligand system, which would be amenable to incorporation into biomolecules, was explored. In an effort to synthesize Re(CO)(NO) labelled thymidine derivatives, thymidine was also functionalized with this chelating system (Chapter 5).

1.6 References

(1) Abram, U. in *Comprehensive Coordination Chemistry II*, (Eds. McCleverty, J. A.; Meyer, T. J.), Pergamon, **2003**, p 271-402.

(2) Alberto, R. in *Comprehensive Coordination Chemistry II*, (Eds. McCleverty, J. A.; Meyer, T. J.), Pergamon, **2003**, p 127-270.

(3) Liu, S.; Edwards, D. S. *Chem. Rev.* **1999**, *99*, 2235-2268.

(4) Liu, S. *Adv. Drug Delivery Rev.* **2008**, *60*, 1347-1370.

(5) Abrams, M. J.; Juweid, M.; Tenkate, C. I.; Schwartz, D. A.; Hauser, M. M.; Gaul, F. E.; Fuccello, A. J.; Rubin, R. H.; Strauss, H. W.; Fischman, A. J. *J. Nucl. Med.* **1990**, *31*, 2022-2028.

(6) Decristoforo, C.; Mather, S. J. *Nucl. Med. Biol.* **1999**, *26*, 389-396.

(7) Marchi, A.; Garuti, P.; Duatti, A.; Magon, L.; Rossi, R.; Ferretti, V.; Bertolasi, V. *Inorg. Chem.* **1990**, *29*, 2091-2096.

(8) Franz, J.; Volkert, W. A.; Barefield, E. K.; Holmes, R. A. *Nucl. Med. Biol.* **1987**, *14*, 569-572.

(9) Smith, C. J.; Katti, K. V.; Volkert, W. A.; Barbour, L. J. *Inorg. Chem.* **1997**, *36*, 3928-3935.

(10) Alberto, R.; Schibli, R.; Waibel, R.; Abram, U.; Schubiger, A. P. *Coord. Chem. Rev.* **1999**, *190-192*, 901-919.

(11) Alberto, R. in *Contrast Agents III*, (Ed. Krause, W.), Springer, **2005,** *252*, p 1-44.

(12) Banerjee, S. R.; Levadala, M. K.; Lazarova, N.; Wei, L.; Valliant, J. F.; Stephenson, K. A.; Babich, J. W.; Maresca, K. P.; Zubieta, J. *Inorg. Chem.* **2002**, *41*, 6417-6425.

(13) Lazarova, N.; Babich, J.; Valliant, J.; Schaffer, P.; James, S.; Zubieta, J. *Inorg. Chem.* **2005**, *44*, 6763-6770.

(14) Pak, J. K.; Benny, P.; Spingler, B.; Ortner, K.; Alberto, R. *Chem.--Eur. J.* **2003**, *9*, 2053-2061.

(15) van Staveren, D. R.; Benny, P. D.; Waibel, R.; Kurz, P.; Pak, J.-K.; Alberto, R. *Helv. Chim. Acta* **2005**, *88*, 447-460.

(16) Schibli, R.; La Bella, R.; Alberto, R.; Garcia-Garayoa, E.; Ortner, K.; Abram, U.; Schubiger, P. A. *Bioconjugate Chem.* **2000**, *11*, 345-351.

(17) Bezerra, C. W. B.; da Silva, S. C.; Gambardella, M. T. P.; Santos, R. H. A.; Plicas, L. M. A.; Tfouni, E.; Franco, D. W. *Inorg. Chem.* **1999**, *38*, 5560-5667.

(18) Hund, H.-U.; Ruppli, U.; Berke, H. *Helv. Chim. Act.* **1993**, *76*, 963-975.

(19) Norton, J. R.; Dolcetti, G. *Inorg. Chem.* **1973**, *12*, 485-487.

(20) Schibli, R.; Marti, N.; Maurer, P.; Spingler, B.; Lehaire, M. L.; Gramlich, V.; Barnes, C. L. *Inorg. Chem.* **2005**, *44*, 683-690.

(21) Lehaire, M. L.; Grundler, P. V.; Steinhauser, S.; Marti, N.; Helm, L.; Hegetschweiler, K.; Schibli, R.; Merbach, A. E. *Inorg. Chem.* **2006**, *45*, 4199-4204.

(22) Kurz, P.; Rattat, D.; Angst, D.; Schmalle, H.; Spingler, B.; Alberto, R.; Berke, H.; Beck, W. *Dalton Trans.* **2005**, 804-810.

(23) Marti, M. A.; Bari, S. E.; Estrin, D. A.; Doctorovich, F. *J. Am. Chem. Soc.* **2005**, *127*, 4680-4684.

(24) Marti, N.; Spingler, B.; Breher, F.; Schibli, R. *Inorg. Chem.* **2005**, *44*, 6082-6091.

(25) Tooyama, Y.; Braband, H.; Spingler, B.; Abram, U.; Alberto, R. *Inorg. Chem.* **2008**, *47*, 257-264.

(26) Davison, A.; Jones, A. G.; Abrams, M. J. *Inorg. Chem.* **1981**, *20*, 4300-4302.

(27) Liu, S.; Edwards, D. S. *Chem. Rev.* **1999**, *99*, 2235-2268.

(28) Pak, J. K.; Benny, P.; Spingler, B.; Ortner, K.; Alberto, R. *Chem.--Eur. J.* **2003**, *9*, 2053-2061.

(29) Celen, S.; De Groot, T. J.; Balzarini, J.; Vunckx, K.; Terwinghe, C.; Vermaelen, P.; Van Berckelaer, L.; Vanbilloen, H.; Nuyts, J.; Mortelmans, L.; Verbruggen, A.; Bormans, G. *Nucl. Med. Biol.* **2007**, *34*, 283-291.

(30) Stephenson, K. A.; Zubieta, J.; Banerjee, S. R.; Levadala, M. K.; Taggart, L.; Ryan, L.; McFarlane, N.; Boreham, D. R.; Maresca, K. P.; Babich, J. W.; Valliant, J. F. *Bioconjugate Chem.* **2004**, *15*, 128-136.

(31) Banerjee, S. R.; Maresca, K. P.; Francesconi, L.; Valliant, J.; Babich, J. W.; Zubieta, J. *Nucl. Med. Biol.* **2005**, *32*, 1-20.

(32) Valliant, J. F.; Riddoch, R. W.; Hughes, D. W.; Roe, D. G.; Fauconnier, T. K.; Thornback, J. R. *Inorg. Chim. Acta* **2001**, *325*, 155-163.

(33) Gariepy, J.; Remy, S.; Zhang, X.; Ballinger, J. R.; Bolewska-Pedyczak, E.; Rauth, M.; Bisland, S. K. *Bioconjugate Chem.* **2002**, *13*, 679-684.

(34) Greenland, W. E. P.; Howland, K.; Hardy, J.; Fogelman, I.; Blower, P. J. *J. Med. Chem.* **2003**, *46*, 1751-1757.

(35) Stephenson, K. A.; Reid, L. C.; Zubieta, J.; Babich, J. W.; Kung, M. P.; Kung, H. F.; Valliant, J. F. *Bioconjugate Chem.* **2008**, *19*, 1087-1094.

(36) Kolb, H. C.; Finn, M. G.; Sharpless, K. B. *Angew. Chem., Int. Ed.* **2001**, *40*, 2004-2021.

(37) Kolb, H. C.; Sharpless, K. B. *Drug Discovery Today* **2003**, *8*, 1128-1137.

(38) Huisgen, R. in *1,3-Dipolar cycloaddition - introduction, survey, mechanism*, (Ed. Padwa, A.), Wiley, **1984**, p 1-176.

(39) Rostovtsev, V. V.; Green, L. G.; Fokin, V. V.; Sharpless, K. B. *Angew. Chem. Int. Ed.* **2002**, *41*, 2596-2599.

(40) Tornoe, C. W.; Christensen, C.; Meldal, M. *J. Org. Chem.* **2002**, *67*, 3057-3064.

(41) Lee, L. V.; Mitchell, M. L.; Huang, S. J.; Fokin, V. V.; Sharpless, K. B.; Wong, C. H. *J. Am. Chem. Soc.* **2003**, *125*, 9588-9589.

(42) Tornoe, C. W.; Sanderson, S. J.; Mottram, J. C.; Coombs, G. H.; Meldal, M. *J. Comb. Chem.* **2004**, *6*, 312-324.

(43) Wu, P.; Fokin, V. V. *Aldrichimica Acta* **2007**, *40*, 7-17.

(44) Meldal, M.; Tornoe, C. W. *Chem. Rev.* **2008**, *108*, 2952-3015.

(45) Chan, T. R.; Hilgraf, R.; Sharpless, K. B.; Fokin, V. V. *J. Am. Chem. Soc.* **2004**, *6*, 2853-2855.

(46) Moore, D. S.; Robinson, S. D. *Adv. Inorg. Chem.* **1988**, *32*, 171-239.

(47) Detz, R. J.; Heras, S. A.; de Gelder, R.; van Leeuwen, P. W. N. M.; Hiemstra, H.; Reek, J. N. H.; van Maarseveen, J. H. *Org. Lett.* **2006**, *8*, 3227-3230.

(48) Maisonial, A.; Serafin, P.; Traikia, M.; Debiton, E.; Thery, V.; Aitken, D. J.; Lemoine, P.; Viossat, B.; Gautier, A. *Eur. J. Inorg. Chem.* **2008**, 298-305.

(49) Monkowius, U.; Ritter, S.; Konig, B.; Zabel, M.; Yersin, H. *Eur. J. Inorg. Chem.* **2007**, 4597-4606.

(50) Fletcher, J. T.; Bumgarner, B. J.; Engels, N. D.; Skoglund, D. A. *Organometallics* **2008**, *27*, 5430-5433.

(51) Li, Y. J.; Huffman, J. C.; Flood, A. H. *Chem. Commun.* **2007**, 2692-2694.

(52) Huang, S.; Clark, R. J.; Zhu, L. *Org. Lett.* **2007**, *9*, 4999-5002.

(53) Fukuzawa, S. I.; Oki, H.; Hosaka, M.; Sugasawa, J.; Kikuchi, S. *Org. Lett.* **2007**, *9*, 5557-5560.

(54) Suijkerbuijk, B.; Aerts, B. N. H.; Dijkstra, H. P.; Lutz, M.; Spek, A. L.; van Koten, G.; Gebbink, R. *Dalton Trans.* **2007**, 1273-1276.

(55) David, O.; Maisonneuve, S.; Xie, J. *Tetrahedron Lett.* **2007**, *48*, 6527-6530.

(56) Schweinfurth, D.; Hardcastle, K. I.; Bunz, U. H. F. *Chem. Commun.* **2008**, 2203-2205.

(57) Arner, E. S. J.; Eriksson, S. *Pharmacol. Ther.* **1995**, *67*, 155-186.

(58) Coppock, D. L.; Pardee, A. B. *Mol. Cell. Biol.* **1987**, *7*, 2925-2932.

(59) Eriksson, S.; Munch-Petersen, B.; Johansson, K.; Eklund, H. *Cell. Mol. Life Sci.* **2002**, *59*, 1327-1346.

(60) Schinazi, R. F.; Mead, J. R.; Feorino, P. M. *AIDS Res. Hum. Retrov.* **1992**, *8*, 963-990.

(61) Eriksson, S.; Wang, J. H. *Nucleos. Nucleot.* **1995**, *14*, 507-510.

(62) Lunato, A. J.; Wang, J. H.; Woollard, J. E.; Anisuzzaman, A. K. M.; Ji, W. H.; Rong, F. G.; Ikeda, S.; Soloway, A. H.; Eriksson, S.; Ives, D. H.; Blue, T. E.; Tjarks, W. *J. Med. Chem.* **1999**, *42*, 3378-3389.

(63) Al-Madhoun, A. S.; Johnsamuel, J.; Yan, J. H.; Ji, W. H.; Wang, J. H.; Zhuo, J. C.; Lunato, A. J.; Woollard, J. E.; Hawk, A. E.; Cosquer, G. Y.; Blue, T. E.; Eriksson, S.; Tjarks, W. *J. Med. Chem.* **2002**, *45*, 4018-4028.

(64) Byun, Y.; Yan, J. H.; Al-Madhoun, A. S.; Johnsamuel, J.; Yang, W. L.; Barth, R. F.; Eriksson, S.; Tjarks, W. *J. Med. Chem.* **2005**, *48*, 1188-1198.

(65) Welin, M.; Kosinska, U.; Mikkelsen, N. E.; Carnrot, C.; Zhu, C. Y.; Wang, L. Y.; Eriksson, S.; Munch-Petersen, B.; Eklund, H. *Proc. Natl. Acad. Sci. U. S. A.* **2004**, *101*, 17970-17975.

(66) Sandrini, M. P. B.; Piskur, J. *Trends Biochem. Sci.* **2005**, *30*, 225-228.

(67) Mikkelsen, N. E.; Johansson, K.; Karlsson, A.; Knecht, W.; Andersen, G.; Piskur, J.; Munch-Petersen, B.; Eklund, H. *Biochemistry* **2003**, *42*, 5706-5712.

(68) Eriksson, S.; Wang, L. Y. *Nucleos. Nucleot.* **1997**, *16*, 653-659.

(69) Kubota, R.; Yamada, S.; Kubota, K.; Ishiwata, K.; Tamahashi, N.; Ido, T. *J. Nucl. Med.* **1992**, *33*, 1972-1980.

(70) Lu, L.; Samuelsson, L.; Bergstrom, M.; Sato, K.; Fasth, K. J.; Langstrom, B. *J. Nucl. Med.* **2002**, *43*, 1688-1698.

(71) Shields, A. F.; Grierson, J. R.; Dohmen, B. M.; Machulla, H. J.; Stayanoff, J. C.; Lawhorn-Crews, J. M.; Obradovich, J. E.; Muzik, O.; Mangner, T. J. *Nat. Med.* **1998**, *4*, 1334-1336.

(72) Tjarks, W.; Wang, J.; Chandra, S.; Ji, W.; Zhuo, J.; Lunato, A. J.; Boyer, C.; Li, Q.; Usova, E. V.; Eriksson, S.; Morrison, G. H.; Cosquer, G. Y. *Nucleos. Nucleot. Nucleic Acids* **2001**, *20*, 695-698.

(73) Goudgaon, N. M.; Elkattan, G. F.; Schinazi, R. F. *Nucleos. Nucleot.* **1994**, *13*, 849-880.

(74) Lesnikowski, Z. J.; Schinazi, R. F. *Pol. J. Chem.* **1995**, *69*, 827-840.

(75) Soloway, A. H.; Tjarks, W.; Barnum, B. A.; Rong, F. G.; Barth, R. F.; Codogni, I. M.; Wilson, J. G. *Chem. Rev.* **1998**, *98*, 1515-1562.

(76) Yamamoto, Y.; Seko, T.; Nakamura, H.; Nemoto, H.; Hojo, H.; Mukai, N.; Hashimoto, Y. *J. Chem. Soc.-Chem. Commun.* **1992**, 157-158.

(77) Rong, F. G.; Soloway, A. H. *Nucleos. Nucleot.* **1994**, *13*, 2021-2034.

(78) Schinazi, R. F.; Goudgaon, N. M.; Fulcrand, G.; Elkattan, Y.; Lesnikowski, Z.; Ullas, G.; Moravek, J.; Liotta, D. C. *Int. J. Radiat. Oncol. Biol. Phys.* **1994**, *28*, 1113-1120.

(79) Rong, F. G.; Soloway, A. H.; Ikeda, S.; Ives, D. H. *Nucleos. Nucleot.* **1997**, *16*, 379-401.

(80) Rong, F. G.; Soloway, A. H.; Ikeda, S.; Ives, D. H. *Nucleos. Nucleot.* **1995**, *14*, 1873-1887.

(81) Al-Madhoun, A. S.; Johnsamuel, J.; Barth, R. F.; Tjarks, W.; Eriksson, S. *Cancer Res.* **2004**, *64*, 6280-6286.

(82) Schmid, M.; Neumaier, B.; Vogg, A. T. J.; Wczasek, K.; Friesen, C.; Mottaghy, F. M.; Buck, A. K.; Reske, S. N. *Nucl. Med. Biol.* **2006**, *33*, 359-366

(83) Schibli, R.; Netter, M.; Scapozza, L.; Birringer, M.; Schelling, P.; Dumas, C.; Schoch, J.; Schubiger, P. A. *J. Organomet. Chem.* **2003**, *668*, 67-74.

(84) Wei, L.; Babich, J. W.; Eckelman, W. C.; Zubieta, J. *Inorg. Chem.* **2005**, *44*, 2198-2209.

(85) Cabrita, M. A.; Baldwin, S. A.; Young, J. D.; Cass, C. E. *Biochem. Cell Biol.* **2002**, *80*, 623-638.

(86) Zhang, J.; Visser, F.; King, K. M.; Baldwin, S. A.; Young, J. D.; Cass, C. E. *Cancer Metastasis Rev.* **2007**, *26*, 85-110.

(87) Yao, S. Y. M.; Ng, A. M. L.; Sundaram, M.; Cass, C. E.; Baldwin, S. A.; Young, J. D. *Mol. Membr. Biol.* **2001**, *18*, 161-167.

(88) Zimmerman, T. P.; Mahony, W. B.; Prus, K. L. *J. Biol. Chem.* **1987**, *262*, 5748-5754.

(89) Kong, X. B.; Zhu, Q. Y.; Vidal, P. M.; Watanabe, K. A.; Polsky, B.; Armstrong, D.; Ostrander, M.; Lang, S. A.; Muchmore, E.; Chou, T. C. *Antimicrob. Agents Chemother.* **1992**, *36*, 808-818.

(90) Paproski, R. J.; Ng, A. M. L.; Yao, S. Y. M.; Graham, K.; Young, J. D.; Cass, C. E. *Mol. Pharmacol.* **2008**, *74*, 1372-1380.

(91) Pennycooke, M.; Chaudary, N.; Shuralyova, I.; Zhang, Y.; Coe, I. R. *Biochem. Biophys. Res. Commun.* **2001**, *280*, 951-959.

(92) Mackey, J. R.; Jennings, L. L.; Clarke, M. L.; Santos, C. L.; Dabbagh, L.; Vsianska, M.; Koski, S. L.; Coupland, R. W.; Baldwin, S. A.; Young, J. D.; Cass, C. E. *Clin. Cancer Res.* **2002**, *8*, 110-116.

“Click-to-Chelate”: Synthesis and installation of metal chelates into biomolecules in a single step

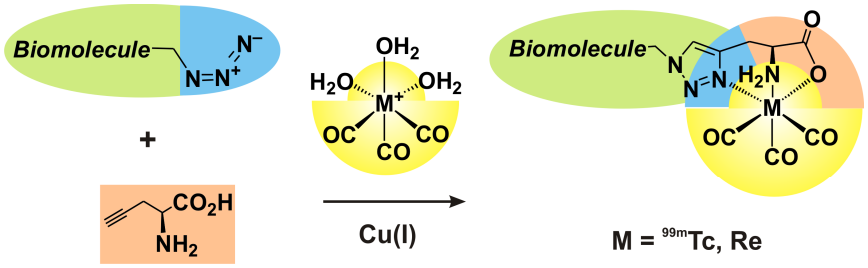

Journal of the American Chemical Society, **2006**, 128(47), 15096

2.1 Abstract

The radiolabelling of biologically active molecules has become an indispensable tool for the assessment of novel drug candidates. To keep pace with the growing number of new targets, innovative and efficient methodologies are needed for the firm attachment of readily available radionuclides with suitable decay characteristics to molecules of biomedical interest. The copper catalyzed cycloaddition of azides and terminal alkynes has been employed for the assembly of two triazole-based, histidine-like chelating systems for the $M(CO)_3$ core (M = ^{99m}Tc, Re), which can be incorporated into any azide/alkyne containing molecule in a single, high-yielding step. A range of representative biomolecules were selected to demonstrate the versatility of the new approach. All could be readily labelled with the $^{99m}Tc(CO)_3$ core at low ligand concentration, even without prior purification of the biomolecule-chelating system conjugate using a one-pot procedure in which the click reaction mixture is labelled directly. Preliminary pharmacological evaluation of a bombesin derivative, functionalized using click chemistry and labelled with technetium-99m, proved the *in vitro* and *in vivo* stability of the novel chelating system. The "click-to-chelate" approach offers a powerful new tool for the modification of biomolecules with metal chelators for potential diagnostic and therapeutic applications.

2.2 Introduction

Many isotopes with suitable decay characteristics for diagnostic applications are transition metal elements or possess metallic character. In order to incorporate radiometals into molecules of biological interest, the target molecule must first be functionalized with an appropriate bifunctional chelating agent to stabilize the metal in a given oxidation state. With ideal decay properties ($T_{1/2}$ = 6 h, 140 keV γ-radiation) and universal availability at low cost from a $^{99}Mo/^{99m}Tc$ generator, technetium-99m remains the most widely used radionuclide in diagnostic nuclear medicine. In recent years, a number of new cores of technetium-99m have been explored as precursors for the radiolabelling of biomolecules.[1] Our group has focused on the development of the complex *fac*-$[^{99m}Tc(CO)_3(H_2O)_3]^+$ as a labelling precursor.[2,3] The three labile water molecules can be readily replaced by a tridentate chelating system to form comparatively small, octahedral $^{99m}Tc(CO)_3$ complexes in which the metal has a low spin, d^6 configuration, and which are stable *in vitro* and *in vivo*.

A variety of bifunctional tridentate ligand systems have been designed to enable the incorporation of the technetium-99m tricarbonyl core into biologically relevant molecules. Chelators typically combine aliphatic and aromatic amines, carboxylic acids and thioethers, and are often based on amino acid scaffolds such as cysteine, lysine and histidine.[4-8] It is well documented, however, that the preparations of such chelators involve multi-step syntheses and their incorporation into biomolecules is often complicated by cross-reactivity with other functional groups present in the chelator and/or biomolecule. To tackle these shortcomings, we set out to investigate the use of Sharpless' click chemistry[9-11] as a means to reduce the complexity of the synthesis of effective metal chelators and improve the efficiency of the incorporation of the chelators into various classes of biologically relevant molecules.

The copper catalyzed [3+2] cycloaddition of azides and terminal alkynes, which forms stable 1,4-bifunctionalized 1,2,3-triazole linkages, has emerged as a transformation of such practicality and broad scope, that it has become the premier example of a click reaction and is synonymous with "click chemistry".[12] Click reactions are characterized by being efficient, selective and devoid of side reactions. Reactions must be insensitive to water and oxygen and require only minimal work-up and purification. The

orthogonal reactivity of alkynes and azides and the mild reaction conditions of the cycloaddition are well suited for the modification of a wide variety of biomolecules. Furthermore alkynes and azides can be readily incorporated into the relevant molecules by standard synthetic transformations or biochemical methods.[13-15] The features of click chemistry are paralleled by the requirements of a novel strategy for the functionalization of biomolecules with metal chelating systems. In addition, we recognized that the 1,4-disubstituted 1,2,3-triazole products of the cycloaddition share structural, electronic and thus potentially coordinative properties with 1,4-disubstituted imidazoles. Both heterocycles are known to be efficient ligands for various transition metals,[16-18] yet surprisingly few examples of 1,2,3-triazole chelators obtained using click chemistry have been reported.[19-21]

We have used click chemistry to facilitate the synthesis of two histidine-like chelating systems for the $^{99m}Tc(CO)_3$ core. The first system is derived from the reaction of propargyl glycine and a suitable azide, and leads to $M(CO)_3$ complexes in which the triazole is coordinated through N3. In the second system, azido alanine is reacted with a suitable alkyne, leading to complexes in which the triazole is coordinated through N2. DFT calculations supported experimental observations, which suggested that the chelating system derived from propargyl glycine was the more efficient ligand for the $M(CO)_3$ core. This chelating system was incorporated into a range of biomolecules in a single step, and the bioconjugates were then labelled efficiently with technetium-99m at low ligand concentrations. *In vitro* and *in vivo* characterization of a bombesin derivative proved the viability of the click chelating system for radiopharmaceutical applications.

2.3 Results and discussion

*N*τ-functionalized histidines have been shown to be extraordinarily good chelators, particularly for organometallic cores of Mo, Tc and Re,[22-24] yet their incorporation into small biomolecules is far from straightforward, requiring a complex multi-step synthetic strategy.[24] Using the copper catalyzed cycloaddition, triazole analogues of *N*τ-functionalized histidine can be synthesized from commercially available propargyl

glycine and a suitable azide (Figure 1, A) or azido alanine[25] and a suitable alkyne (Figure 1, B) in a single step.

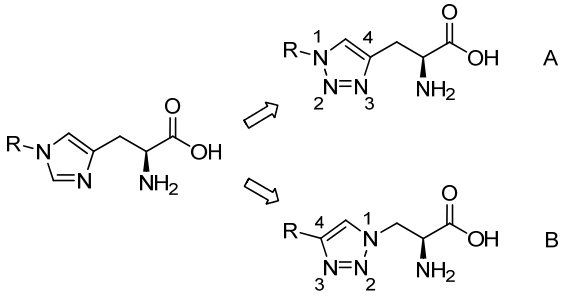

Figure 1. General structure of *N*τ-functionalized histidine and 1,2,3-triazole analogues, which can be readily prepared using click chemistry.

2.3.1 Model complexes

To probe the potential of a "click-to-chelate" approach, four model ligands were synthesized (Scheme 1). L-Propargyl glycine **1** was reacted with benzyl azide **3a** and azido acetate ethyl ester **3b** to form the 1,2,3-triazole-4-yl-alanines **5** and **6**, respectively. Similarly, L-azido alanine was reacted with 3-phenylpropyne **4a** and 4-pentynoic acid ethyl ester **4b** to give the triazole containing products **7** and **8**, respectively. In all cases, the cycloaddition reactions were carried out using similar conditions to those reported by the Sharpless group.[10] One equivalent of alkyne and one equivalent of azide were stirred in a mixture of tertiary butanol and water with 0.1 equivalents of copper (II) acetate and 0.2 equivalents of sodium ascorbate to generate the copper (I) catalyst *in situ*. Reactions were complete after stirring either for 12 hours at room temperature, or for 30 minutes at 100 °C. All of the reactions proceeded almost quantitatively with unprotected substrates, as determined by HPLC or ^{1}H-NMR spectroscopy (see Appendix A). Compound **6** could be conveniently isolated by precipitation from the reaction solution at 0 °C. In general, however, the water solubility of the unprotected ligand systems complicated purification of the triazole products. To facilitate thorough characterization, compound **5** was prepared from *N*α-Boc-L-propargyl glycine, which enabled extraction from the click reaction solution. Analogously, compounds **7** and **8** were prepared from *N*α-Boc-L-azido alanine.

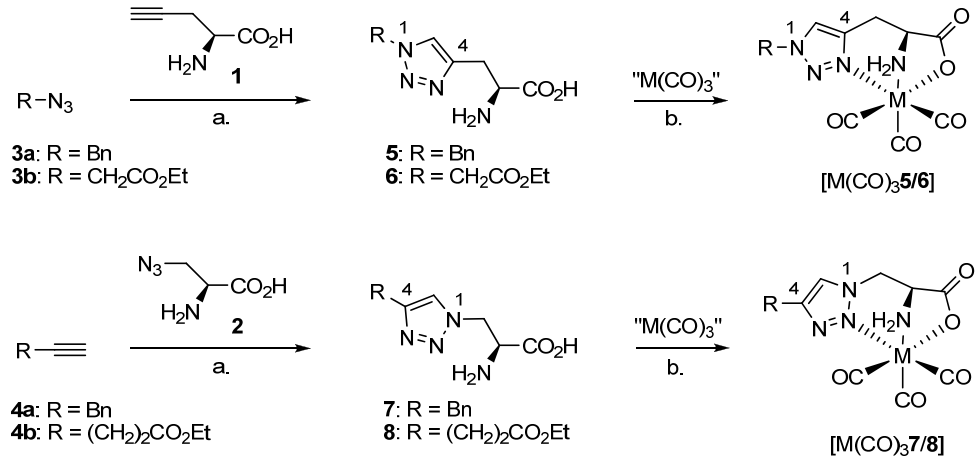

Scheme 1. Preparation of histidine-like triazole containing chelating systems and the corresponding $M(CO)_3$ (M = ^{99m}Tc, Re) complexes: (a) $Cu(OAc)_2.H_2O$, Na(ascorbate), water/*t*BuOH, 25 °C, 12 h or 100 °C, 30 min. (b) M = ^{99m}Tc: $[^{99m}Tc(CO)_3(H_2O)_3]^+$, PBS pH 7.4, 100 °C, 45 min; M = Re: $[Re(CO)_3Br_3]^{2-}$, water or alcohols, 50-65 °C, 1-4 h.

The reactions of ligands **5-8** with $[ReBr_3(CO)_3][NEt_4]_2$ in aqueous or alcoholic media yielded the well-defined neutral complexes $[Re(CO)_3$**5-8**$]$ in high yield (Scheme 1). The complexes were characterized by NMR, IR and elemental analysis. The characteristic features of the NMR spectra of the isolated complexes were consistent with those reported for [Re(CO)$_3$histidine][26] and Tc/Re(CO)$_3$ complexes of *N*τ-functionalized histidine derivatives.[24] NMR analysis provided strong evidence for tridentate coordination of N3 of the 1,2,3-triazole, the *N*α-amine and the carboxylate in the case of $[Re(CO)_3$**5**/**6**$]$, and N2 of the 1,2,3-triazole, the *N*α-amine and the carboxylate in the case of $[Re(CO)_3$**7**/**8**$]$. NMR signals of the metal chelator in the rhenium complexes exhibit a low field shift compared to the corresponding signals of the uncomplexed ligand. Independent signals are observed for the β-CH_2 protons which become distinguishable on coordination to the metal. Coordination of the amine is inferred from the appearance of signals for the NH_2 protons, even in protic solvents, as a result of a large decrease in the rate of H/D exchange. For all of the complexes there are two distinct NH signals with well defined coupling to each other, and in the case of one signal, to the α-proton of the amino acid. Both NH signals disappear after 24 hours in CD_3OD. Representative NMR spectra can be found in Appendix A.

The radioactive complexes $[^{99m}Tc(CO)_3$**5-8**$]$ were obtained as single products from the reactions of ligands **5-8** with the technetium-99m precursor $[^{99m}Tc(CO)_3(H_2O)_3]^+$ in

PBS (Scheme 1). Radiolabelling yields were determined by HPLC and the products were identified by comparison of their γ-HPLC retention times with the UV-HPLC retention times of the corresponding rhenium complexes, a procedure which is common in radiopharmacy. Varying the ligand concentration gave rise to step-sigmoid curves (Figure 2), which allowed the determination of EC_{50} values (ligand concentration necessary to achieve 50% radiolabelling yield). The EC_{50} values for ligands **5** and **6** were $2.5*10^{-7}$ M and $3.0*10^{-7}$ M, respectively. These values were comparable to that of *N*τ-methyl histidine (EC_{50} = ~10^{-7} M), demonstrating the potency of the triazole ligands **5** and **6**. EC_{50} values for ligands **7** and **8** were approximately two orders of magnitude higher (~10^{-5} M), suggesting that coordination of the triazole through N3 gives rise to a more efficient chelating system than coordination through N2.

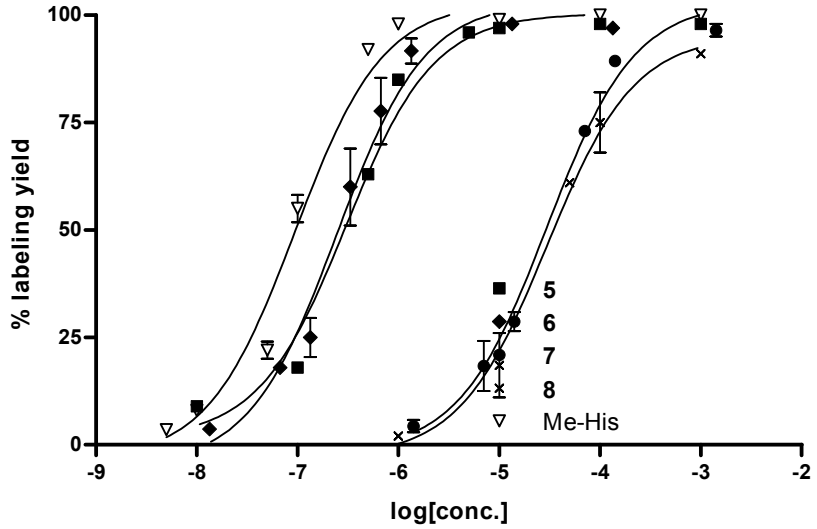

Figure 2. Labelling profiles for the reactions of ligands 5-8 and *N*τ-methyl histidine (Me-His) with $[^{99m}Tc(CO)_3(H_2O)_3]^+$ as a function of ligand concentration.

To further investigate the differing efficiencies of the triazole histidine analogues experimentally, L-propargyl glycine **1** was reacted with L-azido alanine **2** (Scheme 2). The resulting ligand **9** incorporates both the N2, *N*α-amine, carboxylate (κ*N2*,κ*N*α,κ*O*) and the N3, *N*α-amine, carboxylate (κ*N3*,κ*N*ακ*O*) chelating systems, which could give rise to two different complexes. The reaction of **9** with one equivalent of $[ReBr_3(CO)_3][NEt_4]_2$, however, leads to a single product, in which the metal is coordinated exclusively to the N3, *N*α-amine, carboxylate chelating system. 1-D and 2-D NMR analyses show clearly that the coordinated amine is coupled to the α-CH of

the C4 side chain. As further evidence for this mode of coordination, investigation of the reaction of ligand **9** with the technetium-99m precursor $[^{99m}Tc(CO)_3(H_2O)_3]^+$, gave an EC_{50} value of $9.8*10^{-8}$, which is more similar to the values for ligands **5** and **6**, than those of the isomeric ligands **7** and **8**. Density functional theory calculations (Gaussian 03[27]) were performed to calculate the electron densities on each of the atoms in the triazole ring of 1,4-dimethyl-1,2,3-triazole, and for comparison 1,4-dimethylimidazole. The preferential coordination through N3 can be attributed to the higher electron density at this position compared to the N2 nitrogen atom (Figure 3).

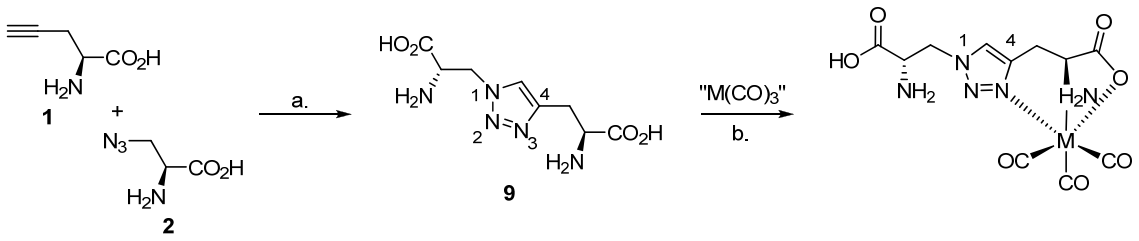

Scheme 2. Preparation of $[M(CO)_3\mathbf{9}]$ (M = ^{99m}Tc, Re): (a) $Cu(OAc)_2.H_2O$, Na(ascorbate), water/*t*BuOH, rt, 12 h. (b) M = ^{99m}Tc: $[^{99m}Tc(CO)_3(H_2O)_3]^+$, PBS pH 7.4, 100 °C, 45 min; M = Re: $[Re(CO)_3Br_3]^{2-}$, water or alcohols, 50-65 °C, 1-4 h.

	imidazole	triazole
N1	-0.399	-0.198
N2	-	-0.071
N3	-0.502	-0.268

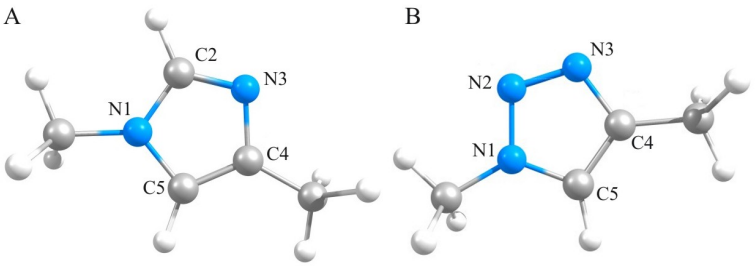

Figure 3. B3LYP/6-31G(d) optimized geometries and natural population analyses for 1,4-dimethylimidazole (A) and 1,4-dimethyltriazole (B) used as models for the histidine and click based ligands, respectively. For further information see the experimental section, 2.5.7 and Appendix A.

2.3.2 Incoporation of the triazole-containing chelating system into biologically relevant molecules

Unlike the multi-step syntheses required for preparation of *N*τ-derivatized histidine derivatives,[17,24] the novel click strategy avoids protective groups and provides optically pure histidine-like 1,4-functionalized triazoles in a single step with quantitative yields. These features are particularly appealing for the functionalization of biomolecules such as carbohydrates with polydentate metal chelates, which is notoriously inefficient using common synthetic strategies, as we and others have experienced.[28,29] Having established that the histidine-like triazole chelator, which coordinates to the $M(CO)_3$ core through N3 is the more efficient ligand system, the click approach was used to install this chelating system into a range of azido-functionalized biomolecules to give compounds **10**-**13** (Figure 4). Unprotected 1-azido-1-deoxy-*β*-D-galactopyranose,[30] 3′-azido-3′-deoxythymidine and an azido-phospholipid derivative were reacted with substrate **1** using the conditions outlined above for the preparation of compounds **5** and **6**. An azido-bombesin derivative was prepared and clicked on solid support[31] to afford compound **13** in excellent yield after cleavage from the resin.

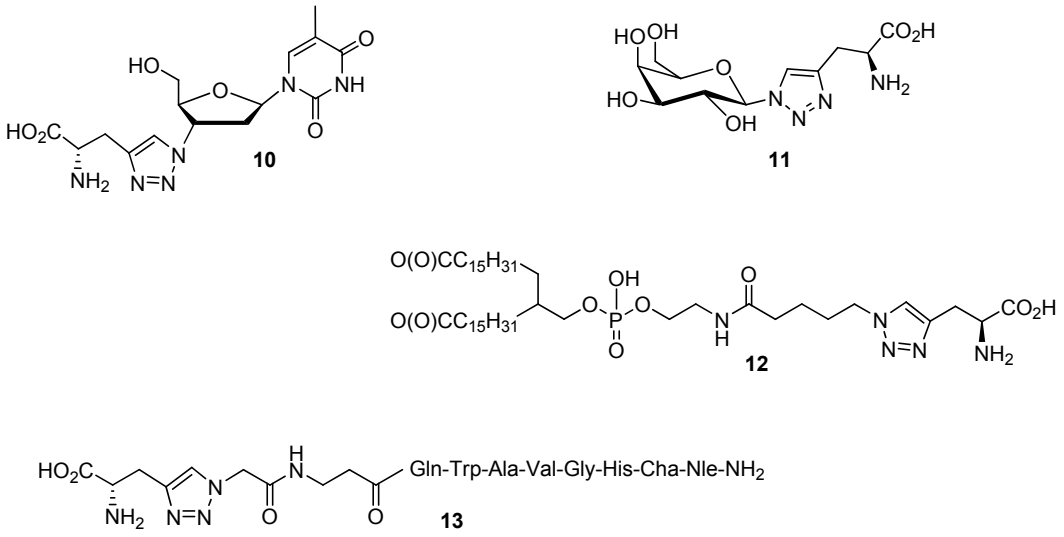

Figure 4. Biomolecules functionalized with a triazole containing chelator for the $M(CO)_3$ core (M = ^{99m}Tc, Re).

2.3.3 One-pot radiolabelling protocol

While the click products represent a class of extraordinarily good chelators, we could show that the individual substrates, for example, alkyne **1** and azide **2**, do not form stable or defined complexes with $[^{99m}Tc(CO)_3(H_2O)_3]^+$. This observation spurred the idea of a one-pot procedure to avoid isolation of the functionalized biomolecule prior to labelling with the $[^{99m}Tc(CO)_3(H_2O)_3]^+$ precursor and thus expedite tracer preparation. Stock solutions of L-propargyl glycine **1**, benzyl azide **3a**, 3′-azido-3′-deoxythymidine and 1-azido-1-deoxy-β-D-galactopyranoside were prepared in water (or methanol for benzyl azide **3a**), along with aqueous solutions of copper (II) acetate and sodium ascorbate. One equivalent of alkyne **1**, 0.1 equivalents of copper acetate, 0.2 equivalents of sodium ascorbate and 1.5 equivalents of **3a**, 3′-azido-3′-deoxythymidine or 1-azido-1-deoxy-β-D-galactopyranoside were heated to 100 °C for 30 minutes. After this time, $[^{99m}Tc(CO)_3(H_2O)_3]^+$ was added and the mixtures were heated for a further 30 minutes (Scheme 3). HPLC analysis confirmed the clean formation of complexes $[^{99m}Tc(CO)_3\mathbf{5}]$, $[^{99m}Tc(CO)_3\mathbf{10}]$ and $[^{99m}Tc(CO)_3\mathbf{11}]$, the identical products to those obtained with pre-synthesized and purified ligands **5**, **10** and **11** (see Appendix A).

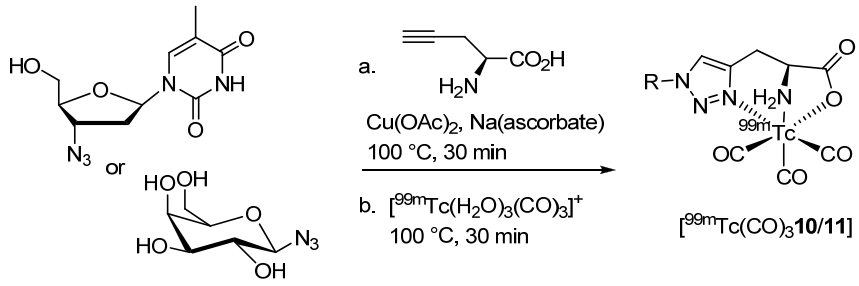

Scheme 3. One-pot procedure to yield the radiolabeled conjugates $[^{99m}Tc(CO)_3\mathbf{10}]$ and $[^{99m}Tc(CO)_3\mathbf{11}]$ in a single step.

For clinical applications it is desirable for ^{99m}Tc-labelled products to be obtained in a single step directly from $[^{99m}TcO_4]^-$ as eluted from the ^{99}Mo/^{99m}Tc generator. We were able to show that this can also be accomplished with the new click ligands by adding a solution of the relevant ligand (**5**, **10**, **11**) to the IsoLink™ kit and heating for 60 minutes at 100 °C.

2.3.4 Pharmacological properties of ^{99m}Tc labelled bombesin derivative

The radiolabelled bombesin derivative [^{99m}Tc(CO)$_3$**13**] was assessed *in vitro* and *in vivo* for its stability and receptor affinity. The radiotracer had high affinity for the gastrin-releasing-peptide (GRP) receptor *in vitro* (K_D = 0.19 ± 0.06 nM). *In vivo* data from CD-1 nu/nu mice revealed a biodistribution pattern comparable to [^{99m}Tc(CO)$_3$*N*αAcHis-BBN] a bombesin analogue with sequence homology in the receptor binding part, but which possesses a histidine chelate.[32,33] [^{99m}Tc(CO)$_3$**13**] exhibited a rapid clearance from the blood pool and most tissues, but showed high uptake in the GRP receptor-positive pancreas and colon (Figure 5). Co-injection of non-radioactive bombesin suppressed specific uptake but did not affect distribution of radioactivity in other tissue and organs, which is evidence that the biological activity and specificity of the peptide was retained (see Appendix A). These preliminary results suggest that the new triazole ligands represent a valuable alternative to histidine-derived chelators for labelling biomolecules. Detailed results are published elsewhere.[34]

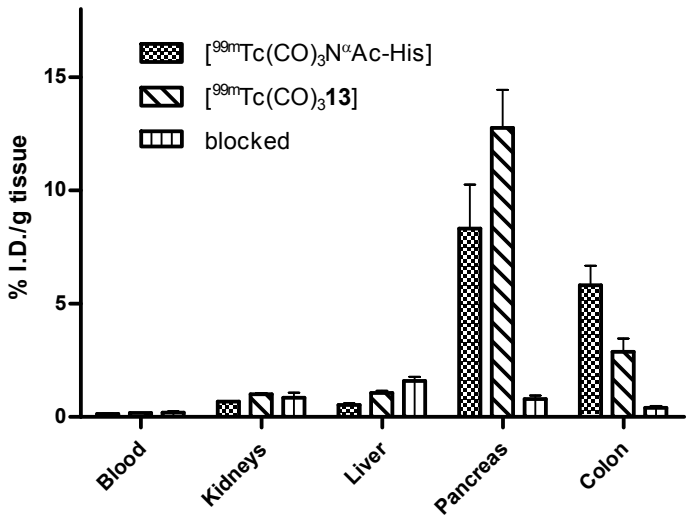

Figure 5. Biodistribution in selected organs and tissue of GRP receptor targeting with radiolabelled bombesin analogue [^{99m}Tc(CO)$_3$**13**] in mice, 1.5 h post injection. To prove the GRP specificity, blocking experiments were perfomed by co-injection of 100 µg non-radioactive bombesin. For comparison, biodistribution data of [^{99m}Tc(CO)$_3$(*N*αAcHis-BBN)], which had already been fully characterized,[32] are shown.

2.4 Conclusions

Click reactions are particularly valuable chemical transformations because they are efficient, selective and devoid of side reactions. The reactions proceed under mild conditions and require minimal work up and purification, providing an ideal framework for the development of a novel strategy for the functionalization of a wide range of biomolecules with chelating systems for the $M(CO)_3$ core. We have shown that the copper catalyzed [3+2] cycloaddition of azides and alkynes can be used to synthesize an efficient histidine-like ligand system for the $M(CO)_3$ core (M = ^{99m}Tc, Re) in which the 1,4-disubstituted triazole forms an integral part of the metal chelating system. Click chemistry not only simplifies the synthesis of efficient metal chelating systems, but also facilitates their incorporation into biologically relevant molecules in a single, high-yielding step.

Using the "click-to-chelate" approach, representatives from four classes of biomolecules could be efficiently labelled with the $^{99m}Tc(CO)_3$ core in a simple two step procedure. Furthermore, a one-pot protocol was developed to allow *in situ* radiolabelling of the click reaction mixtures, without compromising the radiolabelling yields or purity of the bioconjugates. Promising data were obtained with a bombesin derivative functionalized using click chemistry and labelled with technetium-99m, which was stable *in vitro* and *in vivo* and retained substrate affinity for the GRP receptor. These results suggest that the triazole containing chelating system is a viable alternative to established histidine chelators for radiopharmaceutical applications, and in addition the remarkable features of click chemistry offer significant advantages for their preparation and incorporation into a wide range of molecules.

2.5 Experimental details

2.5.1 General methods

Melting points were taken on a Büchi-535 apparatus and are uncorrected. Infrared spectra were recorded on either a Jasco FT/IR-6200 ATR-IR or a Perkin Elmer Spectrum BX II FT-IR, with a Pike MIRacle™ ATR accessory. Nuclear magnetic

resonance spectra were recorded on either a Bruker 400 MHz spectrometer or a 300 MHz Varian Gemini 2000 spectrometer with the corresponding solvent signals as an internal standard. Chemical shifts are reported in parts per million (ppm) relative to tetramethylsilane (0.00 ppm). Values of the coupling constant, *J*, are given in Hertz (Hz); the following abbreviations are used in the description of ^{1}H-NMR spectra: singlet (s), doublet (d), triplet (t), quartet (q), multiplet (m), doublet of doublets (dd), broad singlet (bs). The chemical shifts of complex multiplets are given as the range of their occurrence. Low resolution mass spectra were recorded with a Micromass Quattro microTM API LC-ESI or an LCT Premier ESI-TOF from Waters, using either the negative or positive ionization mode. High resolution mass spectra (High Res. MS) were recorded with a Bruker FTMS 4.7T BioAPEXII (ESI) or an Ionspec Ultima FTMS 4.7T (MALDI). Optical rotation values were measured in a 0.5 mL cell using a Jasco P-1020 polarimeter.

$[^{99m}Tc(CO)_3(H_2O)_3]^+$ was prepared using the Isolink^{TM} kit (Mallinkrodt-Tyco, Petten, the Netherlands). $[Na][^{99m}TcO_4]$ was eluted from a $^{99}Mo/^{99m}Tc$ generator (Mallinckrodt-Tyco, Petten) with a 0.9% saline solution. Commercial Boc-propargylglycine dicyclohexylamine salt (Sigma-Aldrich) was dissolved in ethyl acetate and washed with citric acid (1 M) and brine. The organic extract was dried over Na_2SO_4 and evaporated under reduced pressure to yield the free acid for click reactions. Sep-Pak® columns (Waters) were washed well with methanol and water prior to use. $[Re(CO)_3Br_3][NEt_4]_2$,[35] pentynoic acid ethyl ester,[36] L-azido-alanine,[25] Boc-L-azido-alanine[37] and azido acetic acid[38] were prepared according to literature procedures. QuadraPure-IDATM metal scavenging resin (Sigma-Aldrich) was washed well with methanol prior to use. The Rink amide resin for solid-phase peptide synthesis was obtained from NovaBioChem (Läufelfingen, Switzerland). All other reagents and solvents were obtained from commercial sources (Sigma-Aldrich, Acros, Alfa Aesar, Bachem) and used as supplied unless stated otherwise.

Reactions were monitored by thin layer chromatography (TLC) or HPLC. TLC was performed on EM Science 0.25 mm thick, precoated silica gel 60 F-254 glass supported plates. Plates were visualized by UV, or using solutions of permanganate or ninhydrin. TLC analysis of peptides used EtOAc/n-BuOH/AcOH/H_2O (1:1:1:1) as the eluent, and permanganate for visualization. HPLC was performed on a Merck-Hitachi L-7000

system equipped with an L-7400 tunable absorption detector and a Berthold LB 506 B radiometric detector. Analytical HPLC was performed with either an XTerra® column (MSC18, 5µm, 4.6 x 150 mm, Waters) or a Nucleosil® 5 C18 column (5µm, 4.6 x 250 mm, Macherey-Nagel). An XBridgeTM column (Prep C18, 5µm, 10 x 150 mm, Waters) was used for semi-preparative HPLC. HPLC solvents were either 0.05 M triethylammonium phosphate buffer, pH 2.25 (solvent A) and methanol (solvent B), or water with 0.1% trifluoroacetic acid (solvent A) and acetonitrile (solvent B). Two HPLC gradients were used. Gradient 1: 0 to 15 min, 95% A to 20% A, 15 to 20 min 100% A, and a flow rate of 1 mL/min (analytical) or 3 mL/min (semi-preparative). Gradient 2: 0 to 20 min, 97% A to 0% A, 20 to 25 min, 0% A to 97% A, 25 to 30 min, 97% A, and a flow rate of 1 mL/min.

2.5.2 Ligand synthesis

Compounds **5**, **7**, **8** and **12** were prepared using either *N*α-Boc-propargyl-L-glycine or *N*α-Boc-azido-L-alanine, to facilitate isolation of the triazole ligands. Unlike the water soluble *N*α-deprotected triazole ligands, Boc-protected intermediates could be readily isolated by extraction und purified by flash chromatography on silica gel.

***N*α-Boc-5.** Benzylazide (53 mg, 0.4 mmol), N(α)-Boc-L-propargylglycine (85 mg, 0.4 mmol) copper (II) acetate (7 mg, 0.04 mmol) and sodium ascorbate (16 mg, 0.08 mmol) were mixed in *t*-butanol/water (1:1; 3.0 mL) and stirred at rt overnight. The resulting green solution was diluted with ethyl acetate (5 mL) and washed with brine (2 x 5 mL). The aqueous solutions were extracted with ethyl acetate (2 x 5 mL). The organic extracts were combined, dried over Na_2SO_4 and concentrated under reduced pressure. The crude product was purified by flash chromatography on silica gel with mixtures of CH_2Cl_2/MeOH (20-30%) to afford the Boc-protected intermediate as a pale yellow solid (86 mg, 62%): mp >170 °C (decomp.); IR (neat) ν 3359, 2977, 2927, 1691, 1562, 1402, 1051 cm^{-1}; ^{1}H-NMR (CD_3OD) δ 7.74 (s, 1H), 7.36-7.28 (m, 5H), 5.55 (s, 2H), 4.30 (bs, 1H), 3.27-3.01 (m, 2H), 1.36 (s, 9H) ppm; ^{13}C-NMR (CD_3OD) δ 157.6, 136.8, 130.0,

129.5, 129.0, 124.8 (broad), 80.4, 62.7, 54.9, 30.2, 28.7 ppm (one carbon (carbonyl) not observed); MS (ESI) *m/z* 347.05 $[C_{17}H_{22}N_4O_4]H^+$; $[\alpha]_D^{20}$ = +11.0 (c = 0.9 in $CHCl_3$).

Compound 5. *N*α-Boc-5 (65 mg, 0.19 mmol) was dissolved in CH_2Cl_2/TFA (2:1; 2.0 mL) and stirred at rt overnight. Concentration under reduced pressure followed by repeated dissolution of the residue in MeOH and evaporation under reduced pressure provided compound **5** as a hygroscopic, white solid (68 mg, 98%): mp >195 °C (decomp.); IR (neat) ν 3130, 2930, 2859, 1674, 1592, 1198, 1137, 718 cm^{-1}; ^{1}H-NMR (D_2O containing 0.5% DCl) δ 7.96 (s, 1H), 7.40-7.25 (m, 5H), 5.56 (s, 2H), 4.36 (t, 1H, *J* = 6.2 Hz), 3.37 (d, 2H, *J* = 6.2 Hz) ppm; ^{13}C-NMR (D_2O containing 0.5% DCl) δ 170.4, 162.5 (q, *J* = 36.0 Hz, TFA), 140.6, 134.4, 129.1, 128.8, 128.1, 125.4, 116.1 (q, *J* = 291.8 Hz, TFA), 54.2, 52.2, 25.3 ppm; High Res. MS (MALDI) *m/z* 247.1185 $[C_{12}H_{14}N_4O_2]H^+$ (calc. 247.1195); elemental analysis (calculated %-values for $C_{12}H_{14}N_4O_2(C_2HF_3O_2)_{0.2}$ in parenthesis) C 55.65 (55.35), H 5.69 (5.32), N 21.17 (20.82).

Compound 6. Azidoacetic acid ethyl ester (129 mg, 1.0 mmol), L-propargyl glycine (113 mg, 1.0 mmol), copper (II) acetate (18 mg, 0.1 mmol) and sodium ascorbate (40 mg, 0.2 mmol) were mixed in *t*-butanol/water (1:1; 6.0 mL) and stirred at rt overnight. QuadraPure-IDA® resin (0.2 g) was added and the mixture was gently shaken at rt for 2 h during which the blue colour of the solution faded. The resulting brown solution was decanted and added dropwise to ethanol (100 mL). Filtration at 0 °C yielded compound **6** as a white powder (220 mg, 91%): mp 272-274 °C; IR (neat) ν 3126, 2980, 2909, 1745, 1577, 1491, 14.09, 1220, 1197, 1061 cm^{-1}; ^{1}H-NMR (D_2O) δ 7.95 (s, 1H), 5.40 (s, 2H), 4.31 (q, 2H, *J* = 7.2 Hz), 4.10 (t, 1H, *J* = 6.4 Hz), 3.39 (dd, 1H, *J* = 15.7 and 4.9 Hz), 3.36 (dd, 1H, *J* = 15.7 and 7.1 Hz), 1.31 (t, 3H, *J* = 7.2 Hz) ppm; ^{13}C-NMR (D_2O) δ 173.1, 169.0, 142.1, 125.9, 63.4, 54.3, 51.0, 26.3, 13.2 ppm; High Res. MS *m/z* 243.1090 $[C_9H_{15}N_4O_4]^-$ (calc. 243.1093); elemental analysis (calculated %-values in parenthesis) C 44.51 (44.63), H 5.70 (5.83), N 22.88 (23.13), O 26.52 (26.42); $[\alpha]_D^{20}$ = -10.5 (c = 1.0 in H_2O).

***N*α-Boc-7.** 3-Phenyl-1-propyne (93 µL, 87 mg, 0.75 mmol), *N*α-Boc-L-azidoalanine (173 mg, 0.75 mmol) copper (II) acetate (14 mg, 0.08 mmol) and sodium ascorbate (30

mg, 0.15 mmol) were mixed in *t*-butanol/water (1:1; 6.0 mL) and stirred at rt overnight. The resulting green solution was diluted with ethyl acetate (10 mL) and washed with brine (2 x 10 mL). The aqueous solutions were extracted with ethyl acetate (2 x 5 mL). The organic extracts were combined, dried over Na_2SO_4 and concentrated under reduced pressure. The crude product was purified by flash chromatography on silica gel with mixtures of CH_2Cl_2/MeOH (20-30%) to afford the Boc protected intermediate as a pale yellow solid (177 mg, 68%): mp >190 °C (decomp.); IR (neat) ν 3206, 2980, 1688, 1602, 1368, 1190, 1151, 1066 cm^{-1}; ^{1}H-NMR (CD_3OD) δ 7.59 (s, 1H), 7.35-7.25 (m, 5H), 4.91-4.79 (m, partly covered by HDO signal, 1H, *J* = 4.2 Hz), 4.62 (dd, 1H, *J* = 13.6 and 7.1 Hz), 4.38 (dd, 1H, *J* = 7.1 and 4.2 Hz), 4.00 (s, 2H), 1.33 (s, 9H) ppm; ^{13}C-NMR (CD_3OD) δ 157.5, 140.3, 131.2, 129.7, 129.6, 127.5, 125.1 (broad), 101.5, 80.6, 52.9, 32.6, 28.7 ppm. (One carbon (carbonyl) not observed); MS (ESI) *m/z* 347.02 $[C_{17}H_{22}N_4O_4]H^+$; $[\alpha]_D^{20}$ = +24.7 (c = 0.9 in $CHCl_3$).

Compound 7. *N*α-Boc-7 (113 mg, 0.33 mmol) was deprotected in CH_2Cl_2/TFA (2:1; 3.0 mL) by the procedure described for compound **5** to give a hygroscopic, white solid (**7**, 110 mg, 93%): mp >220 °C (decomp.); IR (neat) ν 3363, 2977, 1710, 1674, 1198, 721 cm^{-1}; ^{1}H-NMR (D_2O containing 0.5% DCl) δ 8.05 (s, 1H), 7.29-7.13 (m, 5H), 5.03 (dd, 1H, *J* = 15.3 and 5.4 Hz), 4.99 (dd, 1H, *J* = 15.3 and 4.5 Hz), 4.64 (dd, 1H, *J* = 5.4 and 4.5 Hz) 4.04 (s, 2H) ppm; ^{13}C-NMR (D_2O containing 0.5% DCl) δ 167.9, 162.1 (q, *J* = 37.0 Hz, TFA), 145.8, 129.0, 128.7, 127.3, 127.0, 115.8 (q, *J* = 289.8 Hz, TFA), 51.9, 50.0, 29.5 ppm; High Res. MS (MALDI) *m/z* 247.1185 $[C_{12}H_{14}N_4O_2]H^+$ (calc. 247.1195); elemental analysis (calculated %-values for $C_{12}H_{14}N_4O_2(C_2HF_3O_2)_{0.08}$ in parenthesis) C 57.59 (57.19), H 5.73 (5.56), N 22.12 (21.94).

***N*α-Boc-8.** Pent-4-ynoic acid ethyl ester (202 mg, 1.60 mmol), *N*α-Boc-L-azidoalanine (369 mg, 1.60 mmol) copper (II) acetate (29 mg, 0.16 mmol) and sodium ascorbate (63 mg, 0.32 mmol) were mixed in *t*-butanol/water (1:1; 12 mL) and stirred at rt overnight. The resulting green solution was diluted with ethyl acetate (10 mL) and washed with brine (2 x 10 mL). The aqueous solutions were extracted with ethyl acetate (2 x 10 mL). The organic extracts were combined, dried over Na_2SO_4 and concentrated under reduced pressure. The crude product was purified by flash chromatography on silica gel with mixtures of CH_2Cl_2/MeOH (15-30%) to afford the Boc-protected intermediate as a

pale yellow oil (233 mg, 41%): IR (neat) ν 3382, 2984, 1694, 1381, 1233, 1192, 1155, 1062, 951 cm^{-1}; ^{1}H-NMR (CD_3OD) δ 7.71 (s, 1H), 4.88-4.82 (m, 1H), 469-4.59 (m, 2H), 4.12 (q, 2H, *J* = 7.1 Hz), 2.98 (t, 2H, *J* = 7.3 Hz), 2.69 (t, 2H, *J* = 7.3 Hz), 1.40 (s, 9H), 1.23 (t, 3H, *J* = 7.1 Hz) ppm; ^{13}C-NMR (CD_3OD) δ 174.1, 157.5, 124.3 (broad), 123.4, 119.2, 80.7, 61.7, 52.6, 34.5, 28.7, 21.8, 14.5 ppm (one carbon (carbonyl) not observed); MS (ESI) *m/z* 357.10 $[C_{15}H_{24}N_4O_6]H^+$; $[\alpha]_D^{20}$ = +8.9 (c = 1.0 in MeOH).

Compound 8. *N*α-Boc-8 (200 mg, 0.56 mmol) was dissolved in CH_2Cl_2/TFA (9:1; 10 mL) and stirred at rt overnight. After concentration under reduced pressure followed by repeated dissolution of the residue in MeOH and evaporation under reduced pressure, compound **8** precipitated as a white solid (62 mg, 43%): mp >200 °C (decomp.); IR (neat) ν 3062, 1728, 1622, 1580, 1483, 1438, 1402, 1323, 1164, 1054, 865 cm^{-1}; ^{1}H-NMR (D_2O/DCl) δ 8.01 (s, 1H), 4.99 (t, 2H, *J* = 4.9 Hz), 4.62 (t, 1H, *J* = 4.9 Hz), 3.96 (q, 2H, *J* = 7.1 Hz), 2.94 (t, 2H, *J* = 7.0 Hz), 2.64 (t, 2H, *J* = 7.0 Hz), 1.04 (t, 3H, *J* = 7.1 Hz) ppm; ^{13}C-NMR (D_2O/DCl/CD_3OD) δ 177.2, 175.5, 169.0, 146.6 (broad), 127.2, 62.8, 58.4, 53.1, 33.3, 20.3, 17.8 ppm; High Res. MS *m/z* 257.1244 $[C_{10}H_{16}N_4O_4]H^+$ (calc. 257.1249); $[\alpha]_D^{20}$ = +4.1 (c = 1.0 in HCl/H_2O).

***N*α-Boc-9.** L-propargyl glycine (173 mg, 0.75 mmol), *N*α-Boc-L-azidoalanine (176 mg, 0.75 mmol) copper (II) acetate (30 mg, 0.15 mmol) and sodium ascorbate (60 mg, 0.30 mmol) were mixed in *t*-butanol/water (2:1; 6 mL) and stirred at rt overnight. The reaction mixture was concentrated under reduced pressure. The crude product was purified by flash chromatography on silica gel with mixtures of CH_2Cl_2/MeOH (5-20%) to afford the Boc-protected intermediate as a white solid (60 mg, 17%): ^{1}H-NMR (MeOD) δ 8.02 (s, 1H), 4.85 (m, 2H), 4.44 (m, 2H), 3.25 (m, 1H), 3.14 (m, 1H), 1.44 (s, 9H), 1.44 (s, 9H) ppm; ^{13}C-NMR (MeOD) δ 157.50, 156.88, 124.42, 80.82, 57.41, 56.22, 53.17, 30.41, 28.95, 28.86 ppm; MS (ESI) *m/z* 444.08 $[C1_8H_{29}N_5O_8]H^+$.

Compound 9. *N*α-Boc-9 (60 mg, 0.14 mmol) was dissolved in CH_2Cl_2/TFA (2:1; 5 mL) and stirred at rt overnight. After concentration under reduced pressure followed by repeated dissolution of the residue in MeOH and evaporation under reduced pressure, the TFA salt of compound **9** precipitated as a white solid (60 mg, 94%): ^{1}H-NMR (D_2O) δ 7.91 (s, 1H), 4.96 (t, *J* = 5.1, 2H), 4.60 (dd, *J* = 5.4, 4.4, 1H), 4.34 (t, *J* = 6.1, 1H),

3.33 (d, *J* = 6.1, 2H) ppm; ^{13}C-NMR (D_2O) δ 170.58, 168.54, 141.27, 125.93, 52.47, 52.25, 48.67, 25.40 ppm; High Res. MS *m/z* 244.1041 $[C_8H_{13}N_5O_4]H^+$ (calc. 244.1040).

Compound 10. 3-Azidothymidine (30.0 mg, 0.112 mmol), L-propargyl glycine (13.0 mg, 0.115 mmol), copper (II) acetate (0.8 mg, 0.004 mmol) and sodium ascorbate (2.2 mg, 0.011 mmol) were mixed in *t*-butanol/water (1:1; 0.5 mL) and stirred at rt overnight. Water (0.5 ml) and QuadraPure-IDA® resin (50 mg) were added and the mixture was gently shaken at 50°C for 2 h during which time the blue colour of the solution disappeared. The solution was added dropwise to methanol (5 mL). Filtration of the resulting suspension yielded compound **10** (34.8 mg, 82 %) as a white solid: mp >190 °C (decomp.); IR (neat) ν 3535, 3426, 3136, 3018, 2990, 2930, 2880, 2815, 2750, 1690, 1665, 1652, 1628, 1598, 1538, 1473, 1410, 1388, 1345, 1306, 1272, 1255, 1235, 1214, 1150, 1093, 1047, 1020, 1000, 955, 929, 902, 882, 857, 785, 761, 669, 614 cm^{-1}; ^{1}H-NMR (D_2O) δ 8.03 (s, 1H), 7.74 (s, 1H), 6.45 (t, *J* = 6.5 Hz, 1H), 5.48 – 5.36 (dd, 1H), 4.79 - 4.77 (m, 1H), 4.50 - 4.43 (m, 1H), 4.08 (s, 1H), 3.90 (dd, *J* = 12.6 and 3.0 Hz, 1H), 3.80 (dd, *J* = 12.6 and 4.2 Hz, 1H), 3.33 (s, 1H), 2.96 (dd, *J* = 14.6, 7.5 and 4.5 Hz, 1H), 2.82 (ddd, 1H, *J* = 14.6, 8.6 and 6.1 Hz), 1.90 (s, 3H) ppm; ^{13}C-NMR (D_2O) δ 185.2, 166.4, 151.4, 137.6, 111.3, 99.9, 85.4, 84.1, 60.4, 59.5, 36.7, 26.2, 21.8, 11.4 ppm; High Res. MS *m/z* 379.1370 $[C_{15}H_{19}N_6O_6]^-$ (calc. for: 379.1372).

***N*α-Boc-11-tetraacetate.** 1-Azido-1-deoxy-β-D-galactopyranoside tetraacetate (187 mg, 0.5 mmol), *N*α-Boc-L-propargylglycine (106 mg, 0.5 mmol) copper (II) acetate (9 mg, 0.05 mmol) and sodium ascorbate (20 mg, 0.10 mmol) were mixed in *t*-butanol/water (1:1; 4.0 mL) and stirred at rt overnight. The resulting green solution was diluted with ethyl acetate (10 mL) and washed with brine (2 x 10 mL). The aqueous solutions were extracted with ethyl acetate (2 x 5 mL) . The organic extracts were combined, dried over Na_2SO_4 and concentrated under reduced pressure. The crude product was purified by flash chromatography on silica gel with mixtures of CH_2Cl_2/MeOH (10-20%) to afford *N*α-Boc-11-tetraacetate as a white solid (217 mg, 74%): mp >190 °C (decomp.);IR (neat) ν 3406, 2977, 2934, 1752, 1684, 1588, 1395, 1366, 1215, 1254 cm^{-1}; ^{1}H-NMR (CD_3OD) δ 7.95 (s, 1H), 6.06 (d, 1H, *J* = 9.2 Hz), 5.65 (t, 1H, *J* = 9.8 Hz), 5.55 (d, 1H, *J* = 2.7 Hz), 5.41 (dd, 1H, *J* = 10.3 and 3.4 Hz), 4.46 (t, 1H, *J* = 6.5 Hz), 4.30- 4.15 (m, 2H), 4.12 (dd, 1H, *J* = 11.4 and 6.9 Hz), 3.38-

3.25 (m, partly covered by CD_3OD signal, 1H, *J* = 5.0 Hz), 3.15 (dd, 1H, *J* = 14.8 and 6.6 Hz), 2.21 (s, 3H), 2.02 (s, 3H), 2.00 (s, 3H), 1.86 (s, 3H), 1.42 (s, 9H) ppm; ^{13}C-NMR (CD_3OD) δ 172.0, 171.9, 171.3, 170.6, 158.3, 146.5, 123.4, 87.0, 80.4, 75.0, 72.4, 69.6, 68.7, 62.6, 49.0, 29.6, 28.8, 20.6, 20.5, 20.4, 20.2 ppm (one quaternary carbon is not visible); MS (ESI) *m/z* 587.12 $[C_{24}H_{34}N_4O_{13}]H^+$ (calc. for: 587.22).

***N*α-Boc-11.** Tetraacetate (152 mg, 0.26 mmol) was dissolved in methanol (2.0 mL) and a catalytic amount of sodium methoxide (1.4 mg, 0.03 mmol) was added. The solution was stirred at rt overnight and then concentrated under reduced pressure to yield *N*α-Boc-12 as a white solid (107 mg, 98%): mp >110 °C (decomp.); IR (neat) ν 3345, 2980, 2930, 1681, 1592, 1398, 1162, 1090, 1054, 886 cm^{-1}; ^{1}H-NMR (CD_3OD) δ 7.99 (s, 1H), 5.54 (d, 1H, *J* = 8.9 Hz), 4.27 (bs, 1H), 4.17 (t, 1H, *J* = 9.1 Hz), 4.09 (bs, 1H), 3.90-3.18 (m, 4H), 3.29-3.07 (m, 2H), 1.29 (s, 9H) ppm; ^{13}C-NMR (CD_3OD) δ 179.4, 157.8, 145.5, 123.4, 90.4, 80.7, 79.9, 75.3, 71.6, 70.5, 62.5, 56.6, 29.9, 28.9 ppm; MS (ESI) *m/z* 419.06 $[C_{16}H_{26}N_4O_9]H^+$ (calc. 419.18).

Compound 11. *N*α-Boc-11 (113 mg, 0.33 mmol) was deprotected in CH_2Cl_2/TFA (2:1; 3.0 mL) by the procedure described for compound 5 to give as an off-white solid (12, 80 mg, 96%): mp >145 °C (decomp.); IR (neat) ν 3298, 2919, 1670, 1438, 1198, 1134, 1093, 1065, 725 cm^{-1}; ^{1}H-NMR (D_2O) δ 8.08 (s, 1H), 5.62 (d, 1H, *J* = 9.2 Hz), 4.15 (t, 1H, *J* = 9.6 Hz), 4.08-4.00 (m, 2H), 3.93 (t, 1H, *J* = 5.9 Hz), 3.81 (dd, 1H, *J* = 9.8 and 3.3 Hz), 3.71 (d ,2H, *J* = 6.0 Hz), 3.34 (dd, 1H, *J* = 15.7 and 5.2 Hz), 3.29 (dd, 1H, *J* = 15.7 and 6.8 Hz) ppm; ^{13}C-NMR (D_2O) δ 172.9, 163.0 (q, *J* = 35.6 Hz), 142.2, 123.6, 116.3 (q, *J* = 291.7 Hz), 87.9, 78.3, 72.9, 69.7, 68.5, 60.8, 54.2, 26.3 ppm; MS (ESI) *m/z* 319.03 $[C_{11}H_{18}N_4O_7]H^+$; $[\alpha]_D^{20}$ = +5.5 (c = 4.2 in MeOH).

Azido-phospholipid intermediate. 5-Azido-pentanoicacid-NHS-ester[39] (48 mg, 0.2 mmol) was dissolved in DMF (1.0 mL) and a solution of 1,2-dipalmitoyl-R/S-glycero-3-phosphoethanolamine (124 mg, 0.18 mmol) and triethylamine (50 μL, 36 mg, 0.36 mmol) in $CHCl_3$/MeOH (2:1; 9.0 mL) was added. The resulting mixture was stirred at rt overnight. After evaporation under reduced pressure the residue was purified by flash chromatography on silica gel with mixtures of CH_2Cl_2/MeOH (10-20%) to afford the azidophospholipid intermediate as a white wax (125 mg, 85 %): mp 80-120 °C; IR

(neat) ν 3385, 2919, 2855, 2096 (N_3), 1735, 1642, 1459, 1237, 1108, 1066 cm^{-1}; ^{1}H-NMR ($CDCl_3$) δ 5.55-5.50 (bs, 2H), 4.25-3.30 (m, 7H), 3.27 (t, 2H, *J* = 6.5 Hz), 2.50-2.20 (m, 7H), 1.75-1.50 (m, 7H), 1.23 (s, 50H), 0.86 (t, 6H, *J* = 7.0 Hz) ppm; ^{31}P-NMR ($CDCl_3$) δ -2.47 ppm; MS (ESI) *m/z* 817.60 $[C_{42}H_{80}N_4O_9P]H^+$ (calc. 817.11).

Compound 12. Azido-phospholipid (100 mg, 0.12 mmol), propargyl glycine (14 mg, 0.12 mmol), copper (II) acetate (5 mg, 0.02 mmol) and sodium ascorbate (10 mg, 0.05 mmol) were mixed in *t*-butanol/water (1:1; 1.5 mL) and stirred at 50 °C for 8 hours. The resulting green solution was filtered and added to acetonitrile (100 mL). Filtration at 0 °C gave a green solid which was dissolved in hot THF (30 mL) and filtered through Celite. Treatment of the blue-green solution with QuadraPure-IDA® resin (0.5 g) at rt for 4 days resulted in a pale yellow solution. Filtration through Celite® and concentration under reduced pressure yielded compound 13 as a colourless oil (65 mg, 60 %): IR (neat) ν 3299, 2923, 2855, 1735, 1652, 1054 cm^{-1}; ^{31}P-NMR ($CDCl_3$): δ -2.29 ppm; MS (ESI) *m/z* 930.60 $[C_{42}H_{80}N_4O_9P]H^+$ (calc. 930.23).

Compound 13. SPPS was performed on a Rink amide polystyrene resin. Fluorenylmethyloxycarbonyl main-chain protected amino acids were used. The Fmoc deprotection was performed in a mixture of 20% piperidine in DMF (2 x 10 min). After filtration and washing of the resin, the couplings were performed by using 3 equivalents of protected amino acid and DIC (3 equiv.) in the presence of HOBt (3 equiv.). The completeness of the couplings was checked with the ninhydrin test. After coupling and deprotection of Fmoc-βAla-OH, azido-acetic acid was coupled using the same protocol. After filtration and washing of the resin (with DMF, iPrOH, DMF), 0.2 eq CuBr, 2 eq DIPEA and 2 eq Fmoc-L-Pra-OH in DMF were added to the resin.[31] The click reaction was left shaking overnight at room temperature, after which the Fmoc protecting groups were removed. The peptide was cleaved from the resin with 10% thioanisole/ethanedithiol (7:3) in TFA. After 3 h the resin was removed by filtration and the filtrate was added dropwise to dry, cold ether to precipitate the product. HPLC purification of the peptide gave an overall yield of 38%. TLC, R_f = 0.58. HPLC, t_R = 13.4 min. MS (ESI) *m/z* 1229.2 $[C_{57}H_{84}N_{18}O_{13}]H^+$.

2.5.3 $Re(CO)_3$ complex synthesis

[$Re(CO)_3$5]. Ligand **5** (9.5 mg, 0.04 mmol) and $[Re(CO)_3Br_3][NEt_4]_2$ (27 mg, 0.04 mmol) were added to a 1:1 mixture of methanol and water (4 mL) and stirred at 65 °C. The reaction was followed by HPLC. After 2 hours all of the starting material had been consumed. The solvent was removed under reduced pressure, and the residue redissolved in water. The crude product was purified using a Sep-Pak column with a water/methanol gradient. The fractions containing the product were combined and the solvent removed under reduced pressure to give [$Re(CO)_3$**5**] as a white powder (15 mg, 82%): IR (neat) ν 2923, 2022, 1902, 1867, 1633, 1074, 734 cm^{-1}; ^{1}H-NMR (CD_3OD) δ 7.97 (s, 1H), 7.49-7.33 (m, 5H), 5.88 (dd, 1H, *J* = 5.8 and 11.2), 5.64 (s, 2H), 5.20 (d, 1H, *J* = 11.2), 4.14-4.04 (m, 1H), 3.36-3.29 (m, 1H, obscured by solvent signal), 3.22 (dd, 1H, *J* = 4.0, 17.7) ppm; ^{13}C-NMR (CD_3OD) δ 198.3, 197.5, 196.7, 184.7, 144.1, 135.4, 130.2, 130.1, 129.6, 126.4, 56.0, 52.7, 27.5 ppm; High Res. MS *m/z* 515.0370 $[C_{15}H_{12}N_4O_5Re]^-$ (calc. 515.0371).

[$Re(CO)_3$6]. Ligand **6** (12 mg, 0.05 mmol) was dissolved in 5 mL ethanol. $[Re(CO)_3Br_3][NEt_4]_2$ (37 mg, 0.05 mmol) was added and the mixture was stirred at 50 °C. The reaction was followed by HPLC. After 2 hours all of the starting material had been consumed. The solvent was removed under reduced pressure, and the residue redissolved in water. The crude product was purified using a Sep-Pak column with a water/methanol gradient. The fractions containing the product were combined and the solvent removed under reduced pressure to give [$Re(CO)_3$**6**] as a white powder (19 mg, 77%): IR (neat) ν 2360, 2337, 2025, 1871, 1748, 1636, 1376, 1220, 656 cm^{-1}; ^{1}H-NMR (CD_3OD) δ 8.07 (s, 1H), 5.89 (dd, 1H, *J* = 5.8 and 11.2 Hz), 5.44 (d, 1H, *J* = 11.2 Hz), 5.38 (d, 1H, *J* = 17.5 Hz), 5.26 (d, 1H, *J* = 17.5 Hz), 4.27 (q, 2H, *J* = 7.1 Hz), 4.15-4.03 (m, 1H), 3.40 (dd, 1H, *J* = 2.6 and 17.6 Hz), 3.35-3.26 (m, 1H), 1.30 (t, 3H, *J* = 7.1 Hz) ppm; ^{13}C-NMR (CD_3OD) δ 198.1, 197.4, 196.7, 184.7, 167.5, 143.9, 128.2, 63.5, 52.8, 52.7, 27.4, 14.3 ppm; High Res. MS *m/z* 511.0272 $[C_{12}H_{12}N_4O_7Re]^-$ (calc. 511.0269); elemental analysis (calculated %-values in parenthesis) C 28.13 (28.18), H 2.77 (2.56), N 10.95 (10.95).

[$Re(CO)_3$7]. Ligand **7** (19.6 mg, 0.08 mmol) and $[Re(CO)_3Br_3][NEt_4]_2$ (59 mg, 0.08 mmol) were added to a 1:1 mixture of methanol and water (8 mL) and stirred at 65 °C.

The reaction was followed by HPLC. After 4 hours all of the strating material had been consumed. The solvent was removed under reduced pressure, and the residue redissolved in water. The crude product was purified using a Sep-Pak column with a water/methanol gradient. The fractions containing the product were combined and the solvent removed under reduced pressure to give [$Re(CO)_3$**7**] as a pale yellow powder (22 mg, 55%): IR (neat) ν 2025, 1876, 1643, 1370, 1147, 729 cm^{-1}; ^{1}H-NMR (CD_3OD) δ 7.92 (s, 1H), 7.34-7.19 (m, 5H), 6.13 (dd, 1H, *J* = 6.0 and 11.1 Hz), 5.50 (d, 1H, *J* = 11.1 Hz), 5.00-4.79 (m, 1H, obscured by H_2O signal), 4.65 (dd, 1H, *J* = 2.9 and 14.9 Hz), 4.41-4.32 (m, 1H, *J* = 2.9 and 6.0 Hz), 4.09 (s, 2H) ppm; ^{13}C-NMR (CD_3OD) δ 197.8, 197.1, 196.1, 181.7, 151.5, 139.3, 129.81, 129.77, 128.8, 127.9, 53.73, 53.68, 32.4 ppm; High Res. MS *m/z* 515.0376 $[C_{15}H_{12}N_4O_5Re]^-$ (calc. for: 515.0371).

[$Re(CO)_3$8]. Ligand **8** (15 mg, 0.06 mmol) was dissolved in 6 mL ethanol. $[Re(CO)_3Br_3][NEt_4]_2$ (45 mg, 0.06 mmol) was added and the mixture was stirred at 50 °C. The reaction was followed by HPLC. After 1 hour all of the starting material had been consumed. The solvent was removed under reduced pressure, and the residue redissolved in water. The crude product was purified using a Sep-Pak column with a water/methanol gradient. The fractions containing the product were combined and the solvent removed under reduced pressure to give [$Re(CO)_3$**8**] as a pale yellow powder (20 mg, 64%): mp >220 °C; IR (neat) ν 2024, 1881, 1716, 1643, 1445, 1375, 1348, 1158, 1034, 910, 836, 654 cm^{-1}; ^{1}H-NMR (CD_3OD) δ 8.04 (s, 1H), 6.13 (dd, 1H, *J* = 5.1 and 10.3 Hz), 5.51 (d, 1H, *J* = 10.3 Hz), 4.97 (d, 1H, *J* = 14.9 Hz), 4.69 (dd, 1H, J = 2.4 and 14.9 Hz), 4.41-4.35 (m, 1H), 4.13 (q, 2H, J =7.2 Hz), 3.04 (t, 2H, *J* = 7.1 Hz), 2.75 (t, 2H, *J* = 7.1 Hz), 1.24 (t, 3H, *J* = 7.2 Hz) ppm; ^{13}C-NMR (CD_3OD) δ 197.8, 197.1, 196.0, 181.6, 174.0, 150.3, 128.7, 61.8, 53.6, 53.6, 33.7, 21.5, 14.5 ppm; MS (ESI) *m/z* 527.04 $[C_{13}H_{15}N_4O_7Re]H^+$.

[$Re(CO)_3$9]. Compound **9** (5 mg, 0.01 mmol) and $[Re(Br)_3(CO)_3][NEt_4]_2$ (8 mg, 0.01 mmol) were dissolved in water (1 mL) and the pH was adjusted to pH 7-8 with an aqueous solution of NEt_4OH (0.2 M). The resulting solution was stirred at 55 °C for 10 h. Purification by semi-preparative HPLC gave the complex [$Re(CO)_3$**9**] as a white solid (3 mg, 80%): IR (neat) ν 3137, 2024, 1881, 1666, 1634, 1197, 1137 cm^{-1}; ^{1}H-NMR (CD_3OD) δ 7.96 (s, 1H), 5.63 (dd, 1H, *J* = 11.1 and 4.8 Hz; exchanges slowly

with deuterium), 5.01 (bd, 1H, *J* = 11.1 Hz; exchanges slowly with deuterium), 4.96 (dd, 1H, *J* = 15.2 and 4.0 Hz), 4.90 (dd, 1H, *J* = 15.2 and 6.6 Hz), 4.29 (dd, 1H, *J* = 6.6 and 4.0 Hz), 4.21-4.17 (m, 1H), 3.32 (dd, 1H, *J* = 18.0 and 2.0 Hz), 3.24 (dd, 1H, *J* = 18.0 and 4.8 Hz) ppm; ^{13}C-NMR (D_2O) δ 197.2, 196.0, 195.6, 184.8, 169.5, 142.8, 127.1, 53.7, 51.4, 50.5, 26.1 ppm; High Res. MS *m/z* 512.0224 $[C_{11}H_{11}N_5O_7Re]^-$ (calc. 512.0216).

[Re(CO)$_3$10]. Compound **10** (15.0 mg, 0.039 mmol) and $[Re(Br)_3(CO)_3][NEt_4]_2$ (30.0 mg, 0.039 mmol) were mixed in methanol/water (1:2; 1.5 mL) and stirred at 80 °C for 1.5 hours. The reaction mixture was concentrated under reduced pressure and the residue was purified by solid phase extraction using a Sep-Pak column and a water/MeCN gradient. The fractions containing the product were evaporated under reduced pressure to give [Re(CO)$_3$**10**] (20.4 mg, 81%) as a white solid: IR (neat) ν 3384, 2948, 2831, 2412, 2324, 2022, 1879, 1627, 1474, 1433, 1373, 1274, 1152, 1095, 1076, 1021, 970, 900, 819, 768, 654, 636 cm^{-1}; ^{1}H-NMR (CD_3OD) δ 8.16 (s, 1H), 7.83 (d, 1H, *J* = 1.0 Hz), 6.38 (t, 1H, *J* = 6.4 Hz), 5.87 (m, 1H, *J* = 5.4 Hz), 5.46 (dt, 1H, *J* = 8.5 and 5.6 Hz), 5.17 (d, 1H, *J* = 11.2 Hz), 4.34 (dt, 1H, *J* = 5.8 and 3.0 Hz), 4.05 (q, 1H, *J* = 4.0 Hz), 3.86 (dd, 1H, *J* = 12.2 and 3.0 Hz), 3.75 (dd, 1H, *J* = 12.2 and 3.2 Hz), 3.33 (dd, 1H, *J* = 17.3 and 2.4 Hz), 3.23 (dd, 1H, *J* = 17.3 and 4.1 Hz), 2.90 (ddd, 1H, *J* = 14.1, 6.7 and 6.2 Hz), 2.76 (ddd, 1H, *J* = 14.1, 8.6 and 6.0 Hz), 1.85 (d, 3H, J =1.0 Hz) ppm; ^{13}C-NMR (CD_3OD) δ 198.2, 197.4, 196.7, 184.6, 166.5, 156.7, 156.4, 152.3, 144.3, 138.4, 126.5, 111.7, 101.5, 86.9, 86.1, 62.3, 62.0, 52.9, 38.9, 27.6, 12.5 ppm; High Res. MS *m/z* 649.0688 $[C_{18}H_{18}N_6O_9Re]^-$ (calc. 649.0698).

[Re(CO)$_3$11]. Carbohydrate ligand **11** (22 mg, 0.05 mmol) and $[Re(Br)_3(CO)_3][NEt_4]_2$ (39 mg, 0.05 mmol) were dissolved in water (3 mL) and the pH was adjusted to pH 7-8 with an aqueous solution of NEt_4OH (10%, 3 drops). The resulting solution was stirred at 50 °C for 3 h. Concentration under reduced pressure followed by HPLC purification of the residue yielded [Re(CO)$_3$**11**] as a white solid (17 mg, 58%): mp >195 °C (decomp.); IR (neat) ν 3274, 3157, 2027, 1889, 1671, 1631, 1391, 1202, 1140, 1086, 1046 cm^{-1}; ^{1}H-NMR (D_2O) δ 8.31 (s, 1H), 5.82-5.70 (m, 1H), 5.76 (d, 1H, *J* = 9.1 Hz), 5.15 (d, 1H, *J* = 12.0 Hz), 4.35-4.28 (m, 1H), 4.16 (t, 1H, *J* = 9.7 Hz), 4.12 (d, 1H, *J* = 3.2 Hz), 4.05 (t, 1H, *J* = 6.0 Hz), 3.91 (dd, 1H, *J* = 9.7 and 3.3 Hz), 3.87-3.80 (m, 2H),

3.49 (dd, 1H, *J* = 18.2 and 2.4 Hz), 3.45 (dd, 1H, *J* = 28.2 and 4.4 Hz) ppm; ^{13}C-NMR (D_2O) δ 197.0, 195.8, 195.4, 184.9, 142.7, 124.9, 88.8, 78.7, 72.7, 69.6, 68.5, 60.8, 51.3, 26.2 ppm; High Res. MS *m/z* 611.0397 $[C_{14}H_{17}N_4O_{10}Re]Na^+$ (calc. 611.0400).

[Re(CO)$_3$13]. An aqueous solution of bombesin derivative **13** (10^{-3} M, 100 µL) was mixed with $[Re(Br)_3(CO)_3][NEt_4]_2$ (10^{-3} M in water, 200 µL). The solution was heated to 100 °C for 60 min. HPLC analysis of the reaction mixture revealed complete consumption of the starting material. Product formation was confirmed by MS. MS (ESI) *m/z* 1499.6 $[C_{60}H_{83}N_{18}O_{16}Re]H^+$, 750.1 $([C_{60}H_{83}N_{18}O_{16}Re]H^+)_2$.

2.5.4 Radiolabelling with $[^{99m}Tc(CO)_3(H_2O)_3]^+$

The precursor $[^{99m}Tc(H_2O)_3(CO)_3]^+$ was prepared according to the literature.[3] 1 mL $[^{99m}TcO_4]^-$ in 0.9% NaCl was added to the IsoLink™ kit (Mallinckrodt-Tyco, Petten, Holland) via the septum. The reaction was heated for 20 minutes at 100 °C. The solution was cooled to room temperature and neutralized (pH 7.2) with 150 µL 1 M HCl and 150 µL 1 M phosphate buffer (pH 7.4).

Stock solutions (10^{-2} to 10^{-7} M) of ligands **5-8** and **10-12** were prepared in PBS, pH 7.4. A solution of $[^{99m}Tc(CO)_3(H_2O)_3]^+$ (50 µL; ~500 MBq/mL) was added to 50 µL of the relevant ligand diluted with 400 µL PBS (pH 7.4) to give final concentrations between 10^{-3} and 10^{-8} M. The reaction mixtures were heated for 50 min at 100 °C. Radiolabelling yields were determined by HPLC. The identity of the products was confirmed by comparison of the γ-traces of the ^{99m}Tc complexes with the UV traces of the corresponding Re complexes. This is common practice with Tc-99m complexes on the n.c.a. level.

One-pot protocol A: Stock solutions (0.01 M) of propargyl glycine, benzyl azide, 3′-azido-3′-deoxythymidine and 1-azido-1-deoxy-β-D-galactopyranoside were prepared in water or methanol (benzyl azide), along with aqueous 0.01 M solutions of copper (II) acetate and sodium ascorbate. Click reactions were performed with 100 µL propargyl glycine, 150 µL benzyl azide, 3′-azido-3′-deoxythymidine or 1-azido-1-deoxy-β-D-

galactopyranoside, 30 µL sodium ascorbate and 15 µL copper (II) acetate. The reaction mixtures were heated at 100 °C for 30 minutes. 200 µL of the precursor $[^{99m}Tc(H_2O)_3(CO)_3]^+$ in PBS buffer (pH 7.4) was added to the crude click solutions. The reaction mixtures were heated again at 100 °C for 30 minutes before product formation was confirmed by γ-HPLC.

One-pot protocol B: 0.9 mL $[^{99m}TcO_4]^-$ in 0.9% NaCl was added to the IsoLink™ kit (Mallinckrodt-Tyco) via the septum. 0.1 mL of stock solution (10^{-4} M in PBS) of **10** or **11** was added. The reactions were heated for 60 min at 100 °C and then cooled to room temperature. The solution was neutralized (pH 7.2) with 150 µL 1 M HCl and 150 µL 1 M phosphate buffer (pH 7.4). The reaction mixtures were analyzed by HPLC.

2.5.5 *In vitro* characterization of $[^{99m}Tc(CO)_3$13]

The human prostate adenocarcinoma cell line PC-3 was purchased from the European Collection of Cell Culture (ECACC; Salisbury, England). Cells were maintained in DMEM GLUTAMAX-I supplemented with 10% FCS, 100 IU/mL penicillin G sodium, 100 µg/mL streptomycin sulphate, 0.25 µg/mL amphotericin B. The cell culture was incubated at 37 °C in an atmosphere containing 7.5% CO_2. The cells were subcultured weekly after detaching them with trypsin/EDTA (0.25%).

Inhibition studies (IC_{50}): PC-3 cells at confluence were placed in 48-well plates (1.5 x 10^5/well). Cells were incubated in triplicate for 1 h at 37 °C in a special binding buffer (0.2 ml final volume per well) including protease inhibitors (50 mM HEPES, 125 mM NaCl, 7.5 mM KCl, 5.5 mM $MgCl_2$, 1 mM EGTA, 5 g/L BSA, 2 mg/L chymostatin, 100 mg/L soybean trypsin inhibitor, 50 mg/L bacitracin) with 150000-250000 cpm of the corresponding $[^{99m}Tc(CO)_3(BBN)]$ complex per well and increasing concentrations of the different unlabelled BBN analogues (0-30000 nM). After incubation cells were washed twice with cold PBS and solubilized with 400 µl (twice) of 1 M NaOH at 37 °C. The radioactivity in the final suspension was measured in a γ-counter. IC_{50} values were

calculated by non-linear regression analysis using GraphPad Prism™. Experiments were performed twice in triplicate.

Saturation studies (K_D): C-3 cells were prepared as described above and were incubated in triplicate with increasing concentrations (0.001 to 1 nM) of the ^{99m}Tc-bombesin analogues for 1 h at 37 °C in the binding buffer already described. The total concentrations of technetium (^{99}Tc + ^{99m}Tc) were estimated according to the method of Bauer and Pabst.[40] After incubation, cells were washed twice with cold PBS and solubilized with 400 µl (twice) of 1 M NaOH at 37 °C. The bound radioactivity was measured in a γ-counter. Non-specific binding was determined under the same conditions by co-incubation of the ^{99m}Tc-bombesin analogues and 1 µM unlabelled BBN. Experiments were performed two to four times in triplicate.

2.5.6 *In vivo* characterization of [^{99m}Tc(CO)$_3$13]

All animal experiments were conducted in compliance with the Swiss animal protection laws and with the ethical principles and guidelines for scientific animal trials established by the Swiss Academy of Medical Sciences and the Swiss Academy of Natural Sciences. Studies were performed with 6 to 8 weeks old female CD-1 nu/nu mice (20-25 g), purchased from Charles River Laboratories (Sulzfeld, Germany). On the day of the assay, three groups of three mice each received the radiolabelled BBN analogue (3.7 MBq/mouse) via intravenous injection into the tail vein. To determine non-specific uptake *in vivo*, another group of three mice received 100 µg of unlabelled bombesin, co-injected with the radiolabelled BBN analogue.

The first three groups of mice were sacrificed 0.5, 1.5 or 5 h after injection by cervical dislocation and dissected. Samples of blood and tissues (heart, lung, spleen, kidneys, stomach, pancreas, ileum, colon, liver, muscle and bone) were removed, wet weighed and the amount of radioactivity was determined with a γ-counter. Results are expressed as a percentage of the injected dose per gram of tissue (%I.D./g).

2.5.7 Density functional theory calculations

All calculations were conducted using density functional theory (DFT) as implemented in the Gaussian 03, Revision C.02 suite of ab initio quantum chemistry programs.[27] Geometry optimizations and vibrational frequency calculations were performed using the restricted B3LYP exchange and correlation functionals and either the double-ζ 6-31G(d) or triple-ζ 6-311+G(d) basis sets for all atoms. Normal SCF and geometry convergence criteria were used and no symmetry constraints were imposed. Harmonic frequency analysis based on analytical second derivates was used to characterize the optimised geometries as local minima.

2.6 References

(1) Banerjee, S. R.; Maresca, K. P.; Francesconi, L.; Valliant, J.; Babich, J. W.; Zubieta, J. *Nucl. Med. Biol.* **2005**, *32*, 1-20.

(2) Alberto, R.; Schibli, R.; Egli, A.; Schubiger, A. P.; Abram, U.; Kaden, T. A. *J. Am. Chem. Soc.* **1998**, *120*, 7987-7988.

(3) Alberto, R.; Ortner, K.; Wheatley, N.; Schibli, R.; Schubiger, P. A. *J. Am. Chem. Soc.* **2001**, *123*, 3135-3136.

(4) Alberto, R. In *Contrast Agents III*, (Ed. Krause, W.), Springer, **2005**, Vol. 252, p 1-44.

(5) van Staveren, D. R.; Benny, P. D.; Waibel, R.; Kurz, P.; Pak, J. K.; Alberto, R. *Helv. Chim. Acta* **2005**, *88*, 447-460.

(6) Stephenson, K. A.; Zubieta, J.; Banerjee, S. R.; Levadala, M. K.; Taggart, L.; Ryan, L.; McFarlane, N.; Boreham, D. R.; Maresca, K. P.; Babich, J. W.; Valliant, J. F. *Bioconjugate Chem.* **2004**, *15*, 128-136.

(7) Levadala, M. K.; Banerjee, S. R.; Maresca, K. P.; Babich, J. W.; Zubieta, J. *Synthesis* **2004**, 1759-1766.

(8) Banerjee, S. R.; Levadala, M. K.; Lazarova, N.; Wei, L.; Valliant, J. F.; Stephenson, K. A.; Babich, J. W.; Maresca, K. P.; Zubieta, J. *Inorg. Chem.* **2002**, *41*, 6417-6425.

(9) Kolb, H. C.; Finn, M. G.; Sharpless, K. B. *Angew. Chem., Int. Ed.* **2001**, *40*, 2004-2021.

(10) Rostovtsev, V. V.; Green, L. G.; Fokin, V. V.; Sharpless, K. B. *Angew. Chem. Int. Ed.* **2002**, *41*, 2596-2599.

(11) Wang, Q.; Chan, T. R.; Hilgraf, R.; Fokin, V. V.; Sharpless, K. B.; Finn, M. G. *J. Am. Chem. Soc.* **2003**, *125*, 3192-3193.

(12) Kolb, H. C.; Sharpless, K. B. *Drug Discovery Today* **2003**, *8*, 1128-1137.

(13) Link, A. J.; Mock, M. L.; Tirrell, D. A. *Curr. Opin. Biotechnol.* **2003**, *14*, 603-609.

(14) Prescher, J. A.; Bertozzi, C. R. *Nat. Chem. Biol.* **2005**, *1*, 13-21.

(15) Wang, L.; Schultz, P. G. *Angew. Chem. Int. Ed.* **2005**, *44*, 34-66.

(16) Moore, D. S.; Robinson, S. D. *Adv. Inorg. Chem.* **1988**, *32*, 171-239.

(17) van Staveren, D. R.; Mundwiler, S.; Hoffmanns, U.; Pak, J. K.; Spingler, B.; Metzler-Nolte, N.; Alberto, R. *Org. Biomol. Chem.* **2004**, *2*, 2593-2603.

(18) Raper, E. S. *Coord. Chem. Rev.* **1996**, *153*, 199-255.

(19) Chan, T. R.; Hilgraf, R.; Sharpless, K. B.; Fokin, V. V. *J. Am. Chem. Soc.* **2004**, *6*, 2853-2855.

(20) Dai, Q.; Gao, W. Z.; Liu, D.; Kapes, L. M.; Zhang, X. M. *J. Org. Chem.* **2006**, *71*, 3928-3934.

(21) Detz, R. J.; Heras, S. A.; de Gelder, R.; van Leeuwen, P.; Hiemstra, H.; Reek, J. N. H.; van Maarseveen, J. H. *Org. Lett.* **2006**, *8*, 3227-3230.

(22) van Staveren, D. R.; Bill, E.; Bothe, E.; Buhl, M.; Weyhermuller, T.; Metzler-Nolte, N. *Chem.--Eur. J.* **2002**, *8*, 1649-1662.

(23) van Staveren, D. R.; Metzler-Nolte, N. *Chem. Commun.* **2002**, 1406-1407.

(24) Pak, J. K.; Benny, P.; Spingler, B.; Ortner, K.; Alberto, R. *Chem.--Eur. J.* **2003**, *9*, 2053-2061.

(25) Link, A. J.; Vink, M. K. S.; Tirrell, D. A. *J. Am. Chem. Soc.* **2004**, *126*, 10598-10602.

(26) Schibli, R.; La Bella, R.; Alberto, R.; Garcia-Garayoa, E.; Ortner, K.; Abram, U.; Schubiger, P. A. *Bioconjugate Chem.* **2000**, *11*, 345-351.

(27) Frisch, M. J.; Trucks, G. W.; Schlegel, H. B.; Scuseria, G. E.; Robb, M. A. *et al.* Gaussian Inc., Wallingford CT, 2004.

(28) Dumas, C.; Petrig, J.; Frei, L.; Spingler, B.; Schibli, R. *Bioconjugate Chem.* **2005**, *16*, 421-428.

(29) Storr, T.; Obata, M.; Fisher, C. L.; Bayly, S. R.; Green, D. E.; Brudzinska, I.; Mikata, Y.; Patrick, B. O.; Adam, M. J.; Yano, S.; Orvig, C. *Chem.--Eur. J.* **2004**, *11*, 195-203.

(30) Kuijpers, B. H. M.; Groothuys, S.; Keereweer, A. R.; Quaedflieg, P.; Blaauw, R. H.; van Delft, F. L.; Rutjes, F. *Org. Lett.* **2004**, *6*, 3123-3126.

(31) Tornoe, C. W.; Christensen, C.; Meldal, M. *J. Org. Chem.* **2002**, *67*, 3057-3064.

(32) Garayoa, E. G.; Schweinsberg, C.; Maes, V.; Ruegg, D.; Blanc, A.; Blauenstein, P.; Tourwe, D. A.; Beck-Sickinger, A. G.; Schubiger, P. A. *Q. J. Nucl. Med. Mol. Imaging* **2007**, *51*, 42-50.

(33) La Bella, R.; Garcia-Garayoa, E.; Langer, M.; Blauenstein, P.; Beck-Sickinger, A. G.; Schubiger, P. A. *Nucl. Med. Biol.* **2002**, *29*, 553-560.

(34) Schweinsberg, C. *PhD Thesis*, **2008**.

(35) Alberto, R.; Egli, A.; Abram, U.; Hegetschweiler, K.; Gramlich, V.; Schubiger, P. A. *Dalton Trans.* **1994**, 2815-2820.

(36) Rosenblum, S. B.; Huynh, T.; Afonso, A.; Davis, H. R. *Tetrahedron* **2000**, *56*, 5735-5742.

(37) Lundquist, J. T.; Pelletier, J. C. *Org. Lett.* **2001**, *3*, 781-783.

(38) Banaszynski, L. A.; Liu, C. W.; Wandless, T. J. *J. Am. Chem. Soc.* **2005**, *127*, 4715-4721.

(39) Seo, T. S.; Li, Z. M.; Ruparel, H.; Ju, J. Y. *J. Org. Chem.* **2003**, *68*, 609-612.

(40) Bauer, R.; Pabst, H. W. *Eur. J. Nucl. Med.* **1982**, *7*, 35-36.

“Click-to-Chelate”: Diverse triazole-containing chelating systems for the $M(CO)_3$ core (M = ^{99m}Tc, Re) and their incorporation into biomolecules of diagnostic and therapeutic interest

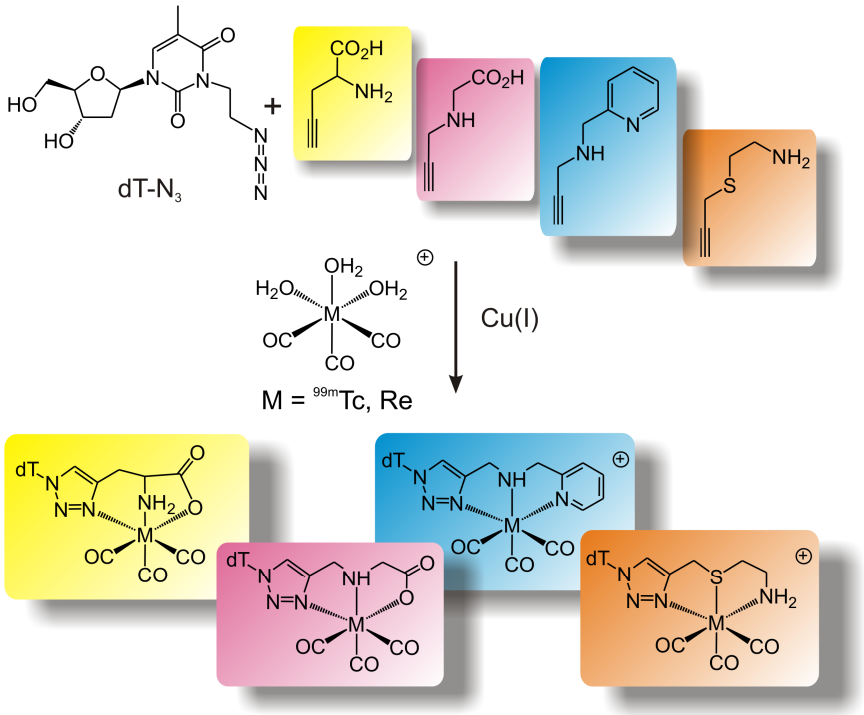

Chemistry - A European Journal, **2008**, 14(20), 6173

3.1 Abstract

The site-specific conjugation of metal chelating systems to biologically relevant molecules is an important contemporary topic in bioinorganic and bioorganometallic chemistry. In this work, we have used the Cu(I) catalyzed cycloaddition of azides and terminal alkynes to synthesize novel ligand systems, in which the 1,2,3-triazole is an integral part of the metal chelating system. A diverse set of bidentate alkyne building blocks with different aliphatic and aromatic backbones and various donor groups were prepared. The bidentate alkynes were reacted with benzyl azide in the presence of a catalytic amount of Cu(I) to form tridentate model ligands. The chelators were reacted with $[ReBr_3(CO)_3]^{2-}$ to form well-defined and stable complexes with different overall charges, structures and hydrophilicities. In all cases tridentate coordination of the ligands, including through N3 of the 1,2,3-triazole ring, was observed. The ligand systems could also be quantitatively radiolabelled with the precursor $[^{99m}Tc(H_2O)_3(CO)_3]^{+}$ at low ligand concentrations. Similarly, the alkynes were reacted with an azido-thymidine derivative to form a series of compounds which could be radiolabelled *in situ* to form single products. Subsequent incubation of the neutral and cationic organometallic ^{99m}Tc thymidine derivatives with human cytosolic thymidine kinase, a key enzyme in tumour proliferation, revealed that all of the compounds maintained substrate activity towards the enzyme. Bioconjugation, radiolabelling and enzymatic reactions were successfully performed in a matter of hours. Thus, click chemistry provides an elegant method for rapidly functionalizing a biologically relevant molecule with a variety of efficient metal chelators suitable for (radio)labelling with the $M(CO)_3$ core (M = ^{99m}Tc, Re), offering new potential for Tc-99m in clinical and preclinical tracer development.

3.2 Introduction

The radiolabelling of biologically active molecules has become an important tool for the non-invasive assessment of novel drug candidates as a result of the high sensitivity of nuclear imaging technologies, such as positron emission tomography (PET) and single photon emission computed tomography (SPECT). In recent years, the focus has mainly been on positron emitting isotopes such as fluorine-18 ($T_{1/2}$ = 109.8 min) and carbon-11 ($T_{1/2}$ = 20.5 min) suitable for PET. Radiolabelling methods for carbon-11 and fluorine-18 are established but still challenging, typically requiring multi-step syntheses, and are by no means quantitative, despite semi- or fully-automated synthesizers.[1] Furthermore, as a result of their short half-lives, such isotopes have to be produced on site by expensive cyclotrons and require extensive laboratory infrastructures, which together prohibit a more widespread application of PET. Radionuclides with suitable decay characteristics for *in vivo* SPECT are usually more readily available and often have longer half-lives (from several hours to several days) which facilitate their handling and processing. In addition, over the last few years, several preclinical small animal SPECT scanners have become available with sub-millimetre spatial resolution and excellent sensitivity, and which outperform comparable PET devices.[2] It is anticipated that this will drive an increased interest in novel SPECT tracers in preclinical research.

One of the most prominent single photon emitting radionuclides is technetium-99m ($T_{1/2}$ = 6 h, 140 keV γ-radiation), the mainstay of diagnostic nuclear medicine. Unlike most PET nuclides, Tc-99m is readily available at low cost from a ^{99}Mo/^{99m}Tc generator system. However, whereas non-metal radionuclides can be covalently attached to the target molecule, stable incorporation of a radiometal such as technetium into a biomolecule requires an appropriate bifunctional chelating agent and an efficient strategy to assemble the desired bioconjugate. Numerous functionalization strategies and bifunctional chelating systems have been reported.[3,4] However, syntheses are invariably multi-step, frequently inefficient, and often require protecting group chemistry to prevent unwanted side reactions during incorporation into the targeting molecule. These are all critical issues, which have to be properly addressed if novel, metal-based SPECT tracers are to become more widespread, particularly in preclinical research.

The use of the Cu(I) catalyzed cycloaddition of azides and terminal alkynes ("click chemistry")[5,6] has only very recently found applications in the design of ligands for transition metals.[7-13] This is surprising given the attractiveness of click chemistry: the Cu(I) catalyzed cycloaddition gives high chemical yields under mild reaction conditions even in aqueous media; the reactions are regiospecific (resulting exclusively in the formation of 1,4-bifunctionalized 1,2,3-triazole products); finally, an additional but often neglected feature of the clicked products is that the 1,2,3-triazole itself is an effective ligand for various transition metals. Our group has recently reported the synthesis of histidine-like chelating systems in which the imidazole ring has been replaced by a 1,4-bifunctionalized 1,2,3-triazole via reaction of an azide or an azide containing biomolecule with propargyl glycine.[13] Their organometallic $^{99m}Tc(CO)_3$ complexes proved to be stable *in vivo*. An appealing aspect of this approach, particularly for potential biomedical applications, is that the click reaction enables simultaneous formation of the chelating system and conjugation to a biomolecule in a single high-yielding step.

We have now extended the scope of the "click-to-chelate" approach. In this work we show that by combining both newly synthesized and commercial, clickable azide and alkyne building blocks with different substituents, various 1,2,3-triazole containing polydentate ligands can be efficiently synthesized. The novel chelating systems give rise to metal complexes of different size, overall charge and hydrophilicity when (radio)labelled with the $M(CO)_3$ core (M = ^{99m}Tc, Re). For proof of concept we applied the modular approach to the parallel synthesis and radiolabelling of a series of organometallic thymidine derivatives. Using this strategy we were able to identify novel organometallic substrates for hTK1 in a matter of hours starting from the organic azide/alkyne building blocks and commercial Na[$^{99m}TcO_4$].

3.3 Results and discussion

3.3.1 Ligand design and synthesis

The technetium/rhenium tricarbonyl core forms highly stable, low spin d^6 complexes with a wide range of ligand systems.[14-17] We have shown that coordination of tridentate chelating systems to the $M(CO)_3$ core efficiently protects the metal centre from ligand exchange reactions, for example, with functional groups of plasma proteins, an observation which in turn leads to better pharmacokinetic profiles for $^{99m}Tc(CO)_3$ complexes with tridentate ligands than for complexes with bidentate ligands.[18] The incorporation of different tridentate chelating systems into azido-functionalized biomolecules requires the synthesis of suitable alkyne building blocks. For our intended purpose and as proof of concept, five suitable alkynes were synthesized (**2**, **4**-**7**), and two commercially available compounds (**1**, **3**) were also investigated (Table 1). The primary considerations for the synthesis of suitable alkynes were structural variation of the ligand (and subsequent complexes), as well as the potential to form complexes with different overall charges and varied hydrophilicities.

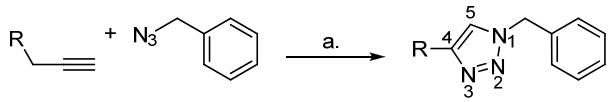

1-7 L1-L7

Scheme 1. General synthesis of ligands **L1**-**L7** using the Cu(I)-catalyzed [3+2] cycloaddition reaction: (a) 0.1 eq. $Cu(OAc)_2.H_2O$, 0.1 eq. sodium ascorbate, *t*BuOH/H_2O, 12 h, room temperature. For R see Table 1.

*N*α-propargyl glycine **2**, was prepared by alkylation of propargyl amine with methyl bromoacetate followed by ester hydrolysis with 1 M sodium hydroxide. 2-Propargyl malonate dimethyl ester is commercially available; the esters were hydrolysed with four equivalents of 1 M sodium hydroxide to give **3**. Alkynes **4** and **5** were prepared in a single step by reductive alkylation of propargyl amine with 2-pyridine carboxaldehyde or 2-thiophene carboxaldehyde, respectively. Selective *S*-alkylation of 2-(amino)ethanethiol and cysteine with propargyl bromide was achieved using Boc-protected precursors; the Boc protecting groups were removed using a 9:1 mixture of

dichloromethane and trifluoroacetic acid to give **6** and **7**, respectively. (See experimental section, 3.5.2 for further details.)

Table 1. EC_{50} values for ligands **L1**-**L7**.

	Alkyne	Ligand	EC50[a] (M)
1	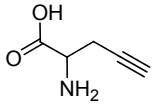	**L1** 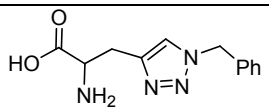	**2.3×10^{-7}**
2	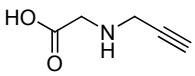	**L2** 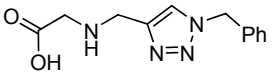	**2.1×10^{-7}**
3	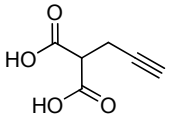	**L3** 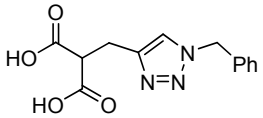	**$> 10^{-3}$**
4	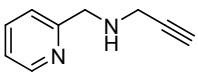	**L4** 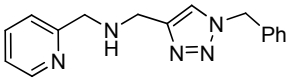	**5.8×10^{-8}**
5	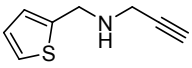	**L5** 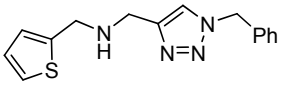	**n/a[b]**
6	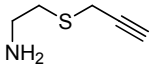	**L6** 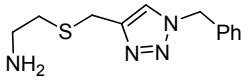	**3.5×10^{-7}**
7	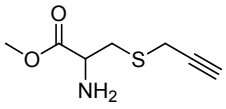	**L7** 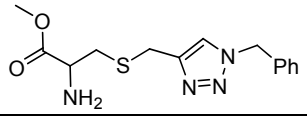	**n/a[c]**

[a] Ligand concentration necessary to achieve 50% radiolabelling yield when reacted with $[^{99m}Tc(CO)_3(H_2O)_3]^+$. [b] Difficult to assess due to lipophilicity of ligand and/or complex. [c] Two products are formed.

Compounds **1**-**6** provide structural variation and a range of donor atoms. Compound **7** is a bifunctional building block, which in addition to being coupled to an azide, can also be coupled to a second molecule of biological interest through either the amine or carboxylic acid group, while still providing a tridentate metal chelating system. Each of the alkyne building blocks was reacted with benzyl azide to form the model triazole-containing ligands **L1**-**L7** (Scheme 1). The [3+2] cycloaddition reactions were performed using similar conditions to those reported by the Sharpless group.[6] One equivalent of azide and one equivalent of alkyne were stirred at room temperature for 12

hours in a mixture of tertiary butanol and water with 0.1 equivalents of copper acetate and 0.2 equivalents of sodium ascorbate to generate Cu(I) *in situ*. For the synthesis of **L2** and **L3** carboxylic acid groups were protected as methyl esters and in the synthesis of **L1**, **L6** and **L7**, primary amines were Boc protected to simplify purification. The yields of the click reaction were typically 60-90% after purification. In all cases the syntheses could also be carried out without protecting the carboxylate and amine groups, but this prohibited efficient purification of the products.

3.3.2 $Re(CO)_3$ complex formation

Rhenium tricarbonyl complexes of all ligands were readily prepared as outlined in Scheme 2 by heating one equivalent of $[ReBr_3(CO)_3][NEt_4]_2$ with one equivalent of the ligand in a mixture of methanol and water (**L1**, **L2**, **L3**, **L6**) or methanol (**L4**, **L5**, **L7**). In all cases, HPLC analyses of the crude reaction mixtures revealed quantitative formation of a single product after 2 hours at 50 °C. Complexes $[Re(CO)_3$**L1**$]$, $[Re(CO)_3$**L3**$]NEt_4$, $[Re(CO)_3$**L4**$]$Br, $[Re(CO)_3$**L6**$]$Br and $[Re(CO)_3$**L7**$]$Br were purified using reverse phase Sep-Pak columns, whereas analytically pure samples of $[Re(CO)_3$**L2**$]$ and $[Re(CO)_3$**L5**$]$Br precipitated from their reaction mixtures directly. Although HPLC analysis confirmed quantitative formation of the products, the isolated yields varied between 40% and 80%, depending on the purification method. All of the complexes were characterized by mass spectrometry, IR spectroscopy, NMR and elemental analysis. Crystals suitable for x-ray structure determination could be obtained for complexes $[Re(CO)_3$**L2**$]$, $[Re(CO)_3$**L3**$]NEt_4$ and $[Re(CO)_3$**L6**$]$Br.

Comparison of the NMR spectra of the complexes with those of the free ligands revealed characteristic differences in chemical shifts and coupling patterns, which allowed assignment of the chemical composition and structure of the chelates. Signals in the proton NMR spectra of the complexes typically occur at higher frequencies than the corresponding signals in the uncomplexed ligand as a result of coordination to the electron deficient metal centre. In $[Re(CO)_3$**L1**$]$, the β-CH_2 protons are no longer magnetically equivalent, and independent resonances are observed for these protons as

well as a more complex coupling pattern for the α-CH proton, suggesting facial coordination of the tridentate ligand. Similarly, in $[Re(CO)_3$**L2**$]$ and $[Re(CO)_3$**L4**-**L7**$]$Br, four distinguishable resonances result from the two CH_2 groups of the chelate rings. In addition, the structures of $[Re(CO)_3$**L4**$]$Br and $[Re(CO)_3$**L7**$]$Br are sufficiently rigid in solution that two independent signals are observed for the benzylic CH_2 protons.

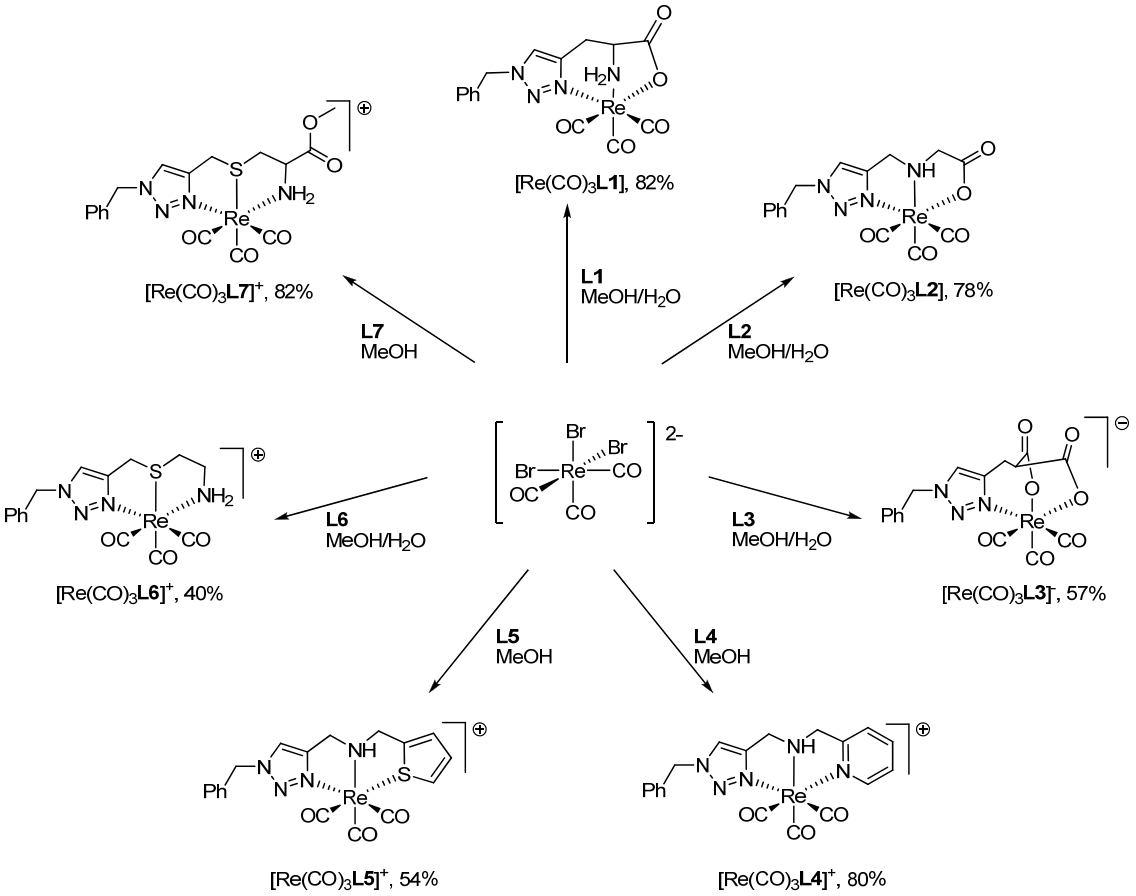

Scheme 2. Synthesis and structures of $Re(CO)_3$ complexes.

In the proton NMR spectra of $[Re(CO)_3$**L1**$]$ and $[Re(CO)_3$**L4**-**L7**$]$Br recorded in $[D_4]$MeOH, protons of the coordinated amine are also observed, since coordination of the amine to the metal results in much slower H/D exchange rates than in the uncomplexed ligand. Similar behaviour has been reported for $^{99}Tc/Re(CO)_3$ complexes containing other primary and secondary amines.[18,19] Differences between the proton NMR spectra of the ligand **L3** and $[Re(CO)_3$**L3**$]NEt_4$ are less pronounced than for all other complexes as a result of the higher symmetry of this complex (C_S compared to C_1 in all other complexes). The different possible diastereoisomers of the $Re(CO)_3$

complexes with the ligands **L2**, **L4**, **L5**-**L7** could not be distinguished in the proton NMR spectra. Representative NMR spectra can be found in Appendix B.

The reaction of the cysteine based ligand **L7** gave the complex, $[Re(CO)_3\mathbf{L7}]Br$, with κ*N3*,κ*S*,κ*N* coordination of the ligand and the methyl ester still intact, as evident from NMR analyses. This type of coordination models the situation in which **L7** is coupled via the cysteine carboxylic acid to another molecule of interest. The hydrolyzed ligand **L7b** (**L7** but without the ester group) can potentially form three, structurally different complexes with the $M(CO)_3$ core: two in which the ligand is coordinated through N3 of the triazole, sulfur and either the primary amine (κ*N3*,κ*S*,κ*N* coordination) or the carboxylate (κ*N3*,κ*S*,κ*O* coordination), and one in which the ligand is coordinated through the sulfur, primary amine and carboxylate (κ*S*,κ*N*,κ*O* coordination). However, the reaction of **L7b** with $[ReBr_3(CO)_3][NEt_4]_2$ led to the formation of only two products after heating in methanol for 2 hours, as shown by HPLC analysis (Scheme 3). Elemental analysis of the purified mixture of products revealed both complexes were neutral. The structures of the products were elucidated from the proton NMR spectrum. The compound with κ*N3*,κ*S*,κ*N* coordination (60%) was identified by signals for the amine protons as observed for $[Re(CO)_3\mathbf{L1}]$ and $[Re(CO)_3\mathbf{L4}$-$\mathbf{L7}]Br$ and two independent resonances for the benzylic CH_2 protons, attributed to coordination of the triazole, as observed for $[Re(CO)_3\mathbf{L4}]Br$ and $[Re(CO)_3\mathbf{L7}]Br$. The complex with κ*S*,κ*N*,κ*O* coordination (40%) was identified by coordination of the primary amine and the equivalence, in this case, of the benzyl CH_2 protons (see Appendix B). The formation of two products is interesting given that with a structurally similar ligand, 2(-2′-pyridyl)ethyl-cysteine, Karagiorgou *et al.* observed exclusive formation of a single complex with κ*S*,κ*N*,κ*O* coordination, without coordinative participation of the pyridyl nitrogen.[21]

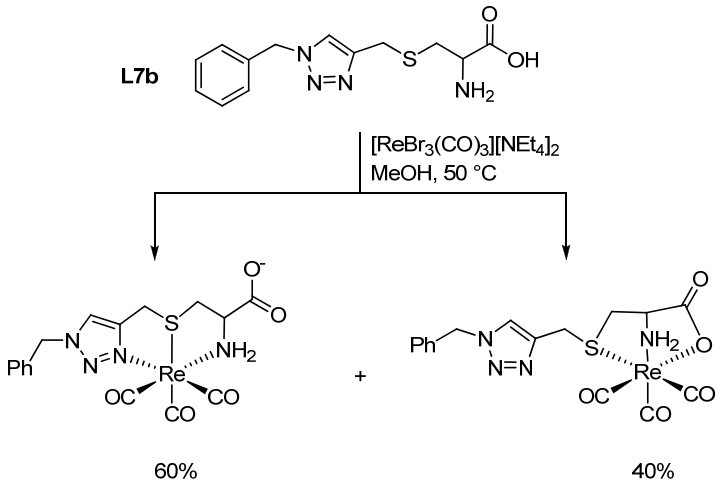

Scheme 3. Reaction of **L7b** with $[ReBr_3(CO)_3][NEt_4]_2$.

The x-ray structure analyses of $[Re(CO)_3\mathbf{L2}]$, $[Re(CO)_3\mathbf{L3}]NEt_4$ and $[Re(CO)_3\mathbf{L6}]Br$ (Figure 1) confirmed the tridentate, facial coordination of the ligands to the metal centre as expected from NMR analyses. All three structures show that the 1,2,3-triazole ligand is coordinated through N3 (see Scheme 1 for numbering scheme). This is consistent with DFT calculations we have reported previously, which predict that the highest electron density is at position N3, followed by N1, with the lowest at position N2 of the triazole ring, favouring N3-coordination.[13] The bond lengths between rhenium and N3 of the triazole are between 2.15 Å and 2.21 Å, which is in good agreement with the Re-N bond length in the bi-1,2,3-triazole-containing complex $[ReCl(Bn\text{-}bta)(CO)_3]$ (Bn-bta: 1,1-dibenzyl-4,4-bi-1*H*-1,2,3-triazole, Re-N = 2.176(6) Å).[12] The bond lengths are also comparable with the Re-N bond lengths in similar $Re(CO)_3$ complexes with imidazole or pyrazole based ligands, which are typically 2.19-2.21 Å.[16,22] Crystallographic data for all structures solved are given in Table 2 in the experimental section (3.5.3).

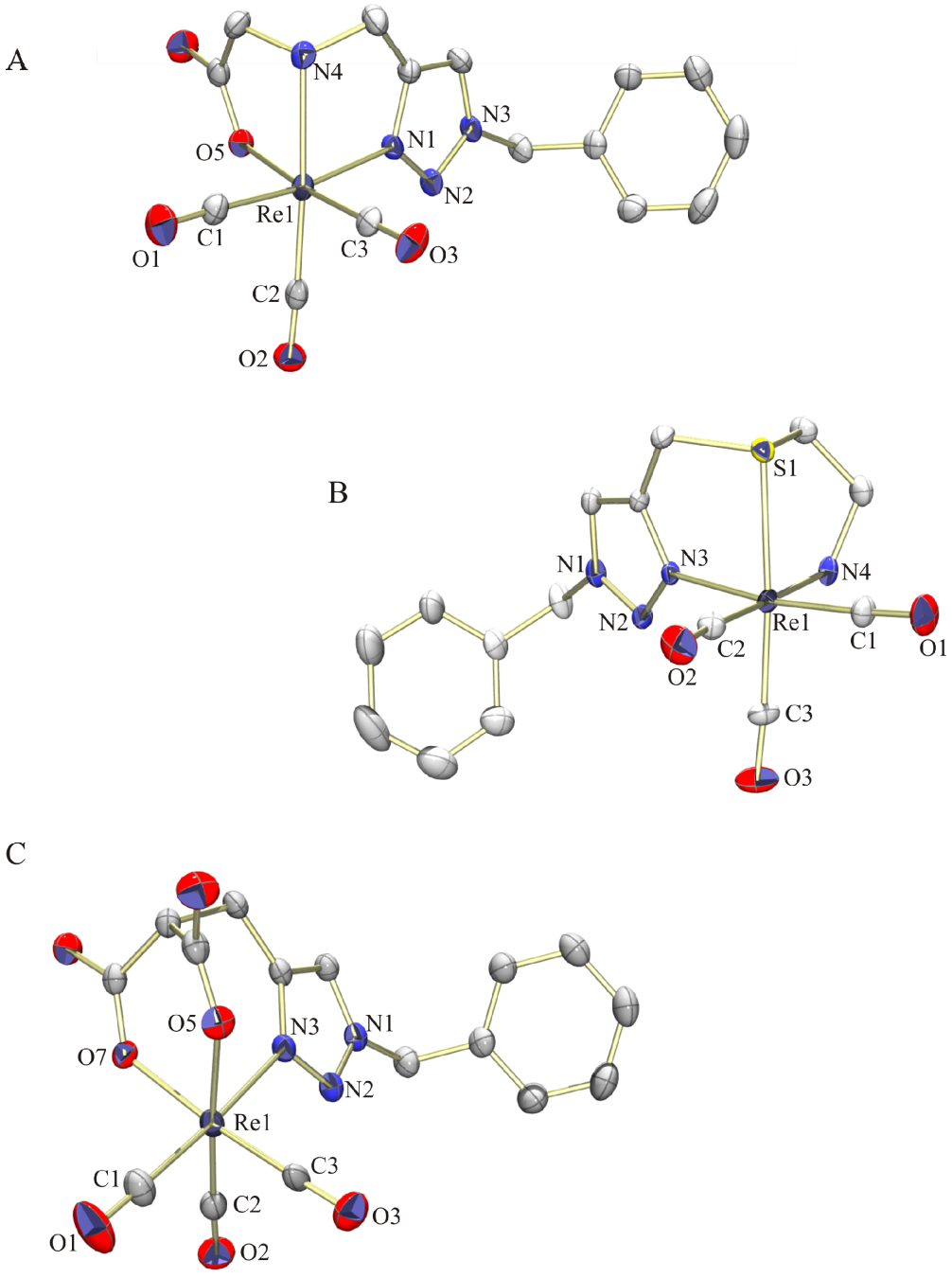

Figure 1. ORTEP-3[20] representations of the neutral complex [Re(CO)$_3$**L2**] (A), the complex anion [Re(CO)$_3$**L3**]$^-$ (B) and the complex cation [Re(CO)$_3$**L6**]$^+$ (C), with thermal ellipsoids shown at 50% probability. Hydrogen atoms are omitted for clarity. Selected bond lengths [Å] and angles [°]: [Re(CO)$_3$**L2**] Re(1)-C(1) 1.919(3), Re(1)-C(2) 1.912(2), Re(1)-C(3) 1.897(3), Re(1)-N(3) 2.15(2), Re(1)-N(4) 2.23(2), Re(1)-O(5) 2.14 (2), C(1)-Re(1)-N(3) 171.96(8), C(3)-Re(1)-N(3) 92.75(9), C(2)-Re(1)-N(4) 170.28(9), N(3)-Re(1)-N(4) 76.53(7), C(3)-Re(1)-O(5) 174.60(8), C(2)-Re(1)-O(5) 94.17(8), N(3)-Re(1)-O(5) 82.46(7); [Re(CO)$_3$**L3**]NEt$_4$ Re(1)-C(1)

1.905(3), Re(1)-C(2) 1.906(3), Re(1)-C(3) 1.898(3), Re(1)-O(5) 2.118(2), Re(1)-O(7) 2.14(2), Re(1)-N(3) 2.199(2), C(1)-Re(1)-N(3) 176.12(1), C(3)-Re(1)-N(3) 94.34(1), C(2)-Re(1)-O(5) 175.96(1), N(3)-Re(1)-O(5) 84.87(8), C(3)-Re(1)-O(7) 174.75(1), C(2)-Re(1)-O(7) 96.29(9), N(3)-Re(1)-O(7) 83.06(8); [$Re(CO)_3$**L6**]Br Re(1)-C(1) 1.909(2), Re(1)-C(2) 1.932(2), Re(1)-C(3) 1.936(2), Re(1)-N(3) 2.18(2), Re(1)-N(4) 2.21(2), Re(1)-S(1) 2.4753(5), C(1)-Re(1)-N(3) 172.28(8), C(3)-Re(1)-N(3) 93.59(8), C(2)-Re(1)-N(4) 177.83(7), N(3)-Re(1)-N(4) 84.16(6), C(3)-Re(1)-S(1) 170.94(6), C(2)-Re(1)-S(1) 97.17(6), N(3)-Re(1)-S(1) 78.23(4).

3.3.3 Radiolabelling with $[^{99m}Tc(CO)_3(H_2O)_3]^+$

It is important, particularly for receptor targeting radiopharmaceuticals, that high labelling yields can be achieved at low ligand concentration to avoid receptor saturation. Thus, potential ligand systems should form defined and stable technetium complexes at micromolar concentrations or lower. The technetium-99m complexes of ligands **L1**, **L2**, **L4** and **L6** were prepared by adding a solution of $[^{99m}Tc(H_2O)_3(CO)_3]^+$ to a solution of the ligand in physiological phosphate buffer (PBS) at pH 7.4, and characterized by comparison of their γ-HPLC traces with the UV-HPLC traces of the corresponding rhenium complexes. Labelling yields were assessed as the ligand concentration was varied between 10^{-3} M and 10^{-8} M, giving rise to step-sigmoid curves. This allowed the determination of EC_{50} values (ligand concentration necessary to achieve 50% labelling yield; Table 1 and Appendix B).

Ligands **L1**, **L2**, **L4** and **L6** proved very efficient, with EC_{50} values in the sub-micromolar range, which are comparable to values reported for *N*τ-functionalized histidine derivatives.[13,16] The radiolabelling of **L3** led to the formation of two products in a 1:1 ratio. Furthermore, a high concentration of the ligand (10^{-2} M) was required to yield detectable amounts of product. The nature of the reaction with $[^{99m}Tc(H_2O)_3(CO)_3]^+$ was surprising given that a well-defined and characterizable $Re(CO)_3$ complex could be synthesized. We do not currently have a plausible explanation for the unusual behaviour. The problems we encountered with **L3** unfortunately precluded the use of building block **3** in our further investigations. **L5** is noticeably more lipophilic than all of the other triazole containing ligands, which

complicated labelling with the $^{99m}Tc(CO)_3$ core in aqueous media and analysis of the Tc-99m complex formed by reverse phase HPLC. The radiolabelling of **L7** also led to the formation of two products, neither of which corresponded to the rhenium complex [$Re(CO)_3$**L7**]. The γ-HPLC trace in fact matched the UV-HPLC trace of the reaction between ligand **L7b** and the rhenium precursor (Scheme 3), which suggested that ligand **L7** was hydrolyzed under the conditions used for Tc-99m labelling. Radiolabelling of **L7b** confirmed this assumption.

3.3.4 Rapid identification of substrates for hTK1 using *in situ* clicked and radiolabelled thymidine derivatives

Click chemistry has already proved an effective tool for the parallel synthesis of large numbers of compounds for biological assays, and allows structure-activity information to be obtained without multi-step syntheses or large amounts of material.[23] These are features which are also attractive in radiopharmaceutical development. In the context of the following experiments, it is noteworthy that the reaction between $[^{99m}Tc(H_2O)_3(CO)_3]^+$ and the potentially bidentate alkyne building blocks **1**-**6** did not result in the formation of well-defined or stable complexes at a comparably low concentration to the tridentate, triazole ligands. The same holds true for the azide component of the click reaction. Thus, the presence of the triazole as a donor group appears to greatly increase the structural uniformity and stability of the resulting $^{99m}Tc(CO)_3$ complexes. As a consequence, there is a unique opportunity to expedite tracer development, since even in presence of excess alkyne or azide, the triazole product is preferentially labelled. We have previously reported a one-pot, two-step procedure in which the crude click reaction mixtures are labelled directly with the $[^{99m}Tc(H_2O)_3(CO)_3]^+$ precursor.[13] The resulting products and radiolabelling yields were found to be almost identical to those when the reactions were performed with the pre-purified, triazole containing ligands, but the one-pot procedure avoids unnecessary purification steps. Thus, with *in situ* radiolabelling, click chemistry can rapidly provide a set of radiolabelled compounds for preliminary *in vitro* screening and assessment.

As proof of the value of the one-pot procedure, we aimed to synthesise, radiolabel and assess *in vitro* a set of novel $^{99m}Tc(CO)_3$-thymidine complexes, in order to identify the structural and physicochemical parameters necessary to maintain activity towards human cytosolic thymidine kinase (hTK1). Technetium labelled thymidine analogues have the potential to act as substrates for hTK1 and therefore as markers for cancer cell proliferation, since hTK1 shows a higher than normal expression in a wide variety of cancer cells.[24] For unknown reasons no Tc/Re-labelled thymidine derivates tested to date have shown substrate activity.[25] It is known that modification of thymidine at position N3 of the pyrimidine base does not necessarily affect its ability to act as a substrate for hTK1.[26] Therefore we synthesized N3-functionalized azido thymidine (**dT-N3**). The synthesis is readily accomplished in four steps from commercially available thymidine. The 3′ and 5′ hydroxyl groups were protected with the *tertiary*-butyldimethylsilyl protecting group,[27] to allow selective alkylation at the N3 position with 1,2-dibromoethane, and to simplify purification. The azido compound is formed by nucleophilic substitution of the bromide with excess sodium azide, followed by removal of the silyl protecting groups with tetrabutylammonium fluoride.

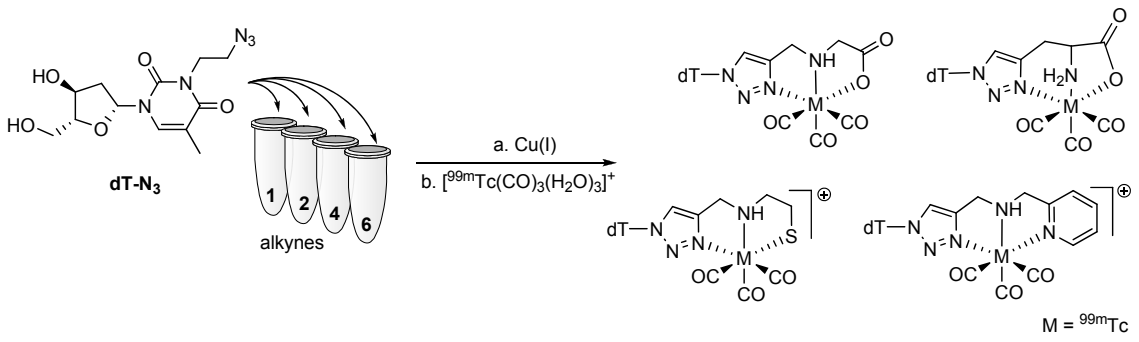

Figure 2. One-pot click reaction and *in situ* radiolabelling of thymidine analogues: (a) 0.1 equivalents $Cu(OAc)_2.H_2O$, 0.2 equiv. sodium ascorbate, 1h, 65 °C; (b) $[^{99m}Tc(CO)_3(H_2O)_3]$+, PBS, 1h, 100 °C.

Based on the labelling profiles of the model ligands with $[^{99m}Tc(H_2O)_3(CO)_3]^+$, four alkynes (**1**, **2**, **4**, **6**) were selected for reaction with the azido-thymidine derivative (Figure 2). Stock solutions of each of the four alkynes were prepared in water (**1**, **2**) or methanol (**4**, **6**), along with aqueous 0.01 M solutions of **dT-N3**, copper (II) acetate and sodium ascorbate. The click reaction was performed on a 100 µL scale with one equivalent of the relevant alkyne, 1.2 equivalents of **dT-N3** (0.2 mg), 0.2 equivalents of

sodium ascorbate and 0.1 equivalents of copper (II) acetate. The reaction mixtures were heated at 65 °C for 60 minutes, after which time product formation was confirmed by mass spectroscopy and HPLC. The precursor $[^{99m}Tc(H_2O)_3(CO)_3]^+$ in PBS buffer (pH 7.4) was added directly to the reaction mixture. The solutions were heated again at 95 °C for 60 minutes before product formation was confirmed by γ-HPLC. Labelling of **dT1**, **dT2**, **dT4** and **dT6** was extremely efficient, with yields greater than 90% in all cases (See Appendix B for more details). The identity of the products was inferred from the successful labelling of the ligands with $[ReBr_3(CO)_3]^{2-}$, which was carried out under the same conditions (analysis by MS).

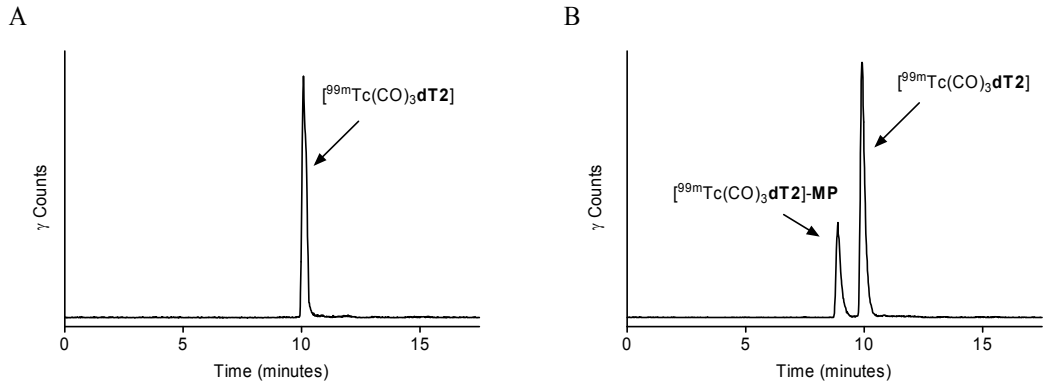

Figure 3. γ-HPLC analysis of the reaction of $[^{99m}Tc(CO)_3$**dT2**] with ATP in the presence of hTK1. (A) Before addition of hTK1; (B) reaction mixture after 3 hours at 37 °C.

The ability of the thymidine analogues to act as substrates for hTK1, and the influence of overall charge and/or structure of the complexes on phosphorylation were investigated with the technetium labelled compounds. The complexes were purified by HPLC and added to a stock solution of ATP, $MgCl_2$ and Tris buffer. Recombinant hTK1 was added, and the solutions were incubated at 37 °C for three hours before being analyzed by HPLC (Figure 3). In all cases, the γ-HPLC traces of the enzymatic reactions revealed two distinguishable ^{99m}Tc containing complexes after incubation with hTK1 (Figure 3B). The first complexes eluted were identified by coinjection of the starting material as the phosphorylated thymidine analogues $[^{99m}Tc(CO)_3$**dTXMP**] (**X** = **1**,**2**,**4**,**6**). These experiments qualitatively identified the first technetium labelled substrates for hTK1, but since all compounds revealed similar phosphorylation by HPLC, could not elucidate whether overall charge or exact structure is more important

in determining the ability of 99m-technetium labelled thymidine analogues to act as substrates for hTK1.

3.4 Conclusions

In this work we present an elegant strategy for the synthesis of 1,2,3-triazole-containing ligands where the 1,2,3-triazole is an integral part of the metal chelating system, while simultaneously coupling them site-specifically to azide-containing organic molecules. The "click-to-chelate" approach represents a significant improvement of classical methods for the incorporation of metal chelating systems into biomolecules, since the reactions are almost quantitative and do not require protecting group chemistry. The potential of this strategy was successfully demonstrated by the parallel synthesis of a set of thymidine analogues with different chelating systems, which could be radiolabelled *in situ* to form technetium complexes of different size and overall charge. Incubation of the radiolabelled thymidine derivatives with human cytosolic thymidine kinase enabled identification of the first metal-containing substrates ever reported for this enzyme. We have shown that the synthesis and incorporation of different metal chelating systems and subsequent radiolabelling do not have to be the rate-determining steps in the development of radiopharmaceuticals. By making functionalization of targeting molecules fast, efficient and predictable, click chemistry could play a crucial role in expediting the development of potential SPECT tracers.

3.5 Experimental details

3.5.1 General methods

All reagents and solvents were obtained from commercial sources (Sigma-Aldrich, Alfa Aesar, Bachem) and used as supplied unless stated otherwise. $[ReBr_3(CO)_3][NEt_4]_2$ was prepared according to the literature procedure.[28] $[Na][^{99m}TcO_4]$ was eluted from a $^{99}Mo/^{99m}Tc$-generator (Mallinckrodt-Tyco, Petten) with a 0.9% saline solution.

Reactions were monitored by HPLC or by thin layer chromatography (TLC) using precoated silica gel 60 F254 aluminium sheets, and visualized by UV absorption or stained with solutions of ninhydrin or $KMnO_4$. HPLC was performed on a Merck-Hitachi L-7000 system equipped with an L-7400 tuneable absorption detector and a Berthold LB 506 B radiometric detector. Analytical HPLC was performed with either an XTerra® column (MSC18, 5 µm, 4.6 x 150 mm, Waters) or a Nucleosil® 5 C18 column (5 µm, 4.6 x 250 mm, Macherey-Nagel). Two HPLC solvent systems were used. System I used aqueous 0.05 M triethylammonium phosphate buffer, pH 2.25 (solvent A), methanol (solvent B), and a gradient as follows: 0 to 15 min, 95% A to 20% A, 1 mL/min; 15 to 20 min 100% A, 1 mL/min. System II used water with 0.1% trifluoroacetic acid (solvent A), acetonitrile (solvent B) and a gradient as follows: 0 to 20 min, 97% A to 0% A, 1 mL/min; 20 to 22 min, 0% A to 97% A, 1 mL/min; 22 to 25 min, 97% A, 1 mL/min. Sep-Pak® columns (Waters) were washed with methanol and water prior to use.

Infrared spectra were recorded on a Perkin Elmer Spectrum BX II FT-IR, with a Pike MIRacle™ ATR accessory. Nuclear magnetic resonance spectra were recorded with a 300 MHz Varian Gemini 2000 spectrometer with solvent signals as an internal standard. Chemical shifts are reported in parts per million (ppm). Residual solvent peaks or water were used as a reference. Values of the coupling constant, *J*, are given in Hertz (Hz). The following abbreviations are used for the description of ^{1}H-NMR spectra: singlet (s), doublet (d), triplet (t), quartet (q), multiplet (m), doublet of doublets (dd), broad singlet (bs). The chemical shifts of complex multiplets are given as the range of their occurrence. Low resolution mass spectra (MS) were recorded with an LCT Premier ESI-TOF instrument from Waters, using either the negative or positive ionization mode. High resolution mass spectra (HR-MS) were recorded with a Bruker FTMS 4.7T BioAPEXII (ESI).

3.5.2 Synthesis and analytical data

***N*-Propargyl-glycine methyl ester (2a).** Propargyl amine (1.5 mL, 23 mmol), methyl bromoacetate (3.3 mL, 35 mmol) and triethylamine (4.9 mL, 35 mmol) were stirred in MeCN (75 mL) at 50 °C. After 12 hours the solvent was removed, and the residue redissolved in CH_2Cl_2. The crude product was purified by column chromatography with CH_2Cl_2 and MeOH (4%). The product was isolated as a yellow oil (2.80 g, 94%). IR ν 3286, 1737, 1437, 1374, 1201, 1139, 1000, 910, 769, 654 cm^{-1}. ^{1}H-NMR ($CDCl_3$) δ 3.74 (s, 3H); 3.52 (s, 2H); 3.48 (d, ^4J(H,H) = 2.4 Hz, 2H); 2.23 (t, ^4J(H,H) = 2.4 Hz, 1H); 1.75 (bs, 1H) ppm. ^{13}C-NMR ($CDCl_3$) δ 172.2, 81.1, 72.0, 51.8, 48.9, 37.5 ppm. MS (ES): *m/z* 128.06 $[C_6H_9NO_2]H^+$.

***N*-Propargyl-glycine (2). 2a** (105 mg, 0.83 mmol) was dissolved in MeOH (2 mL) and 2 equivalents of NaOH (1.65 mL, 1 M solution) were added. The mixture was stirred at room temperature for 1 hour and followed by TLC. When all of the starting material had been consumed, the pH was decreased to approximately 6 with 1 M HCl, and the solvent was removed under vacuum. The product was purified with a Sep-Pak column. The fractions containing the product were evaporated and the product isolated as a white powder (61 mg, 65%). IR ν 3239, 2992, 2780, 2631, 1633, 1614, 1582, 1408, 1308, 931, 904, 741, 705, 669 cm^{-1}. ^{1}H-NMR (D_2O) δ 3.99 (d, ^4J(H,H) = 2.6 Hz, 2H); 3.79 (s, 2H); 3.01 (t, ^4J(H,H) = 2.6 Hz, 1H) ppm. ^{13}C-NMR (D_2O) δ 172.3, 79.8, 57.3, 49.5 (MeOH reference), 46.2, 37.7 ppm. MS (ES): *m/z* 114.05 $[C_5H_7NO_2]H^+$.

2-Propargyl malonic acid (3). 2-Propargyl malonate dimethyl ester (200 mg, 1.18 mmol) was dissolved in MeOH (5 mL) and 4 equivalents of NaOH (4.71 mL, 1 M solution) were added. The yellow solution was stirred at room temperature for 1 hour and followed by TLC. When all of the starting material had been consumed, the pH was decreased to approximately 6 with 1 M HCl to give a colourless solution. The solvent was removed under vacuum and the product was purified with a Sep-Pak column. The fractions containing the product were evaporated under vacuum to give the product as a white powder (126 mg, 75%). IR ν 3274, 1608, 1583, 1439, 1323, 1281, 1175, 62, 851, 668, 628 cm^{-1}. ^{1}H-NMR (D_2O) δ 3.32 (t, ^3J(H,H) = 7.5 Hz, 1H); 2.60 (dd, ^3J(H,H) = 7.5 Hz, ^4J(H,H) = 2.1 Hz, 2H); 2.30 (t, ^4J(H,H) = 2.1 Hz, 1H).

^{13}C-NMR (D_2O) δ 177.6, 83.7, 70.62, 56.6, 49.5 (MeOH reference), 19.9 ppm. MS (ES): *m/z* 143.04 $[C_6H_6O_4]H^+$.

***N*-Propargyl-pyridine-2-methylamine (4).** Propargyl amine (1.29 g, 23.5 mmol) and pyridine-2-carboxaldehyde (0.84 g, 7.9 mmol) were added to MeOH (40 mL) and stirred at room temperature for 30 min. $NaCNBH_3$ (0.74 g, 11.8 mmol) was added and the mixture stirred at room temperature for a further 2 hours. The solvent was evaporated, and the reaction mixture purified by column chromatography with CH_2Cl_2 and MeOH (5%). The product was isolated as a dark orange liquid (0.66 g, 57%). IR ν 3291, 1661, 1594, 1571, 1476, 1435, 1361, 1246, 1151, 1121, 1098, 1050, 1001, 759, 632 cm^{-1}. ^{1}H-NMR ($CDCl_3$) δ 8.56 (m, 1H); 7.65 (m, 1H); 7.32 (m, 1H); 7.17 (m, 1H); 4.00 (s, 2H); 3.50 (d, ^4J(H,H) = 2.4 Hz, 2H); 2.24 (t, ^4J(H,H) = 2.4 Hz, 1H); 1.89 (bs, 1H) ppm. ^{13}C-NMR ($CDCl_3$) δ 159.3, 149.6, 136.6, 122.6, 122.2, 81.9, 71.8, 53.9, 38.0 ppm. MS (ES): *m/z* 147.08 $[C_9H_{10}N_2]H^+$.

***N*-Propargyl-thiophene-2-methylamine (5).** Propargyl amine (2.17 g, 39.5 mmol) and thiophene-2-carboxaldehyde (1.48 g, 13.2 mmol) were added to MeOH (65 mL) and stirred at room temperature for 30 min. $NaCNBH_3$ (1.24 g, 26.3 mmol) was added and the mixture stirred at room temperature for a further 2 hours. The solvent was evaporated, and the reaction mixture purified by column chromatography with CH_2Cl_2 and MeOH (2%). The product was isolated as a yellow liquid (0.87 g, 44%). IR ν 3289, 2843, 1607, 1436, 1368, 1331, 1213, 1166, 1097, 1019, 908, 852, 828, 697, 652, 636 cm^{-1}. ^{1}H-NMR ($CDCl_3$) δ 7.24-7.18 (m, 1H); 6.96-6.90 (m, 2H); 4.04 (s, 2H); 3.40 (d, ^4J(H,H) = 2.4 Hz, 2H); 1.95 (bs, 1H) ppm. ^{13}C-NMR ($CDCl_3$) δ 142.8, 126.8, 125.5, 124.9, 81.7, 72.0, 46.7, 37.0 ppm. MS (ES): *m/z* 152.05 $[C_8H_9NS]H^+$.

***S*-Propargyl-2-(Boc-amino)ethanethiol (6a).** 2-(Boc-amino)ethanethiol (1.00 mL, 5.92 mmol) and propargyl bromide (0.45 mL, 5.99 mmol) were added to a solution of triethylamine (1.25 mL, 8.99 mmol) in MeCN (50 mL). The reaction mixture was stirred at 50 °C and followed by TLC. After 2 hours the solvent was removed and the reaction mixture purified by column chromatography with a mixture of hexane and EtOAc (20%) to give the product as a pale yellow liquid (1.01g, 80%). IR ν 3298, 2977, 2930, 2359, 1694, 1508, 1456, 1392, 1366, 1339, 1251, 1163, 1047, 949, 863, 781, 734, 635 cm^{-1}. ^{1}H-NMR ($CDCl_3$) δ 4.90 (bs, 1H); 3.38 (m, 2H, ^3J(H,H) = 6.4 Hz);

3.26 (d, 2H, ^4J(H,H) = 2.6 Hz); 2.83 (t, 2H, ^3J(H,H) = 6.4 Hz); 2.26 (t, 1H, ^4J(H,H) = 2.6 Hz) ppm. ^{13}C-NMR ($CDCl_3$) δ 155.9, 99.3, 80.0, 71.6, 32.2, 28.6, 25.2, 19.2 ppm. MS (ES): *m/z* 238.07 $[C_{10}H_{17}NO_2S]Na^+$.

***S*-Propargyl-2-aminoethanethiol (6).** **6a** (1.12 g, 5.21 mmol) was dissolved in CH_2Cl_2/TFA (9:1; 50 mL) and stirred at room temperature overnight. The solvent was removed and the crude product purified by column chromatography with CH_2Cl_2 and MeOH (9%) to give the TFA salt of the product as orange oil. The free amine was obtained by dissolving the TFA salt in 1 M sodium hydroxide (10 mL) and extracting into CH_2Cl_2. The organic phase was washed twice with water. The aqueous phases were basified with aqueous NaOH and re-extracted into CH_2Cl_2. The organic phases were collected, dried over Na_2SO_4 and evaporated to give a pale yellow oil (395 mg, 98%). IR ν 3280, 2922, 1657, 1602, 1442, 1414, 1331, 1232, 1184, 1125, 1022, 988, 802, 713, 648 cm^{-1}. ^{1}H-NMR ($CDCl_3$) δ 3.26 (d, ^4J(H,H) = 2.6 Hz, 2H); 2.96 (t, ^3J(H,H) = 6.3 Hz, 2H); 2.81 (t, ^3J(H,H) = 6.3 Hz, 2H) 2.25 (t, ^4J(H,H) = 2.6 Hz, 1H); 1.87 (bs, 2H); 1.42 (s, 9H) ppm. ^{13}C-NMR ($CDCl_3$) δ 80.2, 71.3, 40.9, 36.0, 19.1 ppm. MS (ES): *m/z* 116.06 $[C_5H_9NS]H^+$.

***S*-Propargyl-*N*-Boc-cysteine methyl ester (7a).** *N*-Boc-cysteine methyl ester (1.5 mL, 7.29 mmol) was dissolved in DMF (15 mL). Cs_2CO_3 (2.38 g, 7.30 mmol) and propargyl bromide (0.5 mL, 6.66 mmol) were added and the mixture was stirred at room temperature and followed by TLC. After 3 hours the reaction mixture was diluted with water (30 mL) and the product extracted into EtOAc (50 mL). The organic phase was washed twice with a 1 M $NaHCO_3$ solution and dried over Na_2SO_4. The crude product was purified by column chromatography with CH_2Cl_2 and MeOH (2%) to give a pale yellow solid (1.11 g, 61%). IR ν 3373, 3258, 2986, 2955, 1743, 1681, 1518, 1436, 1422, 1395, 1370, 1320, 1296, 1250, 1238, 1206, 1165, 1079, 1042, 1020, 979, 876, 860, 829, 783, 745, 719, 690 cm^{-1}. ^{1}H-NMR ($CDCl_3$) δ 5.35 (d, 1H, ^3J(H,H) = 7.4 Hz); 4.60-4.54 (m, ^3J(H,H) = 4.8, 7.4 Hz, 1H); 3.77 (s, 3H); 3.31 (dd, ^2J(H,H) = 16.9, ^4J(H,H) = 2.6 Hz, 1H); 3.23 (dd, ^2J(H,H) = 16.9, ^4J(H,H) = 2.6 Hz, 1H); 3.21-3.04 (m, ^3J(H,H) = 4.8 Hz, ^2J(H,H) = 22.7 Hz, 1H); 2.91 (d, ^2J(H,H) = 22.7 Hz, 1H); 2.28 (t, ^4J(H,H) = 2.6 Hz, 1H); 1.44 (s, 9H) ppm. ^{13}C-NMR (CD_3OD) δ 171.6, 154.6, 80.3, 79.3, 53.2, 52.7, 33.7, 28.4, 19.9 ppm. MS (ES): *m/z* 296.07 $[C_{12}H_{19}NO_4S]Na^+$.

***S*-Propargyl-cysteine methyl ester (7).** **7a** (100 mg, 0.45 mmol) was dissolved in CH_2Cl_2/TFA (9:1; 5 mL) and stirred at room temperature overnight. The solvent was removed and the crude product purified by column chromatography with CH_2Cl_2 and MeOH (5%) to give a yellow solid (50 mg, 92%). IR ν 2961, 1748, 1668, 1524, 1441, 1330, 1245, 1184, 1133, 839, 799, 722, 648 cm^{-1}. ^{1}H-NMR (CD_3OD) δ 4.35 (dd, ^3J(H,H) = 4.6, 8.0 Hz, 1H); 3.87 (s, 3H); 3.41 (d, ^4J(H,H) = 2.6 Hz, 2H); 3.36 (dd, ^2J(H,H) = 14.9 Hz, ^3J(H,H) = 4.6, 1H); 3.15 (dd, ^2J(H,H) = 14.9 Hz, ^3J(H,H) = 8.0 Hz, 1H); 2.74 (t, ^4J(H,H) = 2.6 Hz, 1H) ppm. ^{13}C-NMR (CD_3OD) δ 169.6, 79.6, 73.7, 53.9, 53.1, 32.2, 19.9 ppm. MS (ES): *m/z* 174.03 $[C_7H_{11}NO_2S]H^+$.

General procedure A: Cycloaddition reaction between alkynes and benzyl azide. The alkyne (1 equivalent) and benzyl azide (1 equivalent) were added to a 1:1 mixture of tBuOH and water to form a 0.1 mM solution. 0.1 equivalents of $Cu(OAc)_2.H_2O$ and 0.2 equivalents of sodium ascorbate were added and the mixture stirred at room temperature for 12 hours. The product was extracted into EtOAc and washed twice with aqueous NaCl. The aqueous phases were re-extracted with EtOAc. The organic phases were combined, dried over Na_2SO_4 and evaporated. The product was purified by column chromatography with a mixture of CH_2Cl_2 and MeOH.

***N*-Boc-2-(1-benzyl-1H-[1,2,3]triazol-4-ylmethyl)-glycine (L1a).** As per general procedure A, with benzyl azide (375 mg, 2.82 mmol) and N(α)-Boc-L-propargylglycine (600 mg, 2.82 mmol). The crude product was purified by column chromatography with CH_2Cl_2 and MeOH (20%) to give the Boc-protected intermediate as a pale yellow solid (577 mg, 59%). IR ν 3359, 2977, 2927, 1691, 1562, 1402, 1051 cm^{-1}. ^{1}H-NMR (CD_3OD) δ 7.74 (s, 1H), 7.36-7.28 (m, 5H), 5.55 (s, 2H), 4.30 (bs, 1H), 3.27-3.01 (m, 2H), 1.36 (s, 9H) ppm. ^{13}C-NMR (CD_3OD) δ 157.6, 136.8, 130.0, 129.5, 129.0, 124.8, 80.4, 62.7, 54.9, 30.2, 28.7 ppm. MS (ES): *m/z* 347.05 $[C_{17}H_{22}N_4O_4]H^+$.

2-(1-Benzyl-1H-[1,2,3]triazol-4-ylmethyl)-glycine (L1). **L1a** (577 mg, 1.67 mmol) was dissolved in CH_2Cl_2/TFA (9:1; 100 mL) and stirred at room temperature overnight. The solvent was removed under reduced pressure and the residue redissolved in MeOH. After several dissolutions, followed by removal of the solvent, the product precipitated from MeOH as a grey powder. The precipitate was collected and dried under vacuum (258 mg, 63%). IR ν 3130, 2930, 2859, 1674, 1592, 1198, 1137, 718 cm^{-1}. ^{1}H-NMR

(D_2O/DCl) δ 7.96 (s, 1H), 7.40-7.25 (m, 5H), 5.56 (s, 2H), 4.36 (t, 1H, ^3J(H,H) = 6.2 Hz), 3.37 (d, 2H, ^3J(H,H) = 6.2 Hz) ppm. ^{13}C-NMR (D_2O/DCl) δ 170.4, 140.6, 134.4, 129.1, 128.8, 128.1, 125.4, 116.1, 54.2, 52.2, 25.3 ppm. HR-MS (ES): *m/z* 247.1185 $[C_{12}H_{14}N_4O_2]H^+$ (calc. 247.1195).

***N*-(1-Benzyl-1H-[1,2,3]triazol-4-ylmethyl)-glycine methyl ester L2a.** As per general procedure A, with benzyl azide (108 mg, 0.87 mmol) and **2a** (110 mg, 0.81 mmol). The crude product was purified by column chromatography with CH_2Cl_2 and MeOH (5%). The product was isolated as a yellow oil (120 mg, 57%). IR ν 2952, 1737, 1497, 1456, 1436, 1354, 1331, 1214, 1138, 1078, 1049, 1028, 1002, 801, 720, 197, 670 cm^{-1}. ^{1}H-NMR (CD_3OD) δ 7.87 (s, 1H); 7.36-7.34 (m, 4H); 5.58 (s, 2H); 3.87 (s, 2H); 3.68 (s, 3H); 3.41 (s, 2H) ppm. ^{13}C-NMR ($CDCl_3$) δ 172.4, 146.6, 134.7, 129.1, 128.7, 128.1, 121.8, 54.1, 51.9, 49.9, 44.2 ppm. MS (ES): *m/z* 261.40 $[C_{13}H_{16}N_4O_2]H^+$.

***N*-(1-Benzyl-1H-[1,2,3]triazol-4-ylmethyl)-glycine (L2). L2a** (110 mg, 0.42 mmol) was dissolved in a 1:1 mixture of MeOH and water (4 mL) and 2 equivalents of NaOH (34 mg, 0.85 mmol) were added. The mixture was stirred at room temperature for 2 hours and followed by TLC. When all of the starting material had been consumed, the pH was decreased to approximately 6 with 1 M HCl. The white solid which precipitated was collected by filtration and dried under vacuum (61 mg, 60%). IR ν 2853, 2780, 1586, 1557, 1495, 1440, 1397, 1320, 1206, 1122, 1078, 1057, 1018, 906, 862, 842, 718, 692, 669 cm^{-1}. ^{1}H-NMR (CD_3OD) δ 7.89 (s, 1H); 7.39-7.31 (m, 4H); 5.59 (s, 2H); 3.84 (s, 2H); 3.16 (s, 2H) ppm. ^{13}C-NMR (D_2O/DCl) δ 168.3, 137.3, 134.3, 129.0, 128.7, 128.0, 126.6, 54.2, 46.4, 41.2 ppm. MS (ES): *m/z* 247.11 $[C_{12}H_{14}N_4O_2]H^+$.

(1-Benzyl-1H-[1,2,3]triazol-4-ylmethyl)-malonate dimethyl ester (L3a). As per general procedure A, with benzyl azide (299 mg, 2.25 mmol) and 2-propargyl malonate dimethyl ester (382 mg, 2.25 mmol). The crude product was purified by column chromatography with CH_2Cl_2 and MeOH (5%). The methyl ester protected product was isolated as a yellow oil (608 mg, 89%). IR ν 1743, 1728, 1457, 1436, 1325, 1271, 1238, 1219, 1193, 1175, 1148, 1094, 964, 858, 717, 698, 660 cm^{-1}. ^{1}H-NMR (CD_3OD) δ 7.75 (s, 1H); 7.42-7.22 (m, 5H); 5.57 (s, 2H); 3.67 (t, ^3J(H,H) = 6.8 Hz, 1H); 3.26 (d, ^3J(H,H)

= 6.8 Hz, 2H) ppm. ^{13}C-NMR (CD_3OD) δ 170.4, 145.5, 136.9, 129.9, 129.5, 128.9, 124.2, 54.8, 53.0, 52.6, 30.7 ppm. MS (ES): *m/z* 304.10 $[C_{15}H_{17}N_3O_4]H^+$.

(1-Benzyl-1H-[1,2,3]triazol-4-ylmethyl)-malonic acid (L3). **L3a** (500 mg, 1.65 mmol) was dissolved in a 1:1 mixture of MeOH and water and 4 equivalents of NaOH (264 mg, 6.60 mmol) were added. The mixture was stirred at room temperature and followed by TLC. After 2 hours, the pH was decreased to approximately 6 with 1 M HCl and the solvent removed under vacuum. The product was purified with a Sep-Pak column. The fractions containing the product were evaporated and dried under vacuum to give a white crystalline solid (286 mg, 63%). IR ν 2981, 1976, 1731, 1720, 1558, 1431, 1272, 1231, 1174, 1074, 952, 854, 716, 698, 667, 646 cm^{-1}. ^{1}H-NMR (CD_3OD) δ 7.74 (s, 1H); 7.39-7.25 (m, 4H); 5.55 (s, 1H), 3.73 (t, 1H, ^3J(H,H) = 7.7 Hz); 3.22 (d, 2H, ^3J(H,H) = 7.7 Hz) ppm. ^{13}C-NMR (CD_3OD) δ 172.0, 136.8, 130.0, 129.5, 128.9, 124.3, 54.8, 53.0, 26.0 ppm. MS (ES): *m/z* 276.06 $[C_{13}H_{13}N_3O_4]H^+$.

***N*-(1-Benzyl-1H-[1,2,3]triazol-4-ylmethyl)-pyridine-2-methylamine (L4).** As per general procedure A, with benzyl azide (182 mg, 1.4 mmol) and **4** (200 mg, 1.4 mmol). The crude product was purified by column chromatography with CH_2Cl_2 and MeOH (10%) to give a brown oil (253 mg, 66%). IR ν 2926, 1591, 1570, 1456, 1434, 1329, 1219, 1127, 1049, 1029, 994, 759, 720 cm^{-1}. ^{1}H-NMR ($CDCl_3$) δ 8.49 (m, 1H); 7.58 (m, 1H); 7.37 (s, 1H); 7.34-7.29 (m, 3H); 7.20-7.23 (m, 3H); 7.10 (m, 1H); 5.45 (s, 2H); 3.89 (s, 4H); 1.79 (bs, 1H) ppm. ^{13}C-NMR ($CDCl_3$) δ 149.3, 136.6, 129.1, 128.7, 128.2, 122.5, 122.1, 121.8, 54.4, 54.1, 44.3 ppm. HR-MS (ES): *m/z* 280.1562 $[C_{16}H_{17}N_5]H^+$ (calc. 280.1557).

***N*-(1-Benzyl-1H-[1,2,3]triazol-4-ylmethyl)-thiophene-2-methylamine (L5).** As per general procedure A, with benzyl azide (138 mg, 1.0 mmol) and **5** (157mg, 1.0 mmol). The crude product was purified by column chromatography with CH_2Cl_2 and MeOH (3%) to give a yellow oil (131 mg, 46%). IR ν 2963, 1670, 1497, 1455, 1330, 1260, 1218, 1096, 1047, 798, 695 cm^{-1}. ^{1}H-NMR ($CDCl_3$) δ 7.38-7.36 (m, 4H); 7.29-7.25 (m, 2H); 7.21-7.19 (m, 1H); 6.95-6.91 (m, 2H); 5.51 (s, 2H); 4.01 (s, 2H); 3.92 (s, 2H); 1.57 (bs, 1H) ppm. ^{13}C-NMR ($CDCl_3$) δ ppm. HR-MS (ES): *m/z* 285.1171 $[C_{15}H_{16}N_4S]H^+$ (calc. 285.1168).

***S*-(1-benzyl-1H-[1,2,3]triazol-4-ylmethyl)-2-(Boc-amino)ethanethiol (L6a).** As per general procedure A, with benzyl azide (346 mg, 2.60 mmol) and **6a** (560 mg, 2.60 mmol). The crude product was purified by column chromatography with CH_2Cl_2 and MeOH (5%) to give a yellow oil (560 mg, 62%). IR ν 2976, 1698, 1508, 1456, 1391, 1365, 1341, 1270, 1250, 1165, 1048, 1029, 951, 743, 709 cm^{-1}. ^{1}H-NMR ($CDCl_3$) δ 7.44 (s, 1H); 7.40-7.25 (m, 5H); 5.50 (s, 2H); 4.95 (bs, 1H); 3.79 (s, 2H); 3.30 (m, ^3J(H,H) = 6.6, 6.1 Hz, 2H); 2.63 (t, ^3J(H,H) = 6.6 Hz, 2H); 1.43 (s, 9H) ppm. ^{13}C-NMR ($CDCl_3$) δ 129.3, 128.9, 128.2, 121.9, 54.4, 39.6, 31.9, 28.5, 25.8 ppm. MS (ES): *m/z* 349.50 $[C_{17}H_{24}N_4O_2S]H^+$.

***S*-(1-Benzyl-1H-[1,2,3]triazol-4-ylmethyl)-2-(amino)ethanethiol (L6). L6a** (460 mg, 1.32 mmol) was dissolved in CH_2Cl_2/TFA (9:1; 13 mL) and stirred at room temperature overnight. The solvent was removed and the crude product purified by column chromatography with CH_2Cl_2 and MeOH (10%) to give a yellow oil (248 mg, 85%). IR ν 3036, 1673, 1457, 1434, 1200, 1179, 1129, 1057, 837.8, 799, 722 cm^{-1}. ^{1}H-NMR ($CDCl_3$) δ 7.40 (s, 1H); 7.35-7.22 (m, 5H); 5.45 (s, 2H); 3.75 (s, 2H); 3.20 (t, ^3J(H,H) = 6.5 Hz, 2H); 2.86 (t, ^3J(H,H) = 6.5 Hz, 2H); 2.27 (bs, 2H) ppm. ^{13}C-NMR ($CDCl_3$) δ 162.8, 145.2, 134.4, 129.2, 128.9, 128.2, 122.5, 54.3, 38.8, 28.8, 25.4 ppm. HR-MS (ES): *m/z* 271.0983 $[C_{12}H_{16}N_4S]Na^+$ (calc. 271.0988).

***N*-Boc-*S*-(1-benzyl-1H-[1,2,3]triazol-4-ylmethyl)-cysteine methyl ester (L7a).** As per general procedure A, with benzyl azide (202 mg, 1.52 mmol) and **7a** (419 mg, 1.52 mmol). The crude product was purified by column chromatography with CH_2Cl_2 and MeOH (5%) to give a pale yellow solid (544 mg, 88%). IR ν 3388, 3130, 2980, 2932, 2097, 1764, 1685, 1513, 1462, 1436, 1413, 1394, 1370, 1347, 1318, 1285, 1257, 1216, 1169, 1150, 1062, 1052, 1025, 989, 889, 862, 817, 783, 755, 732, 716, 695 cm^{-1}. ^{1}H-NMR ($CDCl_3$) δ 7.41 (s, 1H); 7.40-7.26 (m, 5H); 5.51 (s, 2H); 5.41-5.36 (s, 1H); 4.55-4.51 (s, 1H); 3.80 (s, 2H); 3.73 (s, 3H); 2.98 (dd, ^2J(H,H) = 13.9 Hz, ^3J(H,H) = 5.1 Hz, 1H); 2.90 (dd, ^2J(H,H) = 13.9 Hz, ^3J(H,H) = 5.8 Hz, 1H);1.43 (s, 9H) ppm. ^{13}C-NMR ($CDCl_3$) δ 171.4, 145.3, 134.5, 129.2, 129.0, 128.2, 122.0, 54.4, 53.5, 52.7, 34.2, 28.5, 26.9 ppm. MS (ES): *m/z* 408.12 $[C_{19}H_{26}N_4O_4S]H^+$.

***S*-(1-Benzyl-1H-[1,2,3]triazol-4-ylmethyl)-cysteine methyl ester (L7). L7a** (400 mg, 0.98 mmol) was dissolved in CH_2Cl_2/TFA (9:1; 10 mL) and stirred at room temperature

overnight. The solvent was removed and the crude product redissolved in CH_2Cl_2. The product precipitated as a white solid, which was washed well with CH_2Cl_2 and dried under vacuum (240 mg, 79%). IR ν 3081, 2954, 2029, 1743, 1660, 1525, 1455, 1436, 1330, 1268, 1248, 1179, 1135, 1086, 1052, 986, 900, 869, 833, 802, 748, 721, 712, 700, 641 cm^{-1}. ^{1}H-NMR (CD_3OD) δ 7.91 (s, 1H); 7.47-7.29 (m, 5H); 5.59 (s, 2H); 4.32 (dd, *3J(H,H)* = 8.1, 4.5 Hz); 3.92 (d, ^2J(H,H) = 14.8 Hz, 1H); 3.86 (d, ^2J(H,H) = 14.8 Hz, 1H); 3.81 (s, 3H); 3.17 (dd, ^2J(H,H) = 14.9 Hz, ^3J(H,H) = 4.5 Hz, 1H); 3.00 (dd, ^2J(H,H) = 14.9 Hz, ^3J(H,H) = 8.1 Hz, 1H) ppm. ^{13}C-NMR (CD_3OD) δ 169.7, 146.0, 136.7, 130.1, 129.7, 129.2, 124.3, 55.1, 53.9, 53.3, 32.8, 26.7 ppm. HR-MS (ES): *m/z* 307.1219 $[C_{14}H_{18}N_4O_2S]H^+$ (calc. 307.1223).

***S*-(1-Benzyl-1H-[1,2,3]triazol-4-ylmethyl)-cysteine (L7b).** **L7** (209 mg, 0.68 mmol) was dissolved in a 1:1 mixture of MeOH and water (5 mL) and 2 equivalents of NaOH (54 mg, 1.36 mmol) were added. The mixture was stirred at room temperature for 2 hours and followed by TLC. When all of the starting material had been consumed, the pH was decreased to approximately 6 with 1 M HCl. The white precipitate was collected by filtration and dried under vacuum (94 mg, 47%). IR ν 3060, 1579, 1483, 1413, 1394, 1341, 1302, 1265, 1245, 1212, 1199, 1128, 1104, 1060, 1029, 961, 908, 896, 856, 787, 764, 727, 705, 643, 617 cm^{-1}. ^{1}H-NMR (D_2O) δ 7.88 (s, 1H); 7.38-7.25 (m, 5H); 5.51 (s, 2H); 3.74 (s, 2H); 3.25 (dt, ^3J(H,H) = 5.3, 6.9 Hz, 1H); 2.69 (dd, ^2J(H,H) = 27.9 Hz, ^3J(H,H) = 5.3 Hz, 1H); 2.60 (dd, ^2J(H,H) = 27.9 Hz, ^3J(H,H) = 6.9 Hz, 1H) ppm. MS (ES): *m/z* 293.06 $[C_{13}H_{16}N_4O_2S]H^+$.

General procedure B: $Re(CO)_3$ complex formation. One equivalent of the ligand and one equivalent of $[Re(CO)_3Br_3][NEt_4]_2$ were added to a 1:1 mixture of methanol and water to form a 0.1 mM solution and stirred at 65 °C. The reaction was followed by HPLC. After 3 hours all of the starting material had been consumed. The solvent was removed under reduced pressure, and the residue redissolved in water. The product was purified with a Sep-Pak column and eluted with a 1:2 ratio of water to methanol. The fractions containing the product were combined and the solvent removed under reduced pressure to give $[Re(CO)_3L]$ as a white powder.

$[Re(CO)_3$L1]. As per general procedure B, with **L1** (9.5 mg, 0.04 mmol) and $[Re(CO)_3Br_3][NEt_4]_2$ (27 mg, 0.04 mmol). $[Re(CO)_3$L1] was isolated as a white powder

(15 mg, 82%). Found: C, 34.52; H, 2.72; N, 10.59. Calc. for $C_{15}H_{13}N_4O_5Re$: C, 34.95; H, 2.54; N, 10.87. IR ν 2923, 2022, 1902, 1867, 1633, 1074, 734 cm^{-1}. ^{1}H-NMR (CD_3OD) δ 7.97 (s, 1H), 7.49-7.33 (m, 5H), 5.88 (dd, ^3J(H,H) = 5.8 Hz, ^2J(H,H) = 11.2 Hz, 1H), 5.64 (s, 2H), 5.20 (d ^2J(H,H) = 11.2 Hz, 1H), 4.14-4.04 (m, 1H), 3.36-3.29 (m, 1H), 3.22 (dd, ^2J(H,H) = 17.7, ^3J(H,H) = 4.0 Hz, 1H) ppm. ^{13}C-NMR (CD_3OD) δ 198.3, 197.5, 196.7, 184.7, 144.1, 135.4, 130.2, 130.1, 129.6, 126.4, 56.0, 52.7, 27.5 ppm. HR MS (ES): *m/z* 515.0370 $[C_{15}H_{12}N_4O_5Re]^-$ (calc. 515.0371).

$[Re(CO)_3L2]$. L2 (50 mg, 0.20 mmol) and $[Re(CO)_3Br_3][NEt_4]_2$ (157 mg, 0.20 mmol) were dissolved in a 1:1 mixture of methanol and water (18 mL) and stirred at 65 °C for 3 hours. HPLC analysis confirmed completion of the reaction. The solvent was removed under reduced pressure, and the residue redissolved in methanol. The white precipitate was collected by filtration, washed well with methanol and CH_2Cl_2 and dried under vacuum (80 mg, 78%). Found: C, 34.91; H, 2.54; N, 10.73. Calc. for $C_{15}H_{13}N_4O_5Re$: C, 34.95; H, 2.54; N, 10.87. IR ν 2021, 1921, 1893, 1864, 1658, 1615, 1363, 1343, 1128, 898, 764, 726, 717, 653, 644 cm^{-1}. ^{1}H-NMR (D_6-DMSO) δ 8.41 (s, 1H); 7.45-7.37 (m, 4H); 7.35-7.31 (m, 1H); 5.75 (s, 2H); 4.25 (d, ^2J(H,H) = 16.2Hz, 1H); 4.17 (dd, ^2J(H,H) = 16.2 Hz, ^3J(H,H) = 4.8 Hz, 1H); 3.55 (dd, ^2J(H,H) = 16.9 Hz, ^3J(H,H) = 7.7 Hz, 1H); 3.26 (d, ^2J(H,H) = 16.9 Hz, 1H) ppm. ^{13}C-NMR (d6-DMSO) δ 197.5, 197.0, 196.8, 179.2, 148.7, 134.5, 129.0, 128.7, 128.4, 123.6, 55.0, 54.3, 51.9 ppm. MS (ES): *m/z* 517.03 $[C_{15}H_{13}N_4O_5Re]H^+$. Crystals suitable for X-ray diffraction were obtained by diffusion of hexane into a solution of the complex in EtOH.

$[Re(CO)_3L3]NEt_4$. (36 mg, 0.13 mmol) was dissolved in a 1:1 mixture of methanol and water (13 mL). The solution was neutralized with aqueous NEt_4OH. $[Re(CO)_3Br_3][NEt_4]_2$ (100 mg, 0.13 mmol) was added and the mixture stirred at 65 °C for 3 hours. HPLC analysis confirmed the completion of the reaction. The solvent was removed under reduced pressure, and the residue redissolved in water. The crude product was purified with a Sep-Pak column and eluted with a 1:2 ratio of water to methanol. The fractions containing the product were combined and the solvent removed under reduced pressure to give $[Re(CO)_3L3]NEt_4$ as a white powder (50 mg, 57%). Found: C, 41.31; H, 4.99; N, 8.00. Calc. for $C_{24}H_{31}N_4O_7Re$: C, 42.79; H, 4.64; N, 8.32. IR ν 3386, 2020, 1885, 1609, 1582, 1434, 1417, 1393, 1297, 1162, 1026, 1001, 900, 729, 698 cm^{-1}. ^{1}H-NMR (CD_3OD) δ 7.95 (s, 1H); 7.41-7.38 (m, 4H); 5.64 (s, 2H);

3.54 (t, ^{3}J(H,H) = 4.6 Hz, 1H); 3.35 (d, ^{3}J(H,H) = 4.6 Hz, 2H); 3.32-3.25 (m, 8H); 1.31-1.25 (m, 12H) ppm. ^{13}C-NMR δ 7.6, 27.0, 53.3, 55.9, 126.9, 129.6, 130.1, 130.2, 135.6, 147.3, 179.9, 197.8, 198.4 ppm. HR MS (ES): *m/z* 544.0739 $[C_{16}H_{11}N_3O_7Re]^-$ (calc. 544.0160).

[Re(CO)$_3$L4]Br. As per general procedure B, with **L4** (35 mg, 0.13 mmol) and $[Re(CO)_3Br_3][NEt_4]_2$ (97 mg, 0.13 mmol). The reaction was carried out in methanol. [Re(CO)$_3$L4]Br was isolated as a white powder (51 mg, 65 %). Found: C, 36.66; H, 2.92; N, 10.68. Calc. for $C_{19}H_{17}BrN_5O_3Re$: C, 36.25; H, 2.72; N, 11.13. IR ν 3014, 2873, 2023, 1906, 1494, 1447, 1154, 1112, 1052, 1044, 888, 772, 732, 696, 637, 626 cm^{-1}. ^{1}H-NMR (CD_3OD) δ 8.77 (m, ^{4}J(H,H) = 5.6 Hz, 1H); 7.99 (s, 1H); 7.93 (m, ^{4}J(H,H) = 7.8 Hz, ^{3}J(H,H) = 1.5 Hz, 1H); 7.57 (d, ^{4}J(H,H) = 7.8 Hz, 1H); 7.36-7.31 (m, 4H); 7.12-7.09 (m, 2H); 5.60 (d, ^{2}J(H,H) = 14.8 Hz, 1H); 5.53 (d, ^{2}J(H,H) = 14.8 Hz, 1H); 4.75 (d, ^{2}J(H,H) = 17.0 Hz, 1H); 4.66 (d, ^{2}J(H,H) = 17.0 Hz, 1H) 4.48 (d, ^{2}J(H,H) = 16.6 Hz, 1H); 4.33 (d, ^{2}J(H,H) = 16.6 Hz, 1H) ppm. ^{13}C-NMR δ 161.9, 153.3, 150.9, 141.4, 135.5, 130.1, 130.0, 129.0, 124.6, 124.2, 63.8, 56.2, 53.0 ppm (carbonyl carbons not observed). HR-MS (ES): *m/z* 550.0890 $[C_{19}H_{17}N_5O_3Re]^+$ (calc. 550.0884).

[Re(CO)$_3$L5]Br. **L5** (100 mg, 0.35 mmol) and $[Re(CO)_3Br_3][NEt_4]_2$ (271 mg, 0.35 mmol) were dissolved in methanol (35 mL) and stirred at 65 °C. A precipitate began to form after approximately 1 hour. After 2 hours the reaction mixture was cooled to room temperature and the white precipitate collected by filtration, washed well with methanol and CH_2Cl_2 and dried under vacuum (120 mg, 54%). Found: C, 33.96; H, 2.61; N, 8.62. Calc. for $C_{18}H_{16}N_4O_3ReS$: C, 34.07; H, 2.54; N, 8.83. IR ν 2016, 1913, 1875, 1456, 14334, 1248, 1156, 1138, 1109, 1028, 991, 964, 820, 720, 701, 679, 660, 645, 633 cm^{-1}. ^{1}H-NMR (d6-Acetone) δ 8.17 (s, 1H); 7.53 (dd, ^{4}J(H,H) = 5.1 Hz, ^{3}J(H,H) = 1.0 Hz, 1H); 7.43-7.39 (m, 5H); 7.34 (dd, ^{4}J(H,H) = 3.5 Hz, ^{3}J(H,H) = 1.0 Hz, 1H); 7.08 (dd, ^{4}J(H,H) = 5.1, 3.5 Hz, 1H); 5.77 (s, 2H); 4.84-4.76 (m, 2H); 4.59-4.52 (m, 2H) 4.08-4.00 (m, 1H) ppm. ^{13}C-NMR (D_6-Acetone) δ 197.7, 196.5, 192.3, 149.3, 139.2, 135.5, 130.3, 129.9, 129.6, 129.2, 128.2, 127.8, 123.3, 55.9, 55.6, 48.4 ppm. HR-MS (ES): *m/z* 555.0489 $[C_{18}H_{16}N_4O_3ReS]^+$ (calc. 555.0494).

[Re(CO)$_3$L6]Br. As per general procedure B, with **L6** (78 mg, 0.33 mmol) and $[Re(CO)_3Br_3][NEt_4]_2$ (242 mg, 0.33 mmol). Analytically pure [Re(CO)$_3$L6]Br was

obtained by washing the Sep-Pak purified product with CH_2Cl_2 to remove traces of NEt_4Br (65 mg, 40%). Found: C, 30.20; H, 2.80; N, 9.20. Calc. for $C_{15}H_{16}BrN_4O_3ReS$: C, 30.10; H, 2.69; N, 9.36. ^{1}H-NMR (CD_3OD) δ ppm 8.18 (s, 1H); 7.45-7.41 (m, 5H); 5.70 (s, 2H); 5.26 (bs, 1H); 4.73 (bs, 1H); 4.43 (d, ^2J(H,H) = 17.0 Hz, 1H); 4.21 (d, ^2J(H,H) = 17.0 Hz, 1H); 2.98-2.84 (m, 3H); 2.13-2.02 (m, 1H) ppm. ^{13}C-NMR (CD_3OD) δ 194.6, 192.9, 192.6, 151.6, 135.0, 130.3, 130.25, 129.8, 124.8, 56.7, 44.2, 39.1, 34.2 ppm. MS (ES): *m/z* 519.05 $[C_{15}H_{16}N_4O_3ReS]^+$. Crystals suitable for X-Ray diffraction were obtained by slow evaporation of a solution of the complex in ethanol.

[Re(CO)$_3$L7]Br. As per general procedure B, with **L7** (9.5 mg, 0.04 mmol) and $[Re(CO)_3Br_3][NEt_4]_2$ (27 mg, 0.04 mmol). The reaction was carried out in methanol. $[Re(CO)_3L7]Br$ was isolated as a white powder (15 mg, 82%). ^{1}H-NMR (CD_3OD) δ 8.21 (s, 1H); 7.46-7.40 (m, 5H); 5.73 (d, ^2J(H,H) = 14.7 Hz, 1H); 5.68 (d, ^2J(H,H) = 14.7 Hz, 1H); 5.59-5.52 (m, 1H); 5.40-5.35 (m, 1H); 4.55 (d, ^2J(H,H) = 17.3 Hz, 1H); 4.24 (d, ^2J(H,H) = 17.3 Hz, 1H); 3.23-3.07 (m, 3H) ppm. ^{13}C-NMR (CD_3OD) δ 194.2, 192.5, 192.2, 170.9, 151.4, 135.0, 130.3, 130.2, 129.9, 125.0, 58.1, 56.8, 53.6, 39.9, 34.5 ppm. MS (ES): *m/z* 577.01 $[C_{17}H_{18}N_4O_5ReS]^+$.

[Re(CO)$_3$L7b]Br. As per general procedure B, with **L7b** (46 mg, 0.16 mmol) and $[Re(CO)_3Br_3][NEt_4]_2$ (121 mg, 0.16 mmol). $[Re(CO)_3L7b]Br$ was isolated as a white powder (51 mg, 58%). Found: C, 34.38; H, 2.94; N, 9.82. Calc. for $C_{16}H_{15}N_4O_5ReS$: C, 34.22; H, 2.69; N, 9.98. ^{1}H-NMR (CD_3OD) **Compound A** δ 8.02 (s, 1H); 7.46-7.39 (m, 5H); 5.89 (m, 1H); 5.74 (d, ^2J(H,H) = 14.7 Hz, 1H); 5.66 (d, ^2J(H,H) = 14.7 Hz, 1H); 4.42 (d, ^2J(H,H) = 17.2 Hz, 1H); 4.12 (d, ^2J(H,H) = 17.2 Hz, 1H); 3.90 (m, 1H); 3.47-3.41 (m, 1H); 3.28 (dd, ^2J(H,H) = 13.3 Hz, ^3J(H,H) = 4.8 Hz, 1H); 3.03 (dd, ^2J(H,H) = 13.3 Hz, ^3J(H,H) = 7.4 Hz, 1H) ppm; **Compound B** δ 8.17 (s, 1H); 7.46-7.39 (m, 5H); 5.70(s, 2H); 5.17 (m, 1H); 4.60 (m, 1H); 4.46 (d, ^2J(H,H) = 17.5 Hz, 1H); 4.24 (d, ^2J(H,H) = 17.5 Hz, 1H); 3.32-3.31 (m, 1H); 2.88 (dd, ^2J(H,H) = 14.2 Hz, ^3J(H,H) = 11.4 Hz, 1H); 2.50 (m, 1H) ppm. ^{13}C-NMR (CD_3OD) δ 194.9, 193.1, 193.0, 152.1, 150.9, 135.1, 135.0, 130.4, 130.3, 130.2, 129.9, 129.8, 125.3, 124.5, 56.7, 43.0, 41.3, 34.5, 34.1 ppm. MS (ES): *m/z* 562.77 $[C_{16}H_{16}N_4O_5ReS]^+$.

Table 2. Crystal structure parameters.

	[Re(CO)$_3$**L2**]	[Re(CO)$_3$**L3**]NEt$_4$	[Re(CO)$_3$**L6**]Br
formula	$C_{15}H_{13}N_4O_5Re$	$C_{49}H_{64}Cl_2N_8O_{14}Re_2$	$C_{15}H_{16}BrN_4O_3ReS$
*M*r	515.49	1432.38	598.49
size [mm]	0.13 x 0.13 x 0.09	0.35 x 0.22 x 0.15	0.45 x 0.17 x 0.04
description	colourless block	colourless prism	colourless plate
system	monoclinic	triclinic	monoclinic
space group	$P2_1/c$	P-1	I2/a
a [Å]	9.59717(9)	12.8499(15)	20.3718(2)
b [Å]	14.2008(2)	15.4486(13)	6.59104(7)
c [Å]	24.1727(2)	15.5010(14)	28.9051(4)
α [°]	90	110.452(8)	90
β [°]	91.7106(9)	92.469(8)	105.3580(14)
γ [°]	90	105.905(9)	90
V [Å^3]	3292.98(6)	2739.7(5)	3742.53(7);
Z	8	2	8
D_c [g cm^{-3}]	2.080	1.736	2.124
μ [mm^{-1}]	7.415	4.582	8.762
F(000)	1968	1420	2272
θ range [°]	2.56 to 30.51	2.40 to 28.28	2.84 to 36.32
reflections measured	40584	267324	58404
independent reflections	10048 [R(int) = 0.0342]	13602 [R(int) = 0.0352]	9054 [R(int) = 0.0469]
reflections observed	7409	11494	6991
completeness to θ [%]	99.9	99.9	100
max. and min. transmission	0.5550 and 0.4457	0.5465 and 0.2969	1.0000 and 0.2186
data/restraints/parameters	10048 / 0 / 451	13602 / 0 / 684	9054 / 0 / 233
goodness of fit on F^2	0.896	1.130	1.044
final *R* indices ($I>2\sigma(I)$)	R1 = 0.0208 wR2 = 0.0323	R1 = 0.0245 wR2 = 0.0654	R1 = 0.0260 wR2 = 0.0635
R indices (all data)	R1 = 0.0374 wR2 = 0.0339	R1 = 0.030 wR2 = 0.0697	R1 = 0.0407 wR2 = 0.0683
residual electron [e Å^{-3}]	0.809 and -0.821	2.420 and -0.854	2.082 and -3.612

3.5.3 X-ray crystallography

Crystallographic data were collected at 183(2) K on an Oxford Diffraction Xcalibur system with a Ruby detector ($Mo_{K\alpha}$ radiation, λ = 0.7107 Å) using graphite-monochromated radiation. Suitable crystals were covered with oil (Infineum V8512, formerly known as Paratone N), mounted on top of a glass fiber and immediately transferred to the diffractometer. The program suite CrysAlis^{Pro} was used for data collection, semi-empirical absorption correction and data reduction.[29] Structures were solved with direct methods using SIR97[30] and were refined by full-matrix least-squares methods on F^2 with SHELXL-97.[31] The structures were checked for higher symmetry with the help of the program Platon.[32] CCDC 680569 ([$Re(CO)_3$**L2**]), 680568 ([$Re(CO)_3$**L3**]NEt_4) and 680570 ([$Re(CO)_3$**L6**]Br) contain the supplementary crystallographic data for this paper. These data can be obtained free of charge from The Cambridge Crystallographic Data Centre via www.ccdc.cam.ac.uk/data_request/cif.

3.5.4 Radiolabelling with $[^{99m}Tc(CO)_3(H_2O)_3]^+$

The precursor $[^{99m}Tc(CO)_3(H_2O)_3]^+$ was prepared according to the literature procedure.[33] 1 mL $[^{99m}TcO_4]^-$ in 0.9% NaCl was added to the IsoLink™ kit (Mallinckrodt-Tyco, Petten, Holland) via the septum. The reaction was heated for 20 min at 100 °C. The solution was cooled and neutralized to pH 7.2 with a mixture of 1 M HCl and 1 M phosphate buffer (pH 7.4).

Stock solutions (10^{-2} to 10^{-7} M) of ligands **L1**-**L7** and **L7b** were prepared in PBS, pH 7.4. A solution of $[^{99m}Tc(CO)_3(H_2O)_3]^+$ (50 µL; ~500 MBq/mL) was added to 50 µL of the relevant ligand diluted with 400 µL PBS (pH 7.4) to give final concentrations between 10^{-3} and 10^{-8} M. The reaction mixtures were heated for 60 min at 100 °C. Radiolabelling yields were determined by HPLC. The identity of the products was confirmed by comparison of the γ-traces of the ^{99m}Tc complexes with the UV traces of the corresponding Re complexes.

3.6 References

(1) Ferrieri, R. A. in *Handbook of Radiopharmaceuticals: Radiochemistry and Applications*, (Eds. Welch, M. J., Redvanly, C. S.), John Wiley & Sons, **2003**, p 229-282.

(2) Madsen, M. T. *J. Nucl. Med.* **2007**, *48*, 661-673.

(3) Banerjee, S. R.; Maresca, K. P.; Francesconi, L.; Valliant, J.; Babich, J. W.; Zubieta, J. *Nucl. Med. Biol.* **2005**, *32*, 1-20.

(4) Stephenson, K. A.; Banerjee, S. R.; Sogbein, O. O.; Levadala, M. K.; McFarlane, N.; Boreham, D. R.; Maresca, K. P.; Babich, J. W.; Zubieta, J.; Valliant, J. F. *Bioconjugate Chem.* **2005**, *16*, 1189-1195.

(5) Kolb, H. C.; Finn, M. G.; Sharpless, K. B. *Angew. Chem., Int. Ed.* **2001**, *40*, 2004-2021.

(6) Rostovtsev, V. V.; Green, L. G.; Fokin, V. V.; Sharpless, K. B. *Angew. Chem., Int. Ed.* **2002**, *41*, 2596-2599.

(7) Chan, T. R.; Hilgraf, R.; Sharpless, K. B.; Fokin, V. V. *J. Am. Chem. Soc.* **2004**, *6*, 2853-2855.

(8) Colasson, B.; Save, M.; Milko, P.; Roithova, J.; Schroder, D.; Reinaud, O. *Org. Lett.* **2007**, *9*, 4987-4990.

(9) Dai, Q.; Gao, W. Z.; Liu, D.; Kapes, L. M.; Zhang, X. M. *J. Org. Chem.* **2006**, *71*, 3928-3934.

(10) Detz, R. J.; Heras, S. A.; de Gelder, R.; van Leeuwen, P.; Hiemstra, H.; Reek, J. N. H.; van Maarseveen, J. H. *Org. Lett.* **2006**, *8*, 3227-3230.

(11) Meudtner, R. M.; Ostermeier, R.; Goddard, M.; Limberg, C.; Hecht, S. *Eur. J. Inorg. Chem.* **2007**, *13*, 9834-9840.

(12) Monkowius, U.; Ritter, S.; Konig, B.; Zabel, M.; Yersin, H. *Eur. J. Inorg. Chem.* **2007**, 4597-4606.

(13) Mindt, T. L.; Struthers, H.; Brans, L.; Anguelov, T.; Schweinsberg, C.; Maes, V.; Tourwe, D.; Schibli, R. *J. Am. Chem. Soc.* **2006**, *128*, 15096-15097.

(14) Banerjee, S. R.; Levadala, M. K.; Lazarova, N.; Wei, L.; Valliant, J. F.; Stephenson, K. A.; Babich, J. W.; Maresca, K. P.; Zubieta, J. *Inorg. Chem.* **2002**, *41*, 6417-6425.

(15) Lazarova, N.; Babich, J. W.; Valliant, J. F.; Schaffer, P.; James, S.; Zubieta, J. *Inorg. Chem.* **2005**, *44*, 6763-6770.

(16) Pak, J. K.; Benny, P.; Spingler, B.; Ortner, K.; Alberto, R. *Chem.--Eur. J.* **2003**, *9*, 2053-2061.

(17) van Staveren, D. R.; Benny, P. D.; Waibel, R.; Kurz, P.; Pak, J.-K.; Alberto, R. *Helv. Chim. Acta* **2005**, *88*, 447-460.

(18) Schibli, R.; La Bella, R.; Alberto, R.; Garcia-Garayoa, E.; Ortner, K.; Abram, U.; Schubiger, P. A. *Bioconjugate Chem.* **2000**, *11*, 345-351.

(19) Marti, N.; Spingler, B.; Breher, F.; Schibli, R. *Inorg. Chem.* **2005**, *44*, 6082-6091.

(20) Farrugia, L. J. *J. Appl. Cryst.* **1997**, *30*, 565.

(21) Karagiorgou, O.; Patsis, G.; Pelecanou, M.; Raptopoulou, P.; Terzis, A.; Siatra-Papastaikoudi, T.; Alberto, R.; Pirmettis, I.; Papadopoulos, M. *Inorg. Chem.* **2005**, *44*, 4118-4120.

(22) Vitor, R. F.; Alves, S.; Correia, J. D. G.; Paulo, A.; Santos, I. *J. Organomet. Chem.* **2004**, *689*, 4764-4774.

(23) Lee Lac, V.; Mitchell Michael, L.; Huang, S.-J.; Fokin Valery, V.; Sharpless, K. B.; Wong, C.-H. *J. Am. Chem. Soc.* **2003**, *125*, 9588-9.

(24) Munchpetersen, B.; Cloos, L.; Jensen, H. K. in *Advances in Enzyme Regulation*, Vol. 35, **1995**, p 69-89.

(25) Celen, S.; De Groot, T. J.; Balzarini, J.; Vunckx, K.; Terwinghe, C.; Vermaelen, P.; Van Berckelaer, L.; Vanbilloen, H.; Nuyts, J.; Mortelmans, L.; Verbruggen, A.; Bormans, G. *Nucl. Med. Biol.* **2007**, *34*, 283-291.

(26) Al-Madhoun, A. S.; Johnsamuel, J.; Yan, J. H.; Ji, W. H.; Wang, J. H.; Zhuo, J. C.; Lunato, A. J.; Woollard, J. E.; Hawk, A. E.; Cosquer, G. Y.; Blue, T. E.; Eriksson, S.; Tjarks, W. *J. Med. Chem.* **2002**, *45*, 4018-4028.

(27) Ogilvie, K. K. *Can. J. Chem.* **1973**, *51*, 3799-3807.

(28) Alberto, R.; Egli, A.; Abram, U.; Hegetschweiler, K.; Gramlich, V.; Schubiger, P. A. *Dalton Trans.* **1994**, 2815-2820.

(29) *CrysAlis^{Pro} Software system* **2007**, Oxford Diffraction Ltd., Yarnton, UK.

(30) Altomare, A.; Burla, M. C.; Camalli, M.; Cascarano, G. L.; Giacovazzo, C.; Guagliardi, A.; Moliterni, A. G. G.; Polidori, G.; Spagna, R. *J. Appl. Cryst.* **1999**, *32*, 115-119.

(31) Sheldrick, G. M. *SHELXL97-2: Program for the Refinement of Crystal Structures* **1997**, University of Göttingen, Germany.

(32) Spek, A. L. *J. Appl. Cryst.* **2003**, *36*, 7-13.

(33) Alberto, R.; Ortner, K.; Wheatley, N.; Schibli, R.; Schubiger, A. P. *J. Am. Chem. Soc.* **2001**, *123*, 3135-3136.

"Click-to-Chelate": Functionalization of thymidine with chelating systems for rhenium and technetium and evaluation of organometallic complexes as substrates for human thymidine kinase 1

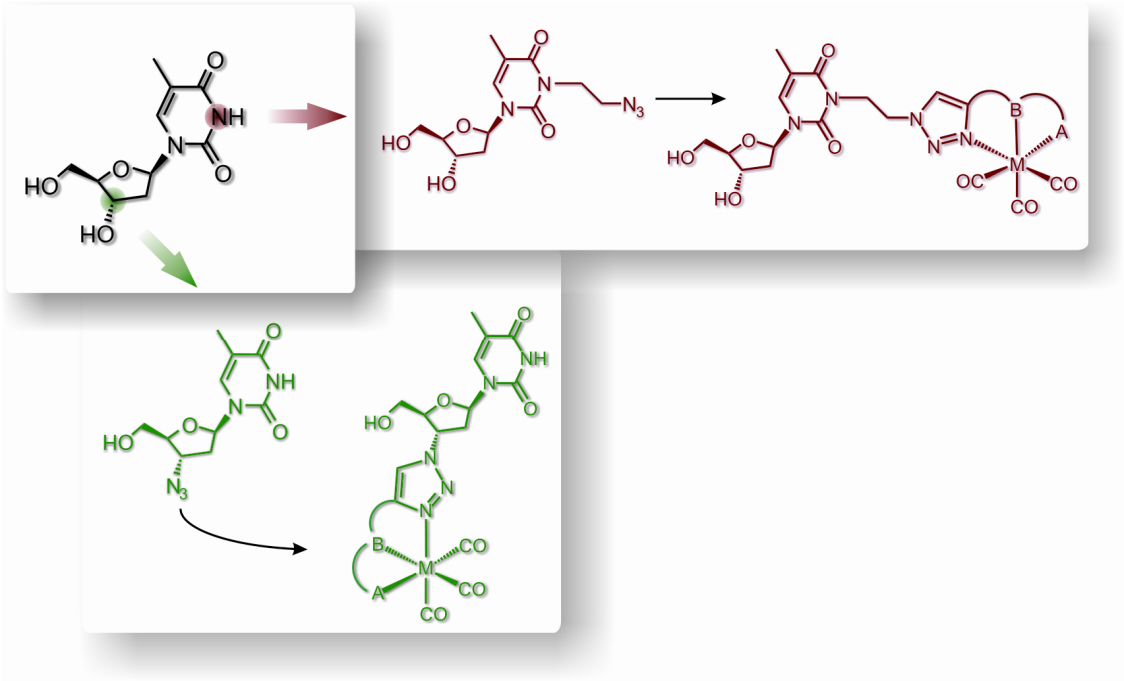

4.1 Abstract

Human cytosolic thymidine kinase (hTK1) has proven to be a suitable target for the non-invasive imaging of cancer cell proliferation using radiolabelled thymidine analogues such as [^{18}F]3′-fluoro-3′-deoxythymidine ([^{18}F]FLT). A thymidine analogue for single photon emission computed tomography (SPECT) incorporating the readily available and inexpensive nuclide technetium-99m would be of considerable practical interest. hTK1 is known to accommodate modification of the structure of the natural substrate thymidine at the positions, N3, C3′ and, to a lesser extent, C5. The copper catalyzed azide-alkyne cycloaddition has been used to synthesize two series of derivatives in which thymidine is functionalized at either the N3 or C3′ position with a chelating system suitable for the $M(CO)_3$ core (M = ^{99m}Tc, Re). Using this strategy, the first organometallic hTK1 substrates in which thymidine is modified at the C3′ position were identified. Furthermore, the click chemistry approach enabled complexes with different structures, overall charges and lipophilicities to be synthesized from a common precursor. Phosphorylation of the organometallic derivatives was measured relative to thymidine. We were able to show that the influence of the overall charge of the derivatives is dependent on the position of functionalization. In the case of the C3′-functionalized derivatives, neutral and anionic substrates were most readily phosphorylated, whereas for the N3-functionalized derivatives, cationic complexes were potentially as good substrates for the enzyme as neutral complexes.

4.2 Introduction

Human Thymidine Kinase 1 (hTK1) is a cytosolic enzyme which catalyzes the γ-phosphate transfer from ATP to the 5′-hydroxyl groups of thymidine (dT) and 2′-deoxyuridine (dUrd). Other hTK1 substrates include 3′-azido-3′-deoxythymdine, AZT and 3′-fluoro-3′-deoxythymidine, FLT, where thymidine has been modified at the C3′-position, and the phosphorylation of which is the first step in their activation as anti-HIV prodrugs.[1,2] It is well documented, however, that hTK1 is among the most selective of the nucleoside kinases, and is particularly sensitive to changes in the structure of the natural substrates dT and dUrd.[3] Eriksson *et al.* have shown that minor modification of the structure at the 5-position is possible, for example, 5-halo and 5-ethyl substitutions are tolerated, but substitution with bulkier groups such as 5-propenyl or 5-(2-chloroethyl) are not.[1,4] More recently, Tjarks and co-workers have shown that hTK1 is also amenable to modification of thymidine at the N3-position.[5,6] Functionalization with a series of bulky carborane derivatives, tethered from N3 of the pyrimidine base with varying spacer length, does not prevent phosphorylation of the nucleoside analogue. The experimental results of substrate activity investigations have all since been rationalized by the determination of the 3-D structure of hTK1, which confirms that hTK1 has a much smaller binding site than other nucleoside kinases.[7]

Unlike the activity of other mammalian deoxyribonucleoside kinases, hTK1 activity is stringently cell cycle regulated.[3] Active enzyme is not found in resting cells, but activity increases dramatically by the time cells reach the S-phase, to coincide with DNA synthesis. A number of thymidine analogues, which aim to target the high hTK1 activity in proliferating cells, have been developed. As potential agents for boron neutron capture therapy, thymidine derivatives incorporating *closo-o-* and *nido-m-*carboranes have been extensively investigated.[5,6,8,9] Similarly, thymidine derivatives labelled with radionuclides suitable for positron emission tomography (PET) have been developed with the goal of monitoring tumour growth and response to therapy.[10-12] However, PET nuclides typically have very short half-lives and their production is expensive, usually requiring an onsite cyclotron. A thymidine analogue labelled with technetium for *in vivo* single photon emission computed tomography (SPECT) would be of considerable interest. Technetium has near perfect decay characteristics for

diagnostic applications ($T_{1/2}$ = 6 h, 140 keV γ-radiation), moreover it is readily available at low cost from a ^{99}Mo/^{99m}Tc generator system.

Numerous functionalization strategies and bifunctional chelating systems which facilitate the incorporation of technetium into biologically relevant molecules have been reported, but they often require multi-step syntheses and lack efficiency. The "click-to-chelate" approach describes a strategy for the synthesis of efficient tridentate chelators for the $M(CO)_3$ core (M = ^{99m}Tc, Re) and their incorporation into biologically relevant molecules.[13] This strategy exploits the remarkable features of the copper catalyzed azide-alkyne cycloaddition[14,15] to aid the design and synthesis of potential technetium labelled radiopharmaceuticals. The most appealing aspect of this approach is that the click reaction allows simultaneous formation of the chelating system and conjugation to a biologically relevant molecule in a single, high-yielding step. A series of suitable alkynes was developed (Figure 1), which can be reacted with any azide functionalized biomolecule to create a set of conjugates with efficient tridentate triazole-containing chelating systems for the $M(CO)_3$ core.[16]

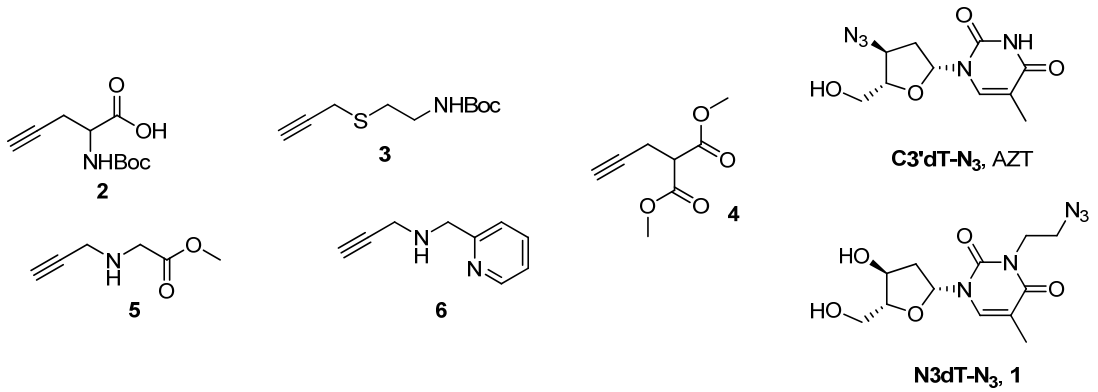

Figure 1. Protected[a] alkyne derivatives **2-6**, which when reacted with a suitable azide lead to tridentate chelating systems for the $M(CO)_3$ core (M = ^{99m}Tc, Re), and the C3′ and N3 functionalized azido-thymidine derivatives.

The aim of this investigation was the synthesis of technetium-labelled thymidine analogues, which have the potential to be used as proliferation markers. We used click

[a] Protected alkynes were used for ease of purification of the triazole-containing products. However, in previous studies we have shown that for radiolabelling purposes it is not necessary to use protected substrates, or indeed to purify the ligands prior to radiolabelling.[13,16]

chemistry to facilitate the parallel synthesis of two series of derivatives, which when labelled with the $M(CO)_3$ core (M = ^{99m}Tc, Re) have varying physical characteristics, such as size, lipophilicity and overall charge. Using this strategy we were able to identify novel organometallic substrates for hTK1 and qualitatively analyze structure-activity relationships. Preliminary investigations were also carried out into the cell-internalizing ability of the complexes in two human glioblastoma cell lines.

4.3 Results and discussion

Thymidine derivatives can incorporate modifications at the C5, N3 or C3′ positions, without losing their ability to act as substrates for hTK1. Experimental evidence and structural characterization rule out the modification of thymidine at the C5 position with a comparatively bulky organometallic complex. Given the promising reports of the N3-functionalized carborane thymidine derivatives,[5,6,9] the N3 position is appealing for functionalization with an $M(CO)_3$ complex (M = ^{99m}Tc, Re). We recently reported the synthesis and *in vitro* evaluation of a small series of technetium labelled thymidine derivatives in which the nucleoside was functionalized at the N3 position and could show that all of the compounds retained activity towards hTK1.[17] While minor modifications at the C3′ position do not dramatically lower affinity and are well-documented, to our knowledge there have not been any systematic investigations into the steric tolerance of hTK1 at this position. Tjarks' group report a small series of compounds in which thymidine has been functionalized at the 3′ position with a carborane, and although the compounds show minimal activity towards hTK1, stability issues prevented thorough characterization.[18] From their elucidation of the structure of hTK1, Welin *et al.* suggest that tolerance of C3′ modification could be a result of the open nature of the C3′/C4′ environment and the proximity of the C3′ substituent to the surface of the enzyme.[7] We reasoned that hTK1 might also accept modification of thymidine at this position with an organometallic complex.

4.3.1 Chemistry

N3-Functionalized thymidine derivatives. Thymidine was functionalized at the N3 position with an azido-ethyl group. The synthesis can be readily accomplished in four steps from commercially available thymidine as shown in Scheme 1. The 3′ and 5′ hydroxyl groups were protected with the *tertiary*-butyldimethylsilyl protecting group,[19] to allow selective alkylation with 1,2-dibromoethane at position N3. The azido compound was formed by nucleophilic substitution of the bromide with excess sodium azide, followed by removal of the silyl protecting groups with tetrabutylammonium fluoride.

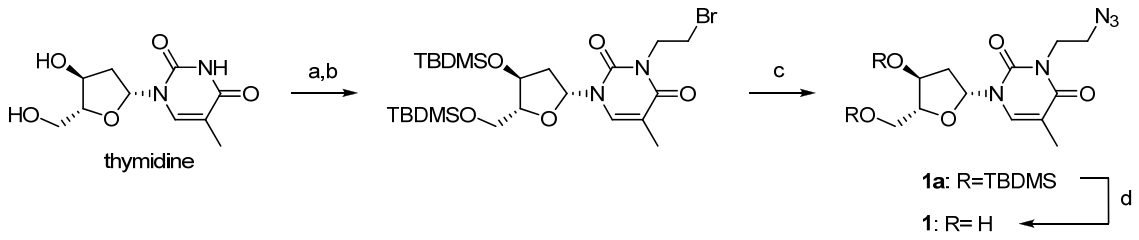

Scheme 1. Functionalization of thymidine at position N3: (a) TBDMSCl, imidazole, DMF (b) $BrCH_2CH_2Br$, Cs_2CO_3, DMF (c) NaN_3, MeCN (d) NBu_4F, THF.

Tridentate chelators for the $M(CO)_3$ core were incorporated into thymidine by reaction of the N3-functionalized azido-thymidine derivative **1** or the *O*-TBDMS protected precursor (**1a**) with a suitable alkyne (Scheme 2). Suitable alkynes (Figure 1) were prepared by alkylation of propargylamine with bromoacetate methyl ester (**5**), alkylation of commercial amines with propargyl bromide (**3** and **6**), or are commercially available (**2** and **4**). Full details of the synthesis of the alkyne components used were recently reported.[16] The copper catalyzed azide-alkyne cycloaddition was performed using standard Sharpless conditions: one equivalent of alkyne and one equivalent of azide were stirred at room temperature for 12 hours in a mixture of *t*BuOH and water with catalytic amounts of copper acetate (0.1 equivalents) and sodium ascorbate (0.1 equivalents).[20] Thymidine derivatives **7** and **8** were prepared from the reactions of the *O*-TBDMS protected N3-functionalized thymidine precursor, **1a**, and alkynes **2** and **3**, respectively. The protected triazole intermediates were purified by silica gel chromatography using mixtures of CH_2Cl_2 and MeOH. In both cases the Boc and TBDMS protecting groups of the products were removed in a single step with HCl in

MeOH. Compounds **7** and **8** were purified by solid phase extraction, although compound **7** could also be recrystallized from MeOH. Similarly, derivative **9** was prepared from the reaction of **1a** with alkyne **4**. The protected intermediate was stirred in HCl/MeOH to remove the TBDMS protecting groups, followed by aqueous NaOH to remove the methyl esters. Thymidine derivative **10** was prepared from the reaction of **1** and alkyne **5**. The intermediate was purified by silica gel chromatography before the methyl ester was removed with aqueous NaOH. In this case, removal of the TBDMS protecting groups from the azido-thymidine derivative **1a** with NBu_4F proved more efficient before the click reaction, as **1** could more easily be separated from excess NBu_4^+ salts than the more hydrophilic triazole product. Both compounds **9** and **10** were purified by solid phase extraction using Sep-Pak® columns. Compound **11** was purified by silica gel chromatography after the reaction of **1** and *N*-propargyl-pyridine-2-methylamine, **6**.

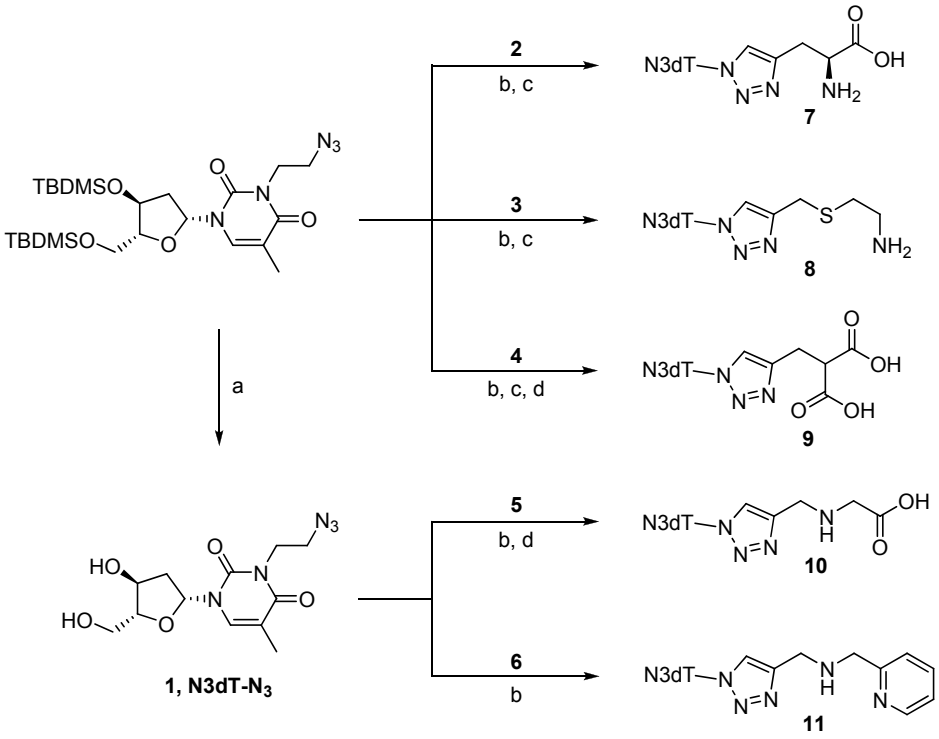

Scheme 2. Incorporation of tridentate chelators into N3-functionalized thymidine: (a) NBu_4F, THF (b) $Cu(OAc)_2.H_2O$, Na(ascorbate), *t*BuOH/H_2O (c) HCl, MeOH (d) NaOH, H_2O.

Compounds **7-9** and **11** have been reported previously.[16] In an evaluation of the scope of the "click-to-chelate" approach, the compounds were synthesized using stock

solutions (10^{-2} M) of the deprotected analogues of alkynes **2**, **3**, **5** and **6**, compound **1**, copper (II) acetate and sodium ascorbate. The reaction solutions were analyzed by MS, to confirm product formation but the small scale (< 0.5 mg) prohibited thorough characterization. The solutions were labelled *in situ* to provide [^{99m}Tc(CO)$_3$**7**], [^{99m}Tc(CO)$_3$**8**]$^+$, [^{99m}Tc(CO)$_3$**10**] and [^{99m}Tc(CO)$_3$**11**]$^+$, and [Re(CO)$_3$**10**], which was analyzed by mass spectroscopy.

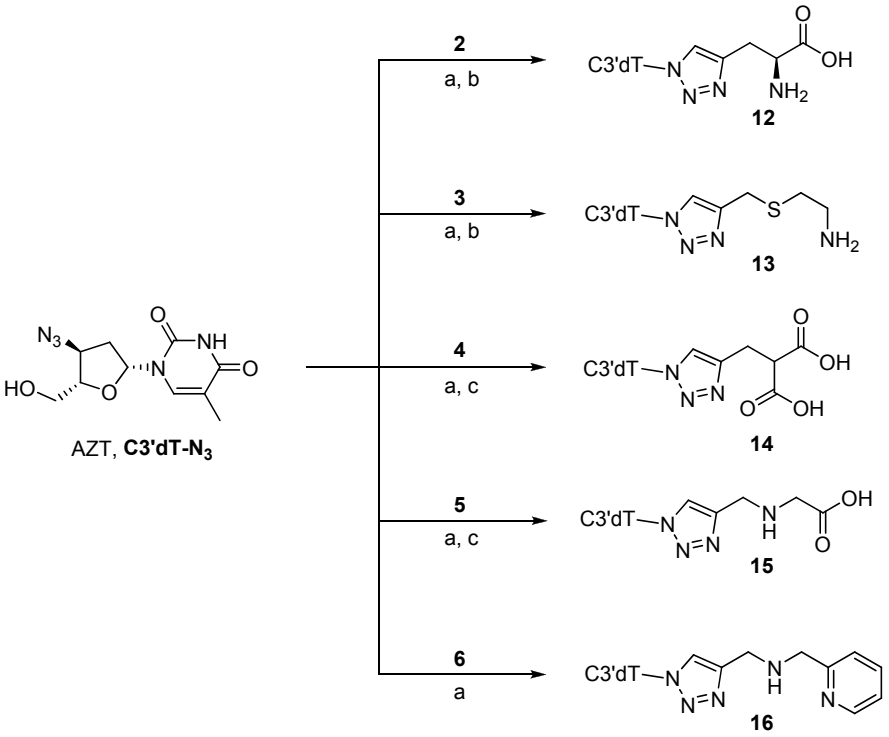

Scheme 3. Synthesis of C3′-functionalized thymidine derivatives: (a) $Cu(OAc)_2.H_2O$, Na(ascorbate), *t*BuOH/H_2O (b) TFA, CH_2Cl_2 (c) NaOH, H_2O.

C3′-Functionalized thymidine derivatives. Thymidine can be readily functionalized at the C3′ position using the "click-to-chelate" approach starting from the commercially available azide 3′-azido-3′-deoxythymidine, AZT. In analogous procedures to the synthesis of the N3-functionalized derivatives described above, tridentate chelators for the M(CO)$_3$ core (M = ^{99m}Tc, Re) were installed at the C3′ position by reacting AZT with alkynes **2**-**6** using standard conditions for the click reaction and as outlined in Scheme 3. Thymidine derivatives **12** and **13** were prepared from the reactions of AZT with alkynes **2** and **3**, respectively. In both cases the Boc-protected triazole products were purified by silica gel chromatography before the Boc protecting groups were

removed in a mixture of trifluoroacetic acid (10%) and CH_2Cl_2. Compounds **12** and **13** were purified by solid phase extraction using Sep-Pak® columns. Thymidine derivatives **14** and **15** were prepared from the reactions of **1** with alkynes **4** and **5**, respectively. The intermediates were purified by silica gel chromatography before the methyl esters were removed with aqueous NaOH. Compounds **14** and **15** were purified by solid phase extraction using Sep-Pak® columns. Compound **16** was purified by silica gel chromatography after the reaction of AZT and *N*-propargyl-pyridine-2-methylamine, **6**.

Synthesis of organometallic thymidine derivatives. The $Re(CO)_3$ complexes of all of the functionalized thymidine derivatives were prepared from the precursor $[ReBr_3(CO)_3][NEt_4]_2$ and a stoichiometric amount of the corresponding ligand in a mixture of MeOH and water at 50 °C. In each case the quantitative formation of the product was observed by HPLC. The crude products were purified by solid phase extraction using SepPak® columns and a water-MeOH gradient. The IR spectra of all of the rhenium complexes revealed the typical *fac*-$Re(CO)_3$ pattern with significantly blue-shifted, intense CO stretching frequencies (around 2020 cm^{-1} and 1880 cm^{-1}) compared with the starting material $[ReBr_3(CO)_3]^{2-}$ (2000 cm^{-1} and 1868 cm^{-1}). NMR analyses provided evidence that the metal core is site-specifically coordinated via the tridentate metal chelating systems introduced at either the N3 or C3′ positions, showing similar features to model complexes which were synthesized with benzyl azide and characterized previously.[16] Typically, the proton NMR spectra showed low field shifts of the protons in the chelating system after metal chelation, as well as independent resonances for the each proton in CH_2 groups of the chelating system which become distinguishable due to a lack of symmetry in the metal chelate. Similar trends in the rate of H/D exchange were also observed. A key difference between the thymidine chelates and the analogous model complexes is the appearance of diastereoisomers, which can be distinguished in some cases by NMR and/or HPLC. For the N3-functionalized complexes $[Re(CO)_3\mathbf{X}]Br$, (**X** = **8**, **11**) and $[Re(CO)_3\mathbf{10}]$, two diastereoisomers can be distinguished by NMR. The differences in chemical shifts of the two isomers are most pronounced for the complex $[Re(CO)_3\mathbf{8}]Br$, and HPLC analysis also revealed two products in this case. For the C3′ complexes HPLC analyses revealed two isomeric products for both $[Re(CO)_3\mathbf{13}]Br$ and $[Re(CO)_3\mathbf{15}]$, but only in the case of

[$Re(CO)_3$**16**]Br were two isomers apparent in the ^1H NMR spectrum. In analogous model complexes, isomers were not distinguishable by either HPLC or NMR.[16] All of the complexes were readily water soluble, which is a prerequisite for *in vitro* assessment. Representative NMR spectra can be found in Appendix C.

Radioactive technetium-99m complexes were prepared with the ligands **7**, **10**, **11**, **12**, **15** and **16**. The complexes were prepared quantitatively by adding the organometallic precursor $[^{99m}Tc(CO)_3(H_2O)_3]^+$ to a solution of the ligand in physiological phosphate buffer (PBS; pH 7.4) and heating for 45 minutes at 95 °C.[21] A single complex was formed with each of the nucleoside derivatives. Characterization of the radioactive complexes was accomplished by comparison of the retention times observed in the γ-HPLC trace with those in the UV-trace of the corresponding rhenium complexes, a procedure which is common in radiopharmacy (see, for example, complexes [^{99m}Tc/$Re(CO)_3$**15**] in Figure 2A/B). Given the experimental limitations, the retention times matched for all pairs of complexes. For *in vitro* and enzymatic studies ^{99m}Tc complexes were separated from unreacted thymidine derivatives by HPLC.

4.3.2 *In vitro* evaluation of the organometallic thymidine derivatives

Substrate activity toward human thymidine kinase. The hTK1 substrate activities of all target rhenium complexes were assessed using a coupled thymidine kinase-pyruvate kinase-lactate dehydrogenase UV assay (λ = 340 nm) as previously described (see Appendix C).[6,22] We were able to show that all of the N3-functionalized and C3′-functionalized rhenium complexes were substrates for hTK1. The results with both series of compounds are presented in Table 1. The phosphorylation of thymidine was arbitrarily set to 100%.

In the first series of compounds, thymidine was functionalized at the N3 position. The overall charges of the derivatives vary, but in all cases there is an ethyl spacer between thymidine and the metal complex. Although the phosphorylation is relatively low compared to thymidine for all of the complexes (>18%), the neutral and cationic complexes appear to be better substrates than the anionic complex. This is consistent with results from Tjarks *et al*., which show that zwitterionic NH_3^+-*nido*-*m*-carborane-

substituted thymidine analogues (with a propyl spacer) have high substrate activity.[23] However, the variation in the phosphorylation of the two cationic complexes (10.9 ± 0.4% and 16.8 ± 0.2% for [Re(CO)$_3$**8**]Br and [Re(CO)$_3$**11**]Br, respectively), suggests that in addition to overall charge, structural differences in the metal chelate also affect the substrate affinity for hTK1. It is not possible, therefore, to rule out structural differences in addition to overall charge as the reason for the lower substrate affinity of the complex [Re(CO)$_3$**9**]NEt$_4$.

Table 1. Phosphorylation of organometallic thymidine complexes [Re(CO)$_3$**7**-**16**].

Compound	Position of functionalization	Overall charge	Phosphorylation [%][a]
[Re(CO)$_3$**7**]	N3	Neutral	17.9 ± 0.1
[Re(CO)$_3$**10**]	N3	Neutral	14.1 ± 0.2
[Re(CO)$_3$**9**]NEt$_4$	N3	Anionic	9.0 ± 0.4
[Re(CO)$_3$**8**]Br	N3	Cationic	10.9 ± 0.4
[Re(CO)$_3$**11**]Br	N3	Cationic	16.8 ± 0.2
[Re(CO)$_3$**12**]	C3′	Neutral	20.3 ± 0.8
[Re(CO)$_3$**15**]	C3′	Neutral	27.6 ± 1.9
[Re(CO)$_3$**14**]NEt$_4$	C3′	Anionic	23.1 ± 1.8
[Re(CO)$_3$**13**]Br	C3′	Cationic	12.5 ± 0.5
[Re(CO)$_3$**16**]Br	C3′	Cationic	14.2 ± 0.2
Thymidine	-	-	100[a]

[a] The phosphroylation of thymidine was arbitrarily set to 100%.

In the second series of complexes, thymidine was functionalized at the C3′ position. For these complexes there is no spacer between the thymidine and metal chelate, but instead the ribose of thymidine is functionalized directly. The phosphorylation data show that in general the C3′-functionalized compounds are better substrates for hTK1 than the N3-functionalized compounds. The neutral complex [Re(CO)$_3$**15**] had the highest relative phosphorylation of 27.6 ± 1.9%. Interestingly, for the C3′-functionalized compounds there appears to be a clearer trend in phosphorylation rate as a function of overall charge. In contrast to the N3-functionalized compounds, where the anionic derivative was least readily phosphorylated (9.0 ± 0.4%), the anionic C3′-functionalized compound (23.1 ± 1.8%) is as comparatively good a substrate as the

neutral C3′-functionalized compounds. The cationic complexes, on the other hand, are much less readily phosphorylated (12.5 ± 0.5% and 14.2 ± 0.2% for [Re(CO)$_3$**13**]Br and [Re(CO)$_3$**16**]Br, respectively). This is perhaps surprising given that the structure of hTK1 co-crystallized with the feedback inhibitor thymidine triphosphate (dTTP) shows the proximity and suspected interaction of the C3′ substituent (in the case of dTTP, a hydroxyl group) with a glycine residue and an aspartic acid residue.[7] There is, however, an arginine residue in the same region of the active site. Interaction between the C3′ substituent and the cationic side chain of arginine may compensate for the loss of interaction with the C3′ hydroxyl group of thymidine, and thus be an explanation for the greater substrate efficiency of the anionic complex compared to the cationic complexes.

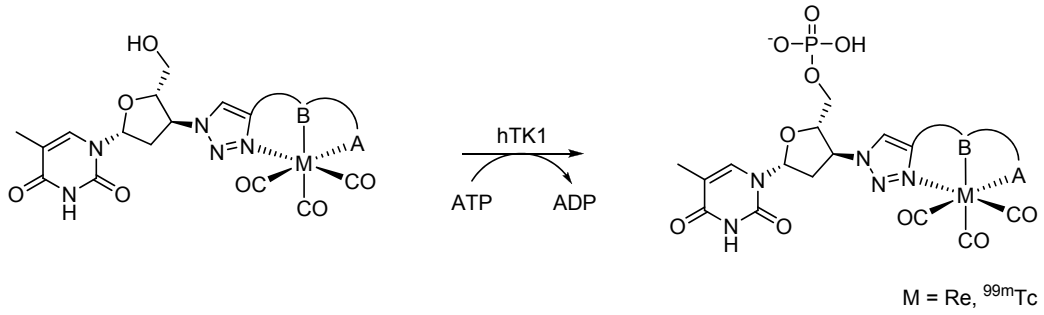

Scheme 4. Phosphorylation of C3′-functionalized ^{99m}Tc/Re(CO)$_3$-labelled thymidine derivatives.

In a second, direct assay the radioactive and non-radioactive complexes [^{99m}Tc/Re(CO)$_3$**X**] (**X** = **7**, **10**, **11**, **12**, **15**, **16**) were incubated with ATP and recombinant hTK1 only (Scheme 4). The enzymatic reactions were analysed by HPLC (UV-trace at λ = 254 nm for the rhenium complexes, γ-trace in the case of the radioactive Tc-99m complexes). For both the ^{99m}Tc and the Re compounds phosphorylation resulted in a measurable shift in retention time on a C_{18} reversed phase column (Figure 2) and the monophosphorylated products [^{99m}Tc/Re(CO)$_3$**X**]-**P** (**X** = **7**, **10**, **11**, **12**, **15**, **16**) were distinguished clearly from the starting material. In the case of the complex [Re(CO)$_3$**15**], the reaction mixture was purified by HPLC, and the fractions collected were analysed by mass spectroscopy. The fraction corresponding to the starting material showed a mass peak at *m/z* = 651.09, $[C_{18}H_{19}N_6O_9Re]H^+$. The more hydrophilic phosphorylated complex, [Re(CO)$_3$**15**]-**P**, revealed a mass peak at *m/z* = 731.03 $[C_{18}H_{20}N_6O_{12}PRe]H^+$. In time dependent HPLC experiments monitoring the

phosphorylation of complex [Re(CO)$_3$**15**], an increase in the concentration of the monophosphorylated species, [Re(CO)$_3$**15**]-**P**, and corresponding decrease in the concentration of the starting complex was observed (see Appendix C for more details).

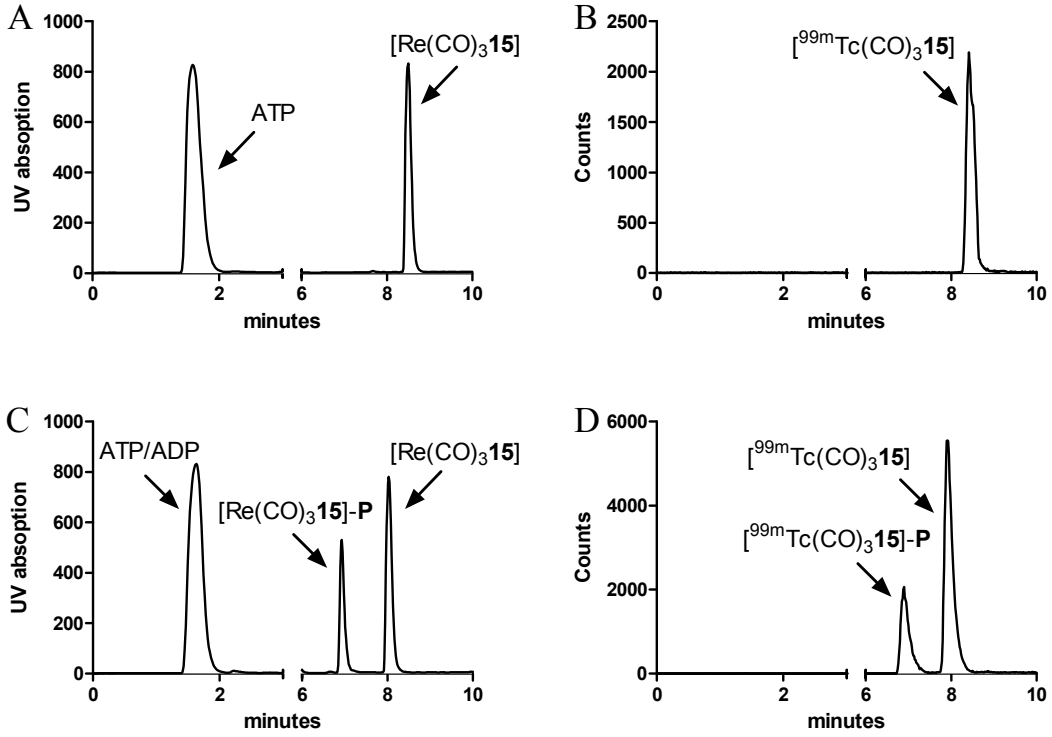

Figure 2. (A) UV-HPLC trace of rhenium complex [Re(CO)$_3$**15**] and ATP before addition of hTK1. (B) γ-HPLC trace of ^{99m}Tc complex [^{99m}Tc(CO)$_3$**15**] and ATP before addition of hTK1. (C) UV-HPLC trace of rhenium complex [Re(CO)$_3$**15**] and ATP after incubation with hTK1 for 1 h at 37 °C. (D) γ-HPLC trace of ^{99m}Tc complex [^{99m}Tc(CO)$_3$**15**] and ATP after incubation with hTK1 for 1 h at 37 °C.

Cell internalization experiments. hTK1 is located in the cytosol, and therefore a potential substrate has to pass through the cell membrane before it can be phosphorylated. If this transport is not achieved actively via nucleoside transporters then it must occur by passive diffusion.[24] This has been suggested as the major cell internalization route for the carborane-thymidine derivatives reported by Tjarks *et al*.[23] By analogy to the N3-functionalized carborane derivatives, we suspected passive diffusion would be the most likely cell internalization route of our N3-functionalized complexes. Similarly, by analogy to AZT, which is not recognized by the ubiquitously expressed human equilibrative nucleoside transporter type 1 (hENT1) and is transported

primarily by passive diffusion,[25] we expected our C3′-functionalized compounds to rely on passive diffusion to accumulate in cells.

In a preliminary study of the cell internalizing ability of the organometallic thymidine derivatives, we investigated the internalization of one $^{99m}Tc(CO)_3$-labelled complex from each series of compounds. The incorporation of the complexes $[^{99m}Tc(CO)_3\mathbf{11}]^+$ and $[^{99m}Tc(CO)_3\mathbf{12}]$ into two human glioblastoma cell lines were measured and compared with the incorporation of ^{125}I-iododeoxyuridine (^{125}IdUrd), using cell lines and conditions established for the incorporation of ^{125}IdUrd.[26,27] Internalization was measured with and without pretreatment with 5-fluorodeoxyuridine (FdUrd), which is known to increase uptake of 5-iododeoxyuridine by inhibiting endogenous thymidine synthesis and inducing upregulation of nucleoside transporters.[26,28] The results for both cell lines, U251 and LN229, and with and without 5-fluorodeoxyuridine pretreatment are presented in Table 2.

Table 2. Internalization into the human glioblastoma cell lines U251 and LN229, with and without pretreatment with 5-fluorodeoxyuridine, as a percentage of the initial activity added.

	U251		LN229	
	Internalization [%]	Internalization after pretreatment with FdUrd[a] [%]	Internalization [%]	Internalization after pretreatment with FdUrd[a] [%]
^{125}IdUrd	14.03 ± 1.69	59.29 ± 2.80	8.81 ± 0.43	39.40 ± 1.39
$[^{99m}Tc(CO)_3\mathbf{11}]^+$	0.13 ± 0.01	0.14 ± 0.01	0.12 ± 0.01	0.15 ± 0.01
$[^{99m}Tc(CO)_3\mathbf{12}]$	0.01 ± 0.00	0.02 ± 0.00	0.01 ± 0.00	0.01 ± 0.00

[a] Cells were incubated with 1 μM FdUrd for 1 hour before addition of the radioactive dT analogue.

The structural similarity between thymidine and ^{125}I-iododeoxyuridine means IdUrd is actively transported into cells, as competition experiments with thymidine show. However, in the absence of any pretreatment, *in vitro* ^{125}IdUrd uptake is relatively low as a result of competition from the endogenous nucleoside pool and a short biological half-life attributable to rapid *in vivo* catabolism and dehalogenation. Several groups have investigated the effect of thymidylate synthase inhibitors such as FdUrd on the DNA incorporation of IdUrd with a view to increasing the therapeutic efficacy of

radioactive IdUrd.[26,29] As shown in Table 2, incubation with 1 μM FdUrd for 1 hour before addition of ^{125}IdUrd leads to an approximately 4-fold increase in internalization of the radioactivity. It has been suggested that this is an absolute increase in the amount of ^{125}IdUrd per cell, rather than an accumulation of cells in the synthesis phase, which only becomes significant after 6 hours following exposure to FdUrd.[27] Unfortunately, neither of the ^{99m}Tc-labelled derivatives tested showed any significant uptake into either cell line. Pretreatment with FdUrd had no effect on the amount of radioactivity associated with the cells, which is further evidence that uptake is not mediated by nucleoside transporters.

4.4 Conclusions

Starting from two azido-functionalized thymidine derivatives, we were able to investigate the influence of the position of the metal complex on the substrate affinity, as well as the influence of charge on the relative phosporylation of two series of novel $M(CO)_3$-labelled thymidine derivatives. The "click-to-chelate" approach was used to synthesize thymidine derivatives functionalized with a tridentate chelator for the $M(CO)_3$ core (M = ^{99m}Tc, Re) at either the N3 or C3′ position of thymidine. All of the conjugates could be readily labelled with the $M(CO)_3$ precursors to form well-defined organometallic complexes, with differing sizes, lipophilicities and overall charges. Incubation of the $Re(CO)_3$ derivatives with ATP in the presence of hTK1 led to the formation of monophosphorylated organometallic thymidine derivatives, which were observed by HPLC and unambiguously identified by mass spectroscopy. In this way, we were able to show that all of the compounds tested, which vary in the position of the metal chelate, hydrophilicity, and overall charge, were substrates for hTK1. For each of the complexes the relative rate of phosphorylation was measured quantitatively compared to thymidine, the natural substrate for hTK1. We could show that for the two sets of compounds investigated the C3′-functionalized thymidine derivatives were on average more readily phosphorylated by hTK1 than the N3-functionalized derivatives. Furthermore, we have shown that the effect of the overall charge of the substrate is dependent on the position of the metal complex. For the N3-functionalized complexes, the neutral and cationic complexes showed similar rates of phosphorylation relative to

thymidine, whereas an anionic complex was less readily phosphorylated. In the case of the C3′-functionalized derivatives the neutral and anionic complexes had similar phosphorylation rates, whereas the cationic complexes were notably less readily phosphorylated.

Unfortunately, preliminary cell internalization experiments did not give promising results. The complexes were obviously too hydrophilic to internalize significantly by passive diffusion and the structure of thymidine had been perturbed significantly enough to prohibit active incorporation via nucleoside transporters. It seems unlikely that any of the current set of compounds will internalize sufficiently to be useful as a proliferation marker. As we have noted before in a similar study of technetium-labelled glucose analogues, the development of radiopharmaceuticals which rely on membrane proteins for active transport to their intracellular targets is complicated by the substrate specificity of the transporter. Target-specific radiopharmaceuticals, which target receptors which themselves facilitate internalization, would appear to show much more promise.

4.5 Experimental details

4.5.1 Chemistry

General methods. All chemicals were purchased from Sigma-Aldrich or Fluka, Buchs, Switzerland. All chemicals and solvents were of reagent grade and were used without further purification unless otherwise stated. The precursor *fac*-$[Re(CO)_3Br_3][NEt_4]_2$[30] was prepared according to the published procedure. $[Na][^{99m}TcO_4]$ was eluted from a $^{99}Mo/^{99m}Tc$-generator (Covidien, Petten) with a 0.9% saline solution. Reactions were monitored by HPLC or by thin-layer chromatography (TLC) using precoated silica gel 60 F_{254} aluminium sheets (Merck), and visualized by UV absorption or stained with a solution of ninhydrin in EtOH. Column chromatography was performed using silica gel 60 (Fluka; particle size 0.04-0.063 mm). Analytical HPLC was performed using a Merck-Hitachi L-7000 system equipped with an L-7400 tunable absorption detector and an XBridge™ C-18 reverse phase column (5 μM, 4.6 x 150 mm, Waters). HPLC solvents were either water with 0.1% TFA (solvent A) and MeCN (solvent B), or water

(solvent A) and MeOH (solvent B) (for purification of ^{99m}Tc complexes) with a flow rate of 1 mL/min. The gradient was as follows: 0-15 min: gradient from 95% A to 20% A; 15-20 min: gradient from 20% A to 95% A; 20-25 min 95% A. Sep-Pak® columns (Waters) were washed with methanol and water prior to use. Nuclear magnetic resonance spectra were recorded on a 400 MHz Bruker spectrometer. ^{1}H and ^{13}C chemical shifts are reported relative to residual solvent peaks or water as a reference. Values of the coupling constant, *J*, are given in Hertz (Hz). The following abbreviations are used for the description of ^{1}H-NMR spectra: singlet (s), doublet (d), triplet (t), quartet (q), multiplet (m), doublet of doublets (dd), broad singlet (bs). The chemical shifts of complex multiplets are given as the range of their occurrence. Infrared spectra were recorded on a Perkin Elmer Spectrum 100 FT-IR, with a universal ATR sampling accessory. Low resolution mass spectra were recorded with a Micromass Quattro micro^{TM} API LC-ESI using either the negative or positive ionization mode. High resolution mass spectra were recorded with a Bruker FTMS 4.7T BioAPEXII.

N3-Functionalized thymidine precursor

3',5'-Di-O-(tert-butyl-dimethyl-silanyl)thymidine. Thymidine (1.00 g, 4.13 mmol) and imidazole (1.18 g, 17.34 mmol) were dissolved in DMF (10 mL) and stirred for 5 minutes at room temperature. TBDMSCl (1.31 g, 8.67 mmol) was added and the reaction stirred at room temperature and followed by TLC. After 16 hours the reaction mixture was diluted with EtOAc (20 mL), and washed twice with 1 M $NaHCO_3$, and once with saturated NaCl. The aqueous phases were re-extracted with EtOAc. The organic phases were combined, dried over Na_2SO_4 and evaporated under reduced pressure to give the product as a colourless liquid (1.90 g, 98%). ^{1}H NMR ($CDCl_3$) δ 8.37 (s, 1H); 7.45 (d, *J* = 0.9, 1H); 6.30 (*J* =7.9, 5.8, 1H); 4.38 (m, 1H); 3.91 (m, *J* = 2.5, 2.4, 2.4, 1H); 3.84 (dd, *J* = 11.4, 2.5, 1H); 3.74 (dd, *J* = 11.4, 2.4, 1H); 2.22 (ddd, *J* = 13.1, 5.8, 2.6, 1H); 2.02-1.89 (m, 1H); 0.90 (s, 9H); 0.87 (s, 9H); 0.09 (s, 6H); 0.05 (s, 6H) ppm. ^{13}C NMR ($CDCl_3$) δ 163.52, 149.90, 135.53, 110.64, 87.69, 84.77, 72.21, 62.87, 41.24, 36.36, 31.07, 25.88, 25.68, 12.33, -4.69, -4.89, -5.34, -5.50 ppm. MS (ESI) *m/z* 941.35 (100%) $[C_{44}H_{84}N_4O_{10}Si_4]H^+$, 471.08 (75%) $[C_{22}H_{42}N_2O_5Si_2]H^+$.

3-(2-Bromoethyl)-3',5'-di-O-(tert-butyl-dimethyl-silanyl)thymidine. 3',5'-Di-O-(tert-butyl-dimethyl-silanyl)-thymidine (1.90 g, 4.04 mmol) was dissolved in DMF (10 mL). Cs_2CO_3 (4.40 g, 12.39 mmol) was added and the mixture was stirred for 5 minutes at room temperature. Dibromoethane (7.76 g, 41.28 mmol) was added and the reaction stirred at room temperature and followed by TLC. After 2 hours the reaction mixture was diluted with EtOAc (20 mL), and washed twice with 1 M $NaHCO_3$, and once with saturated NaCl. The aqueous phases were re-extracted with EtOAc. The organic phases were combined, dried over Na_2SO_4 and evaporated under reduced pressure. The crude product was purified by column chromatography with hexane and EtOAc (20%) to give the pure product as a colorless liquid (2.21 g, 95%). ^{1}H-NMR ($CDCl_3$) δ 7.48 (d, ^4J(H,H)=1.1, 1H); 6.36 (m, J=7.9, 5.8, 1H); 4.45-4.29 (m, 3H); 3.95 (m, 1H); 3.87 (dd, J =11.4, J=2.6, 1H); 3.76 (dd, J =11.4, J=2.4, 1H); 3.54 (t, J=7.2, 2H); 2.30-2.23 (m, 1H); 2.02-1.95 (m, 1H); 1.94 (s, 3H); 0.93 (s, 9H); 0.90 (s, 9H); 0.12 (s, 6H); 0.09 (s, 3H); 0.08 (s, 3H) ppm. ^{13}C-NMR ($CDCl_3$) δ 162.93, 150.48, 133.61, 109.88, 87.68, 85.26, 72.22, 62.85, 42.18, 41.41, 29.49, 27.25, 25.93, 25.73, 13.14, -4.69, -4.87, -5.43, -5.49 ppm. MS (ESI) *m/z* 578.97 (100%) $[C_{24}H_{45}N_2O_5Si_2]H^+$.

3-(2-Azidoethyl)-3',5'-di-O-(tert-butyl-dimethyl-silanyl)thymidine, 1a. 3-(2-Bromoethyl)-3′,5′-di-O-(tert-butyl-dimethyl-silanyl)thymidine (1.03 g, 1.78 mmol) was dissolved in MeCN (20 mL) and 10 equivalents of NaN_3 (1.16 g 17.8 mmol) were added. The reaction mixture was stirred at 80 °C for 16 hours and followed by TLC. After cooling to room temperature the solvent was removed under reduced pressure and the product extracted into EtOAc. and washed twice with water and once with saturated NaCl. The aqueous phases were re-extracted with EtOAc. The organic phases were combined, dried over Na_2SO_4 and evaporated under reduced the pressure to give the pure product as a colorless liquid (750 mg, 80%). ^{1}H-NMR ($CDCl_3$) δ 7.48 (d, J = 0.9, 1H); 6.36 (m, J = 7.9, 5.8, 1H); 4.40 (m, 1H); 4.19 (m, J = 6.3, 1.9, 2H); 3.94 (m, J = 2.4, 1H); 3.87 (dd, J = 11.4, 2.6, 1H); 3.76 (dd, J = 11.4, 2.3, 1H); 3.54 (t, J = 6.3, 2H); 2.30-2.23 (m, 1H); 2.02-1.95 (m, 1H); 1.93 (s, 3H); 0.92 (s, 9H); 0.89 (s, 9H); 0.19 (s, 6H); 0.08 (s, 3H); 0.07 (s, 3H) ppm. ^{13}C-NMR ($CDCl_3$) δ 163.5, 151.0, 134.0, 110.1, 88.0, 85.7, 72.4, 63.1, 48.6, 41.6, 40.0, 26.1, 25.9, 18.5, 18.1, 13.2, -4.5, -4.7, -5.2, -5.3 ppm. MS (ESI) *m/z* 540.65 $[C_{24}H_{45}N_5O_5Si_2]H^+$.

3-(2-Azidoethyl)thymidine (N3dT-N_3), 1. 3-(2-Azidoethyl)-3',5'-di-O-(tert-butyl-dimethyl-silanyl)thymidine (900 mg, 1.67 mmol) was dissolved in THF (20 mL). NBu_4F (1.16 g, 3.68 mmol) was added and the reaction was stirred at room temperature and followed by TLC. After two hours the solvent was removed under reduced pressure and a 1:1 mixture of water and EtOAc (40 mL) was added. The solvent was evaporated from the aqueous phase under reduced pressure and the crude product was purified by column chromatography with a mixture of CH_2Cl_2 and methanol (9%) to give the product as a colourless liquid (500 mg, 96%). ^{1}H-NMR (D_2O) δ 7.69 (d, *J* = 1.1, 1H); 6.30 (m, *J* = 6.7, 1H); 4.47 (m, *J* = 6.4, 4.2, 1H); 4.18 (m, *J* = 7.0, 5.4, 2H); 4.04 (m, *J* = 8.7, 3.8, 1H); 3.85 (dd, *J* = 12.5, 5.0, 1H); 3.77 (dd, *J* = 12.5, 3.6, 1H); 3.56 (t, *J* = 5.8, 2H); 2.44-2.32 (m, 2H); 1.92 (d, *J* =0.98, 3H). ^{13}C-NMR ($CDCl_3$) δ 166.03, 152.21, 136.44, 111.16, 87.24, 86.61, 71.01, 61.76, 49.50 (MeOH), 48.90, 40.94, 39.41, 12.88 ppm. MS (ESI) *m/z* 334.05 $[C_{12}H_{17}N_5O_5]Na^+$.

Alkynes, ***2-6***. N-Boc-2-prpargyl glycine, **2**, and 2-propargyl dimethyl malonate, **4**, are commercially available. Alkynes, **3** and **5** were prepared according to the published procedures,[16] alkyne **6** was prepared from the reaction of pyridine-2-methylamine (0.53 g, 4.89 mmol) and propargyl bromide (0.58 g, 4.89 mmol) in a solution of triethylamine (1.02 mL, 7.34 mmol) in MeCN (50 mL). The reaction mixture was stirred at 50 °C and followed by TLC. After 4 hours the solvent was removed and the reaction mixture purified by column chromatography with CH_2Cl_2 and MeOH (5%). The product was isolated as a yellow liquid (178 mg, 25%). Analytical data are in agreement with those already published.[16]

Triazole-containing ligands

General procedure A: Copper catalyzed azide-alkyne cyclycloaddition. The alkyne (1-2 equivalents) and azide (1 equivalent) were added to a 1:1 mixture of *t*BuOH and water to form a 0.1 mM solution. 0.1 equivalents of $Cu(OAc)_2.H_2O$ and 0.2 equivalents of sodium ascorbate were added and the mixture stirred at room temperature for 12 hours.

Compound 7. As per general procedure A, with **1a** (487 mg, 0.90 mmol) and **2** (192 mg, 0.90 mmol). The product was extracted into EtOAc and washed twice with saturated NaCl. The aqueous phases were re-extracted with EtOAc. The organic

phases were combined, dried over Na_2SO_4 and evaporated under reduced pressure. The crude product was purified by column chromatography with a mixture of CH_2Cl_2 and MeOH (5%) to give the Boc-protected triazole product as a colourless oil (335 mg, 49%). ^{1}H-NMR (CD_3OD) δ 7.79 (s, 1H), 7.56 (s, 1H), 6.22 (t, *J* = 6.7, 1H), 4.85 (s, 4H), 4.62 (t, *J* = 5.8, 2H), 4.46 (m, 1H), 4.36 (m, 2H), 4.25 (s, 1H), 3.92 (m, 1H), 3.84 (ddd, *J* = 23.7, 11.4, 3.2, 2H), 3.17 (s, 2H), 2.27-2.21 (m, 1H), 2.18–2.02 (m, 1H), 1.87 (s, 4H), 1.42 (s, 9H), 0.94 (s, 9H), 0.93 (s, 9H), 0.14 (s, 6H), 0.12 (s, 6H) ppm. ^{13}C-NMR (CD_3OD) δ 164.99, 152.00, 135.98, 110.61, 89.33, 87.16, 73.64, 64.16, 42.03, 28.85, 26.55, 26.34, 19.34, 18.92, 13.48, -4.38, -4.55, -5.12, -5.15 ppm. MS (ESI) *m/z* 753.29 $[C_{34}H_{60}N_6O_9Si_2]H^+$. The intermediate (300 mg, 0.40 mmol) was dissolved in MeOH (20 mL). Concentrated HCl (0.4 mL) was added and the mixture was stirred overnight at rt. The solvent was removed under reduced pressure, and the residue redissolved in a mixture of water and EtOAc (1:1, 15 mL). The aqueous phase was neutralized with 1 M NaOH and concentrated under reduced pressure. The crude product was purified by solid phase extraction using a Sep-Pak® column. The fractions containing the product were evaporated under reduced pressure to give **7** as a white powder (95 mg, 56%).^{1}H-NMR (D_2O) δ 7.75 (s, 1H), 7.47 (d, *J* = 0.9, 1H), 6.01 (t, *J* = 6.6, 1H), 4.53 (m, 2H), 4.27 (m, *J* = 6.4, 4.4, 1H), 4.19 (t, *J* = 5.4, 2H), 3.85 (m, 2H), 3.67 (dd, *J* = 12.5, 3.5, 1H), 3.58 (dd, *J* = 12.5, 5.1, 1H), 3.18 (dd, *J* = 15.7, 4.9, 1H), 3.09 (dd, *J* = 15.7, 7.3, 1H), 2.26-2.05 (m, 2H), 1.68 (s, 3H).ppm. ^{13}C-NMR (D_2O) δ 173.72, 165.71, 151.81, 142.76, 136.62, 125.91, 110.93, 87.46, 86.68, 70.91, 61.85, 55.14, 49.50 (MeOH), 48.70, 41.81, 39.38, 27.11, 12.70 ppm. High Res. MS (ESI) *m/z* 425.1776 $[C_{17}H_{24}N_6O_7]H^+$ (calc. 425.1779).

Compound 8. As per general procedure A, with **1a** (488 mg, 0.90 mmol) and **3** (180 mg, 0.84 mmol). The product was extracted into EtOAc and washed twice with saturated NaCl. The aqueous phases were re-extracted with EtOAc. The organic phases were combined, dried over Na_2SO_4 and evaporated under reduced pressure. The crude product was purified by column chromatography with a mixture of CH_2Cl_2 and MeOH (5%) to give the Boc-protected triazole product as a colourless oil (240 mg, 38%). ^{1}H-NMR ($CDCl_3$) δ 7.58 (s, 1H), 7.44 (d, *J* = 1.0, 1H), 6.23 (m, 1H), 4.61 (t, *J* = 6.0, 2H), 4.38 (m, 3H), 3.91 (q, *J* = 2.5, 1H), 3.84 (dd, *J* = 11.3, 2.5, 2H), 3.77 (s, 2H), 3.73 (dd, *J* = 11.3, 2.5, 1H), 3.29 (m, 2H), 2.61 (t, *J* = 6.6, 2H), 2.24-2.19 (m, 1H), 1.97-

192 (m, 1H), 1.86 (d, *J* = 1.0, 3H), 1.42 (s, 9H), 0.91 (s, 9H), 0.87 (s, 9H), 0.09 (s, 6H), 0.07 (s, 3H), 0.06 (s, 3H).ppm. ^{13}C-NMR ($CDCl_3$) δ 162.96, 150.46, 134.14, 122.15, 109.59, 87.69, 85.28, 71.93, 62.58, 53.51, 47.37, 41.43, 40.39, 39.32, 31.33, 28.11, 25.90, 25.71, 18.39, 17.95, 13.17, -4.64, -4.90, -5.40, -5.49 ppm. High Res. MS (ESI) *m/z* 777.3826 $[C_{34}H_{62}O_7N_6S]Na^+$ (calc. 777.3831). The intermediate (200 mg, 0.27 mmol) was dissolved in MeOH (14 mL). Concentrated HCl (0.28 mL) was added and the mixture was stirred overnight at rt. The solvent was removed under reduced pressure, and the residue redissolved in a mixture of water and EtOAc (1:1, 15 mL). The aqueous phase was neutralized with 1 M NaOH and concentrated under reduced pressure. The crude product was purified by solid phase extraction using a Sep-Pak® column. The fractions containing the product were evaporated under reduced pressure to give **8** as a colourless oil (100 mg, 89%).^{1}H-NMR (CD_3OD) δ 7.92 (s, 1H), 7.83 (d, *J* = 0.9, 1H), 6.17 (t, *J* = 6.6, 1H), 4.68 (t, 2H), 4.45-4.29 (m, 3H), 3.89 (m, 1H), 3.79 (dd, *J* = 12.0, 3.1, 1H), 3.76 (s, 2H), 3.72 (dd, *J* = 12.0, 3.7, 1H), 2.78 (t, *J* = 6.6, 2H), 2.59 (t, *J* = 6.6, 2H), 2.27-2.21 (m, 2H), 2.19-2.12 (m, 2H), 1.86 (d, *J* = 0.9, 3H) ppm. ^{13}C-NMR (CD_3OD) δ 165.18, 152.22, 146.90, 136.83, 125.10, 110.57, 89.06, 87.35, 72.07, 62.84, 42.01, 41.59, 41.37, 35.27, 25.94, 13.26 ppm. High Res. MS (ESI) *m/z* 427.1755 $[C_{17}H_{26}O_5N_6S]H^+$ (calc. 427.1758).

Compound 9. As per general procedure A, with **1a** (200 mg, 0.37 mmol) and **4** (63 mg, 0.37 mmol). The product was extracted into EtOAc and washed twice with saturated NaCl. The aqueous phases were re-extracted with EtOAc. The organic phases were combined, dried over Na_2SO_4 and evaporated under reduced pressure. The crude product was purified by column chromatography with a mixture of CH_2Cl_2 and MeOH (3%) to give the TBDMS and ester protected triazole product (194 mg, 74%). ^{1}H-NMR (CD_3OD) δ 7.43 (s, 1H), 6.24 (dd, *J* = 7.8, 5.8, 1H), 4.56 (t, *J* = 6.3, 2H), 4.37 (dd, *J* = 7.6, 4.9, 3H), 3.91 (q, *J* = 2.5, 1H), 3.84 (dt, *J* = 5.8, 5.1, 2H), 3.75 (t, *J* = 2.2, 1H), 3.72 (s, 7H), 3.28 (d, *J* = 7.6, 2H), 2.22 (ddd, *J* = 13.2, 5.8, 2.7, 1H), 1.95 (ddd, *J* = 13.2, 7.8, 6.1, 1H), 1.87 (d, *J* = 1.1, 3H), 0.91 (s, 9H), 0.88 (s, 9H), 0.09 (s, 6H), 0.06 (d, *J* = 3.8, 6H) ppm. ^{13}C-NMR (CD_3OD) δ 168.87, 162.94, 150.46, 143.77, 133.89, 122.44, 109.86, 87.69, 85.26, 71.93, 62.86, 52.46, 51.09, 47.38, 41.25, 25.78, 25.69, 24.70, 18.26, 17.69, 12.92, -4.99, -5.79 ppm. MS (ESI) *m/z* 710.25 $[C_{32}H_{55}N_5O_9Si_2]H^+$. The intermediate (190 mg, 0.27 mmol) was dissolved in MeOH (15 mL). Concentrated HCl

(0.3 mL) was added and the mixture was stirred overnight at rt. The solvent was removed under reduced pressure, and the residue redissolved in a mixture of water and EtOAc (1:1, 15 mL). The pH of the aqueous phase was increased to 12 with 1 M NaOH and stirred for a further 2 h at rt. After this time the mixture was neutralized with 1 M HCl before the solvent was removed under reduced pressure. The crude product was purified by solid phase extraction using a Sep-Pak® column. The fractions containing the product were evaporated under reduced pressure to give **9** as a white powder (86 mg, 70%). ^{1}H-NMR (CD_3OD) δ 7.69 (s, 1H), 7.61 (s, 1H), 6.13 (t, *J* = 6.5, 1H), 4.64 (m, 2H), 4.42 (dt, *J* = 6.4, 4.2, 1H), 4.34 (m, 2H), 4.05-3.94 (m, 1H), 3.82 (dd, *J* = 12.5, 3.5, 1H), 3.73 (dd, *J* = 12.5, 5.2, 1H), 3.35 (t, *J* = 7.8, 1H), 3.06 (d, *J* = 7.8, 2H), 2.40-2.17 (m, 2H), 1.84 (s, 3H) ppm. ^{13}C NMR (D_2O) δ 146.94, 136.31, 124.25, 110.63, 87.10, 86.74, 70.80, 61.67, 49.50 (MeOH) 39.35, 12.67. MS (ESI) *m/z* 453.84 $[C_{18}H_{23}N_5O_9]H^+$.

Compound 10. As per general procedure A, with **1** (144 mg, 0.46 mmol) and **5** (59 mg, 0.46 mmol). The solvent was removed and the residue redissolved in a mixture of CH_2Cl_2 and MeOH (10%). The crude product was purified by column chromatography with a mixture of CH_2Cl_2 and MeOH (10%) to give the ester protected triazole product (135 mg, 67%). ^{1}H-NMR (CD_3OD) δ 7.90 (s, 1H), 7.83 (d, *J* = 1.0, 1H), 6.17 (t, *J* = 6.6, 1H), 4.68 (t, *J* = 5.7, 2H), 4.37 (t, *J* = 5.6, 3H), 3.92-3.85 (m, 3H), 3.80 (dd, *J* = 12.0, 3.1, 1H), 3.74-3.70 (dd, *J* = 12.0, 3.8, 1H), 3.72 (s, 3H), 2.24 (ddd, *J* = 13.6, 6.2, 3.9, 1H), 2.16 (ddd, *J* = 11.4, 6.6, 1H), 1.85 (d, *J* = 1.0, 3H) ppm. ^{13}C-NMR (CD_3OD) δ 165.08, 152.25, 136.76, 125.04, 110.37, 88.96, 87.10, 71.92, 62.57, 43.87, 42.08, 41.54, 13.13 ppm. High Res. MS (ESI) *m/z* 439.1933 $[C_{18}H_{26}N_6O_7]H^+$ (calc. 439.1936). The intermediate (112 mg, 0.26 mmol) was dissolved in a mixture of H_2O (2 mL) and 1 M NaOH (0.5 mL) and stirred for 2 h at rt. The mixture was neutralized by addition of 1 M HCl, before being concentrated under reduced pressure. The crude product was purified by solid phase extraction using a Sep-Pak® column. The fractions containing the product were evaporated under reduced pressure to give **10** as a white solid (70 mg, 61%). ^{1}H-NMR (CD_3OD) δ 7.97 (s, 1H), 7.82 (s, 1H), 6.16 (t, *J* = 6.6, 1H), 4.68 (t, *J* = 5.6, 2H), 4.37 (m, 3H), 3.98 (s, 2H), 3.90 (q, *J* = 3.4, 1H), 3.79 (dd, *J* = 12.0, 3.1, 1H), 3.72 (dd, *J* = 12.0, 3.8, 1H), 3.31 (s, 2H), 2.25 (ddd, *J* = 13.5, 6.1, 3.8, 1H), 2.15 (ddd, *J* = 13.5, 6.6, 1H), 1.86 (s, 3H) ppm. ^{13}C-NMR (CD_3OD) δ 176.69, 165.06, 152.03,

145.19, 136.79, 125.45, 110.43, 88.81, 87.25, 71.77, 62.64, 52.00, 43.92, 41.88, 41.34, 13.07 ppm. High Res. MS (ESI) *m/z* 425.1776 $[C_{17}H_{24}N_6O_7]H^+$ (calc. 425.1779).

Compound 11. As per general procedure A, with **1** (280 mg, 0.90 mmol) and **6** (131 mg, 0.88 mmol). The product was extracted into EtOAc and washed twice with saturated NaCl. The aqueous phases were re-extracted with EtOAc. The organic phases were combined, dried over Na_2SO_4 and evaporated under reduced pressure. The crude product was purified by column chromatography with a mixture of CH_2Cl_2 and MeOH (5%) to give the pure triazole product as a yellow solid (220 mg, 55%).^{1}H-NMR (CD_3OD) δ 8.53 (d, *J* = 4.5, 1H), 7.96 (s, 1H), 7.86-7.77 (m, 2H), 7.48 (d, *J* = 7.8, 1H), 7.33 (m, 1H), 6.17 (t, *J* = 6.6, 1H), 4.69 (t, *J* = 5.6, 2H), 4.38 (t, *J* = 5.6, 2H), 4.37 (m, 1H), 3.96 (s, 4H), 3.87 (q, *J* = 3.4, 1H), 3.78 (dd, *J* = 12.0, 3.1, 1H), 3.71 (dd, *J* = 12.0, 3.7, 1H), 2.26-2.11 (m, 2H), 1.84 (s, 3H) ppm. ^{13}C-NMR (CD_3OD) δ 165.20, 159.35, 152.25, 150.18, 146.37, 138.93, 136.91, 125.44, 124.40, 124.12, 110.58, 89.06, 87.36, 72.07, 62.84, 53.95, 44.26, 42.13, 41.52, 18.52, 13.22 ppm. High Res. MS (ESI) *m/z* 458.2149 $[C_{21}H_{27}N_7O_5]H^+$ (calc. 458.2146).

Compound 12. As per general procedure A, with AZT (130 mg, 0.49 mmol) and **3** (137 mg, 0.64 mmol). The solvent was removed and the residue redissolved in a mixture of CH_2Cl_2 and MeOH (10%). The crude product was purified by column chromatography with a mixture of CH_2Cl_2 and MeOH (10%) to give the Boc protected triazole product (183 mg, 77%). ^{1}H-NMR (CD_3OD) δ 7.91 (s, 1H), 7.89 (s, 1H), 6.49 (t, *J* = 6.5, 1H), 5.39 (m, 1H), 4.33 (m, 1H), 4.25 (t, *J* = 5.4, 1H), 3.89 (dd, *J* = 12.2, 2.9, 1H), 3.77 (dd, *J* = 12.2, 3.1, 1H), 3.24 (dd, *J* = 14.6, 5.1, 1H), 3.13 (dd, *J* = 14.6, 6.6, 1H), 2.93-2.83 (m, 1H), 2.77-2.64 (m, 1H), 1.91 (s, 3H), 1.41 (s, 9H) ppm. ^{13}C-NMR (CD_3OD) δ 166.29, 152.10, 137.98, 124.35, 111.50, 86.66, 86.40, 80.54, 62.14, 61.07, 38.88, 28.82, 12.51 ppm. High Res. MS (ESI) *m/z* 481.2039 $[C_{20}H_{28}N_6O_8]H^+$ (calc. 481.2041). 485The intermediate (120 mg, 0.25 mmol) was dissolved in a mixture of CH_2Cl_2 (12.5 mL) and TFA (1.25 mL) and stirred overnight at rt. The solvent was removed under reduced pressure, and the residue redissolved in water (1 mL) and neutralized with 5 M NaOH. The crude product was purified by solid phase extraction using a Sep-Pak® column. The fractions containing the product were evaporated under reduced pressure to give **12** as a colourless oil (81 mg, 85%).^{1}H-NMR ($CDCl_3$) δ ^{1}H NMR (400 MHz, MeOD) δ 8.01 (s, 1H), 7.91 (s, 1H), 6.49 (t, *J* = 6.6, 1H), 5.42 (m,

1H), 4.36 (m, 2H), 3.91 (dd, *J* = 12.1, 3.0, 1H), 3.78 (dd, *J* = 12.1, 3.2, 1H), 3.43 (dd, *J* = 15.7, 5.0, 1H), 3.35 (d, *J* = 15.7, 7.3, 1H), 2.94-2.82 (m, 1H), 2.79-2.65 (m, 1H), 1.91 (s, 3H) ppm. ^{13}C-NMR (CD_3OD) δ 170.88, 166.50, 152.48, 142.79, 138.29, 124.79, 111.94, 86.90, 86.55, 62.44, 61.49, 53.79, 39.18, 27.32, 12.61 ppm. High Res. MS (ESI) *m/z* 381.1515 $[C_{15}H_{20}N_6O_6]H^+$ (calc. 381.1517).

Compound 13. As per general procedure A, with AZT (100 mg, 0.37 mmol) and **3** (150 mg, 0.70 mmol). The solvent was removed and the residue redissolved in a mixture of CH_2Cl_2 and MeOH (10%). The crude product was purified by column chromatography with a mixture of CH_2Cl_2 and MeOH (10%) to give the Boc protected triazole product (142 mg, 79%). ^{1}H-NMR (CD_3OD) δ H NMR (400 MHz, MeOD) δ 8.07 (s, 1H), 7.92 (d, *J* = 0.8, 1H), 6.48 (t, *J* = 6.4, 1H), 5.41 (dt, *J* = 8.6, 5.6, 1H), 4.37 (dt, *J* = 5.7, 3.0, 1H), 3.91 (dd, *J* = 12.3, 3.0, 1H), 3.84 (s, 2H), 3.78 (dd, *J* = 12.3, 3.2, 1H), 3.21 (t, *J* = 7.0, 2H), 2.92 (dt, *J* = 12.5, 6.1, 1H), 2.81-2.65 (m, 1H), 2.58 (t, *J* = 7.0, 2H), 1.91 (d, *J* = 0.8, 3H), 1.43 (s, 9H). ppm. ^{13}C-NMR (CD_3OD) δ 166.29, 152.39, 137.97, 111.50, 102.16, 86.67, 86.39, 62.12, 60.79, 38.89, 28.72, 12.50 ppm. High Res. MS (ESI) *m/z* 483.2018 $[C_{20}H_{30}N_6O_6S]H^+$ (calc. 483.2020). The intermediate (130 mg, 0.27 mmol) was dissolved in a mixture of CH_2Cl_2 (13.5 mL) and TFA (1.35 mL) and stirred overnight at rt. The solvent was removed under reduced pressure, and the residue redissolved in water (1 mL) and neutralized with 5 M NaOH. The crude product was purified by solid phase extraction using a Sep-Pak® column. The fractions containing the product were evaporated under reduced pressure to give **13** as a white powder (77 mg, 74%).^{1}H-NMR (CD_3OD) δ 8.08 (s, 1H), 7.90 (d, *J* = 0.8, 1H), 6.49 (t, *J* = 6.5, 1H), 5.42 (dt, *J* = 8.7, 5.2, 1H), 4.44-4.28 (m, 1H), 3.90 (dd, *J* = 12.2, 3.0, 1H), 3.85 (s, 2H), 3.79 (dd, *J* = 12.2, 3.2, 1H), 2.91 (t, *J* = 6.6, 2H), 2.93-2.86 (m, 1H), 2.78-2.72 (m, 1H), 2.69 (t, *J* = 6.6, 2H), 1.89 (d, *J* = 0.8, 3H). ppm. ^{13}C-NMR (CD_3OD) δ 167.49, 153.22, 146.98, 138.33, 124.15, 111.92, 86.84, 86.49, 62.41, 61.39, 50.00, 49.79, 49.58, 49.36, 49.15, 48.94, 48.72, 48.51, 40.92, 39.16, 33.91, 26.14, 12.72 ppm. High Res MS (ESI) *m/z* 383.1498 $[C_{15}H_{22}O_4N_6S]H^+$ (calc. 383.1496).

Compound 14. As per general procedure A, with AZT (70 mg, 0.26 mmol) and **4** (45 mg, 0.26 mmol). The solvent was removed and the residue redissolved in a mixture of CH_2Cl_2 and MeOH (10%). The crude product was purified by column chromatography with a mixture of CH_2Cl_2 and MeOH (5%) to give the ester protected triazole product

(109 mg, 95%). ^{1}H-NMR (CD_3OD) δ 7.90 (s, 1H), 7.90 (d, *J* = 1.1, 1H), 6.46 (t, *J* = 6.5, 1H), 5.38 (dt, *J* = 8.7, 5.5, 1H), 4.33 (dt, *J* = 5.9, 3.2, 1H), 3.92-3.85 (m, 2H), 3.75 (dd, *J* = 12.2, 3.2, 1H), 3.71 (s, 6H), 3.28 (d, *J* = 7.6, 2H), 2.88 (ddd, *J* = 13.9, 6.6, 5.6, 1H), 2.72 (ddd, *J* = 14.3, 8.5, 6.3, 1H), 1.91 (d, *J* = 1.1, 3H). ppm. ^{13}C-NMR (CD_3OD) δ 170.76, 166.69, 152.57, 145.56, 138.53, 124.12, 111.75, 86.89, 86.64, 62.42, 61.14, 53.35, 39.28, 25.85, 12.65 ppm. High Res. MS (ESI) *m/z* 438.1622 $[C_{18}H_{23}N_5O_8]H^+$ (calc. 438.1619). The intermediate (100 mg, 0.23 mmol) was dissolved in a mixture of MeOH (1 mL) and 1 M NaOH (1 mL) and stirred for 2 h at rt. The mixture was neutralized by addition of 1 M HCl, before being concentrated under reduced pressure. The crude product was purified by solid phase extraction using a Sep-Pak® column. The fractions containing the product were evaporated under reduced pressure to give **14** as a white solid (90 mg, 85%). ^{1}H-NMR (D_2O) δ 7.81 (s, 1H), 7.71 (d, *J* = 1.1, 1H), 6.42 (dd, *J* = 7.0, 6.0, 1H), 5.35 (dt, *J* = 8.7, 6.3, 1H), 4.42 (m, 1H), 3.87 (dd, *J* = 12.8, 3.2, 1H), 3.76 (dd, *J* = 12.8, 4.4, 1H), 3.37 (t, *J* = 7.8, 1H), 3.09 (d, *J* = 7.8, 2H), 2.95 (ddd, *J* = 13.0, 6.9, 1H), 2.79 (ddd, *J* = 13.0, 8.8, 5.7, 1H), 1.88 (d, *J* = 1.1, 3H) ppm. ^{13}C-NMR (D_2O) δ 177.87, 151.46, 146.98, 137.65, 122.60, 111.25, 85.47, 84.36, 60.53, 59.25, 58.31, 36.94, 26.39 ppm. MS (ESI) *m/z* 408.17 $[C_{16}H_{18}N_5O_8]^-$.

Compound 15. As per general procedure A, with AZT (200 mg, 0.74 mmol) and **5** (142 mg, 1.12 mmol). The solvent was removed and the residue redissolved in a mixture of CH_2Cl_2 and MeOH (10%). The crude product was purified by column chromatography with a mixture of CH_2Cl_2 and MeOH (10%) to give the ester protected triazole product (140 mg, 48%). ^{1}H-NMR (CD_3OD) δ 8.03 (s, 1H), 7.91 (d, *J* = 0.9, 1H), 6.48 (t, *J* = 6.5, 1H), 5.42 (dt, *J* = 8.6, 5.4, 1H), 4.36 (m, 1H), 3.92 (s, 2H), 3.90 (dd, *J* = 12.2, 3.0, 1H), 3.77 (dd, *J* = 12.2, 3.2, 1H), 3.72 (s, 3H), 3.46 (s, 2H), 2.97-2.83 (m, 1H), 2.80-2.66 (m, 1H), 1.91 (d, *J* = 0.9, 3H) ppm. ^{13}C-NMR (CD_3OD) δ 173.68, 166.61, 152.50, 147.09, 138.39, 124.29, 111.82, 86.85, 86.55, 62.29, 61.18, 52.45, 50.19, 44.39, 39.19, 12.62 ppm. MS (ESI) *m/z* 395.1674 $[C_{16}H_{22}N_6O_6]H^+$ (calc. 395.1674). The intermediate (100 mg, 0.25 mmol) was dissolved in a mixture of H_2O (2 mL) and 1 M NaOH (0.5 mL) and stirred for 2 h at rt. The mixture was neutralized by addition of 1 M HCl, before being concentrated under reduced pressure. The crude product was purified by solid phase extraction using a Sep-Pak® column. The fractions containing the product were evaporated under reduced pressure to give **15** as a white

solid (84 mg, 88%). ^{1}H-NMR (D_2O) δ 8.26 (s, 1H), 7.69 (s, 1H), 6.41 (t, *J* = 6.6, 1H), 5.42 (dt, *J* = 8.7, 5.8, 1H), 4.44 (dd, *J* = 9.5, 4.0, 1H), 4.39 (s, 2H), 3.87 (dd, *J* = 12.7, 3.3, 1H), 3.77 (dd, *J* = 12.7, 4.3, 1H), 3.60 (s, 2H), 2.94 (ddd, *J* = 13.0, 6.6, 1H), 2.80 (ddd, *J* = 14.7, 8.7, 6.2, 1H), 1.86 (s, 3H). ppm. ^{13}C-NMR (D_2O) δ 171.62, 167.14, 152.22, 138.98, 138.36, 126.49, 112.13, 86.24, 84.89, 61.21, 60.47, 49.50 (MeOH) 49.12, 41.69, 37.50, 12.15 ppm. High Res. MS (ESI) *m/z* 381.1519 $[C_{15}H_{20}N_6O_6]H^+$ (calc. 381.1517).

Compound 16. As per general procedure A, with AZT (85 mg, 0.32 mmol) and **6** (100 mg, 0.68 mmol). The product was extracted into EtOAc and washed twice with saturated NaCl. The aqueous phases were re-extracted with EtOAc. The organic phases were combined, dried over Na_2SO_4 and evaporated under reduced pressure. The crude product was purified by column chromatography with a mixture of CH_2Cl_2 and MeOH (5%) to give the pure triazole product as a crystalline yellow solid (92 mg, 69%). ^{1}H-NMR (CD_3OD) δ 8.53 (d, *J* = 4.5, 1H), 7.96 (s, 1H), 7.86-7.77 (m, 2H), 7.48 (d, *J* = 7.8, 1H), 7.36-7.29 (m, 1H), 6.17 (t, *J* = 6.6, 1H), 4.69 (t, *J* = 5.6, 2H), 4.38 (t, *J* = 5.6, 3H), 3.96 (s, 4H), 3.87 (q, *J* = 3.4, 1H), 3.78 (dd, *J* = 12.0, 3.1, 1H), 3.71 (dd, *J* = 12.0, 3.7, 1H), 2.26-2.11 (m, 2H), 1.84 (s, 3H) ppm. ^{13}C-NMR (CD_3OD) δ 166.76, 152.71, 138.36, 124.62, 111.90, 86.86, 86.58, 62.43, 61.46, 39.18, 12.63 ppm. High Res MS (ESI) m/z $[C_{19}H_{23}N_7O_4]H^+$. (calc. 414.1890).

Rhenium complexes. Tricarbonyl rhenium complexes were synthesized according to the following general procedure: One equivalent of thymidine containing ligand and one equivalent of $[ReBr_3(CO)_3][NEt_4]_2$were dissolved in a 1:1 mixture of MeOH and water to form a 0.1 M solution. In the reactions with ligands **9** and **14** the pH of the reaction mixture was adjusted to 7 with aqueous NEt_4OH. The reaction was stirred at 50 °C for 2 h and followed by HPLC. The solvents were removed under vacuum and the residue was purified by solid phase extraction using a Sep-Pak® column and a water-MeOH gradient to give the $Re(CO)_3$ complex as a white or off-white powder.

[Re(CO)$_3$7]. (55 mg, 95%). ^{1}H-NMR (CD_3OD) δ 8.08 (s, 1H), 7.85 (s, 1H), 6.20 (t, *J* = 6.6, 1H), 5.91-5.77 (m, 1H), 5.15 (d, *J* = 11.2, 1H), 4.78 (m, 2H), 4.48-4.34 (m, 2H), 4.08 (m, 1H), 3.92 (m, *J* = 3.3, 1H), 3.80 (dd, *J* = 12.0, 3.0, 1H), 3.73 (dd, *J* = 12.0, 3.8, 1H), 3.38 (m, 1H), 3.27 (dd, *J* = 17.6, 4.3, 1H), 2.39 (ddd, *J* = 13.6, 5.9, 3.6, 1H), 2.24-

2.18 (m, 1H), 1.89 (s, 3H) ppm. ^{13}C-NMR (DMSO) δ 198.26, 197.44, 196.44, 180.16, 162.49, 150.18, 142.22, 135.08, 126.16, 108.26, 87.38, 84.99, 69.95, 61.07, 50.69, 50.60, 48.57, 48.05, 25.97, 12.84 ppm. High Res MS (ESI) *m/z* 695.1106 $[C_{20}H_{23}N_6O_{10}Re]H^+$ (calc. 695.1107).

[Re(CO)$_3$8]Br. (20 mg, 74%). ^{1}H-NMR (CD_3OD) δ 8.26 (s, 1H), 8.22 (s, 1H), 7.88 (d, *J* = 0.9, 1H), 7.87 (d, *J* = 0.9, 1H), 6.27-6.22 (m, 1H), 6.21 (t, *J* = 6.5, 1H), 5.43 (bs, 1H), 5.37 (bs, 1H), 4.87-4.79 (m, 2H), 4.79-4.69 (m, 2H), 4.55-4.47 (m, 2H), 4.47-4.42 (m, 2H), 4.43-4.36 (m, 2H), 4.34 (dd, *J* = 7.6, 4.5, 1H), 4.30 (d, *J* = 3.5, 1H), 4.20 (d, *J* = 11.3, 1H), 4.16 (d, *J* = 11.2, 1H), 4.10 (bs, 2H), 3.93 (dd, *J* = 6.6, 3.3, 1H), 3.91 (dd, *J* = 6.7, 3.4, 1H), 3.81 (t, *J* = 2.8, 1H), 3.78 (t, *J* = 2.7, 1H), 3.76-3.72 (m, 1H), 3.72-3.68 (m, 1H), 3.05-2.88 (m, 3H), 2.88-2.76 (m, 2H), 2.76-2.61 (m, 1H), 2.47 (m, 1H), 2.41-2.29 (m, 1H), 2.27-2.19 (m, 4H), 1.88 (s, 3H), 1.87 (s, 3H) ppm. ^{13}C-NMR (CD_3OD) δ 165.44 (165.29), 152.51, 151.23 (150.97), 137.22 (137.04), 126.03 (125.90), 110.87, 89.10, 87.02, 72.50 (72.37), 63.06 (62.99), 51.44 (51.32), 44.90 (44.38), 42.82 (42.65), 41.14 (41.06), 38.92 (38.59), 34.38 (34.27), 13.11 ppm. High Res MS (ESI) *m/z* 697.1086 $[C_{20}H_{26}N_6O_8ReS]^+$ (calc. 697.1084).

[Re(CO)$_3$9]NEt$_4$. (67 mg, 65%). ^{1}H-NMR (CD_3OD) δ 8.06 (s, 1H), 7.76 (d, *J* = 1.0, 1H), 6.04 (t, *J* = 6.4, 1H), 4.79-4.68 (m, 2H), 4.51-4.42 (m, 1H), 4.40-4.34 (m, 2H), 3.88 (m, 1H), 3.78 (dd, *J* = 12.1, 3.3, 1H), 3.70 (dd, *J* = 12.1, 4.3, 1H), 3.56 (t, *J* = 4.3, 1H), 3.39 (d, *J* = 4.3, 2H), 3.34-3.25 (m, 8H), 2.28 (ddd, *J* = 13.8, 6.3, 4.0, 1H), 2.14-2.05 (m, 1H), 1.87 (d, *J* = 0.9, 3H), 1.33-1.25 (m, 12H) ppm. ^{13}C-NMR (CD_3OD) δ 164.66, 152.10, 147.03, 137.40, 128.06, 88.54, 87.76, 71.76, 62.64, 53.08, 41.86, 41.31, 12.99, 7.42 ppm. MS (ESI) *m/z* 721.90 $[C_{21}H_{21}N_5O_{12}Re]^-$.

[Re(CO)$_3$10]. (96 mg, 84%). ^{1}H-NMR (CD_3OD) δ 8.18 (s, 1H), 7.84 (m, 1H), 7.23-7.12 (m, 1H), 6.26 (m, 1H), 4.81-4.69 (m, 2H), 4.55-4.28 (m, 3H), 3.91 (m, 1H), 3.84-3.68 (m, 3H), 3.35-3.30 (m, 2H), 2.42-2.26 (m, 1H), 2.21 (m, 1H), 1.92-1.84 (m, 3H) ppm. ^{13}C-NMR (CD_3OD) δ 183.90, 165.23, 151.88, 149.46, 136.63, 124.91, 110.45, 88.82, 87.25, 86.96, 71.99, 62.64, 55.73, 53.58, 41.28, 12.98 ppm. High Res MS (ESI) *m/z* 695.1117 $[C_{20}H_{23}N_6O_{10}Re]H^+$ (calc. 695.1107).

[Re(CO)$_3$11]Br. (110 mg, 73%). ^{1}H-NMR (CD_3OD) δ 8.77 (t, *J* = 5.0, 1H), 8.01-7.93 (m, 2H), 7.97 (s, 1H), 7.84 (d, 1H), 7.63 (d, *J* = 8.0, 1H), 7.38 (t, *J* = 6.6, 1H), 6.12 (t,

J = 6.8, 1H), 4.80-4.55 (m, 4H), 4.49 (dd, *J* = 16.7, 8.1, 1H), 4.41 (dt, *J* = 6.1, 3.2, 1H), 4.37-4.21 (m, 3H), 3.99-3.92 (m, 1H), 3.81 (dd, *J* = 12.0, 3.1, 2H), 3.74 (dd, *J* = 12.0, 3.7, 2H), 2.28-2.12 (m, 2H), 1.84 (d, 3H) ppm. ^{13}C-NMR (CD_3OD) δ 164.98 (164.96), 161.85 (161.79), 153.48 (153.46), 152.12 (152.02), 150.64 (150.61), 141.48 (141.45), 136.86, 126.66, 124.57 (124.55), 124.49 (124.43), 110.58 (110.53), 89.10 (89.07), 87.08 (86.92), 72.33 (72.31), 63.96, 62.93 (62.91), 53.13 (53.07), 50.79 (50.56), 41.87 (41.67), 41.27 (41.19), 13.17 ppm. High Res MS (ESI) *m/z* 728.1470 $[C_{24}H_{27}N_7O_8Re]^+$ (calc. 728.1474).

[Re(CO)$_3$12]. (41 mg, 59%). ^{1}H-NMR (CD_3OD) δ 8.20 (s, 1H), 7.86 (s, 1H), 6.44 (t, *J* = 6.4, 1H), 5.90 (dd, *J* = 11.0, 5.8, 1H), 5.58-5.44 (m, 1H), 5.18 (d, *J* = 11.4, 1H), 4.45-4.32 (m, 1H), 4.11 (d, *J* = 3.9, 1H), 3.92 (dd, *J* = 12.2, 2.9, 1H), 3.81 (dd, *J* = 12.2, 3.1, 1H), 3.38 (dd, *J* = 16.0, 1H), 3.26 (dd, *J* = 4.2, 1H), 3.02-2.73 (m, 2H), 1.91 (s, 3H) ppm. ^{13}C-NMR (CD_3OD) δ 197.39, 196.67, 184.57, 166.45, 152.22, 144.06, 138.43, 126.48, 111.81, 86.97, 85.89, 62.30, 62.01, 52.78, 38.68, 27.39, 12.19 ppm. High Res MS (ESI) *m/z* 651.0846 $[C_{18}H_{19}N_6O_9Re]H^+$ (calc. 651.0844).

[Re(CO)$_3$13]Br. (17 mg, 61%). ^{1}H-NMR (CD_3OD) δ 8.41 (s, 1H), 7.88 (s, 1H), 6.48 (t, *J* = 6.3, 1H), 5.55 (m, 1H), 5.32 (bs, 1H), 4.60 (bs, 1H), 4.53 (d, *J* = 17.2, 1H), 4.56-4.47 (m, 1H), 4.24 (d, *J* = 17.2, 1H), 3.93 (dd, *J* = 12.0, 3.1, 1H), 3.86 (dd, *J* = 12.0, 1H), 3.04-2.96 (m, 1H), 2.95-2.87 (m, 1H), 2.92 (m, 2H), 2.86-2.74 (m, 1H), 2.27 (m, 1H) ppm. ^{13}C-NMR (CD_3OD) δ ^{13}C NMR (101 MHz, MeOD) δ 166.42, 152.40, 151.52, 138.40, 125.44, 111.65, 87.03, 86.92, 86.23, 85.88, 63.81, 63.66, 62.60, 62.37, 44.65, 39.03, 34.23, 12.61 ppm. High Res. MS (ESI) *m/z* 653.0818 $[C_{18}H_{22}N_6O_7ReS]^+$ (calc. 653.0822).

[Re(CO)$_3$14]NEt$_4$. (30 mg, 45%). ^{1}H-NMR (CD_3OD) δ 8.20 (s, 1H), 7.89 (d, *J* = 1.1, 1H), 6.46 (t, *J* = 6.4, 1H), 5.57-5.47 (m, 1H), 4.43 (dt, *J* = 6.1, 3.2, 1H), 3.95 (dd, *J* = 12.4, 3.0, 1H), 3.85 (dd, *J* = 12.4, 3.3, 1H), 3.61 (t, *J* = 4.7, 1H), 3.44 (d, *J* = 4.7, 2H), 3.37-3.28 (m, 8H), 3.06-2.93 (m, 1H), 2.84 (ddd, *J* = 14.3, 8.7, 5.8, 1H), 1.93 (d, *J* = 1.1, 3H), 1.35-1.27 (m, 12H) ppm. ^{13}C-NMR (CD_3OD) δ 198.32, 179.91, 179.88, 166.42, 152.23, 147.36, 138.48, 126.96, 111.65, 86.92, 86.10, 62.05, 62.03, 53.82, 53.31, 53.28, 53.25, 38.79, 27.02, 12.46, 7.59 ppm. MS (ESI) *m/z* 678.05 $[C_{19}H_{17}N_5O_{11}Re]^-$.

[Re(CO)$_3$15]. (58 mg, 83%). ^{1}H-NMR (CD_3OD) δ ^{1}H NMR (400 MHz, MeOD) δ 8.32 (s, 1H), 7.86 (d, *J* = 5.6, 1H), 6.46 (q, *J* = 6.8, 1H), 5.62-5.47 (m, 1H), 4.40 (dd, *J* = 5.2, 3.2, 1H), 4.36-4.22 (m, 2H), 3.88 (dd, 1H), 3.83-3.77 (m, 1H), 3.81 (d, *J* = 17.3, 1H), 3.38 (d, *J* = 17.3, 1H), 3.04-2.93 (m, 1H), 2.85-2.76 (m, 1H), 1.91 (s, 3H) ppm. ^{13}C-NMR (CD_3OD) δ 197.37, 196.71, 183.78, 166.35, 152.20, 149.87, 138.37, 124.04, 111.79, 86.68, 85.88, 62.93, 61.86, 56.29, 53.09, 38.38, 12.50 ppm. High Res MS (ESI) *m/z* 651.0838 $[C_{18}H_{19}N_6O_9Re]H^+$ (calc. 651.0844).

[Re(CO)$_3$16]Br. (64 mg, 55%). ^{1}H-NMR (CD_3OD) δ ^{1}H NMR (400 MHz, MeOD) δ 8.83 (t, *J* = 5.9, 1H), 8.15 (s, 1H, isomer A), 8.14 (s, 1H, isomer B), 8.00-7.91 (m, 1H), 7.82 (s, 1H), 7.60 (d, *J* = 7.9, 1H), 7.39 (dd, *J* = 13.2, 6.6, 1H), 6.38 (td, *J* = 6.6, 2.2, 1H), 5.40 (dt, *J* = 9.4, 4.9, 1H), 4.78 (d, *J* = 17.0, 1H), 4.69 (d, *J* = 17.0, 1H), 4.52 (d, *J* = 16.5, 1H), 4.40-4.31 (m, 1H, isomer B), 4.36 (d, *J* = 16.5, 1H), 4.17-4.05 (m, 1H, isomer A), 3.84 (dd, *J* = 12.1, 3.3, 1H, isomer B), 3.79 (dd, *J* = 12.2, 3.3, 1H, isomer A), 3.70 (dd, *J* = 12.1, 3.1, 1H, isomer B), 3.60 (dd, *J* = 12.2, 3.2, 1H, isomer A), 2.90-2.80 (m, 1H, isomer A), 2.72 (ddd, *J* = 14.4, 8.3, 6.4, 1H, isomer A), 2.63 (dd, *J* = 14.0, 7.2, 1H, isomer B), 2.48 (ddd, *J* = 14.1, 6.4, 4.8, 1H, isomer B), 1.90 (s, 3H) ppm. ^{13}C-NMR (CD_3OD) δ 166.27, 161.70, 153.16, 151.89, 150.24, 140.91, 137.97, 126.77, 124.37, 124.07, 111.80, 86.69, 86.48, 85.91, 85.65, 63.87, 63.45, 63.15, 62.27, 62.00, 52.77, 39.16, 38.39, 12.19 ppm. High Res MS (ESI) *m/z* 684.1214 $[C_{22}H_{23}N_7O_7Re]^+$ (calc. 684.1212).

Technetium-99m complexes. The 99m-technetium tricarbonyl complexes of ligands **7**, **10**, **11**, **12**, **15** and **16**, were synthesized according to the following general procedure: A solution of $[^{99m}Tc(CO)_3(H_2O)_3]^+$ (50 µL; ~500 MBq mL^{-1}) was added to a 10^{-3} M solution of the relevant ligand (50 µL) diluted with PBS (400 µL; pH 7.4) to give a final ligand concentration of 10^{-4} M. The reaction mixtures were heated for 45 min at 95 °C. The radioactive product was separated from unlabelled ligand by HPLC. The complexes were characterized by comparison of their HPLC retention times (γ-trace) with those of their rhenium analogues (UV-trace).

4.5.2 *In vitro* analysis

Phosphorylation transfer assays. Thymidine analogues $[Re(CO)_3$**7-16**$]^{0/+/-}$ were assayed at 37 °C for 1 hour in 200 µL of a mixture containing 162.3 µL water, 10 µL 1 M HEPES buffer (pH 7.5), 0.2 µL 1 M DTT, 0.5 µL 1 M $MgCl_2$, 2 µL 100 mM ATP, 5 µL hTK1 (~0.5 mg/mL) and 20 µL of a 10 mM solution of $[Re(CO)_3$**7-16**$]^{0/+/-}$. The reaction mixtures were quenched by addition of 800 µL 5 mM EDTA solution and analyzed by HPLC.

Thymidine analogues $[Re(CO)_3$**X**$]^{0/+}$ (**X** = **7**, **10**, **11**, **12**, **15**, **16**) were also assayed at 37 °C for 1 hour in 200 µL of a mixture containing 112.3 µL water, 10 µL 1 M HEPES buffer (pH 7.5), 0.2 µL 1 M DTT, 0.5 µL 1 M $MgCl_2$, 2 µL 100 mM ATP, 5 µL hTK1 (~0.5 mg/mL), 20 µL of a 10 mM solution of $[Re(CO)_3$**X**$]^{0/+}$ (**X** = **7**, **10**, **11**, **12**, **15**, **16**) and 50 µL of an aqueous solution of $[^{99m}Tc(CO)_3$**X**$]^{0/+}$ (**X** = **7**, **10**, **11**, **12**, **15**, **16**) (~100 kBq). The reaction mixtures were quenched by addition of 800 µL 5 mM EDTA solution and analyzed by HPLC.

Thymidine and thymidine analogues $[Re(CO)_3$**7-16**$]^{0/+/-}$ were assayed at 25 °C for 15 minutes in 200 µL of a mixture containing 155.38 µL water, 10 µL 1 M HEPES buffer (pH 7.5), 0.2 µL 1 M DTT, 0.42 µL 100 mM PEP, 0.5 µL 1 M $MgCl_2$, 7.2 µL 5 mM NADH, 2 µL 100 mM ATP, 0.6 µL pyruvate kinase (1350 U/mL), 0.7 µL lactate dehydrogenase (1420 U/mL), 5 µL hTK1 (~0.5 mg/mL) and 20 µL of a 10 mM solution of thymidine or the thymidine analogue $[Re(CO)_3$**7-16**$]^{0/+/-}$.

For each substrate the linear decrease in UV absorption at 340 nm was measured from 0 to 15 minutes. The gradients of the regression lines between 6 and 12 minutes were compared to thymidine, the phosphorylation of which was assumed to be 100%.

Cell lines and culture. The human glioblastoma cell lines were chosen for their different *p53* expression that could potentially provide them with different repair capacities or FdUrd resistance: U251 (American Type Culture Collection, ATCC) homozygous mutant and the heterozygous line LN229 (a gift from Prof. N. de Tribolet, Service of Neurosurgery, University Hospital, Geneva, Switzerland). Cells were cultured at 37 °C and 5% CO_2 in RPMI 1640 with glutamax I, supplemented with 10% heat-inactivated fetal bovine serum (Chemie Brunschwig AG, Basel, Switzerland),

penicillin (50 units/ml) and streptomycin (0.05 mg/mL; Life Technologies Inc., Grand Island, NY, USA), which was changed twice a week. Cell doubling times in culture flasks were measured by daily counting for 1 week, and were 24.6±2.3 h and 33.7±3.4 h for U251 and LN229, respectively ($n \geq 3$). Mycoplasma contamination is a potential source of increased nucleoside turnover and could therefore modulate FdUrd efficacy. All cells tested negative for four major potential mycoplasma contaminations (Mycoplasma Detection Kit, F. Hoffmann-La Roche Ltd, Basel, Switzerland). The maximal cell culture time after testing was 6 months.

^{125}I-IdUrd production. ^{125}I-IdUrd of high radiochemical purity was prepared from the precursor 5-tri-*n*-butyl-stannyl-2'-deoxyuridine and purified by SepPak® RP-18 cartridges using a modified version of a method originally described by Foulon *et al*.[31,32] Radiochemical purity was repeatedly verified by TLC using polyethyleneimine cellulose F strips (Merck, Darmstadt, Germany) with a mobile phase of 0.2 M ammonium bicarbonate and radioactivity reading on a Tracemaster 20 (Berthold, Bad Wildbad, Germany). In all experiments, ^{125}I-IdUrd represented >98% of overall ^{125}I activity. Contamination with unlabelled IdUrd was avoided in the production of ^{125}I-IdUrd. It was calculated that the standard activity of 5 kBq ^{125}I-IdUrd in 0.5 mL used in the incorporation experiments represented a concentration of 0.2 nM, though this is only an indicative value as it has not been experimentally verified.

Radioactive dT analogue incorporation assay. 24-well culture dishes were plated with 20,000 cells for LN229 and with 15,000 cells for U251. After 3 days, the exponentially growing cells were incubated for 2 h at 37 °C and 5% CO_2 with either 5 kBq ^{125}I-IdUrd, 10 kBq [^{99m}Tc(CO)$_3$**11**], or 10 kBq [^{99m}Tc(CO)$_3$**12**] in 0.5 mL medium. After this time the supernatant was removed and the cells were washed three times with PBS. The cells were detached with 300 µL of 1 M NaOH. Radioactivity was measured in a gamma counter (Wizard 3" 1480 automatic gamma counter, Wallac Oy, Turku, Finland) and the results expressed as a percentage of the initial activity added. In the FdUrd pre-treatment assay, cells were pre-treated with 1 µM FdUrd and incubated for 1 hour at 37 °C and 5% CO_2. After this time the supernatant was removed and the cells were washed twice with PBS (pH 7.4) before either 5 kBq ^{125}I-IdUrd, 10 kBq [^{99m}Tc(CO)$_3$**11**], or 10 kBq [^{99m}Tc(CO)$_3$**12**] was added in 0.5 mL fresh medium.

4.6 References

(1) Eriksson, S.; Kierdaszuk, B.; Munch-Petersen, B.; Oberg, B.; Johansson, N. G. *Biochem. Biophys. Res. Commun.* **1991**, *176*, 586-592.

(2) Schinazi, R. F.; Mead, J. R.; Feorino, P. M. *AIDS Res. Hum. Retrov.* **1992**, *8*, 963-990.

(3) Eriksson, S.; Munch-Petersen, B.; Johansson, K.; Eklund, H. *Cell. Mol. Life Sci.* **2002**, *59*, 1327-1346.

(4) Eriksson, S.; Wang, J. H. *Nucleos. Nucleot.* **1995**, *14*, 507-510.

(5) Al-Madhoun, A. S.; Johnsamuel, J.; Yan, J. H.; Ji, W. H.; Wang, J. H.; Zhuo, J. C.; Lunato, A. J.; Woollard, J. E.; Hawk, A. E.; Cosquer, G. Y.; Blue, T. E.; Eriksson, S.; Tjarks, W. *J. Med. Chem.* **2002**, *45*, 4018-4028.

(6) Byun, Y.; Thirumamagal, B. T. S.; Yang, W.; Eriksson, S.; Barth, R. F.; Tjarks, W. *J. Med. Chem.* **2006**, *49*, 5513-5523.

(7) Welin, M.; Kosinska, U.; Mikkelsen, N. E.; Carnrot, C.; Zhu, C. Y.; Wang, L. Y.; Eriksson, S.; Munch-Petersen, B.; Eklund, H. *Proc. Natl. Acad. Sci. U. S. A.* **2004**, *101*, 17970-17975.

(8) Lunato, A. J.; Wang, J. H.; Woollard, J. E.; Anisuzzaman, A. K. M.; Ji, W. H.; Rong, F. G.; Ikeda, S.; Soloway, A. H.; Eriksson, S.; Ives, D. H.; Blue, T. E.; Tjarks, W. *J. Med. Chem.* **1999**, *42*, 3378-3389.

(9) Johnsamuel, J.; Lakhi, N.; Al-Madhoun, A. S.; Byun, Y.; Yan, J. H.; Eriksson, S.; Tjarks, W. *Bioorg. Med. Chem.* **2004**, *12*, 4769-4781.

(10) Conti, P. S.; Alauddin, M. M.; Fissekis, J. R.; Schmall, B.; Watanabe, K. A. *Nucl. Med. Biol.* **1995**, *22*, 783-789.

(11) Shields, A. F.; Grierson, J. R.; Dohmen, B. M.; Machulla, H. J.; Stayanoff, J. C.; Lawhorn-Crews, J. M.; Obradovich, J. E.; Muzik, O.; Mangner, T. J. *Nat. Med.* **1998**, *4*, 1334-1336.

(12) Gardelle, O.; Roelcke, U.; Vontobel, P.; Crompton, N. E. A.; Guenther, I.; Blauenstein, P.; Schubiger, A. P.; Blattmann, H.; Ryser, J. E.; Leenders, K. L.; Kaser-Hotz, B. *Nucl. Med. Biol.* **2001**, *28*, 51-57.

(13) Mindt, T. L.; Struthers, H.; Brans, L.; Anguelov, T.; Schweinsberg, C.; Maes, V.; Tourwe, D.; Schibli, R. *J. Am. Chem. Soc.* **2006**, *128*, 15096-15097.

(14) Tornoe, C. W.; Christensen, C.; Meldal, M. *J. Org. Chem.* **2002**, *67*, 3057-3064.

(15) Kolb, H. C.; Sharpless, K. B. *Drug Discovery Today* **2003**, *8*, 1128-1137.

(16) Struthers, H.; Spingler, B.; Mindt, T. L.; Schibli, R. *Chem.--Eur. J.* **2008**, *14*, 6173-6183.

(17) Desbouis, D.; Struthers, H.; Spiwok, V.; Küster, T.; Schibli, R. *J. Med. Chem.* **2008**, *51*, 6689-6698.

(18) Yan, J. H.; Naeslund, C.; Al-Madhoun, A. S.; Wang, J. H.; Ji, W. H.; Cosquer, G. Y.; Johnsamuel, J.; Sjoberg, S.; Eriksson, S.; Tjarks, W. *Bioorg. Med. Chem. Lett.* **2002**, *12*, 2209-2212.

(19) Ogilvie, K. K. *Can. J. Chem.* **1973**, *51*, 3799-3807.

(20) Rostovtsev, V. V.; Green, L. G.; Fokin, V. V.; Sharpless, K. B. *Angew. Chem. Int. Ed.* **2002**, *41*, 2596-2599.

(21) Alberto, R.; Ortner, K.; Wheatley, N.; Schibli, R.; Schubiger, A. P. *J. Am. Chem. Soc.* **2001**, *123*, 3135-3136.

(22) Kornberg, A.; Pricer, W. E. *J. Biol. Chem.* **1951**, *193*, 481-495.

(23) Byun, Y.; Yan, J. H.; Al-Madhoun, A. S.; Johnsamuel, J.; Yang, W. L.; Barth, R. F.; Eriksson, S.; Tjarks, W. *J. Med. Chem.* **2005**, *48*, 1188-1198.

(24) Zhang, J.; Visser, F.; King, K. M.; Baldwin, S. A.; Young, J. D.; Cass, C. E. *Cancer Metastasis Rev.* **2007**, *26*, 85-110.

(25) Yao, S. Y. M.; Ng, A. M. L.; Sundaram, M.; Cass, C. E.; Baldwin, S. A.; Young, J. D. *Mol. Membr. Biol.* **2001**, *18*, 161-167.

(26) Dupertuis, Y. M.; Vazquez, M.; Mach, J. P.; De Tribolet, N.; Pichard, C.; Slosman, D. O.; Buchegger, F. *Cancer Res.* **2001**, *61*, 7971-7977.

(27) Perillo-Adamer, F.; Delaloye, A. B.; Genton, C. S.; Schaffland, A. O.; Dupertuis, Y. M.; Buchegger, F. *Eur. J. Nucl. Med. Mol. Imaging* **2006**, *33*, 613-620.

(28) Armstrong, R. D.; Diasio, R. B. *Cancer Res.* **1980**, *40*, 3333-3338.

(29) Lawrence, T. S.; Davis, M. A.; McKeever, P. E.; Maybaum, J.; Stetson, P. L.; Normolle, D. P.; Ensminger, W. D. *Cancer Res.* **1991**, *51*, 3900-3905.

(30) Alberto, R.; Egli, A.; Abram, U.; Hegetschweiler, K.; Gramlich, V.; Schubiger, P. A. *J. Chem. Soc., Dalton Trans.* **1994**, 2815-2820.

(31) Foulon, C. F.; Adelstein, S. J.; Kassis, A. I. *J. Nucl. Med.* **1996**, *37*, S1-S3.

(32) Schaffland, A. O.; Delaloye, A. B.; Kosinski, M.; Dupertuis, Y. M.; Buchegger, F. *Nucl. Med. Commun.* **2004**, *25*, 461-468.

Organometallic $\{Re(CO)_3\}^+$ and $\{Re(CO)_2(NO)\}^{2+}$ labelled substrates for human thymidine kinase 1: A side by side comparison of their substitution reactions and substrate activity

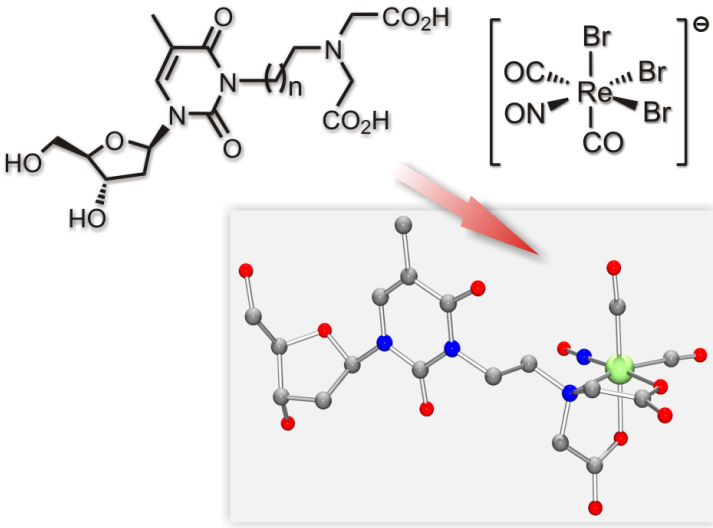

Inorganic Chemistry, **2009**, accepted

5.1 Abstract

Thymidine was functionalized at position N3 with a tridentate iminodiacetic acid (IDA) chelating system and a potentially tetradentate mercaptoethyliminodiacetic acid chelating system. Spacers of different length (ethyl and butyl) were introduced between the chelators and thymidine. The derivatives were labelled with the $\{Re(CO)_2(NO)\}^{2+}$ and $\{Re(CO)_3\}^{+}$ cores to give isostructural complexes with different overall charges. All complexes were analyzed by NMR, MS and IR, and in addition the x-ray structure of a $\{Re(CO)_2(NO)\}^{2+}$ labelled thymidine derivative functionalized at the N3 position was solved. The ligands incorporating the potentially tetradentate mercaptoethyl-iminodiacetic acid chelating system coordinated tridentately through iminodiacetic acid to both the $\{Re(CO)_2(NO)\}^{2+}$ core and the $\{Re(CO)_3\}^{+}$ core. This was surprising given that the reaction of $[Re(CO)_2(NO)Br_3]NEt_4$ with the model ligand ethylmercaptoethyl-iminodiacetic acid led to dissociation of a carbonyl ligand and formation of a monocarbonyl-mononitrosyl complex, as confirmed by x-ray structure analysis. All of the organometallic thymidine derivatives were substrates for hTK1. Neutral $Re(CO)_2(NO)$-labelled thymidine derivatives revealed substrate activity ranging from 24-40%, and the structurally analogous anionic $Re(CO)_3$-labelled thymidine derivatives from 20-38% compared with the natural substrate thymidine.

5.2 Introduction

Technetium-99m is the mainstay of diagnostic nuclear medicine using single photon emission computed tomography (SPECT). The optimal decay properties (γ-emission, 140 keV, $T_{1/2}$ = 6.0 hours) and ready availability at low cost are considerable advantages. In addition there are two medically interesting radionuclides of rhenium, rhenium-186 and rhenium-188, which are suitable for radionuclide therapy (mean β-emission energy of 0.8 MeV and 0.36 MeV, respectively, $T_{1/2}$ = 17 hours and 3.7 days, respectively). Over the last decade, our group has put much emphasis on the development and application of the organometallic precursors $[M(CO)_3(H_2O)_3]^+$ (M = ^{99m}Tc, ^{188}Re).[1,2] In fact, two $^{99m}Tc(CO)_3$ labelled compounds, a tumour affine neurotensin analogue and a vitamin B12 derivative, are currently in clinical phase I trials.[3,4] Buoyed by the success and properties of the $[^{99m}Tc(CO)_3(H_2O)_3]^+$ precursor, there has been a renewed interest in other low oxidation state organometallic cores of technetium as potential radiolabelling precursors.[5] A prominent example arises from the replacement of a carbonyl ligand by an isolobal nitrosyl ligand to give the $\{M(CO)_2(NO)\}^{2+}$ core (M = Tc, Re). Not only does the core have an additional positive charge, but the presence of a nitrosyl group is known to considerably effect transition metal centres and their coordination spheres.[6] For potential radiopharmaceutical applications, this may improve the pharmacokinetic profiles of compounds labelled with the $\{M(CO)_2(NO)\}^{2+}$ core compared to their $\{M(CO)_3\}^+$ labelled analogues. For example, the Valliant group recently reported a series of metallocarboranes, which were evaluated as ligands for the estrogen receptor.[7] Nitrosylation of the negatively charged $[Re(CO)_3L]^-$ compound to give the neutral compound $[Re(CO)_2(NO)L]$ resulted in a noticeable increase in receptor affinity.

The chemistry of mixed carbonyl-nitrosyl complexes of rhenium in organic solvents is well established,[8-11] and the chemistry in aqueous media has more recently been investigated.[12-15] A comparative study of the ligand exchange reactions of $[Re(CO)_3Br_3][NEt_4]_2$ and $[Re(CO)_2(NO)Br_3]NEt_4$ with a series of potential chelating systems revealed that stable complexes are formed with ligands containing carboxylic acids and aromatic and aliphatic amines.[14] A surprising result of this investigation was the dissociation of a carbonyl ligand to give monocarbonyl-mononitrosyl complexes of

the form [Re(CO)(NO)L] when the mixed carbonyl-nitrosyl precursor was reacted with ligands with four coordinating groups. Although the survey of ligands was small, the presence of at least two carboxylic acid groups has been suggested as a prerequisite for this behaviour.

We recently reported the first $M(CO)_3$-labelled substrates for human thymidine kinase 1 (hTK1).[16,17] Our interest in hTK1 is a result of the potential for selective targeting of proliferating cells due to often dramatically increased hTK1 activity.[18-20] The key to nucleoside metabolism is the rapid enzyme-mediated intracellular phosphorylation of nucleosides to nucleotides, which renders them unable to penetrate biological membranes and thus results in the "trapping" of phosphorylated nucleosides inside cells. Confirming recognition and phosphorylation by hTK1 is therefore the first step in the development of thymidine based radiopharmaceuticals. We are interested in the influence of the overall charge of $M(CO)_3$ thymidine derivatives on their substrate activity. In two independent studies we found that among the compounds tested, neutral and negatively charged thymidine complexes were better substrates than cationic derivatives. However, there were significant differences in the chelating systems of the cationic, neutral and negatively charged organometallic thymidine derivatives, and variation in their substrate activity as a result of structural differences cannot be excluded. We hypothesized that comparing derivatives labelled with the dicationic *fac*-$\{M(CO)_2(NO)\}^{2+}$ core with those labelled with the *fac*-$\{M(CO)_3\}^{+}$ core, while keeping the chelating systems constant, would provide a more accurate assessment of the influence of the charge of the organometallic thymidine derivative on its phosphorylation rate. For this purpose, thymidine was functionalized with an iminodiacetic acid chelating system and with the mercaptoethyliminodiacetic acid chelating system, and reacted with $[Re(CO)_3Br_3][NEt_4]_2$ and $[Re(CO)_2(NO)Br_3]NEt_4$. In parallel to these experiments, we investigated the general coordinative behaviour of the potentially tetradentate ligand ethylmercaptoethyliminodiacetic acid with the $Re(CO)_3$ and $Re(CO)_2(NO)$ cores under aqueous conditions.

5.3 Results and discussion

5.3.1 Functionalization of thymidine with iminodiacetic acid

Iminodiacetic acid (IDA) is a tridentate ligand, which is amenable to incorporation into biomolecules and further functionalization through the secondary amine. Tridentate coordination to the $\{M(CO)_3\}^+$ and $\{M(CO)_2(NO)\}^{2+}$ cores gives an anionic complex $[M(CO)_3IDA]^-$, in the case of the tricarbonyl core, and an isostructural but neutral complex $[M(CO)_2(NO)IDA]$ with the dicarbonyl-nitrosyl core. We functionalized thymidine with an iminodiacetic acid chelating system at the N3 position as previously described.[16] Two analogues were prepared with either a 2-carbon ($\mathbf{L^1}$) or 4-carbon ($\mathbf{L^2}$) spacer between thymidine and the metal chelator, as previous studies of the effect of spacer length on the rate of phosphorylation by our group and others have shown that increasing spacer length increases the relative amount of phosphorylation.[16,21]

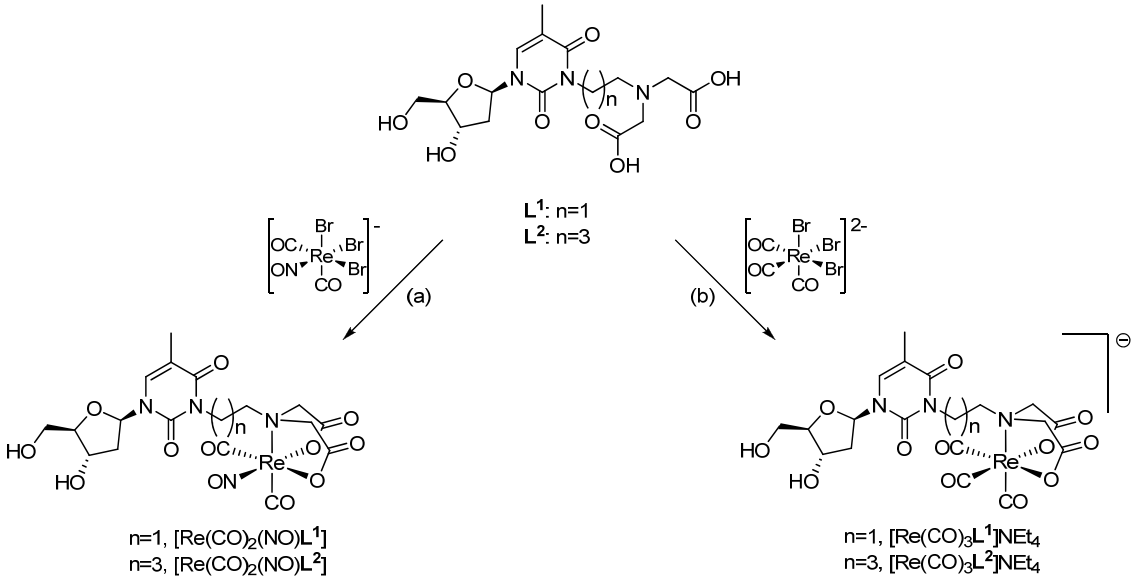

Scheme 1. Reactions of the thymidine derivatives $\mathbf{L^1}$ and $\mathbf{L^2}$ with the precursors $[Re(CO)_3Br_3][NEt_4]$ and $[Re(CO)_2(NO)Br_3]NEt_4$: (a) $MeOH/H_2O$, 60 °C, 2 h; (b) $MeOH/H_2O$, 60 °C, 12 h.

Ligands $\mathbf{L^1}$ and $\mathbf{L^2}$ were reacted with the precursors $[Re(CO)_3Br_3][NEt_4]_2$ and $[Re(CO)_2(NO)Br_3]NEt_4$ in mixtures of methanol and water (Scheme 1). The complex $[Re(CO)_3\mathbf{L^1}]$ had been prepared and characterized previously.[16] Synthesis and characterization of $[Re(CO)_3\mathbf{L^2}]$ gave similar results (see experimental section, 5.5.3).

The reactions with $[Re(CO)_2(NO)Br_3]NEt_4$ proceeded more slowly than those with $[Re(CO)_3Br_3][NEt_4]_2$, as has been observed with other ligand systems in comparative studies of the reactions of the two precursors.[14] For both $\mathbf{L^1}$ and $\mathbf{L^2}$, formation of the $Re(CO)_2(NO)$ complexes was reliably observed by HPLC after 6 hours heating at 60 °C. In the case of $[Re(CO)_2(NO)\mathbf{L^1}]$ the pure product precipitated as a pale yellow crystalline solid from the reaction mixture as the volume of solvent was reduced. The complex $[Re(CO)_2(NO)\mathbf{L^2}]$ was more soluble and could be purified from the reaction mixture by solid phase extraction. Salts were removed by washing well with water before the product was eluted with a mixture of water and methanol (20%). IR, NMR, mass spectroscopy and elemental analysis provided clear evidence for the formation of single structural isomers. The IR spectra are typical of dicarbonyl-nitrosyl rhenium complexes, with strong absorption bands at approximately 2100, 2000 and 1800 cm^{-1}, corresponding to the CO ligands and the NO group, respectively.

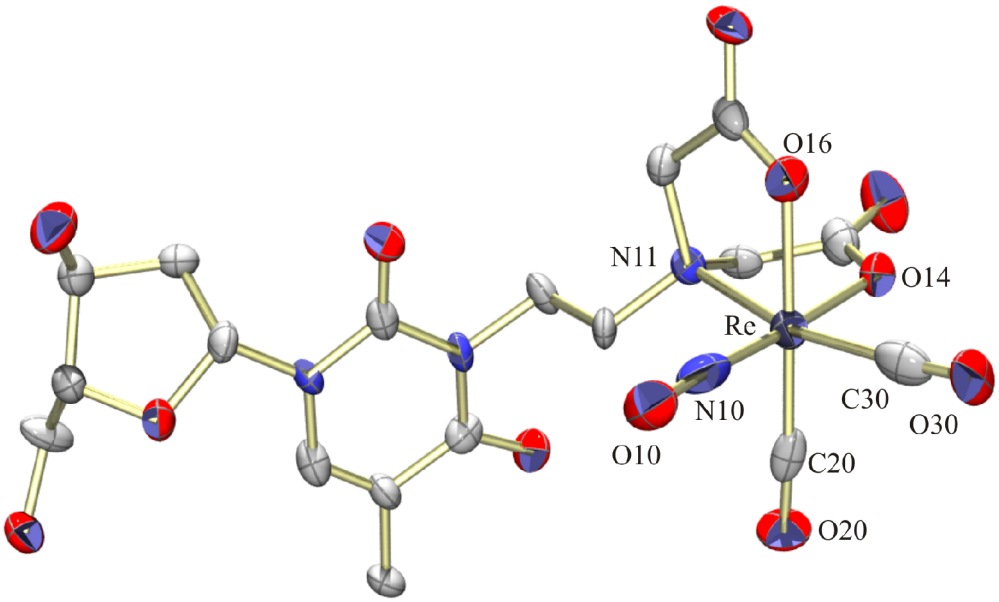

Figure 1. ORTEP-3[22] representation of the neutral complex $[Re(CO)_2(NO)\mathbf{L^1}]$ with thermal ellipsoids shown at 50% probability. Hydrogen atoms are omitted for clarity. Selected bond lengths [Å] and angles [°]: Re-N(10) 1.86(1), Re-C(20) 1.87(2), Re-C(30) 2.00(2), Re-O(14) 2.049(9), Re-O(16) 2.063(9), Re-N(11) 2.210(8), N(10)-Re-C(20) 91.1(5), N(10)-Re-C(30) 90.6(5), C(20)-Re-C(30) 93.1(5), N(10)-Re-O(14) 176.8(4), C(20)-Re-O(14) 92.1(4), C(30)-Re-O(14) 89.7(4), N(10)-Re-O(16) 93.5(4), C(20)-Re-O(16) 173.2(4), C(30)-Re-O(16) 91.9(5),

O(14)-Re-O(16) 83.3(3), N(10)-Re-N(11) 99.8(5), C(20)-Re-N(11) 94.4(4), C(30)-Re-N(11) 167.1(5), O(14)-Re-N(11) 79.5(4), O(16)-Re-N(11) 79.9(3).

Table 1. Crystal data and structure refinement for [$Re(CO)_2(NO)\mathbf{L}^1$] and [$Re(CO)(NO)\mathbf{L}^3$].

	$Re(CO)_2(NO)\mathbf{L}^1$	$Re(CO)(NO)\mathbf{L}^3$
formula	$C_{18}H_{21}N_4O_{12}Re$	$C_9H_{13}N_2O_6ReS$
*M*r	671.59	463.47
temperature [K]	173(2)	200(2)
wavelength [Å]	0.71069	0.71073
crystal size [mm^3]	0.18 x 0.077 x 0.020	0.4 x 0.05 x 0.05
crystal system	orthorhombic	monoclinic
space group	$P2_12_12_1$	$P2_1/c$
a [Å]	6.991(5)	13.419(1)
b [Å]	9.738(5)	6.827(1)
c [Å]	32.511(5)	14.785(1)
α [°]	90	90
β [°]	90	106.83(1)
γ [°]	90	90
volume [$Å^3$]	2213(2)	1296.5(2)
Z	4	4
density (calculated) [Mg m^{-3}]	2.015	2.375
absorption coefficient [mm^{-1}]	5.564	9.558
F(000)	1312	880
θ range for data collection [°]	2.44 – 26.77	2.88 – 29.48
reflections collected	16321	9112
independent reflections	4687 [R(int) = 0.0827]	3462 [R(int) = 0.0747]
completeness to θ [%]	99.3 (θ = 26.77°)	95.8 (θ = 29.48°)
absorption correction	integration	integration
max. and min. transmission	0.8874 and 0.6506	0.847 and 0.328
refinement method	full-matrix least squares on F^2	full-matrix least squares on F^2
data / restraints / parameters	4687 / 0 / 317	3462 / 0 / 172
goodness-of-fit on F^2	0.998	0.858
final R indices [$I>2\sigma(I)$]]	R1 = 0.0538, wR2 = 0.1214	R1 = 0.0377, wR2 = 0.0918
R indices (all data)	R1 = 0.0804, wR2 = 0.1330	R1 = 0.0686, wR2 = 0.1054
absolute structure parameter	0.00(2)	-
largest diff. peak and hole [e $Å^{-3}$]	1.154 and -1.358	1.444 and -3.167

The lack of symmetry in the *fac*-[Re(CO)$_2$(NO)] core caused the NCH$_2$ protons to appear as four doublets in the ^{1}H-NMR spectrum, two AB spin systems. Crystals of [Re(CO)$_2$(NO)**L^1**] suitable for x-ray analysis were obtained by dissolving the complex in hot water and allowing the solution to cool slowly to room temperature. The structure is shown in Figure 1 (crystallographic data are reported in Table 1) and as expected, as a stronger π-donor, a carboxylic acid is coordinated *trans* to the NO ligand. The coordination of the ligand to the metal core is in agreement with the published structure of [Re(CO)$_2$(NO)IDA].[14]

5.3.2 Reaction of the Re(CO)$_3$ and Re(CO)$_2$(NO) cores with ethylmercapto-ethyliminodiacetic acid, L^3

Ethylmercaptoethyliminodiacetic acid **L^3** (Scheme 2) is reported in the literature as a ligand for technetium (V),[23] and also as a bifunctional chelator for the M(CO)$_3$ core,[24] where it adopts κ*S*,κ*N*,κ*O*-coordination when it is amidically coupled through one of the carboxylic acids to a biomolecule. Until now, however, the coordinative behaviour of **L^3** has not been investigated with either the [M(CO)$_3$]$^+$ or the [M(CO)$_2$(NO)]$^{2+}$ core to model the situation where the chelator is coupled through the thioether to a biomolecule rather than through a carboxylic acid group.

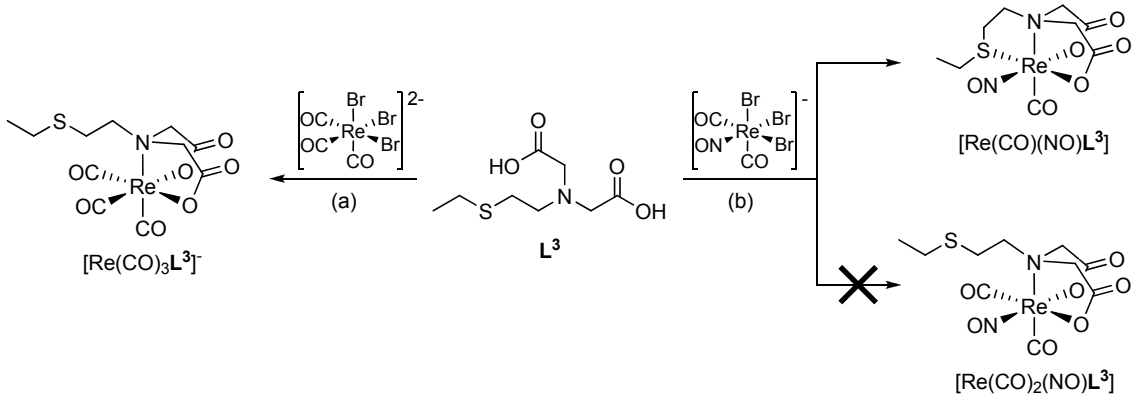

Scheme 2. Reaction of **L^3** with the precursors [Re(CO)$_3$Br$_3$][NEt$_4$] and [Re(CO)$_2$(NO)Br$_3$]NEt$_4$: (a) MeOH/H$_2$O, 60 °C, 2 h; (b) MeOH/H$_2$O, 60 °C, 12 h.

We synthesized and characterized the complex $[Re(CO)_3\mathbf{L^3}]^-$. Data from mass spectroscopy were in agreement with the data already published.[24] However, from NMR spectroscopic analyses we concluded that the ligand coordinates to the metal preferentially through iminodiacetic acid (adopting κ*O*,κ*N*,κ*O'*-coordination) and not through the thioether, amine and one of the carboxylic acids as previously suggested. Assignment of the nature of the coordination of the ligand is based on a comparison of the ^{1}H-NMR spectra of the free ligand and the complex. The ^{1}H-NMR spectrum of the free ligand $\mathbf{L^3}$ has a singlet corresponding to the four equivalent CH_2 protons of the acetic acid groups, which is replaced by two doublets in the spectrum of the complex, as the CH_2 protons are no longer equivalent (see also Figure 3 and Appendix D).

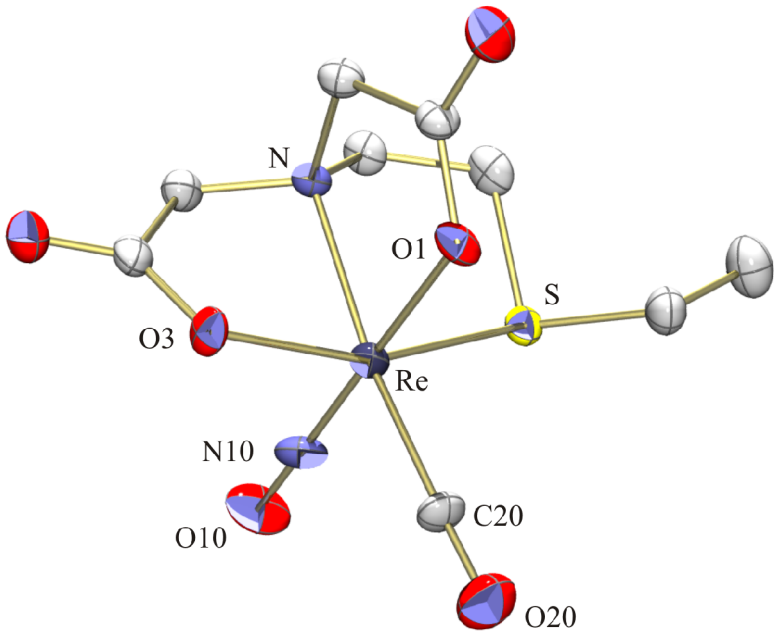

Figure 2. ORTEP-3[22] representation of the neutral complex $[Re(CO)_2(NO)\mathbf{L^3}]$ with thermal ellipsoids shown at 50% probability. Hydrogen atoms are omitted for clarity. Selected bond lengths [Å] and angles [°]: Re-N(10) 1.773(6), Re-C(20) 1.955(7), Re-O(1) 2.059(5), Re-O(3) 2.099(5), Re-N 2.161(6), Re-S 2.39(2), N(10)-Re-C(20) 91.6(3), N(10)-Re-O(1) 179.0(2), C(20)-Re-O(1) 88.6(3), N(10)-Re-O(3) 93.9(3), (20)-Re-O(3) 102.3(3), O(1)-Re-O(3) 87.0(2), N(10)-Re-N 100.1(3), C(20)-Re-N 168.3(3), O(1)-Re-N 79.7(2), O(3)-Re-N 76.7(2), N(10)-Re-S 90.3(2), C(20)-Re-S 95.8(2), O(1)-Re-S 88.75(16), O(3)-Re-S 161.29(15), N-Re-S 84.58(16).

When ligand $\mathbf{L^3}$ was reacted with $[Re(CO)_2(NO)Br_3]NEt_4$ in a mixture of methanol and water at 60 °C for 12 hours the dissociation of one of the carbonyl ligands and

formation of the neutral complex [Re(CO)(NO)$\mathbf{L^3}$] was observed (Scheme 2). The formation of a monocarbonyl-mononitrosyl complex was immediately apparent from the IR spectrum of the product which shows only one strong CO stretching band at 1971 cm^{-1} and an NO stretching band at 1709 cm^{-1}. As for the tricarbonyl complex, the ^{1}H-NMR spectrum is consistent with coordination of both carboxylic acids since the four equivalent NCH_2 protons of the iminodiacetic part of the ligand all become distinguishable in the spectrum of the complex, which in this case lacks symmetry. Similarly, coordination of the sulphur is assumed by a more complicated coupling pattern for the protons in the two CH_2 groups of the ethyl spacer between the amine and the thioether. The composition of the product was confirmed by mass spectroscopy and x-ray crystallography (Figure 2). Crystallographic data are reported in Table 1.

5.3.3 Synthesis of thymidine derivatives $\mathbf{L^4}$ and $\mathbf{L^5}$

Functionalization of thymidine with the mercaptoethyliminodiacetic acid chelating system and either a 2-carbon ($\mathbf{L^4}$) or 4-carbon ($\mathbf{L^5}$) spacer was achieved using a procedure similar to the synthesis of $\mathbf{L^1}$ and $\mathbf{L^2}$ (Scheme 3).[16] Thymidine was protected with the TBDMS protecting group to allow selective alkylation with a dibromoalkane at the N3 position and more ready purification of intermediates. Nucleophilic substitution with *N*-Boc-aminoethanethiol installed the thioether and amine components of the chelating system. The protected intermediates were then fully deprotected in a mixture of methanol and concentrated HCl. Selective alkylation of the primary amines was achieved with methyl bromoacetate in a mixture of acetonitrile and methanol. Ligands $\mathbf{L^4}$ and $\mathbf{L^5}$ were obtained by saponification with aqueous NaOH in methanol. The products were purified by solid phase extraction. Full details of the synthesis of all thymidine containing ligands can be found in the experimental section, 6.5.2.

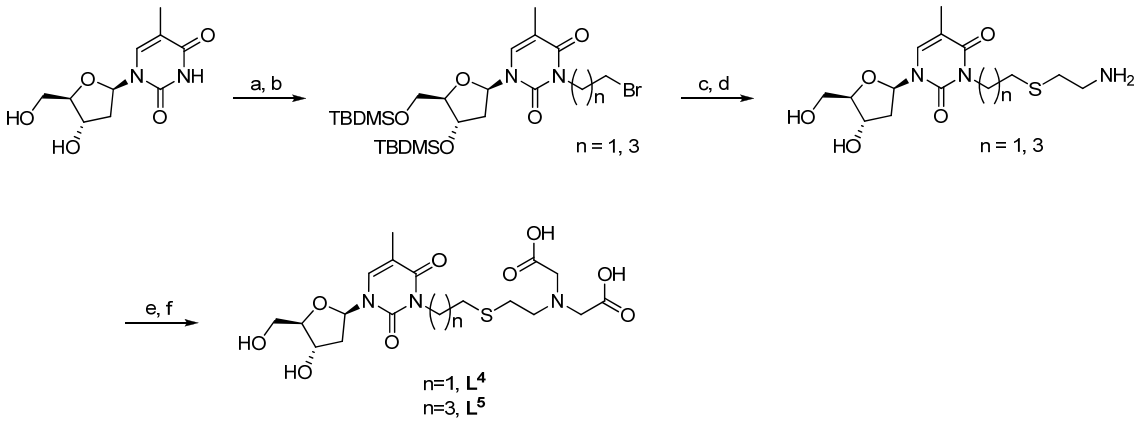

Scheme 3. Synthesis of thymidine containing ligands $\mathbf{L^4}$ and $\mathbf{L^5}$: (a) TBDMSCl, imidazole, DMF; (b) $Br(CH_2)_nBr$, Cs_2CO_3, DMF; (c) $HSCH_2CH_2NHBoc$, Cs_2CO_3, DMF; (d) HCl, MeOH; (e) $BrCH_2CO_2Me$, TEA, MeCN; (f) NaOH, H_2O.

5.3.4 Reactions with $[Re(CO)_2(NO)Br_3]NEt_4$ and $[Re(CO)_3Br_3]NEt_4$

Ligands $\mathbf{L^4}$ and $\mathbf{L^5}$ were reacted with the precursor $[Re(CO)_2(NO)Br_3]NEt_4$ in a mixture of water and methanol (Scheme 4). The reaction mixtures were heated at 60 °C for 6 hours and followed by HPLC. In the reaction with $\mathbf{L^4}$ a single product formed in quantitative yield, which could be isolated by solid phase extraction of the reaction mixture. In light of the model complex formed with $\mathbf{L^2}$, we had expected the product of the reaction with $\mathbf{L^4}$ to be a monocarbonyl-mononitrosyl complex. However, IR and mass spectroscopic analyses revealed the product complex to have retained the $Re(CO)_2(NO)$ core. Elemental analysis confirmed the composition of a neutral complex, suggesting the ligand was coordinated through the iminodiacetic acid part of the chelator (κ*N*,κ*O*,κ*O′*). This was supported by NMR analysis, which showed the four CH_2 protons of the acetic acid groups had all become distinguishable as a result of coordination to the metal centre. Furthermore, IR analysis of the product showed no evidence of an uncoordinated carboxylic acid. We postulated that a ligand with a longer spacer between thymidine and the metal chelating system might be more amenable to tetradentate coordination on steric grounds. However, in the reaction with $\mathbf{L^5}$, which has a butyl rather than an ethyl spacer between thymidine and the potentially tetradentate chelating system, the tridentate κ*N*,κ*O*,κ*O′* coordinated complex,

$[Re(CO)_2(NO)\mathbf{L^5}]$, was again the major product of the reaction. Characterization and analysis of the complex was consistent with an analogous structure to that of $[Re(CO)_2(NO)\mathbf{L^4}]$.

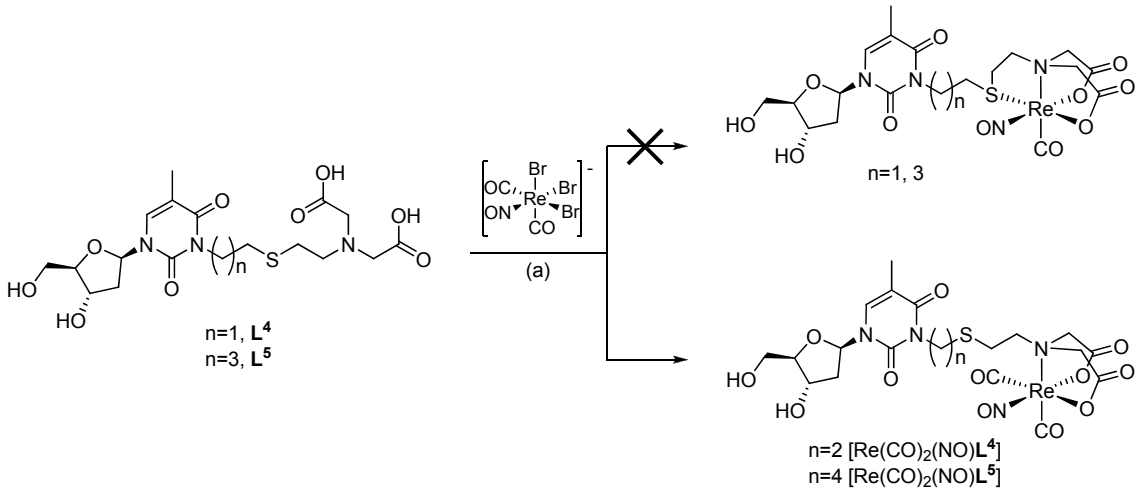

Scheme 4. Reactions of $\mathbf{L^4}$/$\mathbf{L^5}$ with $[Re(CO)_2(NO)Br_3]NEt_4$: (a) $MeOH/H_2O$, 60 °C, 12 h.

We investigated whether the dissociation of a carbonyl ligand was pH dependent in the cases of $\mathbf{L^4}$ and $\mathbf{L^5}$. Initially the reactions were carried out at pH 5, which led to the products described above. Both reactions were also performed at pH 3 and pH 8, however, in neither case did this have any impact on the HPLC trace of the reaction. Increasing the pH from 5 to 8 led only to a decrease in the yield of the reaction, as a result of the instability of the dicarbonyl-nitrosyl precursor in solution at higher pH, which is apparent from the darkening of the initially bright yellow reaction solution.

The $Re(CO)_3$ complexes of $\mathbf{L^4}$ and $\mathbf{L^5}$ were also synthesized and, as expected from the coordination complex formed with the model ligand $\mathbf{L^3}$, the ligands were coordinated in both cases through iminodiacetic acid to give anionic complexes. As for the model complex $[Re(CO)_3\mathbf{L^3}]^-$, the most convincing evidence for this mode of coordination comes from the ^1H NMR spectra of the complexes. As shown in Figure 3, the ^1H-NMR spectrum of the free ligand has a singlet at 3.77 ppm, with relative intensity 4, corresponding to the four equivalent CH_2 protons of the acetic acid groups. In the complex, the two protons of each CH_2 group become distinguishable. The protons appear as two doublets, each with intensity 2 as a result of the C_s symmetry of the

complex, and have a ^{2}J coupling constant of 16.4 Hz. Identical coupling patterns are seen in the ^{1}H-NMR spectra of complexes $[Re(CO)_3\mathbf{L^1}]NEt_4$ and $[Re(CO)_3\mathbf{L^2}]NEt_4$.

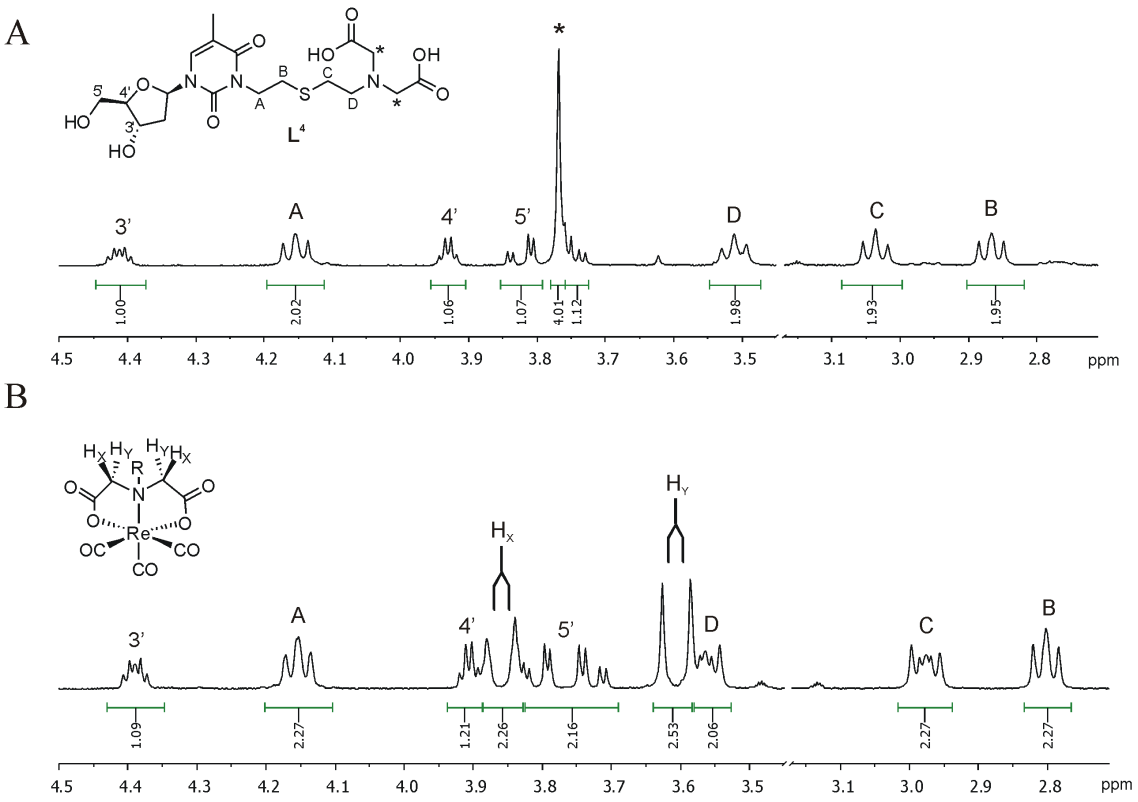

Figure 3. (A) Aliphatic region of the ^{1}H-NMR spectrum of $\mathbf{L^4}$ with numbering scheme and (B) aliphatic region of the ^{1}H-NMR spectrum of $[Re(CO)_3\mathbf{L^4}]^-$ and scheme for coordination of the ligand. The solvent signals ([D_4]MeOH) have been omitted for clarity.

5.3.5 *In vitro* evaluation of the organometallic complexes of the thymidine derivatives $\mathbf{L^1}$, $\mathbf{L^2}$, $\mathbf{L^4}$ and $\mathbf{L^5}$

The hTK1 substrate activities of the organometallic thymidine derivatives $[Re(CO)_3\mathbf{L^1/L^2}][NEt_4]$, $[Re(CO)_2(NO)\mathbf{L^1/L^2}]$, $[Re(CO)_3\mathbf{L^4/L^5}][NEt_4]$ and $[Re(CO)_2(NO)\mathbf{L^4/L^5}]$ were assessed using a coupled thymidine kinase-pyruvate kinase-lactate dehydrogenase UV assay (λ = 340 nm) as previously described (Scheme 5; see Appendix D for more details).[25,26] The results are presented in Table 2. The phosphorylation of thymidine (dT) was arbitrarily set to 100%.

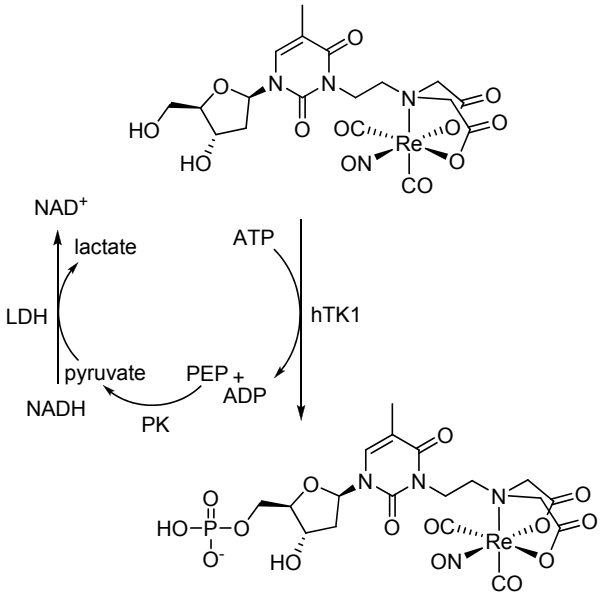

Scheme 5. Phosphorylation of $[Re(CO)_2(NO)\mathbf{L^1}]$ and coupled hTK1, PK, LDH assay.

The organometallic complex of $\mathbf{L^1}$, $[Re(CO)_3\mathbf{L^1}]^-$, showed a relative phosphorylation of 29.9 ± 2.0% compared to the natural substrate thymidine, which was slightly lower (33.8 ± 2.4%) than had been measured in our previous studies.[16] The isostructral neutral complex $[Re(CO)_2(NO)\mathbf{L^1}]$ revealed a very similar phosphorylation rate of 28.9 ± 2.4%. A more significant difference in substrate activity was observed between the anionic $Re(CO)_3$ derivative $[Re(CO)_3\mathbf{L^2}]^-$ (27.6 ± 2.7%) and the neutral $Re(CO)_2(NO)$ derivative $[Re(CO)_2(NO)\mathbf{L^2}]$ (40.2 ± 1.6%) which have a butyl spacer separating the metal complex and thymidine. This is presumably because the length of the spacer determines with which amino acid residues of the enzyme the metal complex interacts. On the other hand, the neutral derivatives $[Re(CO)_2(NO)\mathbf{L^4}/\mathbf{L^5}]$ (phosphorylation 24.4 ± 0.6% and 27.8 ± 2.1%, respectively) with the mercaptoethyliminodiacetic acid chelating system showed comparatively low relative phosphorylation compared to $[Re(CO)_2(NO)\mathbf{L^2}]$. This is contrary to the results obtained for the series of anionic $Re(CO)_3$-IDA-thymidine complexes $[Re(CO)_3\mathbf{L^1}/\mathbf{L^2}/\mathbf{L^5}]^-$ and a series of neutral $Re(CO)_3$-Cys-thymidine complexes, where a continuous increase in substrate activity was observed as the spacer was elongated.[16] For reasons which are not yet known, the phosphorylation of complex $[Re(CO)_3\mathbf{L4}]^-$ is not consistent with this trend. Whether the differences in the chelating system, spacer or the metal core are responsible for these controversial results needs to be investigated further.

Table 2. Phosphorylation of organometallic thymidine derivatives relative to dT [%][a]

Compound	$[Re(CO)_3\mathbf{L}][NEt_4]$	$[Re(CO)_2(NO)\mathbf{L}]$
$\mathbf{L^1}$	29.9 ± 2.0	28.9 ± 2.4
$\mathbf{L^2}$	27.6 ± 2.7	40.2 ± 1.6
$\mathbf{L^4}$	19.9 ± 2.4	24.4 ± 0.6
$\mathbf{L^5}$	38.3 ± 1.3	27.8 ± 2.1

[a] Mean ± SD values are based on three experiments per compound. The phosphorylation of dT was arbitrarily set to 100%.

5.4 Conclusions

The use of isostructural but differently charged organometallic precursors and complexes is a valuable tool for the evaluation of the influence of charge on substrate affinity, since structural differences arising from the use of different ligand systems can be avoided. Isostructural neutral and anionic organometallic $Re(CO)_2(NO)$- and $Re(CO)_3$-labelled complexes of N3-functionalized thymidine derivatives were synthesized and characterized. Derivatives $\mathbf{L^4}$ and $\mathbf{L^5}$, functionalized with a potentially tetradentate mercaptoethyliminodiacetic acid chelator, revealed exclusively tridentate coordination through the iminodiacetic acid part of the chelating system with both the tricabonyl and the dicarbonyl-mononitrosyl precusor. This is surprising in the case of the $\{Re(CO)_2(NO)\}^{2+}$ core, since the reaction of the model ligand ethylmercaptoethyliminodiacetic acid, $\mathbf{L^3}$, with $[Re(CO)_2(NO)Br_3]NEt_4$ induced dissociation of one of the carbonyl ligands and led exclusively to the formation of the complex $[Re(CO)(NO)\mathbf{L^3}]$.

In the case of the tridentate IDA-functionalized derivative $\mathbf{L^1}$ both the neutral and anionic thymidine derivatives were equally good substrates for hTK1, with relative phosphorylation rates of 28.9% and 29.9% compared with the value for the natural substrate. The neutral derivatives $[Re(CO)_2(NO)\mathbf{L^4}/\mathbf{L^5}]$ which are structurally similar to $[Re(CO)_2(NO)\mathbf{L^1}/\mathbf{L^2}]$, but have a longer, sulphur-containing spacer were also substrates for hTK1. However, increasing the spacer length did not lead to higher substrate

activity. Thus, the substrate activity of organometallic rhenium thymidine derivatives appears to be influenced by a combination of multiple parameters including charge, chelating system, spacer length and spacer composition, as well as other factors such as subtle changes of the metal core.

5.5 Experimental details

5.5.1 General methods

All chemicals were purchased from Sigma-Aldrich or Fluka, Buchs, Switzerland. All chemicals and solvents were of reagent grade and were used without further purification unless otherwise stated. The precursors *fac*-$[Re(CO)_2(NO)Br_3]NEt_4$[8-11] and *fac*-$[Re(CO)_3Br_3][NEt_4]_2$[27] were prepared according to published procedures. Reactions were monitored by HPLC or by thin layer chromatography (TLC) using precoated silica gel 60 F_{254} aluminium sheets (Merck), and visualized by UV absorption or stained with a solution of ninhydrin in EtOH. Column chromatography was performed using silica gel 60 (Fluka; particle size 0.040-0.063 mm). Analytical and semi-preparative HPLC were performed using a Merck-Hitachi L-7000 system equipped with an L-7400 tunable absorption detector and either an XBridge™ C-18 reverse phase column (5 µM, 4.6 x 150 mm, Waters) or an XBridge™ Prep C-18 reverse phase column (5 µM, 10 x 150 mm, Waters). HPLC solvents were water with 0.1% TFA (solvent A) and MeCN (solvent B) with a flow rate of 1 mL/min for analytical HPLC and 3 mL/min for semi-preparative HPLC. The analytical system was as follows: 0-15 min: gradient from 95% A to 20% A; 15-20 min: gradient from 20% A to 95% A; 20-25 min 95% A. The semi-preparative system was as follows: 0-14 min: gradient from 85% A to 40% A; 14-16 min: gradient from 40% A to 85% A; 16-17 min 85% A. Sep-Pak® columns (Waters) were washed with methanol and water prior to use. Nuclear magnetic resonance spectra were recorded on a 400 MHz Bruker spectrometer. ^{1}H and ^{13}C chemical shifts are reported relative to residual solvent peaks or water as a reference. The chemical shifts of complex multiplets are given as the range of their occurrence. Infrared spectra were recorded on a Perkin Elmer Spectrum 100 FT-IR, with a universal ATR sampling accessory. Low resolution mass spectra were recorded with a Micromass Quattro

micro^{TM} API LC-ESI using either the negative or positive ionization mode. High resolution mass spectra were recorded with a Bruker FTMS 4.7T BioAPEXII.

5.5.2 Ligand synthesis

The syntheses of $\mathbf{L^1}$, $\mathbf{L^2}$, $\mathbf{L^4}$ and $\mathbf{L^5}$ are outlined in Scheme 6. Ethylmercapto-ethyliminodiacetic acid $\mathbf{L^3}$ was prepared according to a literature procedure.[24]

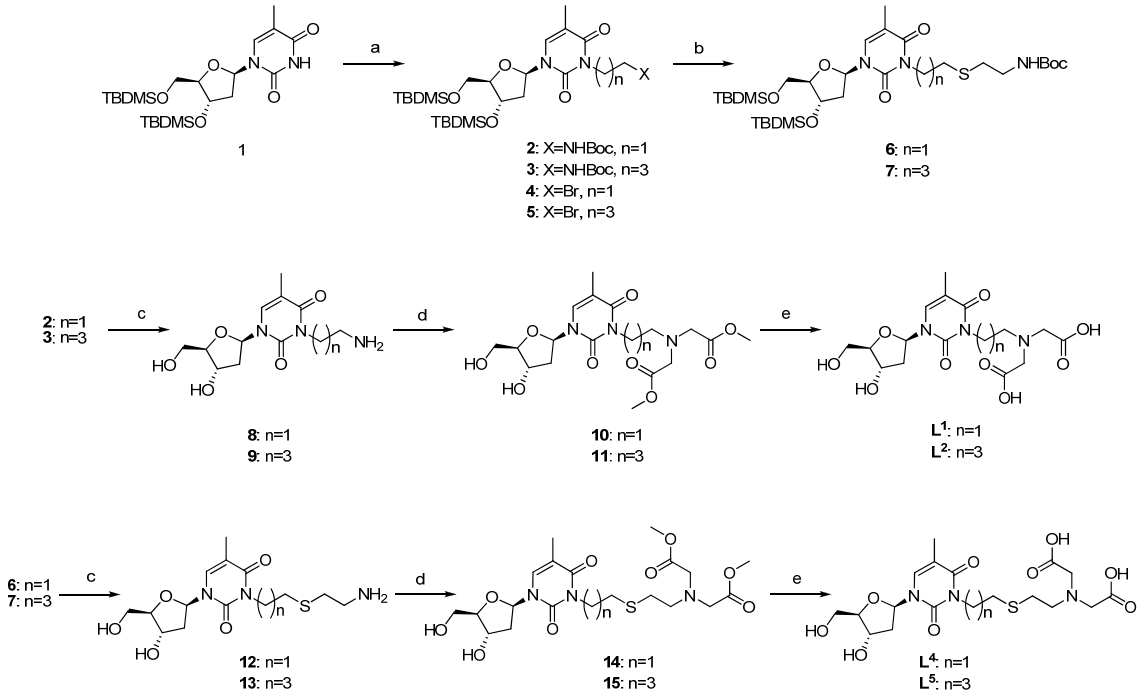

Scheme 6. Synthesis of thymidine containing ligands $\mathbf{L^3}$-$\mathbf{L^6}$: (a) $Br(CH_2)_nX$, Cs_2CO_3, DMF; (b) $HSCH_2CH_2NHBoc$, Cs_2CO_3, DMF; (c) HCl, MeOH; (d) $BrCH_2CO_2Me$, TEA, MeCN; (e) NaOH, H_2O.

Compound 1. Thymidine (1.00 g, 4.13 mmol) and imidazole (1.18 g, 17.34 mmol) were dissolved in DMF (10 mL) and stirred for 5 min at rt. TBDMSCl (1.31 g, 8.67 mmol) was added and the reaction stirred overnight at rt. After work-up, the crude product was purified by column chromatography with CH_2Cl_2 and MeOH (5%) to give 1 as a colorless liquid (1.90 g, 98%). ^{1}H NMR ($CDCl_3$) δ 8.37 (s, 1H), 7.45 (d, J = 0.9 Hz, 1H), 6.30 (m, J = 7.9, 5.8 Hz, 1H), 4.38 (m, 1H), 3.91 (m, J = 2.5, 2.4, 2.4 Hz, 1H), 3.84 (dd, J = 11.4, 2.5 Hz, 1H), 3.74 (dd, J = 11.4, 2.4 Hz, 1H), 2.22 (ddd, J = 13.1,

5.8, 2.6 Hz, 1H), 2.02-1.89 (m, 1H), 0.90 (s, 9H), 0.87 (s, 9H), 0.09 (s, 6H), 0.05 (s, 6H) ppm. ^{13}C NMR ($CDCl_3$) δ 164.3, 150.8, 136.2, 111.5, 88.5, 85.5, 73.0, 63.7, 42.1, 19.1, 18.7, 13.2, 26.4, -4.0, -4.7 ppm. MS *m/z* 941.35 $[C_{44}H_{84}N_4O_{10}Si_4]H^+$, 471.08 $[C_{22}H_{42}N_2O_5Si_2]H^+$.

General procedure A: Alkylation of **1**

1 was dissolved in DMF (2.5 mL/mmol). Cs_2CO_3 was added and the mixture was stirred for 5 min at rt. After addition of the $X(CH_2)_nBr$, the reaction was stirred for 2 h at rt. The reaction mixture was diluted with EtOAc (5 x reaction volume), washed with water (5 x reaction volume) and twice with 1 M $NaHCO_3$ (5 x reaction volume). The aqueous phases were re-extracted with EtOAc. The organic phases were combined, dried over Na_2SO_4 and evaporated under reduced pressure. The crude product was purified by column chromatography.

Compound 2. As per general procedure A, with **1** (0.95 g, 2.01 mmol), Cs_2CO_3 (2.20 g, 6.75 mmol) and *N*-Boc-aminobromoethane (0.70 g, 3.13 mmol). The product was purified by column chromatography with CH_2Cl_2 and MeOH (2%) to give **2** as a colorless oil (1.20 g, 97%). ^{1}H NMR ($CDCl_3$) δ 7.44 (d, *J* = 0.97 Hz, 1H), 6.32 (m, *J* = 5.9 Hz, 1H), 4.58 (bs, 1H), 4.38 (m, 1H), 4.09 (m, 2H), 3.91 (m, 1H), 3.84 (dd, *J* = 11.4, 2.6 Hz, 1H), 3.74 (dd, *J* = 11.4, 2.5 Hz, 1H), 3.43 (m, 2H), 2.26 (m, 1H), 1.98 (m, 1H), 1.90 (d, *J* = 0.97 Hz, 3H), 1.43 (s, 9H), 0.91 (s, 9H), 0.87 (s, 9H), 0.09 (s, 6H), 0.06 (s, 3H), 0.05 (s, 3H) ppm. ^{13}C NMR ($CDCl_3$) δ 163.72, 156.09, 151.02, 133.60, 110.22, 87.96, 85.70, 72.45, 63.17, 41.60, 41.02, 28.59, 27.61, 26.13, 25.93, 25.14, 13.44, -4.47, -4.63, -5.12, -5.26 ppm. MS m/z 614.20 $[C_{29}H_{55}N_3O_7Si_2]H^+$.

Compound 3. As per general procedure A, with **1** (0.94 g, 1.99 mmol), Cs_2CO_3 (0.97 g, 2.99 mmol) and *N*-Boc-amino-4-bromobutane (0.50 g, 1.99 mmol). The product was purified by column chromatography with CH_2Cl_2 and MeOH (2%) to give **3** as a colorless oil (1.09 g, 85%). ^{1}H NMR (CD_3OD) δ 7.44 (d, *J* = 0.97 Hz, 1H), 6.32 (m, *J* = 5.9 Hz, 1H), 4.58 (bs, 1H), 4.38 (m, 1H), 4.09 (m, 2H), 3.98-3.87 (m, 3H), 3.84 (dd, *J* = 11.4, 2.6 Hz, 1H), 3.74 (dd, *J* = 11.4, 2.5 Hz, 1H), 3.13 (m, 2H), 2.26 (m, 1H), 1.98 (m, 1H), 1.90 (d, *J* = 0.97 Hz, 3H), 1.62 (m, 2H), 1.49 (m, 2H), 1.43 (s, 9H), 0.91 (s, 9H), 0.87 (s, 9H), 0.09 (s, 6H), 0.06 (s, 3H), 0.05 (s, 3H) ppm. ^{13}C NMR (CD_3OD) δ 163.72,

156.09, 151.02, 133.60, 110.22, 87.96, 85.70, 72.45, 63.17, 41.60, 41.02, 28.59, 27.61, 26.13, 25.93, 25.14, 18.58, 18.18, 13.44, -4.47, -4.63, -5.12, -5.26 ppm. MS *m/z* 642.25 $[C_{31}H_{59}N_3O_7Si_2]H^+$.

Compound 4. As per general procedure A, with **1** (1.90 g, 4.04 mmol), Cs_2CO_3 (4.40 g, 12.39 mmol) and dibromoethane (7.76 g, 41.28 mmol). The product was purified by column chromatography with hexane and EtOAc (20%) to give **5** as a colorless liquid (2.21 g, 95%). ^{1}H-NMR ($CDCl_3$) δ 7.48 (d, *J* = 1.1 Hz, 1H), 6.36 (m, *J* = 7.9, 5.8 Hz, 1H), 4.45-4.29 (m, 3H), 3.95 (m, 1H), 3.87 (dd, *J* = 11.4, 2.6 Hz, 1H), 3.76 (dd, *J* = 11.4, 2.4 Hz, 1H), 3.54 (t, *J* = 7.2 Hz, 2H), 2.30-2.23 (m, 1H), 2.02-1.95 (m, 1H), 1.94 (s, 3H), 0.93 (s, 9H), 0.90 (s, 9H), 0.12 (s, 6H), 0.09 (s, 3H), 0.08 (s, 3H) ppm. ^{13}C-NMR ($CDCl_3$) δ 163.1, 150.7, 133.9, 110.0, 87.9, 85.6, 72.3, 63.0, 42.2, 41.6, 29.5, 25.8, 25.7, 18.4, 18.0, 13.3, -4.6, -4.8, -5.4, -5.4 ppm. MS *m/z* 578.97 $[C_{24}H_{45}BrN_2O_5Si_2]H^+$. Anal. calcd. for $C_{24}H_{45}BrN_2O_5Si_2$: C, 49.90; H, 7.85; N, 4.85. Found: C, 49.95; H, 7.89; N, 4.83.

Compound 5. As per general procedure A, with **1** (3.00 g, 6.37 mmol), Cs_2CO_3 (4.15 g, 12.74 mmol) and dibromobutane (4.13 g, 19.11 mmol). The product was purified by column chromatography with hexane and EtOAc (20%) to give **5** as a colorless liquid (3.66 g, 95%). ^{1}H NMR (CD_3OD) δ 7.43 (d, *J* = 1.3 Hz, 1H), 6.34 (m, *J* = 7.8, 5.8 Hz, 1H), 4.38 (m, *J* = 5.8, 2.6 Hz, 1H), 3.93 (m, 2H), 3.91 (m, 1H), 3.84 (dd, *J* = 11.4, 2.6 Hz, 1H), 3.74 (dd, *J* = 11.4, 2.6 Hz, 1H), 3.41 (t, *J* = 6.7 Hz, 2H), 2.27-2.21 (m, 1H), 2.02-1.94 (m, 1H), 1.90 (s, 3H), 1.89 (m, 2H), 1.77 (m, 2H), 0.91 (s, 9H), 0.87 (s, 9H), 0.09 (s, 6H), 0.06 (s, 3H), 0.05 (s, 3H) ppm. ^{13}C NMR (CD_3OD) δ 163.6, 150.9, 133.6, 110.0, 87.9, 85.6, 72.6, 63.2, 41.7, 40.5, 33.2, 30.4, 26.6, 26.1, 25.9, 18.6, 18.2, 13.4, -4.4, -4.7, -5.2, -5.3 ppm. MS *m/z* 607.31 $[C_{26}H_{49}BrN_2O_5Si_2]H^+$.

Compound 6. 2-(Boc-amino)ethanethiol (0.31 g, 1.72 mmol) was dissolved in DMF (10 mL). Cs_2CO_3 (0.68 g, 2.09 mmol) was added and the mixture was stirred for 5 min at rt. After addition of **4** (1.10 g, 1.90 mmol), the reaction was stirred for 2 h at rt. The reaction mixture was diluted with EtOAc (50 mL), washed with water (50 mL) and twice with 1 M $NaHCO_3$ (50 mL). The aqueous phases were re-extracted with EtOAc. The organic phases were combined, dried over Na2SO4 and evaporated under reduced pressure. The crude product was purified by column chromatography with hexane and

EtOAc (20%) to give 6 as a colorless oil (0.89 g, 77%). ^{1}H NMR (CD_3OD) δ 7.44 (d, *J* = 1.0 Hz, 1H), 6.33 (m, *J* = 7.8, 5.8 Hz, 1H), 5.00 (bs, 1H) 4.38 (m, 1H), 4.15-4.05 (m, 2H), 3.91 (q, *J* = 2.4, 1H), 3.84 (dd, *J* = 11.4, 2.5 Hz, 1H), 3.73 (dd, *J* = 11.4, 2.5 Hz, 1H), 3.36-3.26 (m, 2H), 2.71-2.78 (m, 4H), 2.26-2.21 (m, 1H), 2.01-1.93 (m, 1H), 1.94 (d, *J* = 0.8, 3H), 1.41 (s, 9H), 0.89 (s, 9H), 0.87 (s, 9H), 0.09 (s, 6H), 0.06 (s, 3H), 0.05 (s, 3H) ppm. ^{13}C NMR (CD_3OD) δ 163.5, 156.0, 150.9, 133.9, 110.2, 87.9, 85.5, 72.3, 63.1, 60.5, 41.6, 40.5, 32.2, 28.8, 28.7, 26.2, 26.0, 18.6, 18.3, 14.4, 13.5, -4.5, -4.7, -5.2, -5.2 ppm. High Res MS *m/z* 674.3684 $[C_{31}H_{59}N_3O_7SSi_2]H^+$ (calc. 674.3685).

Compound 7. 2-(Boc-amino)ethanethiol (0.57 g, 3.23 mmol) was dissolved in DMF (15 mL). Cs_2CO_3 (1.70 g, 5.21 mmol) was added and the mixture was stirred for 5 min at rt. After addition of **5** (2.13 g, 3.51 mmol), the reaction was stirred for 2 h at rt. The reaction mixture was diluted with EtOAc (75 mL), washed with water (75 mL) and twice with 1 M $NaHCO_3$ (75 mL). The aqueous phases were re-extracted with EtOAc. The organic phases were combined, dried over Na_2SO_4 and evaporated under reduced pressure. The crude product was purified by column chromatography with hexane and EtOAc (20%) to give **7** as a colorless oil (1.61 g, 71%). ^{1}H NMR (CD_3OD) δ 7.44 (d, *J* = 1.0 Hz, 1H), 6.33 (m, *J* = 7.8, 5.8 Hz, 1H), 5.00 (bs, 1H) 4.38 (m, 1H), 4.00-3.90 (m, 3H), 3.84 (dd, *J* = 11.4, 2.5 Hz, 1H), 3.73 (dd, *J* = 11.4, 2.5 Hz, 1H), 3.30 (m, 2H), 2.63 (t, *J* = 6.4 Hz, 2H), 2.55 (t, *J* = 7.3 Hz, 2H), 2.26-2.21 (m, 1H), 2.01-1.93 (m, 1H), 1.94 (d, *J* = 0.8, 3H), 1.41 (s, 9H), 0.89 (s, 9H), 0.87 (s, 9H), 0.09 (s, 6H), 0.06 (s, 3H), 0.05 (s, 3H) ppm. ^{13}C NMR (CD_3OD) δ ^{13}C NMR (101 MHz, $CDCl_3$) δ 163.7, 151.1, 133.6, 110.3, 88.0, 85.7, 72.5, 63.2, 41.6, 40.9, 32.5, 31.5, 28.6, 27.2, 27.0, 26.2, 26.0, 18.6, 18.2, 13.5, -4.4, -4.6, -5.1, -5.2 ppm. MS *m/z* 702.52 $[C_{33}H_{63}N_3O_7SSi_2]H^+$.

General procedure B: Removal of silyl and Boc protecting groups.

The protected intermediate was dissolved in MeOH (50 mL/mmol). Concentrated HCl (1 mL/mmol) was added and the reaction was stirred for 6 hours at rt. The solvents were removed under reduced pressure, and the residue redissolved in a mixture of EtOAc and water (1:1, 25 mL/mmol). The aqueous phase was neutralized with 1 M NaOH and evaporated under reduced pressure. The residue was purified by solid phase extraction using a Sep-Pak® column.

Compound 8. As per general procedure B, with **2** (478 mg, 0.78 mmol). **8** was isolated as a white solid (180 mg, 81%). ^{1}H NMR (CD_3OD) δ 7.91 (s, 1H), 6.33 (t, *J* = 6.7 Hz, 1H), 4.41 (m, 1H), 4.25 (t, *J* = 5.6 Hz, 2H), 3.93 (m, *J* = 3.3 Hz, 1H), 3.81 (dd, *J* = 12.0, 3.4 Hz, 1H), 3.75 (dd, *J* = 12.0, 3.4 Hz, 1H), 3.22 (t, *J* = 5.6 Hz, 2H), 2.26 (m, 2H), 1.94 (3H, s) ppm. ^{13}C NMR (CD_3OD) δ 165.8, 152.9, 137.1, 111.0, 89.2, 87.4, 72.3, 62.9, 41.4, 40.1, 40.0, 13.3 ppm. MS *m/z* 285.99 $[C_{12}H_{19}N_3O_5]H^+$.

Compound 9. As per general procedure B, with **3** (1.00 g, 1.56 mmol). **9** was isolated after extraction into EtOH as the HCl salt (480 mg, 88%). ^{1}H NMR (CD_3OD) δ ^{1}H NMR (400 MHz, $CDCl_3$) δ 7.87 (d, *J* = 1.1, 1H), 6.31 (dd, *J* = 8.4, 5.0, 1H), 4.40 (dt, *J* = 6.4, 3.4, 1H), 4.01-3.94 (m, 2H), 3.92 (q, *J* = 3.4, 1H), 3.80 (dd, *J* = 12.1, 3.2, 1H), 3.74 (dd, *J* = 12.1, 3.7, 1H), 3.01-2.92 (m, 2H), 2.33-2.15 (m, 2H), 1.91 (d, *J* = 1.1, 3H), 1.78-1.60 (m, 4H) ppm. ^{13}C NMR (CD_3OD) δ 165.9, 150.7, 136.7, 110.9, 89.6, 87.0, 71.3, 62.7, 57.3, 41.2, 40.7, 28.2, 27.2, 13.7 ppm. MS *m/z* 313.81 $[C_{14}H_{23}N_3O_5]H^+$.

General procedure C: Alkylation with methyl bromoacetate.

The alkylated thymidine derivative was dissolved in MeCN (10 mL/mmol) or MeCN/MeOH (10:1, 10 mL/mmol). Triethylamine (10 equivalents) and methyl bromoacetate (4 equivalents) were added and the mixture was stirred at 50 °C overnight. The solvent was removed under reduced pressure and the crude product purified by column chromatography.

Compound 10. As per general procedure C, with **8** (200 mg, 0.70 mmol), triethylamine (0.98 mL, 7.01 mmol) and methyl bromoacetate (0.27 mL, 2.80 mmol). The product was purified by column chromatography with a mixture of CH_2Cl_2 and MeOH (5%) to give **10** as waxy white solid (271 mg, 90%). ^{1}H NMR (CD_3OD) δ 7.83 (s, 1H), 6.27 (t, *J* = 6.6 Hz, 1H), 4.40 (m, 1H), 4.02 (m, *J* = 6.3 Hz, 2H), 3.90 (m, 1H), 3.81 (dd, *J* = 12.1, 3.2 Hz, 1H), 3.74 (dd, *J* = 12.1, 3.7 Hz, 1H), 3.57 (s, 3H), 3.57 (s, 3H), 2.94 (t, *J* = 6.3 Hz, 2H), 2.26 (m, 2H), 1.90 (s, 3H) ppm. ^{13}C NMR (CD_3OD) δ 173.5, 165.8, 152.6, 136.6, 110.7, 89.0, 87.4, 72.1, 62.9, 55.8, 52.1, 41.6, 40.0, 13.4 ppm. MS *m/z* 429.99 $[C_{18}H_{27}N_3O_9]H^+$. Anal. calcd. for $C_{18}H_{27}N_3O_9$: C, 50.35; H, 6.34; N, 9.79. Found: C, 49.42; H, 6.32; N, 9.34.

Compound 11. As per general procedure C, with **9** (625 mg, 1.79 mmol), triethylamine (0.81 mL, 5.84 mmol) and methyl bromoacetate (0.40 mL, 4.38 mmol). The product was purified by column chromatography with a mixture of CH_2Cl_2 and MeOH (3%). Extraction into THF removed excess ammonium salts to give **11** as a white solid (311 mg, 38%). ^{1}H NMR (CD_3OD) δ 7.83 (d, *J* = 1.1, 1H), 6.30 (t, *J* = 6.6, 1H), 4.40 (dt, *J* = 6.7, 3.5, 1H), 3.97-3.88 (m, 3H), 3.80 (dd, *J* = 12.1, 3.2, 1H), 3.73 (dd, *J* = 12.1, 3.7, 1H), 3.68 (s, 6H), 3.52 (s, 4H), 2.79-2.65 (m, 2H), 2.36-2.12 (m, 2H), 1.91 (d, *J* = 1.1, 3H), 1.70-1.57 (m, 2H), 1.52-1.42 (m, 2H) ppm. ^{13}C NMR (CD_3OD) δ 175.9, 168.0, 154.9, 138.9, 113.2, 91.4, 89.7, 74.6, 65.3, 58.3, 57.7, 54.5, 44.5, 43.9, 28.7, 28.6, 15.7 ppm. MS *m/z* 457.88 $[C_{20}H_{31}N_3O_9]H^+$.

Compound 12. As per general procedure B, with **6** (512 mg, 0.73 mmol). **12** was isolated as the HCl salt (250 mg, 66%). ^{1}H NMR (CD_3OD) δ 7.88 (d, *J* = 1.0, 1H), 6.31 (t, *J* = 6.8, 1H), 4.40 (dt, *J* = 6.4, 3.4, 1H), 4.19-4.08 (m, 2H), 3.92 (q, *J* = 3.3, 1H), 3.81 (dd, *J* = 12.0, 3.2, 1H), 3.77-3.68 (m, 1H), 3.20 (t, *J* = 6.8, 2H), 2.90 (t, *J* = 6.8, 2H), 2.85-2.76 (m, 2H), 2.34-2.15 (m, 2H), 1.92 (d, *J* = 1.0, 3H) ppm. ^{13}C NMR (CD_3OD) δ 165.5, 152.5, 136.9, 110.9, 89.1, 87.3, 72.3, 62.9, 41.5, 41.4, 39.9, 29.8, 29.5, 13.3 ppm. MS *m/z* 367.84 $[C_{14}H_{23}N_3O_5S]Na^+$.

Compound 13. As per general procedure B, with **7** (1.50 g, 2.14 mmol). After extraction into EtOH, **13** was isolated as the HCl salt (850 mg, 97%). ^{1}H NMR (CD_3OD) δ7.85 (d, *J* = 1.3, 1H), 6.31 (t, *J* = 6.8, 1H), 4.40 (m, 1H), 3.94 (m, 3H), 3.80 (dd, *J* = 3.1, 12.0, 1H), 3.73 (dd, *J* = 3.8, 12.0, 1H), 3.11 (t, *J* = 6.8, 2H), 2.78 (t, *J* = 6.8, 2H), 2.64 (t, *J* = 6.3, 2H), 2.33-2.15 (m, 2H), 1.91 (d, *J* = 1.3, 3H), 1.79-1.69 (m, 2H), 1.68-1.56 (m, 2H) ppm. ^{13}C NMR (CD_3OD) δ 172.3, 160.0, 144.4, 118.1, 97.0, 94.4, 79.9, 70.8, 40.1, 40.0, 36.2, 36.0, 31.0, 22.6 ppm. MS *m/z* 374.07 $[C_{16}H_{27}N_3O_5S]H^+$.

Compound 14. As per general procedure C, with **12** (250 mg, 0.66 mmol), triethylamine (0.46 mL, 3.30 mmol) and methyl bromoacetate (0.18 mL, 2.00 mmol). The product was purified by column chromatography with a mixture of CH_2Cl_2 and MeOH (3%) to give **14** (156 mg, 48%) as a white solid. ^{1}H NMR (CD_3OD) δ 7.84 (d, *J* = 1.1, 1H), 6.30 (t, *J* = 6.7, 1H), 4.39 (dt, *J* = 6.8, 3.6, 1H), 4.15- 4.05 (m, 2H), 3.91 (q, *J* = 3.4, 1H), 3.80 (dd, *J* = 12.0, 3.2, 1H), 3.73 (dd, *J* = 12.0, 3.7, 1H), 3.69 (s, 6H), 3.59 (s, 4H), 2.95 (m, 2H), 2.78-2.66 (m, 4H), 2.34-2.16 (m, 2H), 1.91 (d, *J* = 1.1, 3H)

ppm. ^{13}C NMR (CD_3OD) δ 173.5, 165.3, 152.3, 136.7, 110.86, 88.9, 87.2, 72.2, 62.9, 55.8, 52.2, 48.1, 41.7, 41.3, 30.6, 29.8, 13.3 ppm. MS *m/z* 489.87 $[C_{20}H_{31}N_3O_9S]H^+$.

Compound 15. As per general procedure C, with **13** (800 mg, 1.95 mmol), triethylamine (0.81 mL, 5.85 mmol) and methyl bromoacetate (0.54 mL, 5.85 mmol). The product was purified by column chromatography with a mixture of CH_2Cl_2 and MeOH (3%) to give **15** (608 mg, 61%) as a white solid. ^{1}H NMR (CD_3OD) δ 7.30 (d, *J* = 1.2, 1H), 6.12 (t, *J* = 6.8, 1H), 4.52 (d, *J* = 2.7, 1H), 3.94 (q, *J* = 3.2, 1H), 3.91-3.83 (m, 3H), 3.77 (d, *J* = 12.0, 1H), 3.64 (s, 6H), 3.52 (s, 4H), 2.93-2.81 (m, 2H), 2.58-2.52 (m, 3H), 2.52-2.45 (m, 3H), 2.41-2.19 (m, 2H), 1.85 (d, *J* = 1.2, 3H), 1.70-1.60 (m, 4H), 1.58-1.48 (m, 2H) ppm. ^{13}C NMR (CD_3OD) δ 171.9, 163.5, 151.1, 135.0, 110.5, 87.7, 87.1, 71.7, 62.6, 60.6, 55.2, 54.8, 51.9, 40.4, 32.1, 30.5, 27.3, 27.0, 21.2, 13.5 ppm. MS *m/z* 489.87 $[C_{22}H_{35}N_3O_9S]H^+$.

General procedure D: Ester hydrolysis

The ester protected intermediate was dissolved in a mixture of methanol (4 mL/mmol) and 1 M NaOH (4 mL/mmol) and stirred for 2 h at rt. The mixture was neutralized by addition of 1 M HCl, before being concentrated under reduced pressure. The reaction mixture was purified by solid phase extraction using a Sep-Pak® column. The fractions containing the product were evaporated under reduced pressure.

3-{2-[Bis(carboxymethyl)amino]ethyl}thymidine (L^1): As per general procedure D, with **10** (1.29 g, 3.01 mmol) to give $\mathbf{L^1}$ (1.06 g, 68%). ^{1}H NMR (D_2O) δ 7.73 (s, 1H), 6.33 (t, *J* = 6.6 Hz, 1H), 4.51 (m, *J* = 10.1, 5.2 Hz, 1H), 4.40 (m, *J* = 5.7, 2.7 Hz, 2H), 4.07 (m, *J* = 8.4, 4.4 Hz, 1H), 3.90 (s, 3H), 3.88 (dd, *J* = 12.6, 3.5 Hz, 1H), 3.81 (dd, *J* = 12.6, 5.2 Hz, 1H), 3.54 (t, *J* = 5.6 Hz, 2H), 2.46 (t, *J* = 5.6 Hz, 2H), 1.98 (s, 3H) ppm. ^{13}C NMR (D_2O) δ 170.1, 165.7, 152.0, 136.2, 110.6, 86.6, 86.2, 70.2, 61.1, 57.0, 54.6, 46.7, 38.7, 12.2 ppm. High Res MS *m/z* 400.1362 $[C_{16}H_{22}N_3O_9]^-$ (calc. 400.1360).

3-{4-[Bis(carboxymethyl)amino]butyl}thymidine (L^2): As per general procedure D, with **11** (300 mg, 0.66 mmol) to give $\mathbf{L^2}$ (106 mg, 37%). ^{1}H NMR (D_2O) δ 7.69 (d, *J* = 1.0, 1H), 6.36 (t, *J* = 6.6, 1H), 4.54-4.48 (m, 1H), 4.08 (dd, *J* = 8.9, 3.9, 1H), 4.01 (t, *J* = 6.7, 2H), 3.90 (dd, *J* = 12.4, 3.6, 1H), 3.86-3.78 (m, 5H), 3.37-3.30 (m, 2H), 2.50-2.37 (m, 2H), 1.97 (d, *J* = 1.0, 3H), 1.86-1.69 (m, 4H) ppm. ^{13}C NMR (D_2O) δ 170.5, 165.7,

151.7, 135.6, 110.6, 86.5, 85.9, 70.4, 61.1, 57.1, 55.6, 40.6, 38.7, 23.8, 21.2, 12.3 ppm. High Res MS *m/z* 428.1659 $[C_{18}H_{26}N_3O_9]^-$ (calc. 428.1675).

3-{2-[S-(Bis(carboxymethyl)aminoethylthio)]ethyl}thymidine (L^4): As per general procedure D, with 14 (156 mg, 0.32 mmol) to give $\mathbf{L^4}$ after extraction into EtOH (140 mg, 88%). 1H NMR (CD_3OD) δ 1H NMR (400 MHz, MeOD) δ 7.87 (d, *J* = 1.0, 1H), 6.32 (t, *J* = 6.7, 1H), 4.43 (m, 1H), 4.15 (m, 2H), 3.93 (q, *J* = 3.5, 1H), 3.82 (dd, *J* = 12.0, 3.2, 1H), 3.77 (s, 4H), 3.74 (dd, *J* = 12.0, 3.7, 1H), 3.51 (t, 2H), 3.04 (t, *J* = 7.3, 2H), 2.85 (t, 2H), 2.31 (m, 1H), 2.23 (m, 1H), 1.93 (d, *J* = 1.0, 3H) ppm. ^{13}C NMR (CD_3OD) δ 170.1, 165.6, 152.5, 136.8, 111.2, 88.6, 87.3, 71.9, 62.6, 56.9, 55.7, 41.2, 41.0, 29.3, 26.8, 13.3 ppm. High Res MS *m/z* 460.1398 $[C_{18}H_{26}N_3O_9]^-$ (calc. 460.1395).

3-{4-[S-(Bis(carboxymethyl)aminoethylthio)]butyl}thymidine (L^5): As per general procedure D, with 16 (550 mg, 1.06 mmol) to give $\mathbf{L^5}$ as the HCl salt (484 mg, 93%). ^{1}H NMR (CD_3OD) δ 7.71 (s, 1H), 6.38 (t, *J* = 6.5, 1H), 4.53 (m, 1H), 4.10 (m, , 1H), 4.00 (t, *J* = 6.6, 2H), 3.88 (s, 3H), 3.94-3.81 (m, 2H), 3.54 (t, *J* = 6.6, 2H), 3.00 (t, *J* = 6.8, 2H), 2.73 (t, *J* = 6.7, 2H), 2.52-2.35 (m, 2H), 1.98 (s, 3H), 1.77 (m, 2H), 1.70 (m, 2H) ppm. ^{13}C NMR (CD_3OD) δ 171.0, 165.7, 152.5, 136.6, 111.1, 88.6, 87.2, 72.0, 62.7, 58.4, 55.4, 41.9, 41.1, 31.9, 27.7, 27.6, 27.2, 13.4 ppm. MS m/z 487.98 $[C_{20}H_{30}N_3O_9]^-$.

5.5.3 Complex formation

The synthesis and characterization of $[Re(CO)_3\mathbf{L^3}]NEt_4$[16] have been reported previously. Mixed carbonyl-nitrosyl complexes were prepared using the following general procedure unless stated otherwise. One equivalent of the ligand $\mathbf{L^1}$-$\mathbf{L^5}$ was dissolved in a 2:1 mixture of MeOH and water to form a 0.1 M solution. One equivalent of $[Re(CO)_2(NO)Br_3]NEt_4$ was added and the reaction mixtures were stirred at 65 °C. The reactions with thymidine containing ligands $\mathbf{L^1}$, $\mathbf{L^2}$, $\mathbf{L^4}$ and $\mathbf{L^5}$ were followed by HPLC. After 6 hours the solvents were removed under vacuum and the residue was purified by solid phase extraction using a Sep-Pak® column with a water-MeOH gradient. The fractions containing the product were evaporated under reduced pressure. Tricarbonyl complexes of ligands $\mathbf{L^1}$-$\mathbf{L^5}$ were prepared according to the

following general procedure unless stated otherwise. One equivalent of the ligand **L[1]**-**L[5]** was dissolved in a 1:1 mixture of MeOH and water to form a 0.1 M solution. One equivalent of $[ReBr_3(CO)_3][NEt_4]_2$ was added and the reaction mixtures were stirred at 65 °C. All complexation reactions with thymidine containing ligands **L[1]**, **L[2]**, **L[4]** and **L[5]** were followed by HPLC. After 2 hours the solvents were removed under vacuum and the residue was purified by solid phase extraction using a Sep-Pak® column with a water-MeOH gradient. The fractions containing the product were evaporated under reduced pressure.

$[Re(CO)_2(NO)L^1]$. As per general procedure except that the pure product is poorly soluble in both water and methanol and was isolated by precipitation from the reaction solution. Yield 46%. Anal. calcd. for $C_{18}H_{21}N_4O_{12}Re$: C, 32.19; H, 3.15; N, 8.34. Found: C, 31.78; H, 3.34; N, 8.21. ^{1}H NMR (CD_3OD) δ 7.84 (d, *J* = 1.1, 1H), 6.21 (t, *J* = 6.7, 1H), 4.31 (d, *J* = 16.9, 1H), 4.25 (m, 1H), 4.22-4.14 (m, 3H), 4.07 (dd, *J* = 16.0, 2.0, 1H), 4.01 (dd, *J* = 16.0, 4.4, 1H), 3.79 (q, *J* = 3.7, 1H), 3.71 (m, 1H), 3.66-3.52 (m, 4H), 2.13 (m, 2H), 1.86 (d, *J* = 1.1, 3H) ppm. ^{13}C NMR (CD_3OD) δ 188.9, 187.9, 178.2, 177.1, 162.63, 150.3, 135.2, 108.5, 87.4, 84.9, 70.1, 65.7, 62.3, 61.9, 61.1, 36.9, 12.9 ppm. IR ν 3309, 2939, 2112, 2029, 1782, 1712, 1687, 1655, 1627, 1462, 1434, 1357, 1335, 1321, 1236, 1177, 1109, 1059, 1031, 999, 981, 943, 927, 911, 850, 788, 769, 649 cm^{-1}. MS *m/z* 672.94 $[C_{18}H_{21}N_4O_{12}Re]H^+$.

$[Re(CO)_3L^1]NEt_4$. As per general procedure. Yield 63%. ^{1}H NMR (CD_3OD) δ 7.88 (s, 1H), 6.33 (t, *J* = 6.6 Hz, 1H), 4.41 (m, 1H), 4.29 (m, *J* = 6.4 Hz, 2H), 3.93 (m, *J* = 3.4 Hz, 1H), 3.86 (t, *J* = 7.3 Hz, 2H), 3.76 (m, 4H), 3.55 (t, *J* = 7.3 Hz, 2H), 3.31 (m, 8H, NEt_4^+), 2.32 (m, 1H), 2.24 (m, 1H), 1.94 (s, 3H), 1.31 (m, 12H, NEt_4^+) ppm. ^{13}C NMR (CD_3OD) δ 198.7, 197.9, 182.6, 165.2, 152.2, 137.0, 110.8, 89.0, 87.3, 72.1, 66.9, 63.8, 62.8, 53.3 (NEt_4), 41.4, 38.6, 13.2, 7.7 (NEt_4) ppm. IR ν 3385, 2932, 2017, 1863, 1697, 1624, 1466, 1375, 1320, 1272, 1185, 1173, 1092, 1057, 999.6, 946.3, 908, 770, 752, 660, 643, 608 cm^{-1}. High Res MS *m/z* 670.0675 $[C_{19}H_{21}N_3O_{12}Re]^-$ (calc. 670.0689).

$[Re(CO)_2(NO)L^2]$. As per general procedure. Yield 77%. Anal. calcd. for $C_{20}H_{25}N_4O_{12}Re$: C, 34.33; H, 3.60; N, 8.01. Found: C, 34.10; H, 3.86; N, 7.85. ^{1}H NMR (CD_3OD) δ 7.87 (d, *J* = 0.8, 1H), 6.32 (t, *J* = 6.7, 1H), 4.40 (dt, *J* = 6.4, 3.4, 1H), 4.26 (d, *J* = 16.7, 1H), 4.16 (d, *J* = 16.7, 1H), 4.02 (t, *J* = 6.6, 3H), 3.98 (m, 1H),

3.92 (m, 1H), 3.81 (dd, *J* = 12.1, 3.2, 1H), 3.73 (dd, *J* = 12.1, 3.7, 1H), 3.68 (m, 1H), 3.64-3.53 (m, 1H), 2.33-2.24 (m, 1H), 2.24-2.17 (m, 1H), 1.92 (d, *J* = 0.8, 3H), 1.86-1.76 (m, 2H), 1.77-1.67 (m, 2H) ppm. ^{13}C NMR (CD_3OD) δ 182.1, 180.6, 165.7, 152.6, 136.8, 110.9, 102.4, 89.1, 87.3, 72.3, 71.0, 63.9, 63.6, 62.9, 41.4, 41.2, 25.7, 23.0, 13.3 ppm. IR ν 3409, 2941, 2107, 2030 1779, 1684, 1660, 1626, 1469, 1357, 1311, 1276, 1194, 1090, cm^{-1}. MS *m/z* 700.87 $[C_{20}H_{25}N_4O_{12}Re]H^+$.

$[Re(CO)_3L^2]NEt_4$. As per general procedure. Yield 55%. ^{1}H NMR (CD_3OD) δ 7.84 (d, *J* = 0.9, 1H), 6.30 (t, *J* = 6.6, 1H), 4.43-4.35 (m, 1H), 4.00 (t, *J* = 6.5, 2H), 3.92 (q, *J* = 3.4, 1H), 3.80 (dd, *J* = 12.0, 3.2, 1H), 3.74 (d, *J* = 16.2, 2H), 3.73 (dd, *J* = 12.0, 4.3, 2H), 3.51 (d, *J* = 16.2, 2H), 3.40-3.36 (m, 2H), 3.30 (m, 8H, NEt_4^+), 2.30 (m, 1H), 2.21 (m, 1H), 1.91 (d, *J* = 0.9, 3H), 1.72 (m, 4H), 1.36-1.23 (m, 12H, NEt_4^+), ppm. ^{13}C NMR (CD_3OD) δ 199.0, 183.0, 165.7, 152.6, 136.7, 110.8, 89.0, 87.3, 72.2, 70.3, 64.2, 62.9, 53.4 (NEt_4), 41.5, 26.0, 23.3, 13.3, 7.7 (NEt_4) ppm. IR ν 3363, 2952, 2019, 1865, 1693, 1624, 1575, 1467, 1393, 1366, 1279, 1185, 1173, 1092, 1055, 1000, 912, 771, 660, 643 cm^{-1}. High Res MS *m/z* 698.0987 $[C_{21}H_{25}N_3O_{12}Re]^-$ (calc. 698.0991).

$[Re(CO)(NO)L^3]$. As per general procedure except that the pH of the reaction solution was increased to 7 with 1 M NaOH after dissolution of the ligand. Yield 40%. ^{1}H NMR ($CDCl_3$) δ 3.63 (d, *J* = 15.8, 1H), 3.61 (d, *J* = 5.2, 1H), 3.56 (d, *J* = 5.2, 1H), 3.53 (d, *J* = 15.8, 1H), 3.45-3.29 (m, 2H), 2.84-2.66 (m, 2H), 2.54 (q, *J* = 7.4, 2H), 1.23 (t, *J* = 7.4, 3H) ppm. ^{13}C NMR ($CDCl_3$) δ 179.8, 176.9, 67.7, 64.4, 62.9, 27.1, 26.5, 14.7 ppm. IR ν 2981, 1971, 1709, 1655, 1593, 1486, 1457, 1394, 1362, 1327, 1173, 1137, 1083, 1002, 925, 908, 786, 740 cm^{-1}. MS *m/z* 464.69 $[C_9H_{13}N_2O_6ReS]H^+$.

$[Re(CO)_3L^3]NEt_4$. As per general procedure except that the pH of the reaction solution was increased to 7 with 1 M NaOH after dissolution of the ligand and the product was isolated by precipitation as the reaction solution was concentrated. Yield 65%. ^{1}H NMR (CD_3OD) δ 3.76 (d, *J* = 16.5, 2H), 3.56 (d, *J* = 16.5, 2H), 3.52-3.45 (m, 2H), 3.29 (m, 9H), 2.95-2.82 (m, 2H), 2.63 (q, *J* = 6.9, 2H), 1.31-1.28 (m, 15H) ppm. ^{13}C NMR (CD_3OD) δ 182.6, 70.1, 64.0, 53.3 (NEt_4), 27.6, 27.0, 15.4, 7.6 (NEt_4) ppm. IR ν 2944, 2707, 2507, 2025, 1941, 1917, 1890, 1738, 1667, 1616, 1590, 1457, 1433, 1423, 1382, 1346, 1264, 1230, 1205, 1191, 1102, 1058, 990, 959, 919, 883, 794, 764, 702, 649, 630, 610 cm^{-1}. MS *m/z* 489.67 $[C_{11}H_{13}NO_7ReS]^-$.

[Re(CO)$_2$(NO)L^4]. As per general procedure. Yield 39%. Anal. calcd. for $C_{20}H_{25}N_4O_{12}ReS$: C, 32.83; H, 3.44; N 7.66. Found: C, 32.31; H, 3.74; N 7.42. ^{1}H NMR (CD_3OD) δ 7.88 (s, 1H), 6.33 (t, *J* = 6.7, 1H), 4.46-4.36 (m, 2H), 4.31 (d, *J* = 16.6, 1H), 4.17 (t, *J* = 6.9, 2H), 4.09 (m, *J* = 16.6, 2H), 3.91 (m, 2H), 3.85-3.71 (m, 3H), 3.09 (t, 2H), 2.85 (m, 2H), 2.37-2.17 (m, 2H), 1.93 (s, 3H) ppm. ^{13}C NMR (CD_3OD) δ 190.0, 187.0, 181.9, 180.3, 165.3, 152.4, 136.8, 110.9, 89.0, 87.2, 72.2, 70.4, 63.9, 63.5, 62.8, 41.5, 41.5, 29.5, 26.7, 13.2 ppm. IR ν 3283, 2940, 2108, 2027, 1781, 1711, 1687, 1651, 1625, 1461, 1434, 1357, 1334, 1320, 1260, 1236, 1176, 1162, 1108, 1096, 1058, 1031, 998, 981, 943, 927, 911, 881, 850, 788, 768, 753, 649, 631 cm^{-1}. High Res MS *m/z* 733.0824 $[C_{20}H_{25}N_4O_{12}ReS]H^+$ (calc. 733.0819).

[Re(CO)$_3$L^4]Na. As per general procedure. Yield 85%. ^{1}H NMR (CD_3OD) δ 7.84 (d, *J* = 1.2, 1H), 6.30 (t, *J* = 6.6, 1H), 4.43-4.35 (m, 1H), 4.15 (t, 2H), 3.91 (q, *J* = 3.5, 1H), 3.86 (d, *J* = 16.4, 2H), 3.81 (dd, *J* = 12.1, 3.2, 1H), 3.73 (dd, *J* = 12.1, 3.7, 1H), 3.61 (d, *J* = 16.4, 2H), 3.56 (m, 2H), 3.02-2.94 (m, 2H), 2.80 (t, 2H), 2.30 (m, 1H), 2.22 (m, 1H), 1.92 (d, *J* = 1.2, 3H) ppm. ^{13}C NMR (CD_3OD) δ 182.7, 165.1, 136.6, 110.7, 88.8, 87.2, 71.9, 63.8, 62.7, 53.2, 41.4, 41.2, 29.4, 26.7, 13.1 ppm. IR ν 3387, 2938, 2027, 1877, 1731, 1698, 1624, 1467, 1361, 1280, 1229, 1187, 1092, 1056, 995, 919, 784, 767, 648 cm^{-1}. High Res MS *m/z* 777.0581 $[C_{21}H_{26}N_3O_{12}ReSNa]Na^+$ (calc. 777.0584).

[Re(CO)$_2$(NO)L^5]. As per general procedure except that the product was purified by semi-preparative HPLC. Yield 47%. ^{1}H NMR (CD_3OD) δ 7.80 (d, *J* = 0.9, 1H), 6.28 (t, *J* = 6.7, 1H), 4.36 (dt, *J* = 6.7, 3.5, 1H), 4.31 (d, *J* = 17.2, 1H), 4.22 (d, *J* = 16.3, 1H), 4.00 (m, 3H), 3.92 (t, *J* = 7.2, 2H), 3.88 (m, 1H), 3.77 (m, 2H), 3.72-3.61 (m, 2H), 2.91 (t, 3H), 2.66 (t, *J* = 7.2, 2H), 2.29-2.19 (m, 1H), 2.19-2.10 (m, 1H), 1.87 (d, *J* = 0.9, 3H), 1.71 (m, 2H), 1.61 (m, 2H) ppm. ^{13}C NMR (CD_3OD) δ 171.1, 170.2, 165.6, 152.5, 136.6, 110.9, 89.0, 87.2, 72.3, 62.9, 41.8, 41.4, 32.7, 28.3, 27.7, 27.6, 13.4 ppm. IR ν 3397, 2936, 2109, 2034, 1784, 1743, 1688, 1662, 1627, 1469, 1358, 1313, 1268, 1192, 1177, 1131, 1268, 1192, 1177, 1131, 1093, 1053, 984, 915, 834, 798, 770, 752, 720, 636 cm^{-1}. MS *m/z*.760.95 $[C_{22}H_{29}N_4O_{12}ReS]H^+$.

[Re(CO)$_3$L^5]NEt$_4$. As per general procedure. Yield 40%. ^{1}H NMR (CD_3OD) δ 7.74 (d, *J* = 1.1, 1H), 6.22 (t, *J* = 6.6, 1H), 4.31 (dt, *J* = 6.7, 3.5, 1H), 3.88 (t, *J* = 6.9, 2H), 3.83 (m, 1H), 3.75-3.60 (m, 5H), 3.47 (d, *J* = 16.0, 2H), 3.42-3.36 (m, 2H), 2.84-2.75

(m, 2H), 2.56 (t, *J* = 7.1, 2H), 2.25-2.06 (m, 2H), 1.82 (d, *J* = 1.1, 3H), 1.69-1.62 (m, 3H), 1.61-1.49 (m, 1H) ppm. ^{13}C NMR (CD_3OD) δ 182.8, 163.4, 163.1, 119.8, 116.9, 89.0, 87.3, 72.3, 70.2, 64.1, 62.9, 41.8, 41.4, 32.8, 28.5, 28.1, 27.0, 13.4 ppm. IR ν 3374, 2932, 2286, 2026, 1881, 1692, 1623, 1469, 1365, 1266, 1189, 1092, 1053, 991, 918, 769, 649, 624, 608 cm^{-1}. MS *m/z* 757.96 $[C_{23}H_{29}N_3O_{12}ReS]^-$.

5.5.4 X-ray crystallography

The intensities for the x-ray determinations were collected on a STOE IPDS 2T instrument with $Mo_{K\alpha}$ radiation. Standard procedures were applied for data reduction and absorption correction. Structure solution and refinement were performed with SHELXS97 and SHELXL97.[28] Hydrogen atom positions were calculated for idealized positions and treated with the 'riding model' option of SHELXL. CCDC 713659 ($[Re(CO)_2(NO)\mathbf{L^2}]$) and 713658 ($[Re(CO)(NO)\mathbf{L^3}]$) contain the supplementary crystallographic data for this paper. These data can be obtained free of charge from The Cambridge Crystallographic Data Centre via www.ccdc.cam.ac.uk/data_request/cif.

5.5.5 Phosphorylation transfer assays

Thymidine and the organometallic thymidine derivatives $[Re(CO)_3\mathbf{L^1/L^2}][NEt_4]$, $[Re(CO)_2(NO)\mathbf{L^1/L^2}]$, $[Re(CO)_3\mathbf{L^4/L^5}][NEt_4]$ and $[Re(CO)_2(NO)\mathbf{L^4/L^5}]$ were assayed at 25 °C for 15 minutes in 200 µL of a mixture containing 155.38 µL water, 10 µL 1 M HEPES buffer (pH 7.5), 0.2 µL 1 M DTT, 0.42 µL 100 mM PEP, 0.5 µL 1 M $MgCl_2$, 7.2 µL 5 mM NADH, 2 µL 100 mM ATP, 0.6 µL pyruvate kinase (1350 U/mL), 0.7 µL lactate dehydrogenase (1420 U/mL), 5 µL hTK1 (~0.5 mg/mL) and 20 µL of a 10 mM 1:1 DMSO/water solution of thymidine, $[Re(CO)_3\mathbf{L^1/L^2}][NEt_4]$, $[Re(CO)_2(NO)\mathbf{L^1/L^2}]$, $[Re(CO)_3\mathbf{L^4/L^5}][NEt_4]$ or $[Re(CO)_2(NO)\mathbf{L^4/L^5}]$. For each substrate the linear decrease in UV absorption at 340 nm was measured from 0 to 15 minutes. The gradients of the regression lines between 6 and 12 minutes were compared to thymidine, the phosphorylation of which was assumed to be 100%.

5.6 References

(1) Alberto, R.; Schibli, R.; Egli, A.; Schubiger, P. A. *J. Am. Chem. Soc.* **1998**, *120*, 7987-7988.

(2) Alberto, R.; Schibli, R.; Waibel, R.; Abram, U.; Schubiger, A. P. *Coord. Chem. Rev.* **1999**, *190-192*, 901-919.

(3) Buchegger, F.; Bonvin, F.; Kosinski, M.; Schaffland, A. O.; Prior, J.; Reubi, J. C.; Blauenstein, P.; Tourwe, D.; Garayoa, E. G.; Delaloye, A. B. *J. Nucl. Med.* **2003**, *44*, 1649-1654.

(4) Waibel, R.; Treichler, H.; Schaefer, N. G.; van Staveren, D. R.; Mundwiler, S.; Kunze, S.; Kuenzi, M.; Alberto, R.; Nuesch, J.; Knuth, A.; Moch, H.; Schibli, R.; Schubiger, P. A. *Cancer Res.* **2008**, *68*, 2904-2911.

(5) Schibli, R.; Schubiger, P. A. *Eur. J. Nucl. Med. Mol. Imaging* **2002**, *29*, 1529-1542.

(6) Bezerra, C. W. B.; da Silva, S. C.; Gambardella, M. T. P.; Santos, R. H. A.; Plicas, L. M. A.; Tfouni, E.; Franco, D. W. *Inorg. Chem.* **1999**, *38*, 5560-5667.

(7) Causey, P. W.; Besanger, T. R.; Valliant, J. F. *J. Med. Chem.* **2008**, *51*, 2833-2844.

(8) Hund, H.-U.; Ruppli, U.; Berke, H. *Helv. Chim. Act.* **1993**, *76*, 963-975.

(9) Norton, J. R.; Dolcetti, G. *Inorg. Chem.* **1973**, *12*, 485-487.

(10) Zingales, F.; Trovati, A.; Cariati, F.; Uguagliati, P. *Inorg. Chem.* **1971**, *10*, 507-510.

(11) Zingales, F.; Trovati, A.; Uguagliati, P. *Inorg. Chem.* **1971**, *10*, 510-513.

(12) Kurz, P.; Rattat, D.; Angst, D.; Schmalle, H.; Spingler, B.; Alberto, R.; Berke, H.; Beck, W. *Dalton Trans.* **2005**, 804-810.

(13) Lehaire, M. L.; Grundler, P. V.; Steinhauser, S.; Marti, N.; Helm, L.; Hegetschweiler, K.; Schibli, R.; Merbach, A. E. *Inorg. Chem.* **2006**, *45*, 4199-4204.

(14) Marti, N.; Spingler, B.; Breher, F.; Schibli, R. *Inorg. Chem.* **2005**, *44*, 6082-6091.

(15) Schibli, R.; Marti, N.; Maurer, P.; Spingler, B.; Lehaire, M. L.; Gramlich, V.; Barnes, C. L. *Inorg. Chem.* **2005**, *44*, 683-690.

(16) Desbouis, D.; Struthers, H.; Spiwok, V.; Küster, T.; Schibli, R. *J. Med. Chem.* **2008**, *51*, 6689-6698.

(17) Struthers, H.; Spingler, B.; Mindt, T. L.; Schibli, R. *Chem.--Eur. J.* **2008**, *14*, 6173-6183.

(18) Hengstschläger, M.; Knofler, M.; Mullner, E. W.; Ogris, E.; Wintersberger, E.; Wawra, E. *J. Biol. Chem.* **1994**, *269*, 13836-13842.

(19) Hengstschläger, M.; Pusch, O.; Hengstschläger-Ottnad, E.; Ambros, P. F.; Bernaschek, G.; Wawra, E. *DNA Cell Biol.* **1996**, *15*, 41-51.

(20) Munch-Petersen, B.; Cloos, L.; Jensen, H. K. in *Advances in Enzyme Regulation*, Vol. 35, **1995**, p 69-89.

(21) Al-Madhoun, A. S.; Johnsamuel, J.; Yan, J. H.; Ji, W. H.; Wang, J. H.; Zhuo, J. C.; Lunato, A. J.; Woollard, J. E.; Hawk, A. E.; Cosquer, G. Y.; Blue, T. E.; Eriksson, S.; Tjarks, W. *J. Med. Chem.* **2002**, *45*, 4018-4028.

(22) Farrugia, L. J. *J. Appl. Cryst.* **1997**, *30*, 565.

(23) Chiotellis, E.; Stassinopoulou, C. I.; Varvarigou, A.; Vavouraki, H. *J. Med. Chem.* **1982**, *25*, 1370-1374.

(24) Luyt, L. G.; Bigott, H. M.; Welch, M. J.; Katzenellenbogen, J. A. *Bioorg. Med. Chem.* **2003**, *11*, 4977-4989.

(25) Byun, Y.; Thirumamagal, B. T. S.; Yang, W.; Eriksson, S.; Barth, R. F.; Tjarks, W. *J. Med. Chem.* **2006**, *49*, 5513-5523.

(26) Kornberg, A.; Pricer, W. E. *J. Biol. Chem.* **1951**, *193*, 481-495.

(27) Alberto, R.; Egli, A.; Abram, U.; Hegetschweiler, K.; Gramlich, V.; Schubiger, P. A. *J. Chem. Soc. Dalton Trans.* **1994**, 2815-2820.

(28) Sheldrick, G. M. *SHELXL97-2: Program for the Refinement of Crystal Structures* **1997**, University of Göttingen, Germany.

Conclusions

6.1 The "click-to-chelate" approach

The labelling of bioactive molecules with technetium-99m and the corresponding coordination chemistry of technetium-99 and rhenium complexes have been intensively investigated for over 30 years. It is difficult to imagine established procedures will be improved in terms of either labelling efficiency or the direct impact of the metal complex on pharmacokinetic properties. Nonetheless, advances in imaging technology and the identification of new targets for the diagnosis and monitoring of numerous diseases have renewed interest in technetium labelling for the preclinical assessment of drugs, and warrant further improvement of labelling techniques and conjugation strategies. It is likely that conjugation strategies which are widely applicable and facilitate more rapid assessment of structure-activity relationships, will gain particular prominence.

The "click-to-chelate" approach describes a strategy for the synthesis of efficient tridentate chelators for the $M(CO)_3$ core (M = ^{99m}Tc, Re) and their incorporation into biologically relevant molecules. By exploiting the remarkable features of the copper catalyzed azide-alkyne cycloaddition, many of the problems associated with "classical" functionalization strategies, such as time-consuming multi-step syntheses, have been overcome. The most elegant feature of the "click-to-chelate" approach is that the triazole product of the cycloaddition forms an integral part of the chelating system. This means that the cycloaddition reaction enables simultaneous formation of the chelating system and conjugation to a biologically relevant molecule in a single, high-yielding step. Furthermore, the orthogonal reactivity of alkynes and azides means that a wide range of biomolecules can be derivatized without any protecting group chemistry. The synthesis of a triazole-containing histidine-like chelating system and its incorporation into various biomolecules is reported in Chapter 2.

A set of alkynes was developed, which can be reacted with any azide-functionalized biomolecule to create a series of conjugates with efficient, tridentate, triazole-containing chelating systems, as described in Chapter 3. Through the structural differences of the alkynes, metal chelates are formed with varying physicochemical properties such as charge, size and lipophilicity. In addition we have shown that neither the alkyne or azide components of the click reaction form stable complexes with the $M(CO)_3$ core and

that, therefore, the products of the click reactions can be labelled *in situ*, without prior purification. For the purposes of radiopharmaceutical development this is a most valuable characteristic, helping to facilitate a much more efficient process of *in vitro* screening of novel drug candidates. The only prerequisite for use of the "click-to-chelate" strategy is that the biomolecule to be functionalized and radiolabelled incorporates an accessible azide. The availability of a one-pot labeling protocol and the efficiency of the triazole chelators, however, mean very little of the azide-containing biomolecule is required. For example, the click reaction can be performed with only microlitres of a 10^{-2} M solution and labelling of the triazole-containing ligands with $^{99m}Tc(CO)_3$ typically requires a ligand concentration of approximately 10^{-5} M, corresponding to less that 0.5 mg of material for a low molecular weight biomolecule. The use of this approach was illustrated by the synthesis and *in vitro* evaluation of two series of thymidine derivatives, as reported in Chapter 4.

We have shown that chelating systems, which coordinate to the metal through N3 of the triazole, can be incorporated into any azide-containing molecule by the reaction with a suitable alkyne. A tridentate ligand system can also be prepared from the reaction of a suitably functionalized azide with any alkyne-containing molecule, as has been shown, for example, with azido-alanine and various alkynes (Chapter 2). In this case, the tridentate ligand is assumed to coordinate to the metal through N2 of the triazole. Radiolabelling experiments showed, however, that these ligands are less efficient chelators for the $M(CO)_3$ core than the ligands which coordinate through N3 of the triazole. This is presumably because N3 is significantly more electronegative than N2, and as a result, coordinates more readily. When this work was started, very few triazole-containing chelating systems synthesized using the CuAAC reaction had been reported, and none had been structurally characterized. Although there are examples in the literature of triazole-containing ligand systems, which coordinate to a metal through N2 of the triazole,[1] the majority of chelating systems derived from the CuAAC reaction, which have since been reported, have been designed to coordinate to the metal through N3. Debiton *et al.* report two series of bidentate triazole-containing ligands for platinum, where the triazole is functionalized at either C4 or N1.[2] Pt complexes in which the ligands coordinate to the metal through N3 of the triazole have been structurally characterized. They were unable, however, to isolate any complexes in

which the ligands are coordinated through N2, supporting our own observations that coordination through N3 is more favourable.

6.2 Technetium-labelled thymidine analogues

Over the last four years our group has invested considerable effort into the development of technetium-labelled thymidine analogues for the visualization of hTK1 expression. Despite the narrow substrate specificity, structure-activity relationships and elucidation of the crystal structure of the enzyme suggested that modification of thymidine was most likely to be possible at the N3 and C3′ positions.[3,4] Promising reports of carborane-thymidine derivatives, in which thymidine is functionalized at the N3 position and which maintain activity towards hTK1, initiated interest in N3-functionalized radiometal-thymidine analogues.[5,6] However, while other attempts have failed,[7,8] we have shown that using the technetium/rhenium tricarbonyl core, thymidine can indeed be functionalized with a metal complex at the N3 position and maintains activity towards the enzyme.[9,10] Perhaps more remarkably, we were able to functionalize the ribose at the C3′ position with a technetium complex and show that the phosphorylation of these derivatives at the C5′ position is also catalyzed by hTK1 (Chapter 4). It is noteworthy that no thymidine derivatives functionalized with a carborane at the C3′ position have been shown to maintain activity towards the enzyme.

The $M(CO)_3$ core has been incorporated into thymidine using a variety of chelating systems. Using a "classical" functionalization strategy, the influence of the overall charge of the bioconjugate and the spacer length between thymidine and the metal complex were investigated.[9] However, the "click-to-chelate" approach provided a much faster and more straightforward means to investigate structure-activity relationships, and enabled the influence of the position of functionalization, as well as the overall charge and structure of the metal chelate to be assessed (Chapter 4). Although trends can be observed within certain series of derivatives, no consistent correlation between the ability to act as a substrate for the enzyme and the influence of one of these factors could be identified. It is therefore difficult to draw generalized conclusions about the influence of each of the structural and physicochemical properties, and is likely that the

ability of a given derivative to act as a substrate is determined by the interplay of a combination of these factors. A large number of technetium-labelled thymidine derivatives which are recognized by hTK1 as substrates have now been successfully identified. However, if these compounds are to find use as proliferation markers, their lack of cellular uptake must be addressed.

6.3 Labelling with the $\{Re(CO)_2(NO)\}^{2+}$ core

Iminodiacetic acid had previously been identified as a suitable chelating system for the $\{M(CO)_2(NO)\}^{2+}$ core, which forms neutral organometallic complexes, and which is amenable to further functionalization.[11] Thymidine was functionalized at the N3 position with an iminodiacetic acid chelating system and reacted with the $[Re(CO)_2(NO)(H_2O)_3]^{2+}$ precursor to provide the first example of a biomolecule labelled with the $\{Re(CO)_2(NO)\}^{2+}$ core. It has also been shown that in some circumstances, one of the carbonyl ligands of the $\{M(CO)_2(NO)\}^{2+}$ core is labile and complexes of the form [M(CO)(NO)L] can be prepared in combination with tetradentate ligands which contain iminodiacetic acid and either a third carboxylic acid or pyridine as the fourth coordinating group.[11] Since neither of these ligand systems can be readily incorporated into a biomolecule, we chose to investigate mercaptoethyliminodiacetic acid as a potentially tetradentate ligand (Chapter 5). A model monocarbonyl-mononitrosyl complex could be readily synthesized with ethylmercaptoethyliminodiacetic acid, yet when the chelating system was incorporated into thymidine, only tridentate coordination of the ligand was observed. In order to determine the factors which lead to dissociation of a carbonyl ligand a more thorough investigation of ligand systems, their structures and the combination of donor groups, as well as the reaction conditions for complex formation is required.

It has been a common strategy in the search for target-specific radiopharmaceuticals labelled with the $M(CO)_3$ core to evaluate the influence of the charge of the metal chelate on the biological properties of the compound.[12] Inevitably, this requires modification of the metal chelating system, which is necessarily accompanied by a change in the structure (and other properties) of the metal complex, as we have shown

in Chapter 4. The isostructural precursors $[M(CO)_2(NO)(H_2O)_3]^{2+}$ and $[M(CO)_3(H_2O)_3]^{+}$ provide an alternative method of investigating the influence of charge, without needing to take into account concomitant structural changes. The two approaches were compared with a series of thymidine derivatives, designed to act as substrates for hTK1. In the first series of complexes, thymidine was functionalized with three different chelating systems which, when labelled with the $M(CO)_3$ core, gave rise to a neutral complex, a cationic complex and an anionic complex. The relative rates of phosphorylation were compared to assess the influence of the overall charge, and it was found that within this series, the neutral complex was the best substrate, followed by the anionic complex, while the cationic complex was much less readily phosphorylated. In the second series of complexes to be investigated, thymidine derivatives functionalized with iminodiacetic acid-containing chelating systems were labelled with the $\{Re(CO)_3\}^{+}$ core to give anionic complexes, and with the $\{Re(CO)_2(NO)\}^{2+}$ core to give neutral complexes, as described in Chapter 5. It was surprising to find that in this series of complexes, the rates of phosphorylation were almost identical within experimental error for each pair of isostructural neutral and anionic complexes. These results suggest that for N3-functionalized thymidine derivatives, the structure has a greater influence on the compound's ability to act as a substrate for hTK1 than its overall charge.

6.4 Outlook

As the conclusions outlined above highlight, several questions arose during the course of this work, which need to be addressed further:

- Is the "click-to-chelate" approach restricted to labelling with the $M(CO)_3$ core, or can the same approach be used for the preparation of triazole-containing chelating systems for other cores of technetium and rhenium?
- Does the poor cellular uptake of technetium-99m labelled thymidine derivatives prevent the development of a thymidine-based SPECT tracer, or are there ways to improve the cell uptake?
- Is the application of a mixed nitrosyl-carbonyl technetium-labelled compound in radiopharmacy a realistic goal?

6.4.1 Chelating Systems for the $\{MO\}^{3+}$ Core

We have shown that the "click-to-chelate" approach can be very successfully applied to the functionalization of biomolecules with efficient chelating systems for the $M(CO)_3$ cores technetium and rhenium. It has been proven that the $^{99m}Tc(CO)_3$ labelled compounds are stable *in vitro* and *in vivo*, and it has very recently been shown in the case of a folic acid derivative, which incorporates a triazole-containing $^{99m}Tc(CO)_3$ chelate, that the compounds are also suitable for SPECT imaging.[13] In many ways $[^{99m}Tc(CO)_3(H_2O)_3]$ is an excellent labelling precursor, and the stability of the complexes it forms with tridentate chelators is often cited as its primary advantage. However, as part of a potential radiopharmaceutical, there are also circumstances where such high stability could be disadvantageous, and a less stable $^{99m}Tc^{V}O$-labelled complex which underwent more rapid decomposition and washout from non-target organs and tissues *in vivo* might be preferred.

Preliminary investigations as part of this thesis suggest that the "click-to-chelate" approach also provides a practical functionalization strategy for labelling with the $\{MO\}^{3+}$ core. It is well documented that suitable chelating systems for the $\{MO\}^{3+}$

core incorporate combinations of amines, amides, thiols and carboxylic acids, and can be based on tripeptide sequences such as Gly-Gly-Cys.[14] Semi-rigid ligands, which incorporate pyridyl and imidazolyl groups are also reported to form stable complexes with the $\{MO\}^{3+}$ cores of both ^{99m}Tc and Re.[15,16] This led us to believe that tetradentate, triazole-containing chelating systems which also include amines, amides, thiols or carboxylic acids would form suitable chelating systems for the $\{MO\}^{3+}$ core.

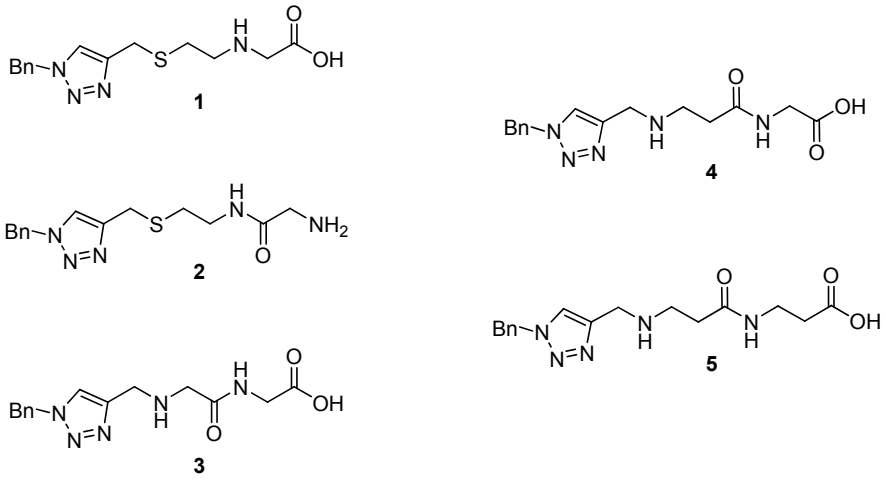

Figure 1. Examples of triazole-containing ligand systems for the $\{MO\}^{3+}$ core.

The synthesis of tetradentate, triazole-containing chelating systems for the $\{MO\}^{3+}$ core requires first the synthesis of a tridentate alkyne component. Suitable alkynes were derived from compounds which had already been synthesized, for example, *S*-propargyl-2-aminoethanethiol and *N*-propargyl glycine, as well as *N*-propargyl β-alanine, using standard alkylation and coupling reactions. Triazole-containing chelating systems were prepared from the reaction with benzyl azide (Figure 1). Model complexes containing the $\{Re^{V}O\}^{3+}$ core were prepared from the reaction with the Re(V) precursor $ReOCl_3(PPh_3)_2$. X-ray structure analysis of the complex formed with ligand **4** confirmed the expected coordination of the tetradentate ligand including through N3 of the triazole (Figure 2).

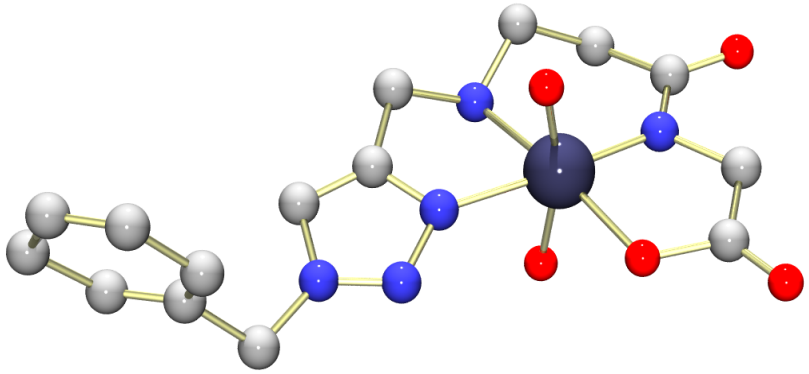

Figure 2. Preliminary crystal structure of an Re(V) complex, with the tetradentate triazole-containing chelating system **4**. An OH group occupies the position *trans* to the oxo ligand.

Not only will the extension of the "click-to-chelate" approach facilitate the parallel synthesis of MO-labelled conjugates, but it will also enable a straightforward comparison of $M(CO)_3$- and MO-labelled compounds from a single azide precursor. However, given that triazoles are known to coordinate to a range of metals, the "click-to-chelate" approach is by no means limited to the preparation of bioconjugates to be labelled with technetium and rhenium. The same strategy will almost certainly be applied to couple metal complexes to organic and bioorganic molecules in other areas of bioorganometallic and medicinal inorganic chemistry, and recent examples from the literature indicate that potential applications are already being explored.[17]

6.4.2 Technetium-labelled thymidine analogues

The incorporation of technetium into any potential target-specific radiopharmaceutical is defined by the requirement for a metal chelating system to be installed, to coordinate and stabilize the metal. Significant modification of the overall structure of the molecule is therefore unavoidable, even if the metal chelate is tethered at a reasonable distance from the pharmacophore. The cellular uptake of nucleosides and nucleoside analogues is typically mediated by nucleoside transporters and most commonly by the ubiquitously expressed human equilibrative nucleoside transporter hENT1. If nucleoside analogues are not actively transported, they require sufficient lipophilicity

and ideally a large concentration gradient to accumulate by passive diffusion. The high specific activity of technetium-99m radiopharmaceuticals means, however, that they are used in very low concentrations, which are not conducive to high rates of passive diffusion.

One approach to increasing the cellular uptake of technetium-labelled thymidine analogues would be the design of a compound which is more likely to be recognized by the hENT1 transporter, than the C3′ or N3 functionalized derivatives so far evaluated. hENT1 in fact has a relatively broad permeant selectivity, and is able to recognize a wide range of natural and synthetic purine- and pyrimidine-based nucleosides.[18] However, it is well documented that modifications of the ribose at the C3′ position are not well tolerated and AZT, for example, is not actively transported by hENT1.[19] Modifications of the pyrimidine ring appear to be preferred in terms of hNT1 transportability, but it seems likely that distancing the metal chealte from the nucleoside interferes with recognition. In this respect it may also be disadvantageous to introduce a charged metal complex, which could be more likely to interfere with the transport protein than a neutral complex, as well as less likely to internalize by passive diffusion. By contrast, increasing the spacer between thymidine and the metal complex has a positive influence on the substrate efficacy towards hTK1. We have also shown, using isostructural but differently charged $Re(CO)_3$ and $Re(CO)_2(NO)$ labelled derivatives, that structural considerations rather than overall charge appear more critical in determining a compound's ability to be a substrate for hTK1. The challenge in designing a compound likely to be recognized by nucleoside transporters, therefore, is to maintain substrate affinity for hTK1 which, while tolerant to modifications at either the C3′ or N3 positions, has the most restricted substrate specificity of the four deoxyribonucleoside kinases.

A second and perhaps more realistic approach would be to incorporate a secondary targeting molecule to aid membrane permeation. Although hTK1 tolerates modifications to thymidine and deoxyuridine at the N3 and C3′ positions, it is not known whether it would accept a compound modified at both positions as a substrate. It is conceivable that this would require more dramatic conformational changes in the enzyme, which in turn would lead to a loss or decrease in enzyme activity. However, an interesting target might incorporate a technetium/rhenium chelate at the C3′ position of

thymidine in combination with either a lipophilic group, or a membrane permeable arginine-rich peptide at the N3 position, or vice versa (Figure 3). Eriksson *et al.* investigated thymidine analogues which had minor modifications at two positions, such as 3′-fluoro-5-fluorodeoxyuridine, and their results suggest that the dual-functionalized compounds were less good substrates than either of the corresponding mono-functionalized compounds.[20] This is not necessarily surprising, and in order to maintain sufficient activity towards the enzyme, the combination of spacer length, metal chelate structure and nature of the secondary targeting molecule would need to be optimized.

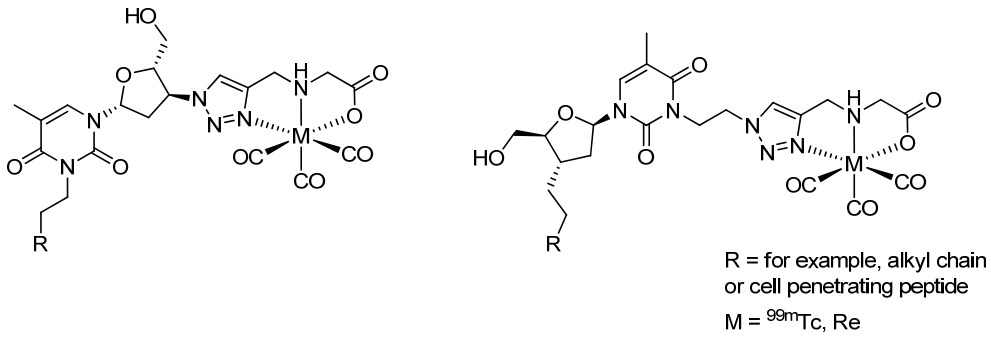

Figure 3. Potential dual-functionalized thymidine derivatives.

From the wealth of information about the expression of hTK1 in various proliferative tissues and the successful application of radiolabelled thymidine analogues for use as PET tracers, it is obvious that thymidine kinase is an attractive target for diagnostic imaging, and that a technetium-labelled thymidine analogue would have considerable practical consequences. On the other hand, given the structural modification necessary to prepare technetium-labelled target-specific radiopharmaceuticals, the development of technetium-labelled compounds, which must first rely on membrane proteins for active transport to an intracellular target, will always be complicated by the substrate specificity of the transporter. In this respect, hTK1 might not be the most suitable target for a technetium based tracer. For technetium-labelled compounds, targeting receptors, which themselves facilitate internalization, would appear to be the more sensible strategy.

6.4.3 The $\{M(CO)_2(NO)\}^{2+}$ core

Use of the isostructural precursors $[Re(CO)_2(NO)Br_3]^-$ and $[Re(CO)_3Br_3]^{2-}$ provided an elegant method of investigating the effect of overall charge on the ability of organometallic thymidine complexes to act as substrates for hTK1. While no differences were observed, overall charge is a parameter which is likely to have a more critical influence on other pharmacological properties. For example, if two isostructural but differently charged complexes were to show measurable cell uptake, then as a result of their differing charge, the lipophilicity and membrane permeability of the complexes would almost certainly be different. The overall charge is also much more likely to influence the *in vivo* properties of any potential radiopharmaceuticals, such as the rate and route of excretion of the compound. There are examples in the literature where nitrosylation has also been employed to improve the *in vitro* properties of corresponding tricarbonyl-labelled compounds,[21] but such effects are difficult to predict and can only be evaluated on a case-by-case basis. This is relatively straightforward using the $Re(CO)_2(NO)$ core because the chemistry is established, and this is likely to remain a useful tool for structure optimization or for a better understanding of structure-activity relationships. It seems unlikely, however, that labelling with the $\{^{99m}Tc(CO)_2(NO)\}^{2+}$ core will find applications in radiopharmacy, since the synthesis of the $[^{99m}Tc(CO)_2(NO)(H_2O)_3]^{2+}$ precursor from pertechnetate on the tracer level is challenging, particularly when compared with the synthesis of $[^{99m}Tc(CO)_3(H_2O)_3]^+$. Unfortunately, there is a lack of convincing evidence to suggest that $^{99m}Tc(CO)_2(NO)$-labelled compounds have sufficiently improved pharmacokinetics to warrant the additional complexity of their preparation.

6.5 References

(1) Huang, S.; Clark, R. J.; Zhu, L. *Org. Lett.* **2007**, *9*, 4999-5002.

(2) Maisonial, A.; Serafin, P.; Traikia, M.; Debiton, E.; Thery, V.; Aitken, D. J.; Lemoine, P.; Viossat, B.; Gautier, A. *Eur. J. Inorg. Chem.* **2008**, 298-305.

(3) Welin, M.; Kosinska, U.; Mikkelsen, N. E.; Carnrot, C.; Zhu, C. Y.; Wang, L. Y.; Eriksson, S.; Munch-Petersen, B.; Eklund, H. *Proc. Natl. Acad. Sci. U. S. A.* **2004**, *101*, 17970-17975.

(4) Arner, E. S. J.; Eriksson, S. *Pharmacol. Ther.* **1995**, *67*, 155-186.

(5) Tjarks, W.; Wang, J.; Chandra, S.; Ji, W.; Zhuo, J.; Lunato, A. J.; Boyer, C.; Li, Q.; Usova, E. V.; Eriksson, S.; Morrison, G. H.; Cosquer, G. Y. *Nucleos. Nucleot. Nucleic Acids* **2001**, *20*, 695-698.

(6) Barth, R. F.; Yang, W. L.; Al-Madhoun, A. S.; Johnsamuel, J.; Byun, Y.; Chandra, S.; Smith, D. R.; Tjarks, W.; Eriksson, S. *Cancer Res.* **2004**, *64*, 6287-6295.

(7) Celen, S.; De Groot, T. J.; Balzarini, J.; Vunckx, K.; Terwinghe, C.; Vermaelen, P.; Van Berckelaer, L.; Vanbilloen, H.; Nuyts, J.; Mortelmans, L.; Verbruggen, A.; Bormans, G. *Nucl. Med. Biol.* **2007**, *34*, 283-291.

(8) Schmid, M.; Neumaier, B.; Vogg, A. T. J.; Wczasek, K.; Friesen, C.; Mottaghy, F. M.; Buck, A. K.; Reske, S. N. *Nucl. Med. Biol.* **2006**, *33*, 359-366

(9) Desbouis, D.; Struthers, H.; Spiwok, V.; Küster, T.; Schibli, R. *J. Med. Chem.* **2008**, *51*, 6689-6698.

(10) Struthers, H.; Spingler, B.; Mindt, T. L.; Schibli, R. *Chem.--Eur. J.* **2008**, *14*, 6173-6183.

(11) Marti, N.; Spingler, B.; Breher, F.; Schibli, R. *Inorg. Chem.* **2005**, *44*, 6082-6091.

(12) Müller, C.; Dumas, C.; Hoffmann, U.; Schubiger, P. A.; Schibli, R. *J. Organomet. Chem.* **2004**, *689*, 4712-4721.

(13) Mindt, T. L.; Muller, C.; Melis, M.; de Jong, M.; Schibli, R. *Bioconjugate Chem.* **2008**, *19*, 1689-1695.

(14) Liu, S.; Edwards, D. S. *Chem. Rev.* **1999**, *99*, 2235-2268.

(15) Rajagopalan, R.; Grummon, G. D.; Bugaj, J.; Hallemann, L. S.; Webb, E. G.; Marmion, M. E.; Vanderheyden, J. L.; Srinivasan, A. *Bioconjugate Chem.* **1997**, *8*, 407-415.

(16) Kurti, L.; Papagiannopoulou, D.; Papadopoulos, M.; Pirmettis, L.; Raptopoulou, C. P.; Terzis, A.; Chlotellis, E.; Harmata, M.; Kuntz, R. R.; Pandurangi, R. S. *Inorg. Chem.* **2003**, *42*, 2960-2967.

(17) Ziegler, T.; Hermann, C. *Tetrahedron Lett.* **2008**, *49*, 2166-2169.

(18) Zhang, J.; Visser, F.; King, K. M.; Baldwin, S. A.; Young, J. D.; Cass, C. E. *Cancer Metastasis Rev.* **2007**, *26*, 85-110.

(19) Yao, S. Y. M.; Ng, A. M. L.; Sundaram, M.; Cass, C. E.; Baldwin, S. A.; Young, J. D. *Mol. Membr. Biol.* **2001**, *18*, 161-167.

(20) Kosinska, U.; Carnrot, C.; Eriksson, S.; Wang, L.; Eklund, H. *FEBS J.* **2005**, *272*, 6365-6372.

(21) Causey, P. W.; Besanger, T. R.; Valliant, J. F. *J. Med. Chem.* **2008**, *51*, 2833-2844.

Supplementary information for chapter 2

A1 Synthesis of triazole-containing ligands with unprotected click substrates

All of the click reactions investigated proceeded quantitatively with unprotected substrates, as determined by HPLC or ^{1}H-NMR (Table 1). The water solubility of most of the unprotected triazole ligand systems complicated their isolation and purification. Only unprotected triazole ligands **6**, **10** and **13** could be conveniently isolated from their reaction solutions. All other triazole products prepared in solution were synthesized in 2-3 steps from protected substrates.

Table 1. Conversion of click substrates after 45 min at 75 ^{o}C: a) 25 mM in D_2O, conversion of substrates determined by ^{1}H-NMR; b) products which precipitated from the reaction mixture were dissolved for NMR measurement by adding a drops of DCl and gently heating; c) 0.2 mM in water, conversion of substrates determined by HPLC.

Alkyne substrate	Azide substrate	Product (conversion)	
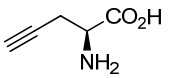	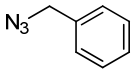	**5**	(>95%[a,b])
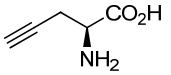	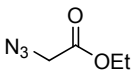	**6**	(>95%[a])
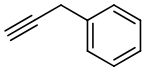	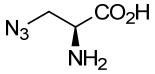	**7**	(>95%[a,b])
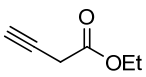	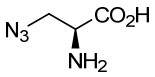	**8**	(>95%[a])
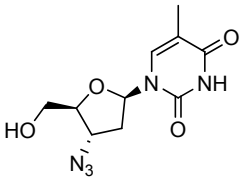	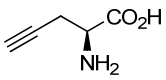	**10**	(>95%[c])
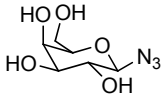	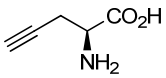	**11**	(>95%[a])

A2 Representative NMR analysis of triazole-containing ligands and their $Re(CO)_3$ complexes

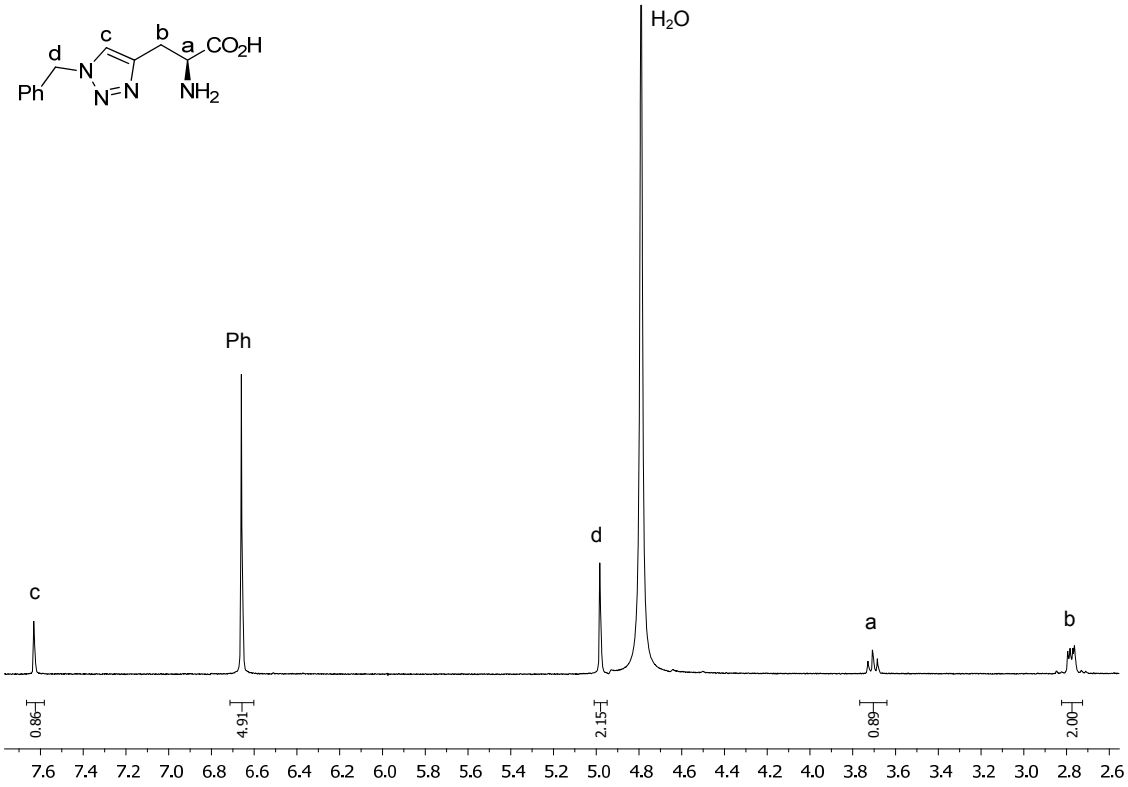

Figure 1. ^{1}H-NMR spectrum of compound **5**.

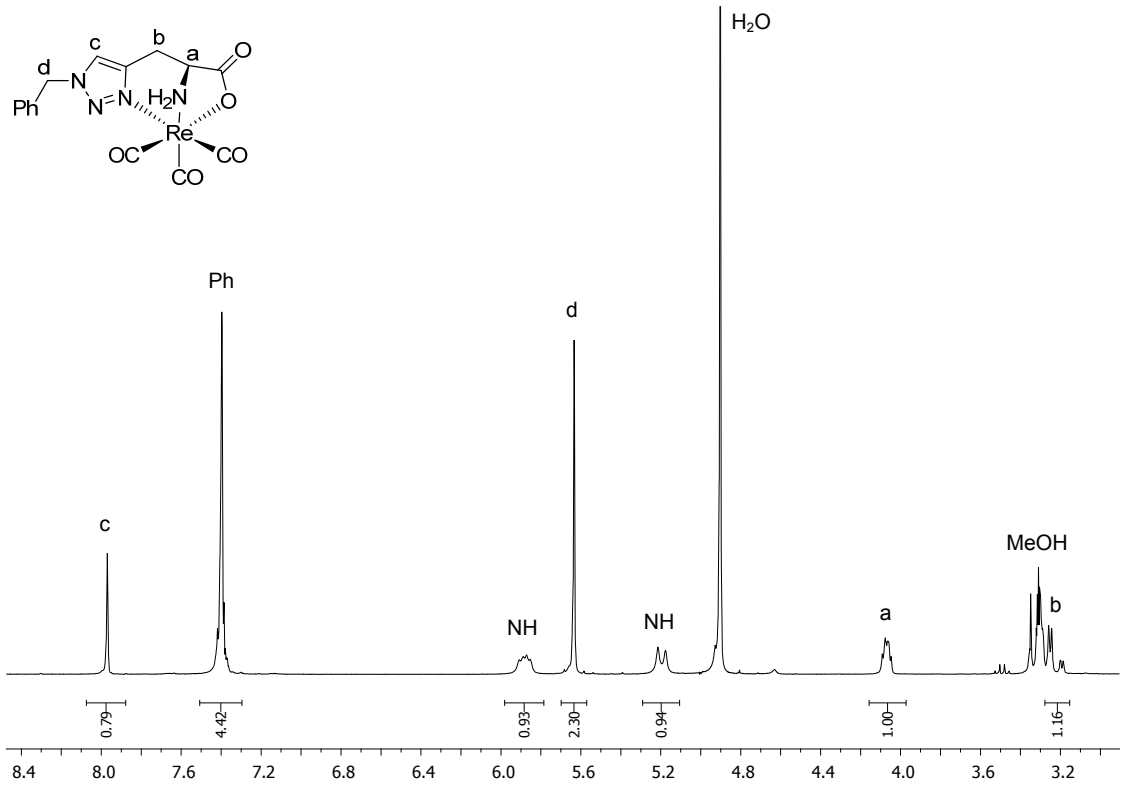

Figure 2. ^{1}H-NMR spectrum of compound [Re(CO)$_3$**5**].

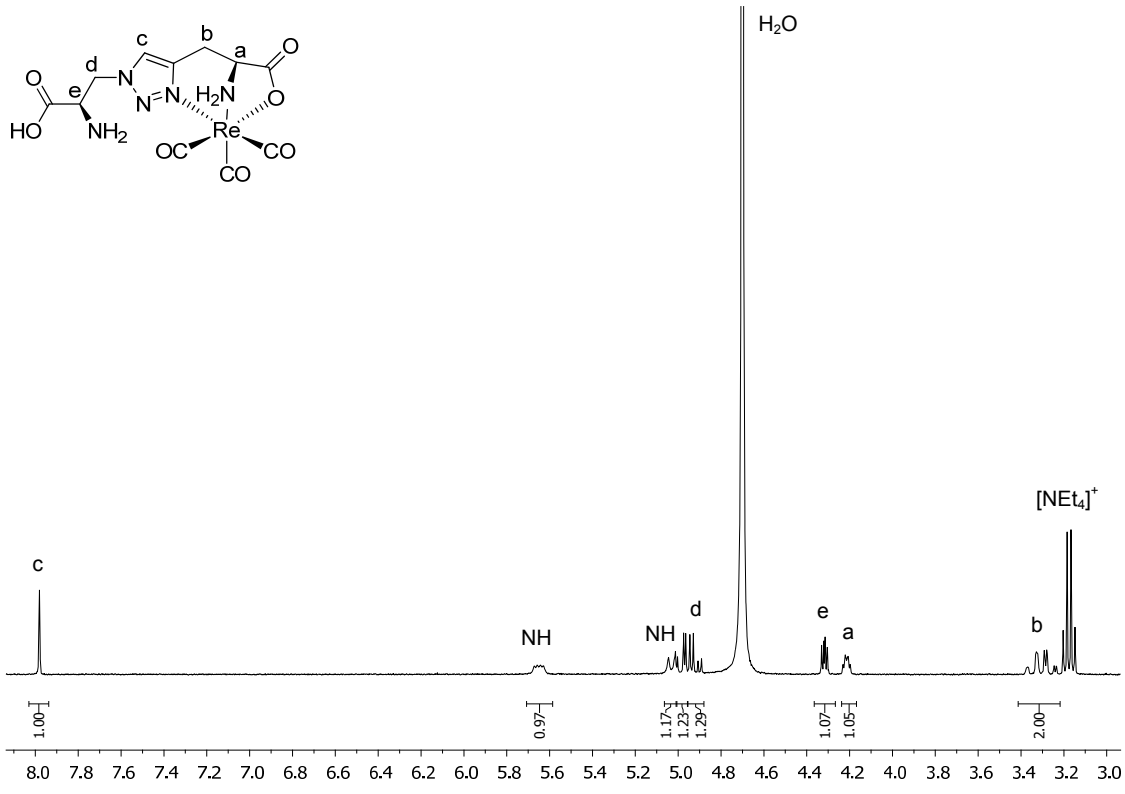

Figure 3. ^{1}H-NMR spectrum of compound [Re(CO)$_3$**9**].

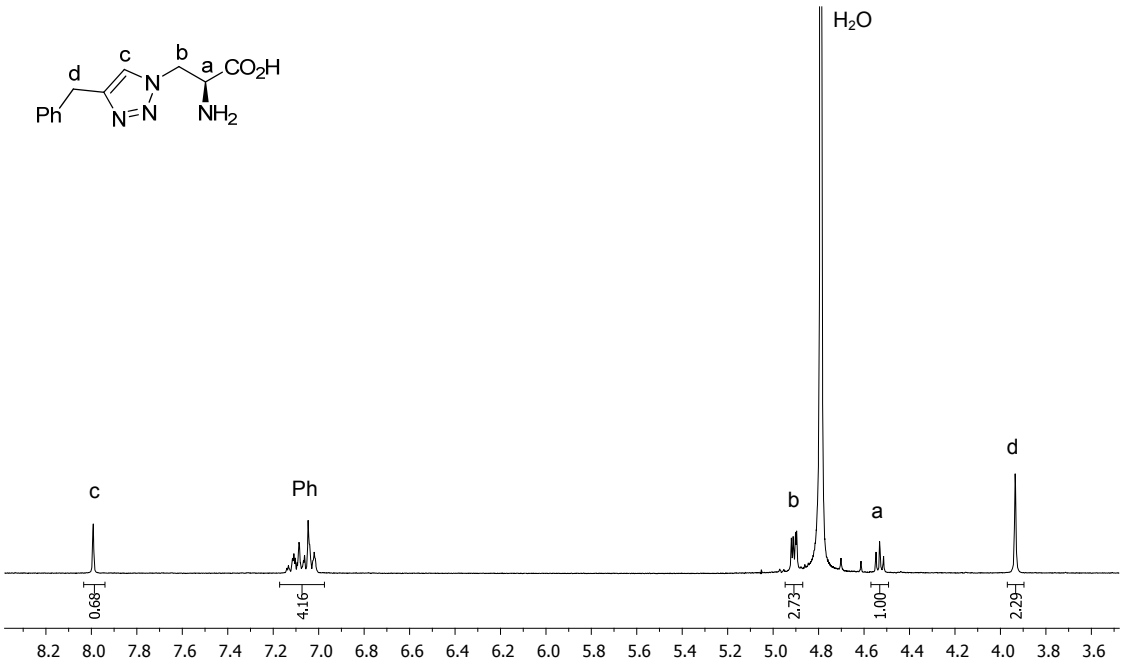

Figure 4. [1]H-NMR spectrum of compound compound **7.**

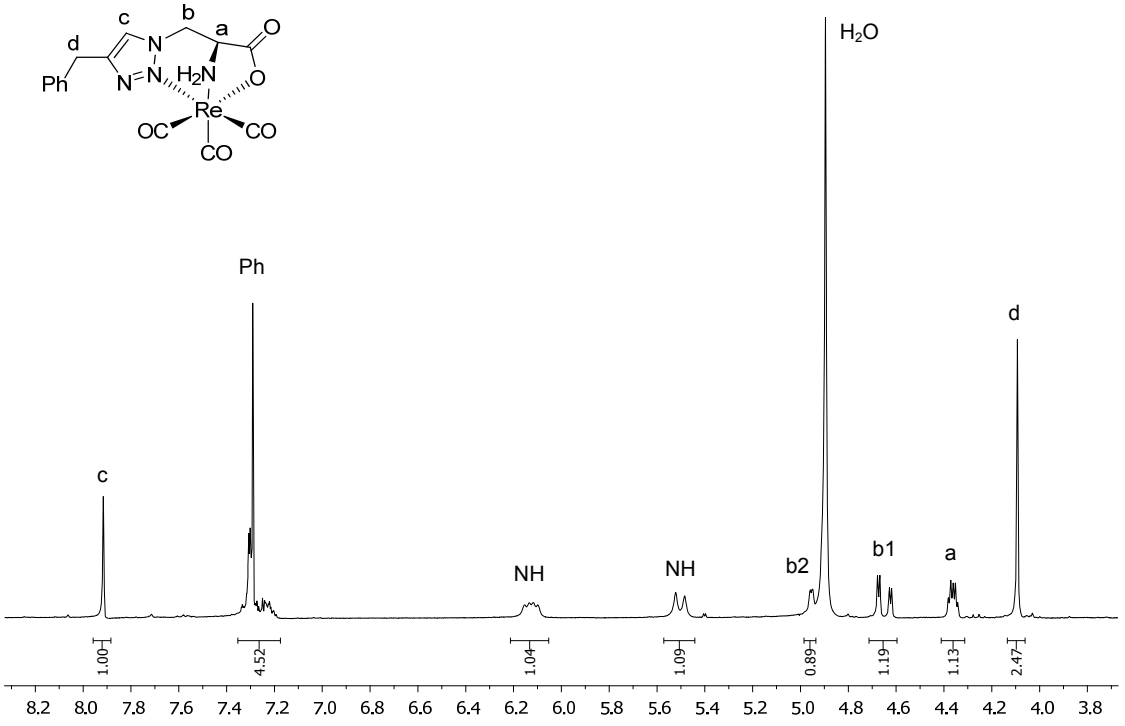

Figure 5. [1]H-NMR spectrum of compound [$Re(CO)_3$**7**].

A3 Radiolabelling efficiencies of the triazole-containing ligands

Table 2. Radiolabelling efficiencies of ligands **5-9**. EC_{50} values correspond to the ligand concentration necessary to achieve 50% radiolabelling yield in the conversion of $[^{99m}Tc(CO)_3(H_2O)_3]^+$ to $[^{99m}Tc(CO)_3\mathbf{L}]$.

	Ligand, **L**	EC_{50} value
5	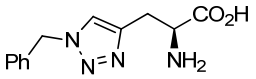	2.45×10^{-7}
6	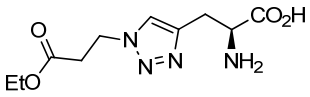	3.02×10^{-7}
7	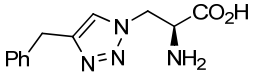	2.97×10^{-5}
8	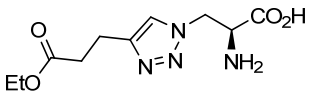	2.96×10^{-5}
9	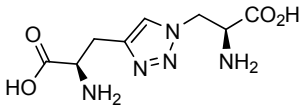	9.81×10^{-8}
Nτ-MeHis	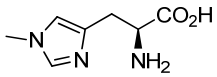	9.47×10^{-8}

A4 DFT Calculations

All calculations were conducted using density functional theory (DFT) as implemented in the Gaussian 03, Revision C.02 suite of *ab initio* quantum chemistry programs.[1] Geometry optimizations and vibrational frequency calculations were performed using the restricted B3LYP exchange and correlation functionals and either the double-ζ 6-31G(d) or triple-ζ 6-311+G(d) basis sets for all atoms. Normal SCF and geometry convergence criteria were used and no symmetry constraints were imposed. Harmonic frequency analysis based on analytical second derivates was used to characterize the optimized geometries as local minima.

[1] Frisch, M. J.; Trucks, G. W.; Schlegel, H. B.; Scuseria, G. E.; Robb, M. A. *et al.* Gaussian Inc., Wallingford CT, 2004.

Figure 6 shows the B3LYP/6-31G(d) optimized geometries and atom numbering scheme for 1,4-dimethylimidazole and 1,4-dimethyltriazole, used as models for the histidine and click based ligands respectively. The Cartesian coordinates for the optimized structures are given in Table 3 below. Mulliken population analysis and Natural population analysis charges on the atoms of the imidazole and triazole rings are given in Table 4.

Table 3. Cartesian coordinates for the optimized structures of 1,4-dimethylimidazole and 1,4-dimethyltriazole.

1,4-Dimethylimidazole				**1,4-Dimethyltriazole**			
B3LYP/6-31G(d)				**B3LYP/6-31G(d)**			
7	1.088731000	-0.090134000	-0.000104000	7	-1.062618000	0.084371000	0.000000000
6	0.608147000	1.188692000	-0.000038000	7	-0.643424000	-1.200536000	0.000000000
7	-0.705946000	1.233387000	0.000026000	7	0.661155000	-1.188628000	0.000000000
6	-1.117087000	-0.085824000	0.000001000	6	1.105173000	0.105509000	0.000000000
6	-0.020716000	-0.916196000	-0.000060000	6	0.000000000	0.930740000	0.000000000
1	1.272352000	2.044191000	0.000004000	1	-0.111268000	2.004848000	0.000000000
1	0.073909000	-1.992662000	-0.000084000	6	2.562250000	0.445378000	0.000000000
6	-2.568004000	-0.455011000	0.000056000	1	3.062194000	0.030207000	0.882291000
1	-3.078395000	-0.049540000	0.881840000	1	3.062194000	0.030207000	-0.882291000
1	-3.078533000	-0.049042000	-0.881478000	1	2.713897000	1.529073000	0.000000000
1	-2.699123000	-1.542052000	-0.000305000	6	-2.482197000	0.384928000	0.000000000
6	2.479898000	-0.500940000	0.000071000	1	-2.756916000	0.954591000	0.893167000
1	2.712620000	-1.093401000	0.891564000	1	-2.756916000	0.954591000	-0.893167000
1	2.712312000	-1.094887000	-0.890454000	1	-3.010326000	-0.569293000	0.000000000
1	3.111933000	0.390286000	-0.000722000				
B3LYP/6-311+G(d)				**B3LYP/6-311+G(d)**			
7	1.088086000	-0.088825000	-0.000067000	7	-1.061640000	0.081473000	0.000000000
6	0.608145000	1.187965000	-0.000014000	7	-0.640121000	-1.198739000	0.000000000
7	-0.704518000	1.228401000	0.000039000	7	0.661537000	-1.184883000	0.000000000
6	-1.117727000	-0.087708000	0.000003000	6	1.105613000	0.106002000	0.000000000
6	-0.020650000	-0.914969000	-0.000046000	6	-0.000126000	0.927395000	0.000000000
1	1.266820000	2.045334000	-0.000020000	1	-0.111987000	1.999836000	0.000000000
1	0.073574000	-1.990027000	-0.000089000	6	2.559957000	0.445873000	0.000000000
6	-2.566207000	-0.455095000	0.000022000	1	3.058781000	0.032127000	0.880238000
1	-3.074085000	-0.049633000	0.879955000	1	3.058781000	0.032127000	-0.880238000
1	-3.074196000	-0.049229000	-0.879659000	1	2.713682000	1.526845000	0.000000000
1	-2.700944000	-1.539265000	-0.000218000	6	-2.481135000	0.384988000	0.000000000
6	2.479515000	-0.501277000	0.000089000	1	-2.753071000	0.953188000	0.891450000
1	2.710901000	-1.091608000	0.889791000	1	-2.753071000	0.953188000	-0.891450000
1	2.710631000	-1.092968000	-0.888773000	1	-3.013999000	-0.563435000	0.000000000
1	3.112753000	0.385770000	-0.000697000				

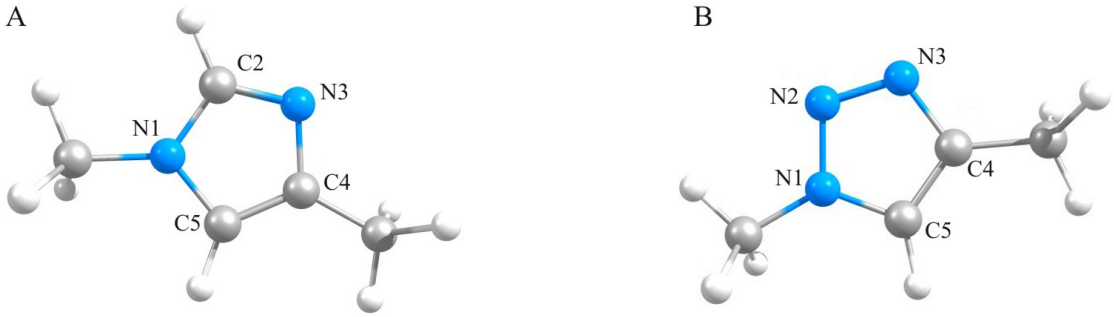

Figure 6. B3LYP/6-31G(d) optimized geometries and natural population analyses for 1,4-dimethylimidazole (A) and 1,4-dimethyltriazole (B) used as models for the histidine and click based ligands, respectively.

From the atomic charge analysis using different two basis sets and the two different methods (MPA and NPA) it can been seen that Mulliken charges are highly sensitive to the basis set used whereas the Natural population charges vary less between the two calculations.

Table 4. Mulliken population analysis (MPA) and Natural population analysis (NPA) charges on the atoms of the imidazole and triazole rings. The atomic numbering is shown in Figure 6.

	Imidazole				**Triazole**			
	B3LYP/6-31G(d)		B3LYP/6-311+G(d)		B3LYP/6-31G(d)		B3LYP/6-311+G(d)	
Atom	MPA	NPA	MPA	NPA	MPA	NPA	MPA	NPA
N1	-0.365	-0.399	0.283	-0.412	-0.218	-0.198	0.409	-0.208
N2	-	-	-	-	-0.083	-0.071	-0.098	-0.078
C2	0.196	0.187	-0.042	0.217	-	-	-	-
N3	-0.474	-0.502	-0.125	-0.511	-0.327	-0.268	-0.188	-0.277
C4	0.232	0.106	0.517	0.107	0.259	0.083	0.442	0.086
C5	-0.028	-0.106	-0.468	-0.083	-0.014	-0.086	-0.545	-0.060

A5 One-pot radiolabelling with the $[^{99m}Tc(CO)_3(H_2O)_3]^+$ precursor

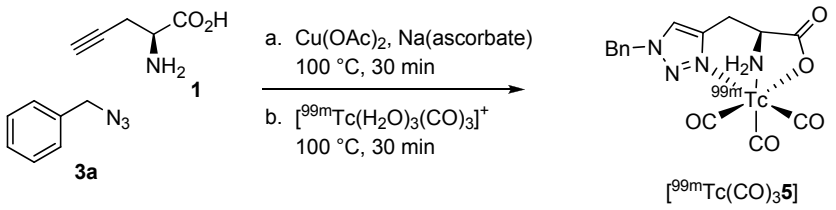

Scheme 1. *In situ* radiolabelling of the click reaction between **1** and **3a**.

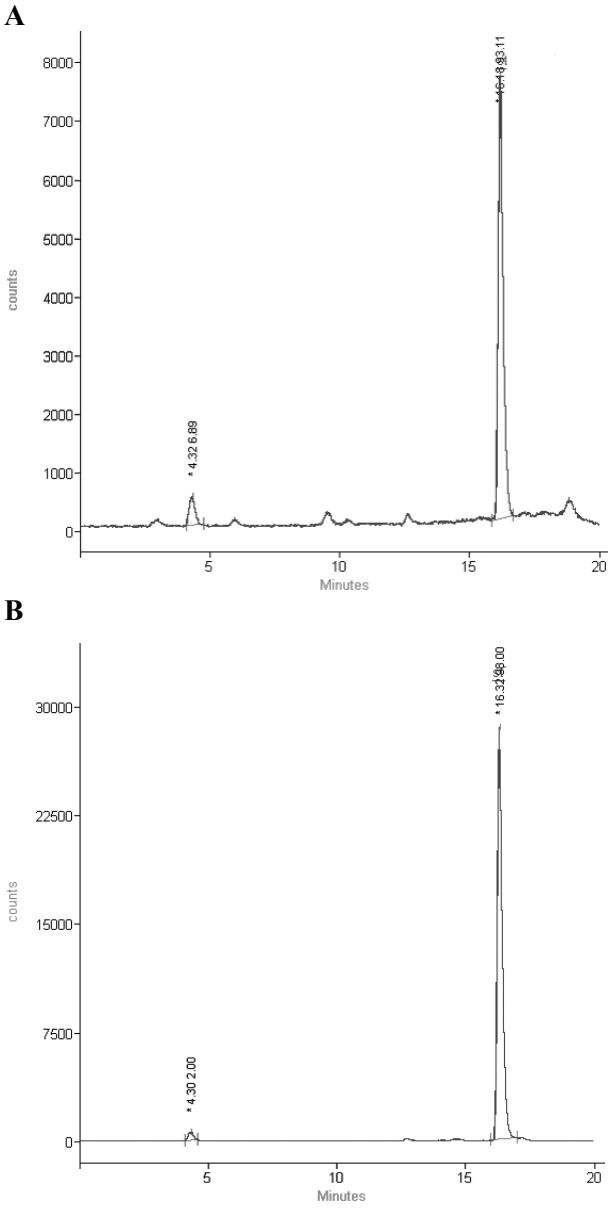

Figure 7. (A) HPLC trace of the one-pot radiolabelling of the reaction between **1** and **3a**; (B) HPLC trace of the radiolabelling of ligand **5**.

A6 Pharmacological Characterization of [^{99m}Tc(CO)$_3$9]

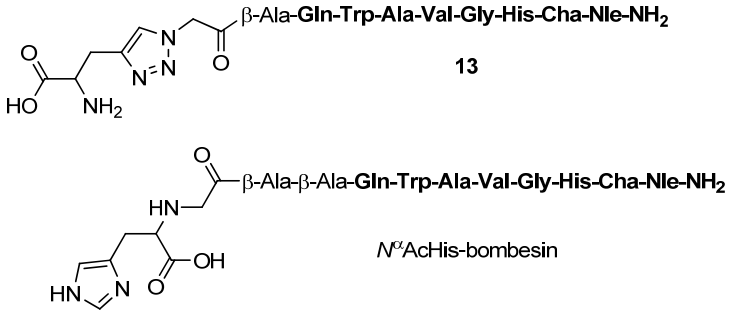

Figure 8. Amino acid sequence of bombesin derivatives included in these studies (receptor binding sequence in bold).

Table 5. IC_{50} and K_D values of bombesin analogues.

	n	IC_{50} [nM]*	n	K_D [nM]**
13	2	1.96 ± 1.55	3	0.19 ± 0.06
N^{α}AcHis-BBN	2	5.10 ± 1.75	2	0.19 ± 0.12

* non-radiolabelled peptides. ** ^{99m}Tc-labelled peptides

Table 6. Biodistribution (% I.D./g) of [^{99m}Tc(CO)$_3$$N^{\alpha}$AcHis-BBN] and [^{99m}Tc(CO)$_3$**13**] in CD-1 mice 1.5 h post injection of the radiotracers. Animals received the labelled analogue by i.v. administration. Data are mean ± SD (n = 3), expressed as a percentage of the injected dose per gram of tissue.

Organ	**13**	**13** (blocked)*	N^{α}AcHis-BBN	N^{α}AcHis-BBN (blocked)*
Blood	0.17 ± 0.01	0.19 ± 0.08	0.13 ± 0.01	0.35 ± 0.14
Heart	0.08 ± 0.02	0.16 ± 0.08	0.05 ± 0.01	0.14 ± 0.06
Kidneys	0.99 ± 0.11	0.84 ± 0.40	0.67 ± 0.04	1.36 ± 0.60
Liver	1.05 ± 0.17	1.59 ± 0.31	0.52 ± 0.13	1.66 ± 0.02
Pancreas	12.76 ± 2.91	0.80 ± 0.27	8.31 ± 3.36	3.73 ± 0.52
Stomach	0.89 ± 0.26	0.28 ± 0.10	0.68 ± 0.08	0.60 ± 0.09
Colon	2.87 ± 1.01	0.40 ± 0.15	5.80 ± 1.52	0.80 ± 0.01
Muscle	0.08 ± 0.07	0.37 ± 0.38	0.03 ± 0.02	0.60 ± 0.77
Bone	0.10 ± 0.03	0.20 ± 0.21	0.10 ± 0.05	0.24 ± 0.01

* Coinjection of 100 µg unlabelled bombesin

Supplementary information for chapter 3

B1 Representative NMR analysis of triazole-containing ligands and complexes

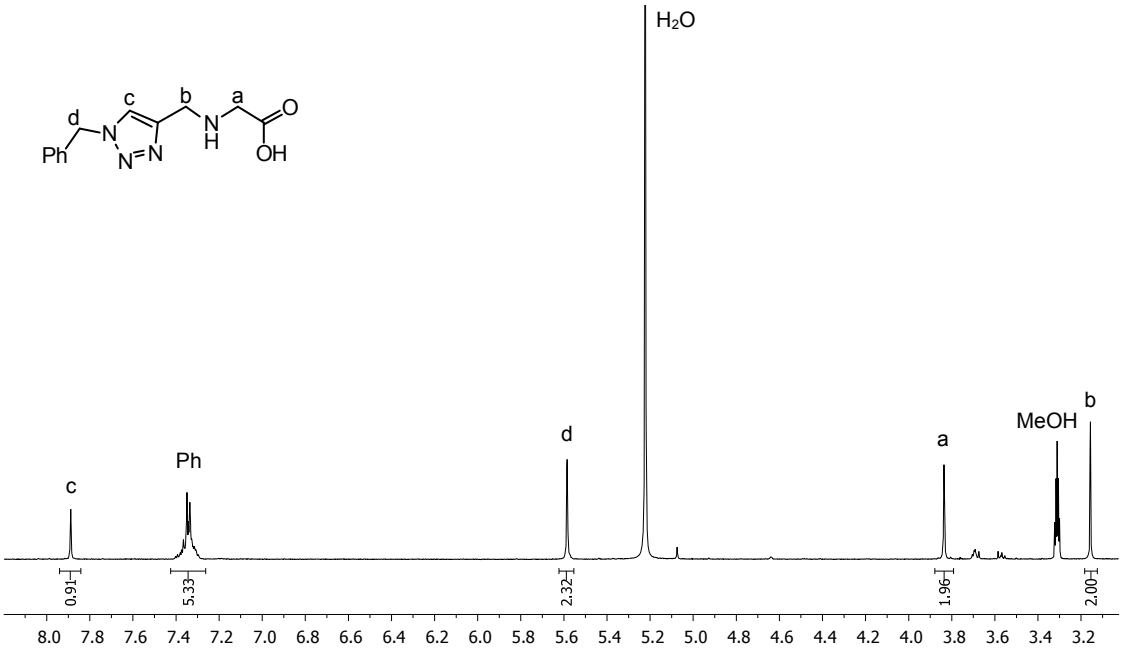

Figure 1. [1]H-NMR spectrum of **L2**.

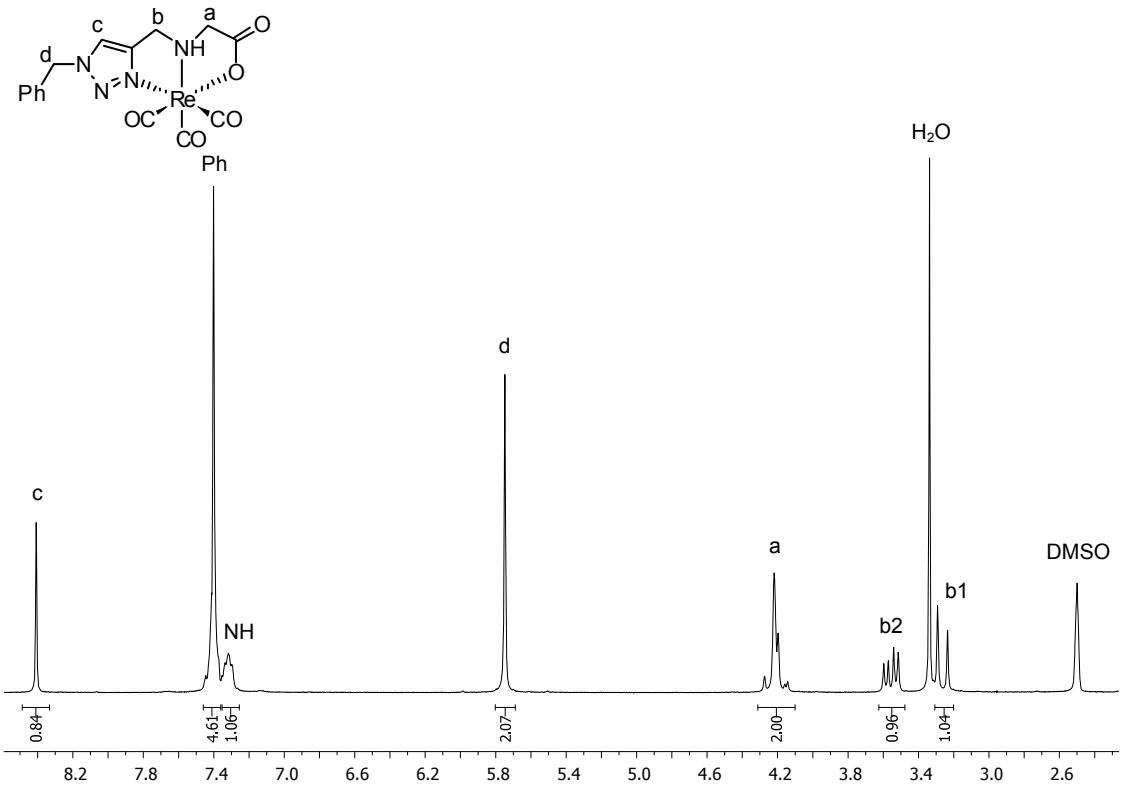

Figure 2. [1]H-NMR spectrum of [$Re(CO)_3$**L2**].

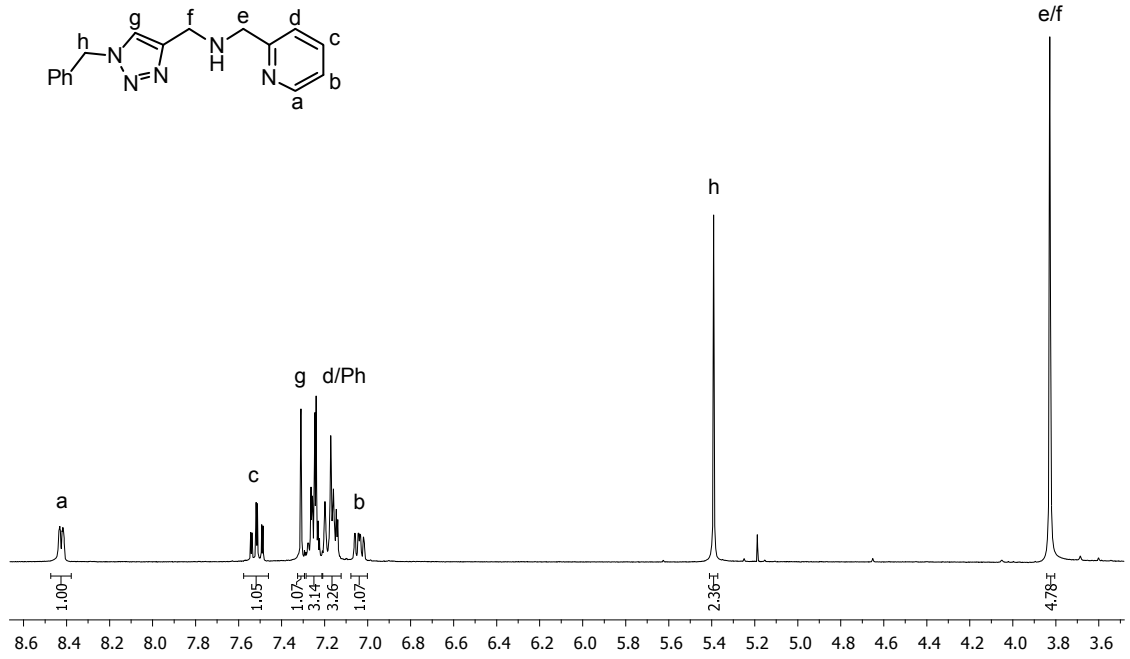

Figure 3. [1]H-NMR spectrum of **L4**.

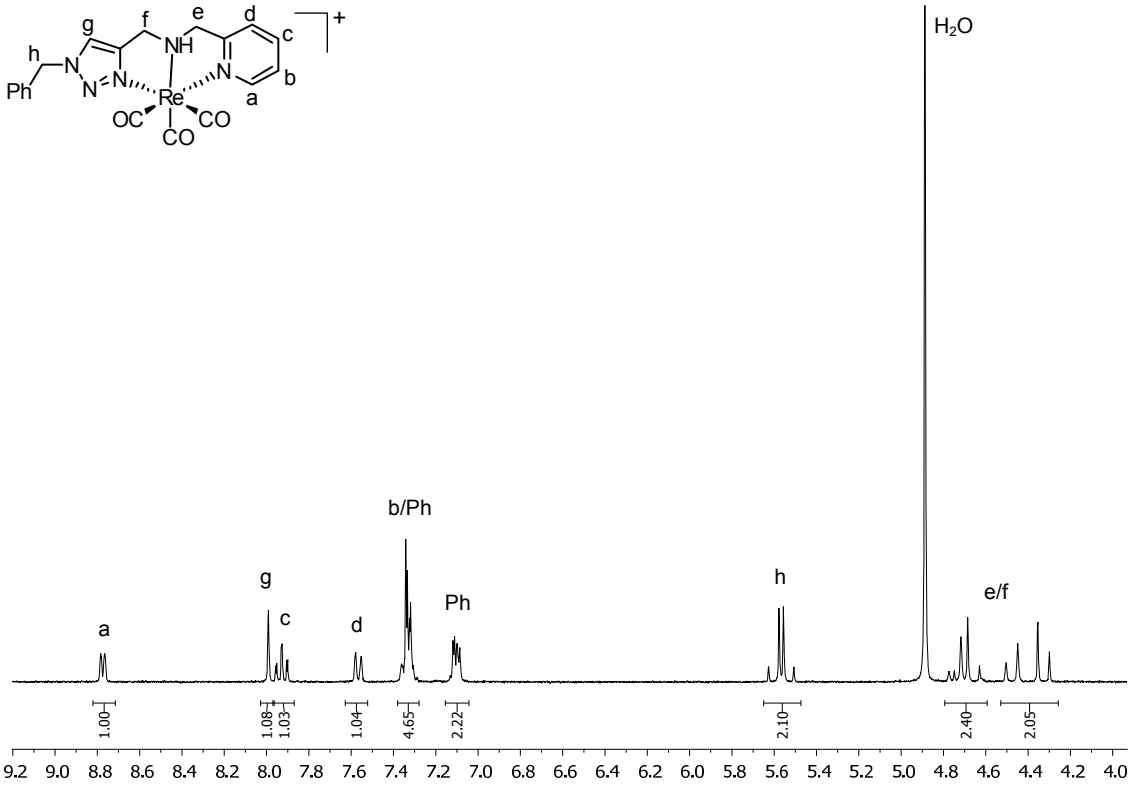

Figure 4. [1]H-NMR spectrum of $[Re(CO)_3\mathbf{L4}]^+$.

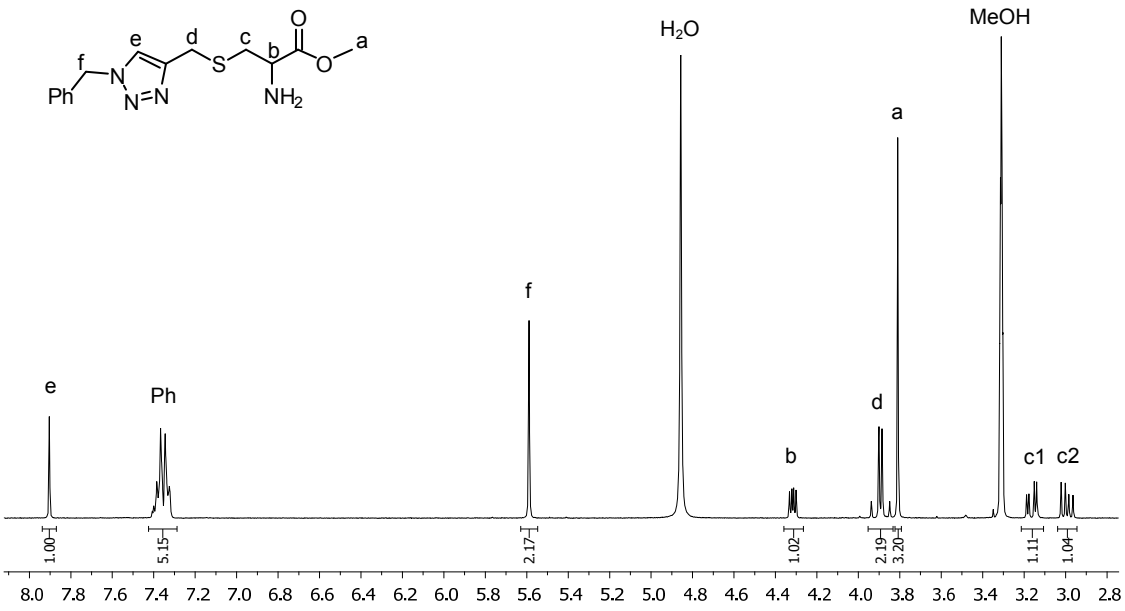

Figure 5. [1]H-NMR spectrum of **L7**.

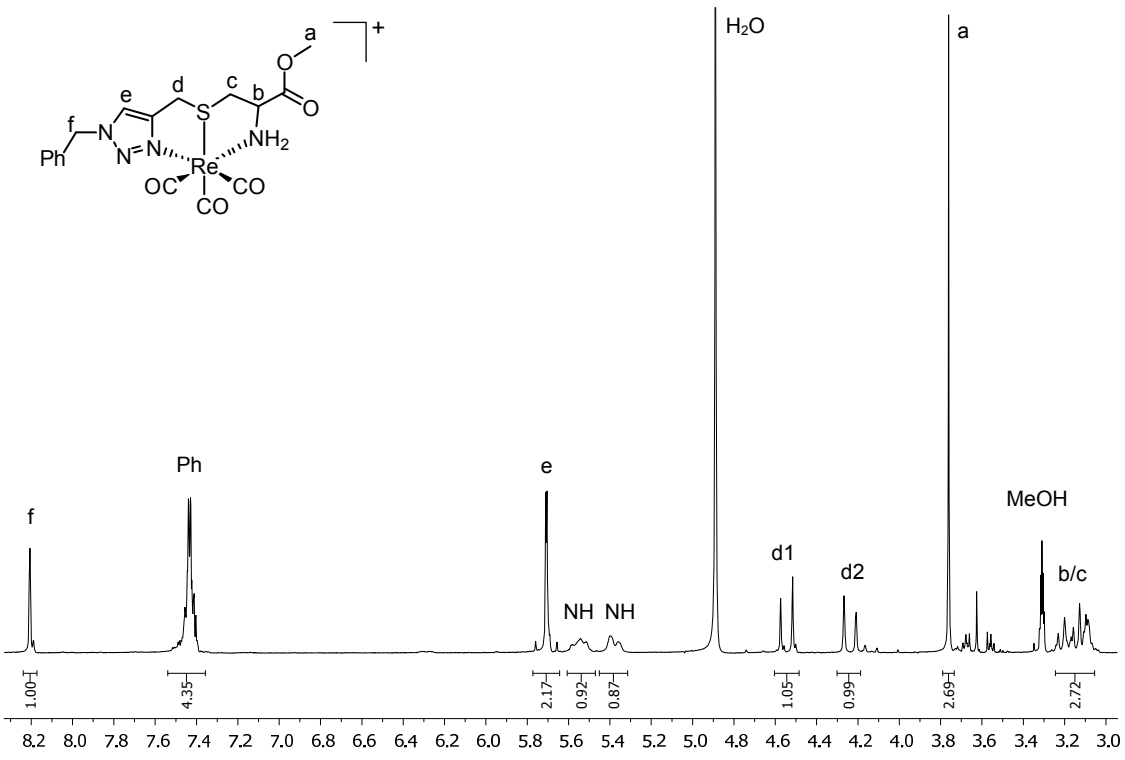

Figure 6. [1]H-NMR spectrum of $[Re(CO)_3$**L7**$]Br$.

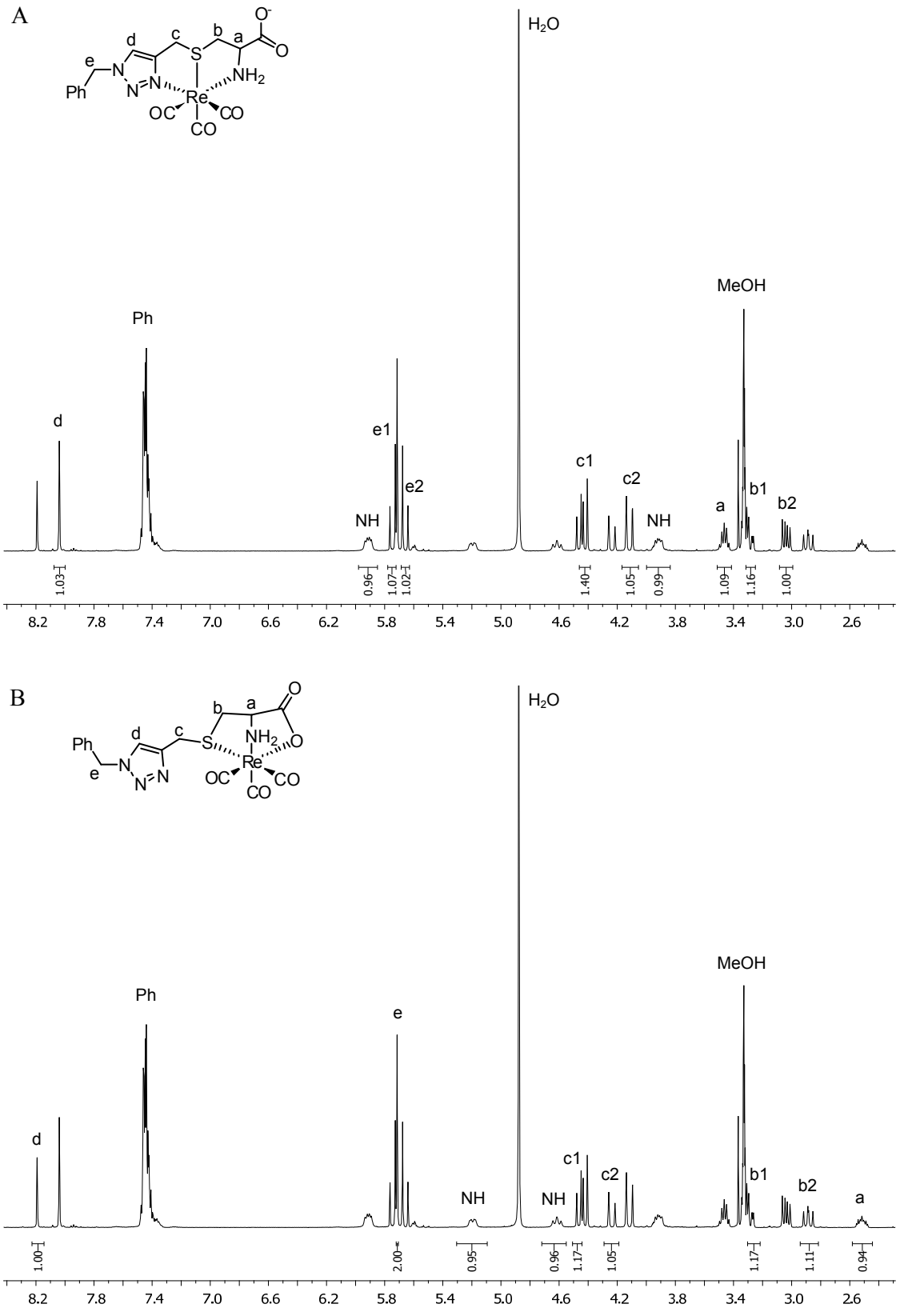

Figure 7. ^{1}H-NMR spectrum of [Re(CO)$_3$**L7b**]: (A) signals from the complex in which the triazole is coordinated; (B) signals from the complex in which coordination is through cysteine.

B2 Labelling efficiencies

The relative efficiencies of ligands **L1**, **L2**, **L4** and **L6** (Table 1) were assessed by comparing the yield of the reaction with $[^{99m}Tc(CO)_3(H_2O)_3]^+$ as the ligand concentration was varied between 10^{-3} M and 10^{-8} M, which gave rise to the step-sigmoid curves shown in Figure 8. EC_{50} values (concentration necessary to achieve 50% labelling yield) are in the sub-micromolar range, and are comparable with values already reported for the most efficient chelating systems for the $\{^{99m}Tc(CO)_3\}^+$ core.

Table 1. Radiolabelling efficiencies.

Ligand, **L**	EC_{50} value
L1 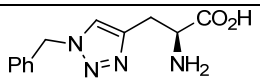	2.5×10^{-7}
L2 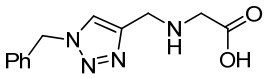	2.1×10^{-7}
L4 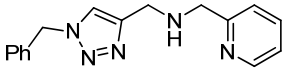	5.8×10^{-8}
L6 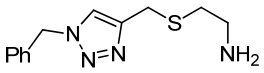	3.5×10^{-7}

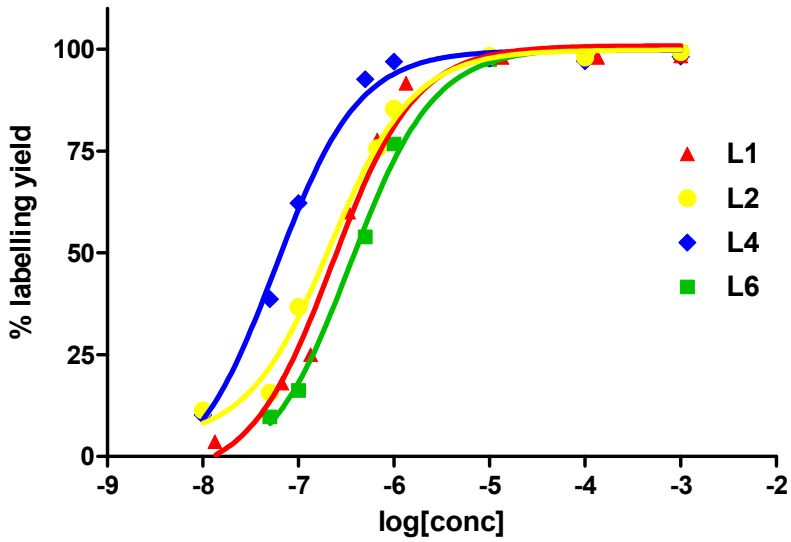

Figure 8. Labelling profiles for the reactions of ligands **L1**, **L2**, **L4** and **L6** with $[^{99m}Tc(CO)_3(H_2O)_3]^+$ as a function of ligand concentration.

B3 HPLC analysis of the synthesis and radiolabelling of thymidine derivatives

Alkynes **1**, **2**, **4** and **6** (Figure 9) were reacted with **dT-N_3**. 0.01 M solutions were prepared of each of the alkynes in water (**1**, **2**) or methanol (**4**, **6**). Aqueous 0.01 M solutions of **dT-N_3**, copper acetate and sodium ascorbate were prepared. All five reactions were carried out simultaneously. 60 µL **dT-N_3**, 50 µL alkyne, 10 µL sodium ascorbate and 5 µL copper acetate were added to an Eppendorf vial and heated at 65 °C for 60 minutes. Formation of the products was confirmed by HPLC (Figure 10) and mass spectroscopy.

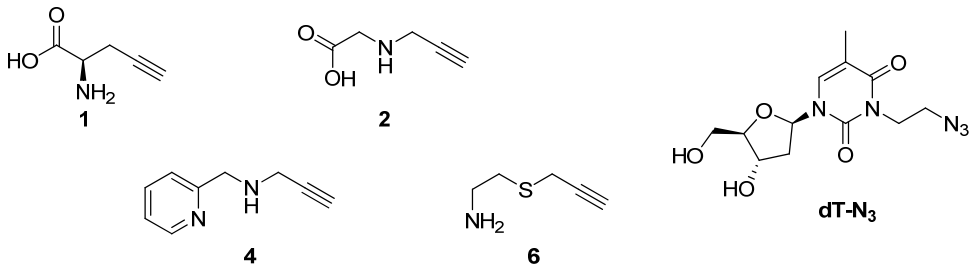

Figure 9. Alkynes **1**, **2**, **4**, **6** and **dT-N_3**.

A

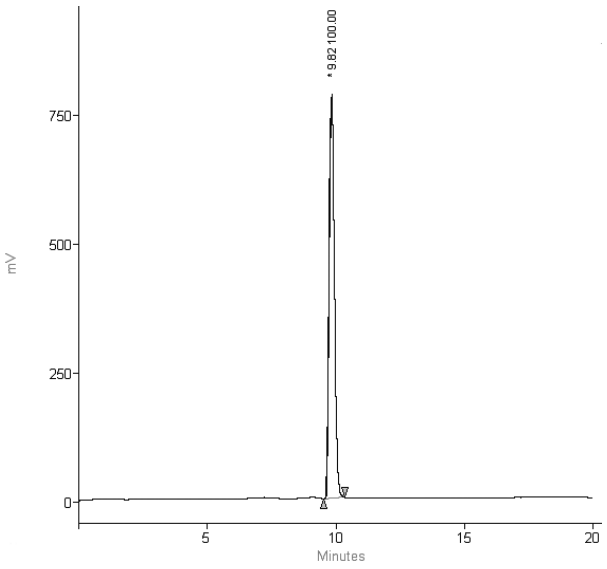

B

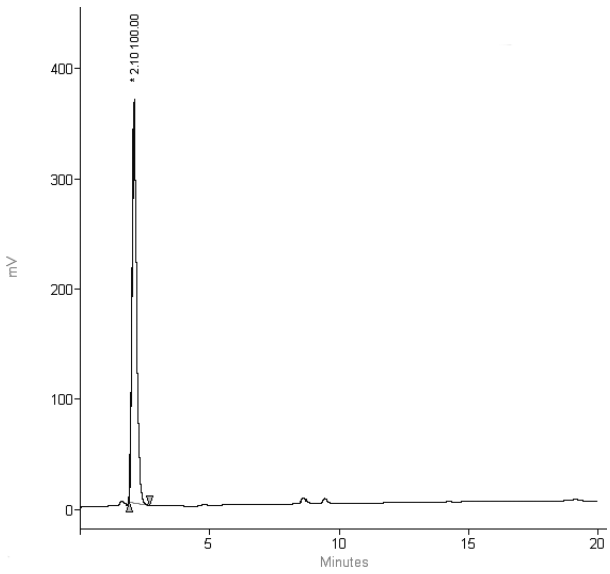

C

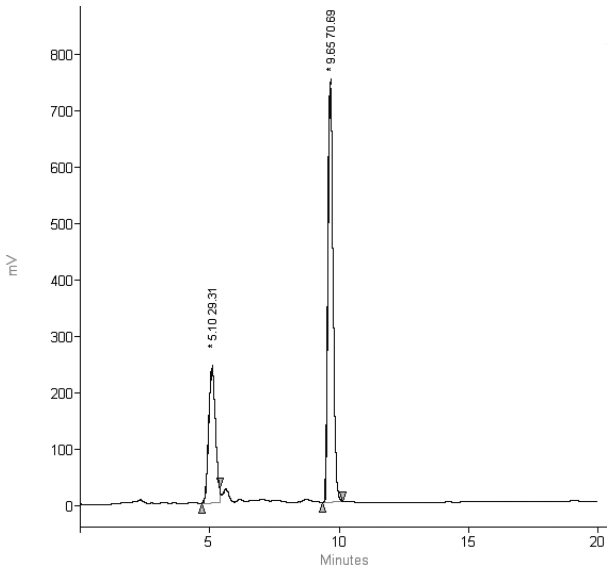

Figure 10. UV HPLC analysis of the click reaction between **1** and **dT-N_3**: (A) **dT-N_3**; (B) reaction mixture without **dT-N_3**; (C) Click reaction mixture after 1 h at 65 °C.

The click reaction mixtures were labelled directly with $[^{99m}Tc(OH_2)_3(CO)_3]^+$. 50 µL of a $[^{99m}Tc(OH_2)_3(CO)_3]^+$ solution were added to 20 µL of the click reaction diluted with 180 µL PBS buffer (pH 7.4), to give a ligand concentration of approximately 2.9 x 10^{-4} M. The reaction mixtures were heated at 100 °C for 60 minutes before the formation of the products was confirmed by HPLC. All of the labelled compounds were obtained in approximately 90% yield. Figure 11 shows two representative γ-HPLC traces.

A

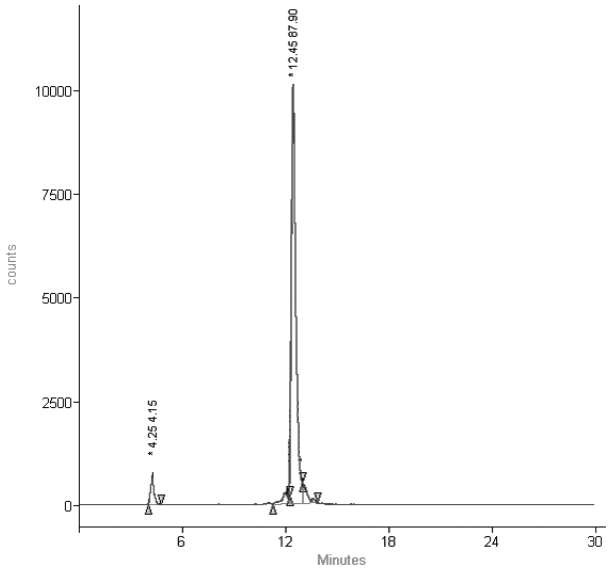

B

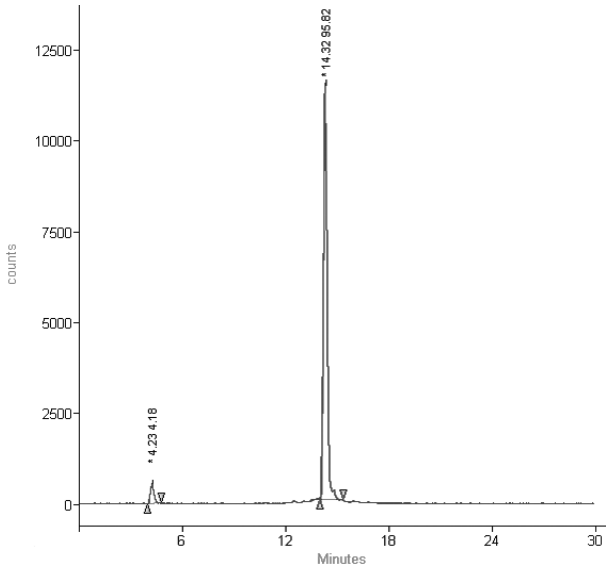

Figure 11. γ-HPLC traces from the radiolabeling of reactions between **2** and **dT-N_3** to give [^{99m}Tc(CO)$_3$**dT2**] (A), and **4** and **dT-N_3** to give [^{99m}Tc(CO)$_3$**dT4**]$^+$ (B).

Supplementary information for chapter 4

C1 Representative NMR analysis of functionalized thymidine derivatives

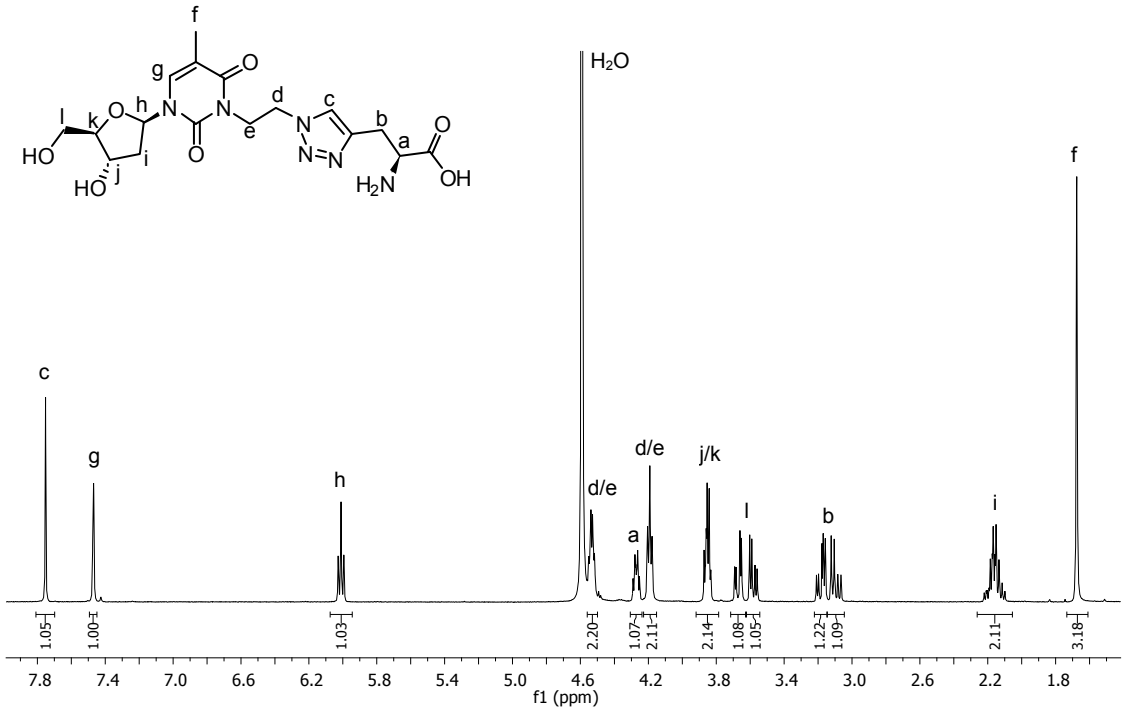

Figure 1. [1]H-NMR of compound **7**.

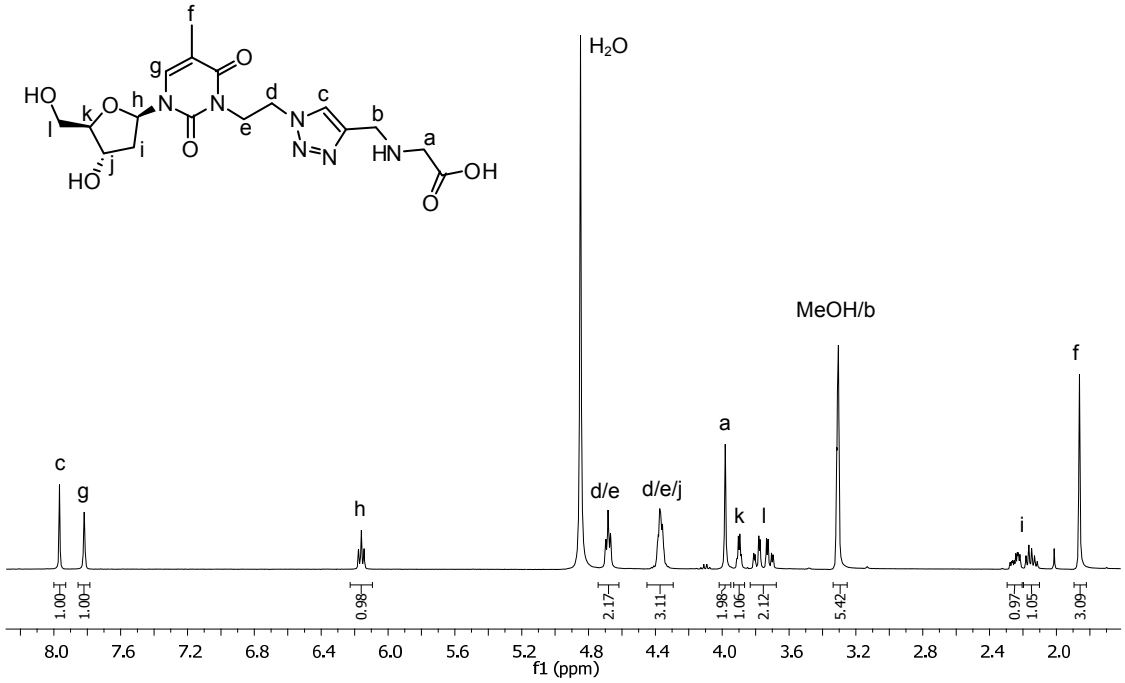

Figure 2. [1]H-NMR of compound **10**.

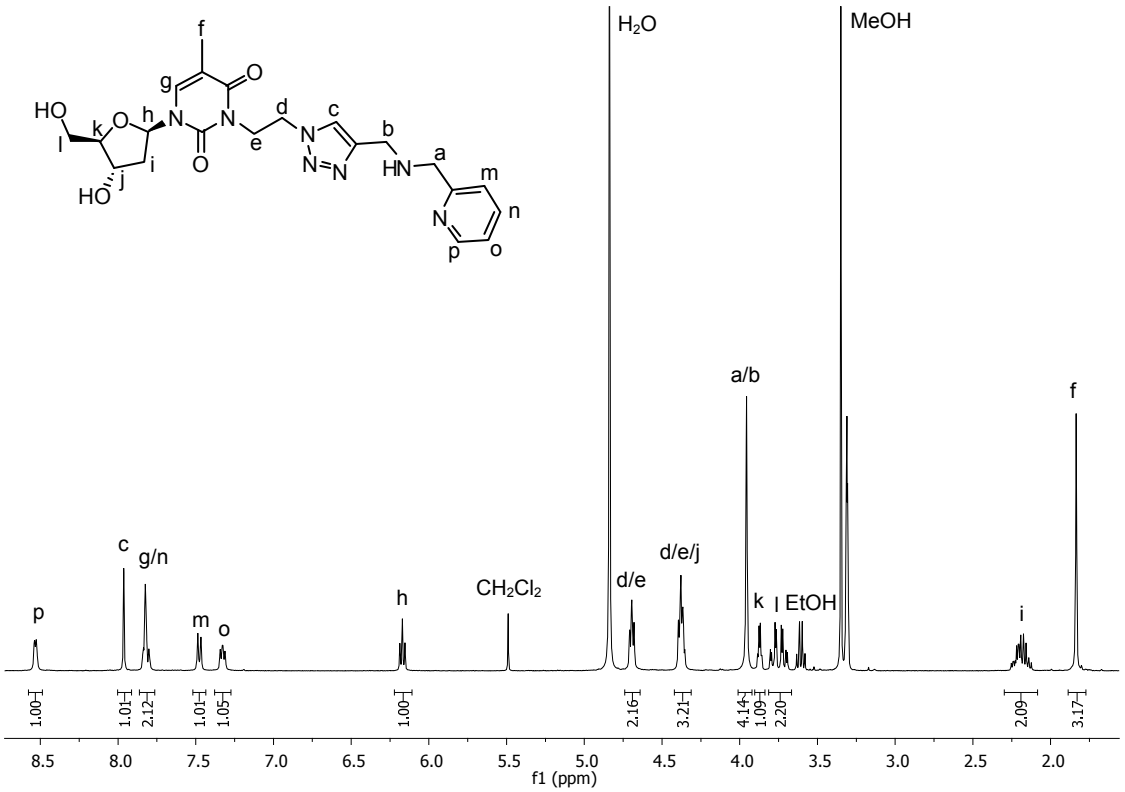

Figure 3. [1]H-NMR of compound **11**.

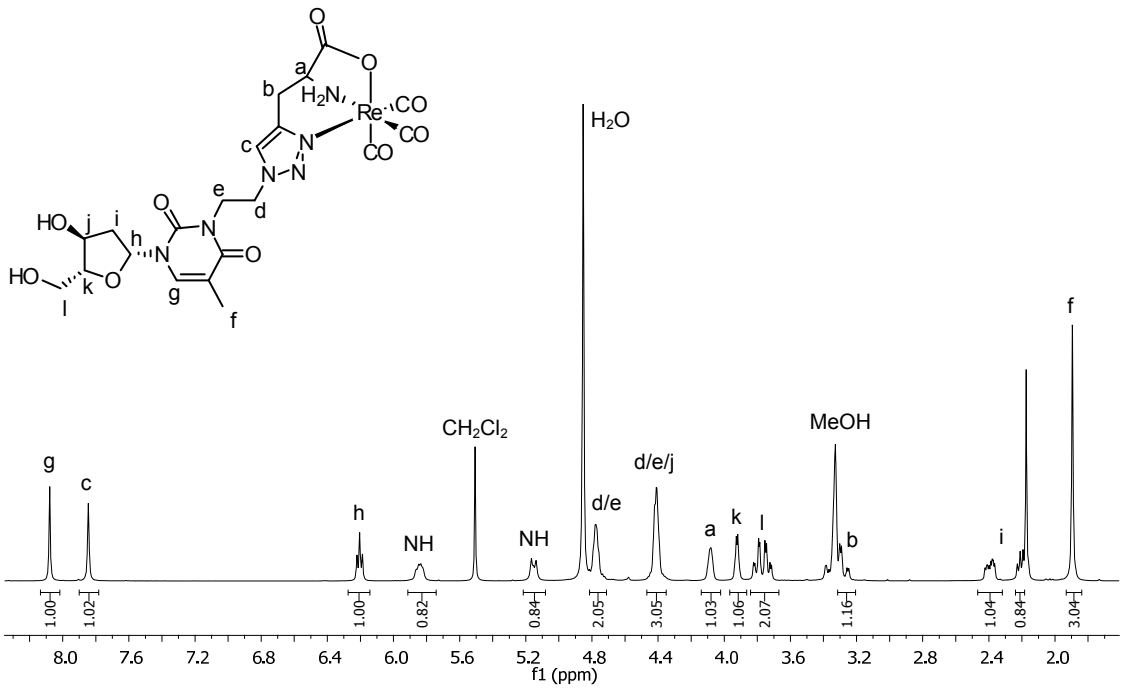

Figure 4. [1]H-NMR of [$Re(CO)_3$**7**].

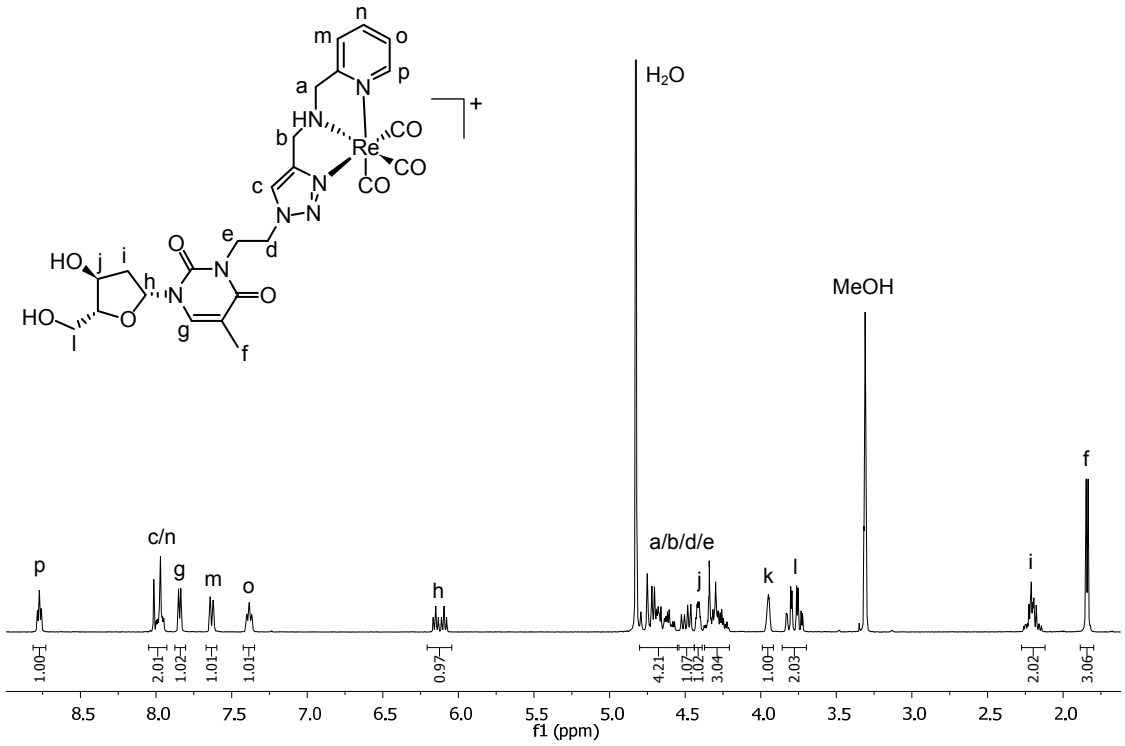

Figure 5. ^{1}H-NMR of [Re(CO)$_3$**11**]Br.

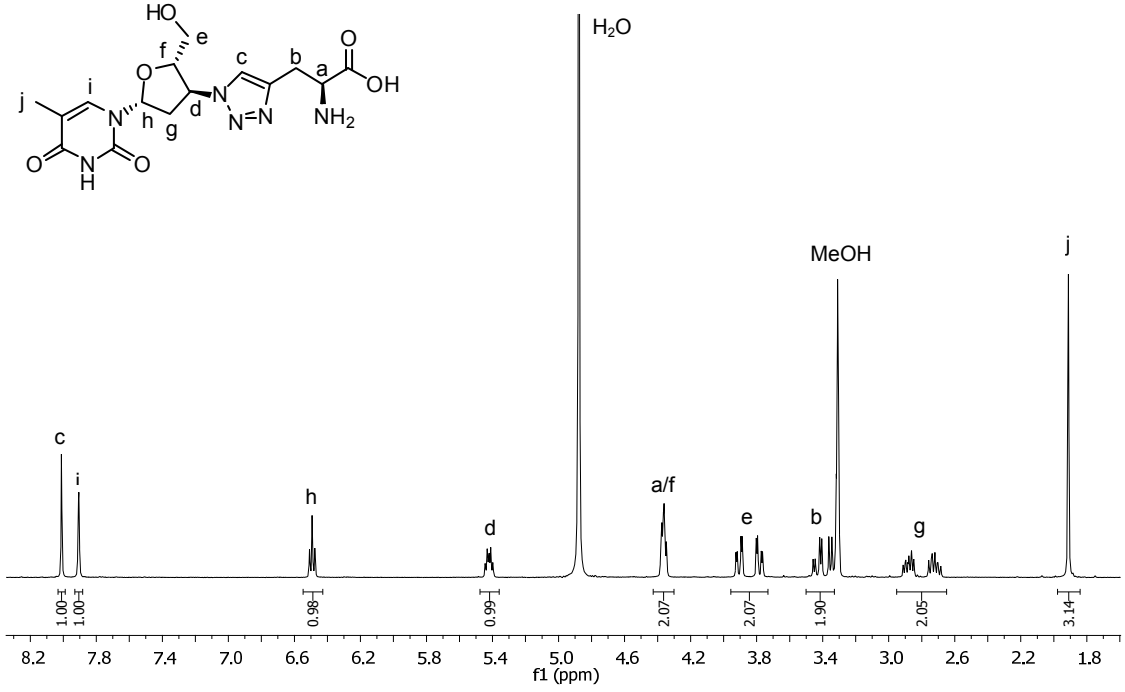

Figure 6. ^{1}H-NMR of compound **12**.

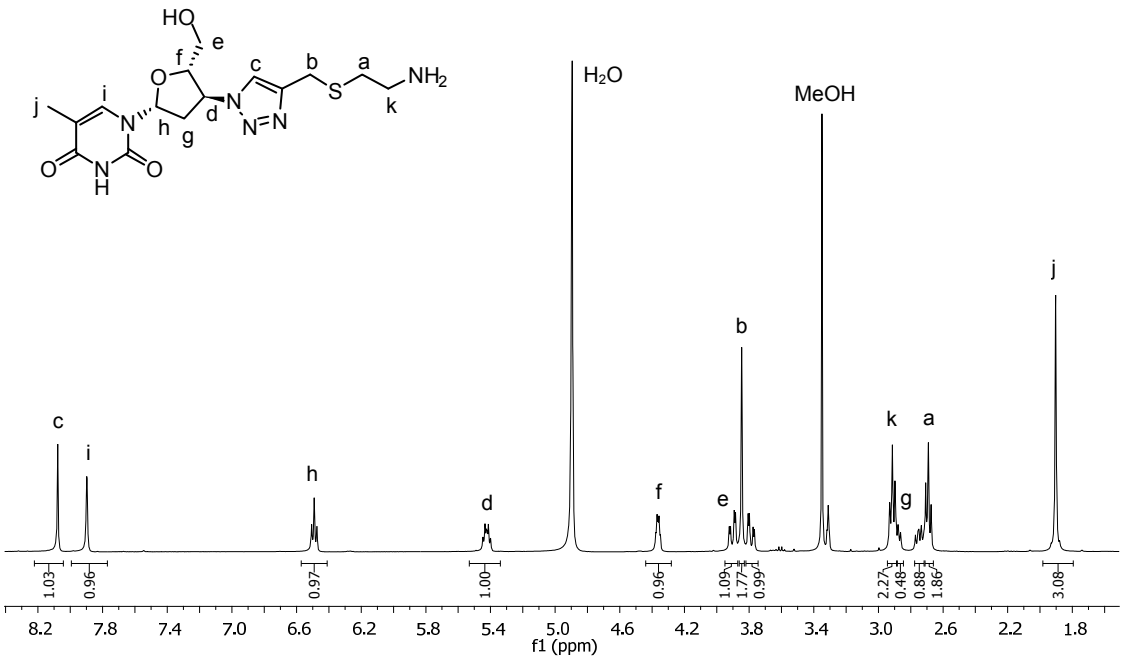

Figure 7. [1]H-NMR of compound **13**.

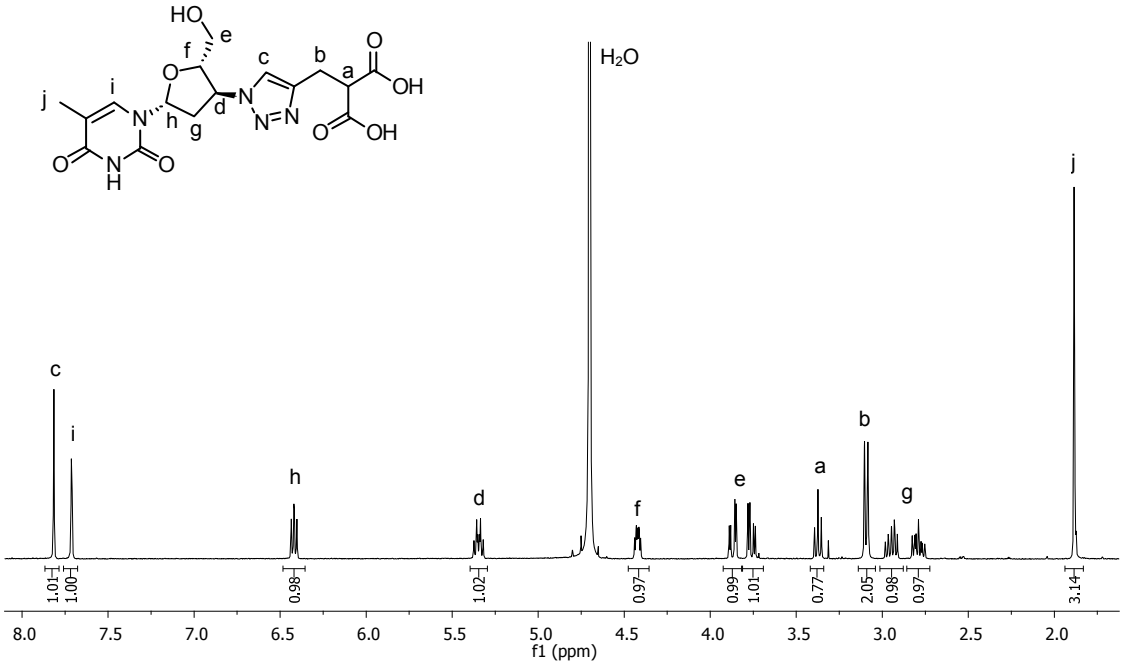

Figure 8. [1]H-NMR of compound **14**.

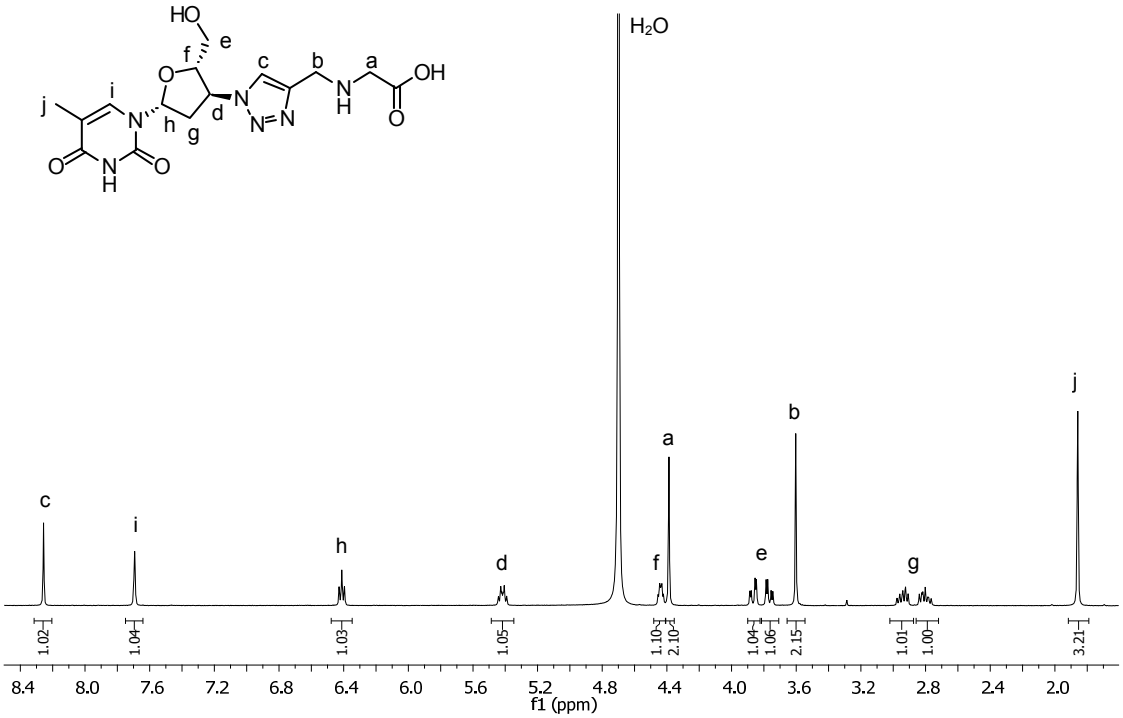

Figure 9. [1]H-NMR of compound **15**.

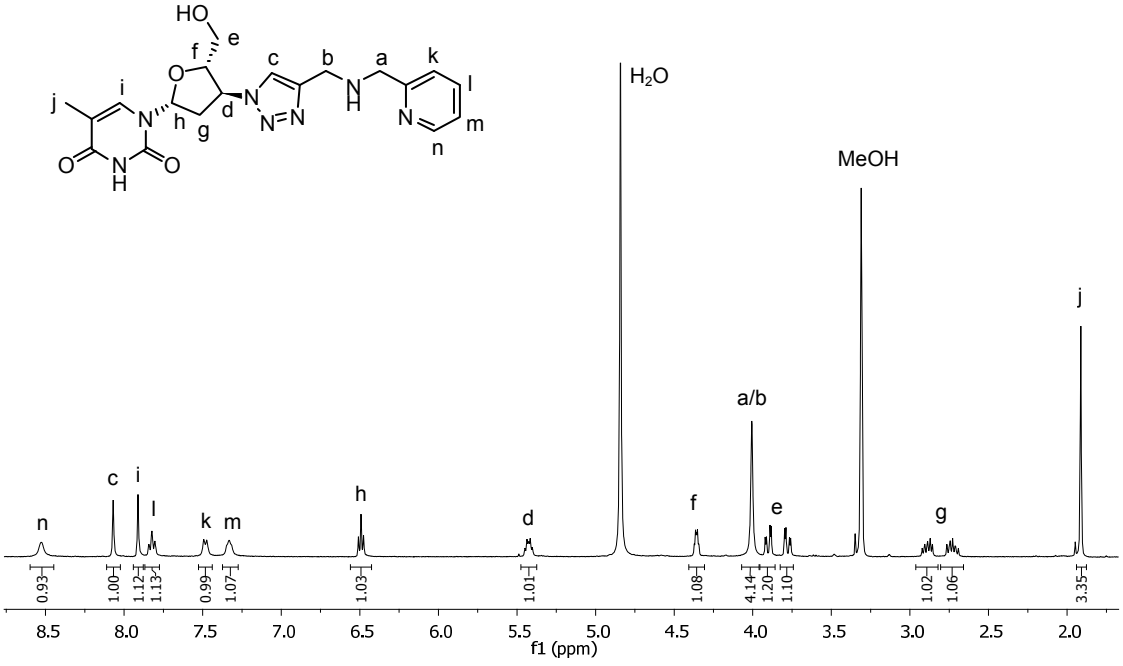

Figure 10. [1]H-NMR of compound **16**.

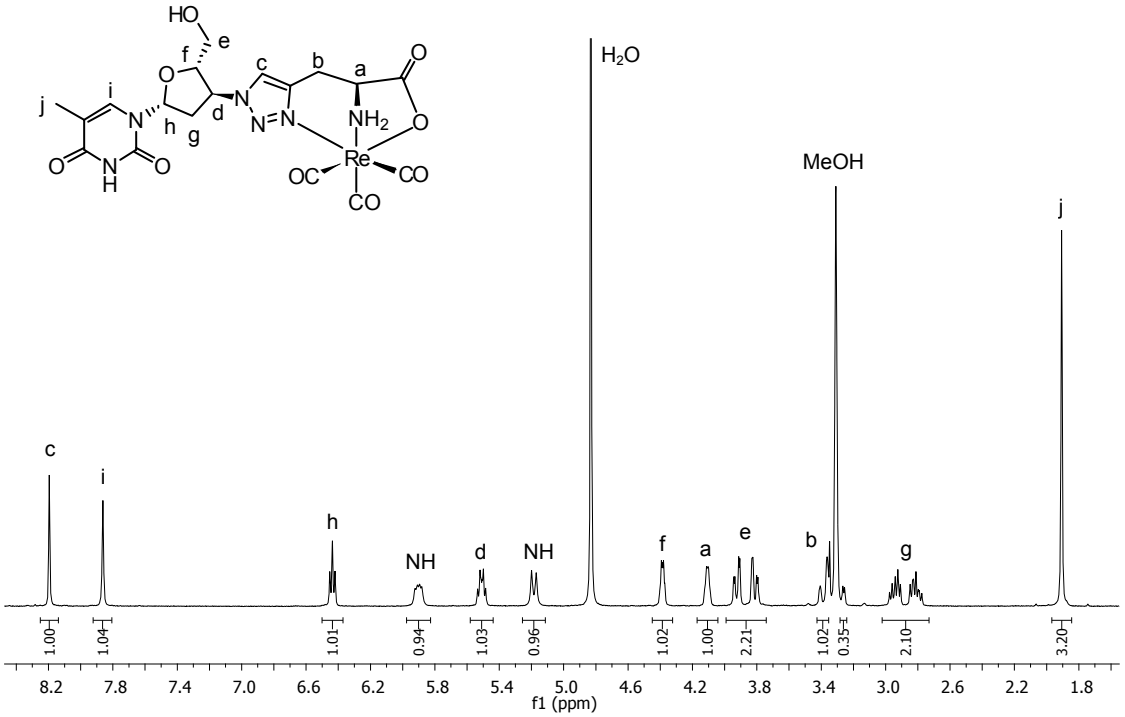

Figure 11. ^{1}H-NMR of [Re(CO)$_3$**12**].

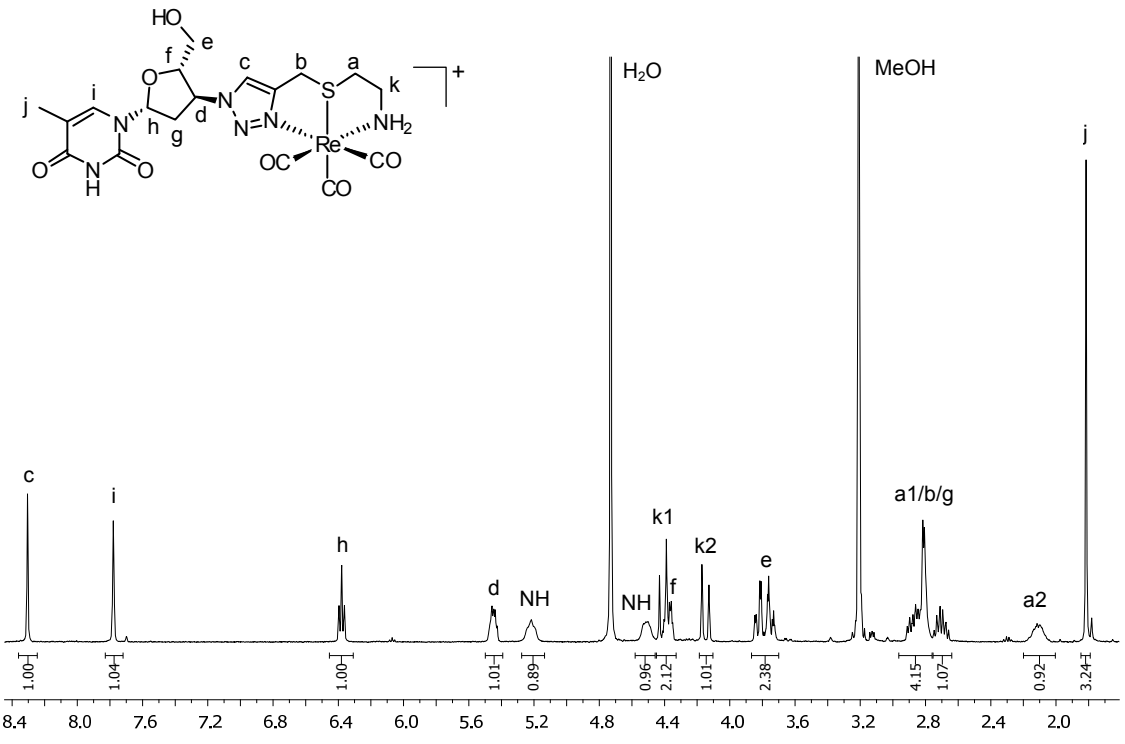

Figure 12. ^{1}H-NMR of [Re(CO)$_3$**13**]Br.

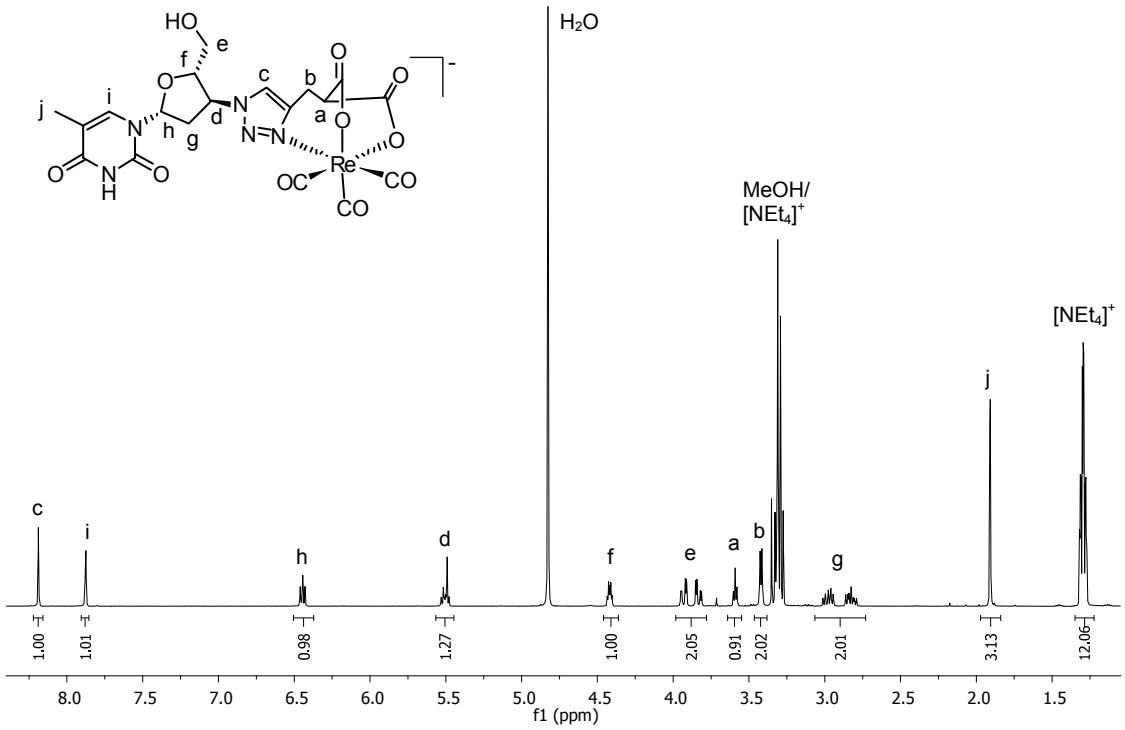

Figure 13. ^{1}H-NMR of [Re(CO)$_3$**14**]NEt$_4$.

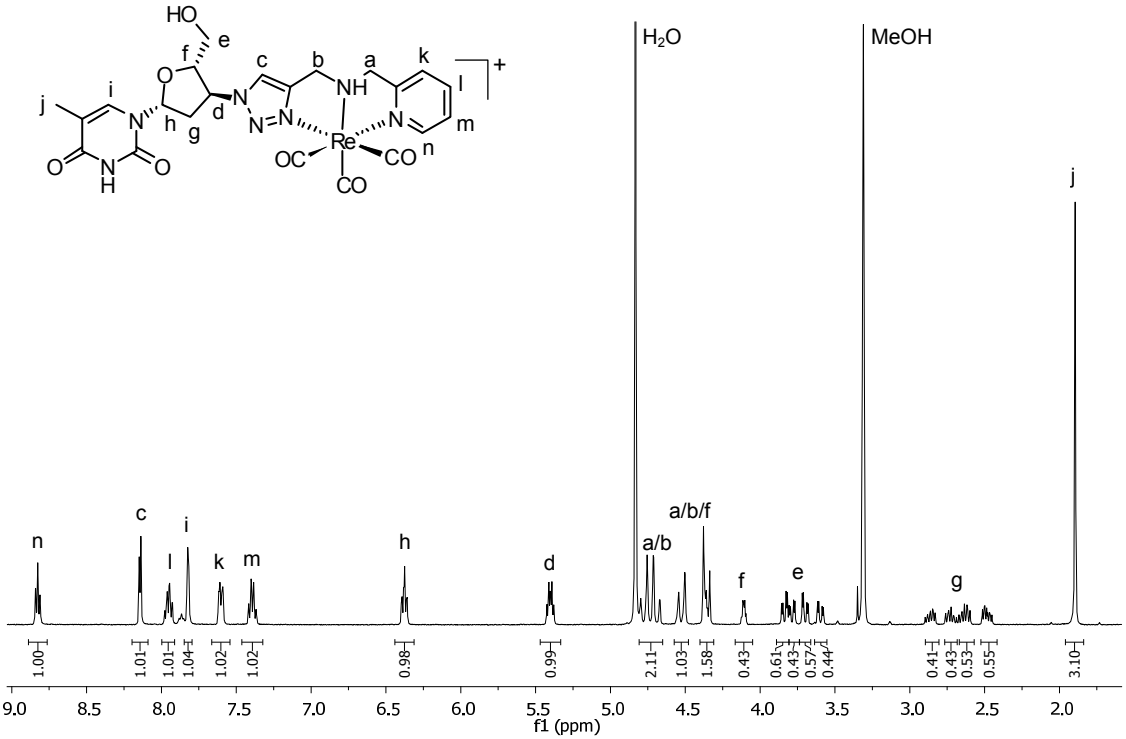

Figure 14. ^{1}H-NMR of [Re(CO)$_3$**16**]Br.

C2 UV analysis of PK/LDH coupled hTK1 phosphorylation assay

The quantification of the phosphorylation of all rhenium-labelled thymdine analogues relative to the natural substrate thymdine was achieved using a coupled hTK1-PK-LDH assay (Scheme 1). Phosphorylation of the dT analogue results in the formation of ADP, which is coupled to the oxidation of NADH to NAD^+. The decrease in NADH concentration was monitored by UV spectroscopy (NADH absorbs strongly at 340 nm, whereas NAD^+ does not).

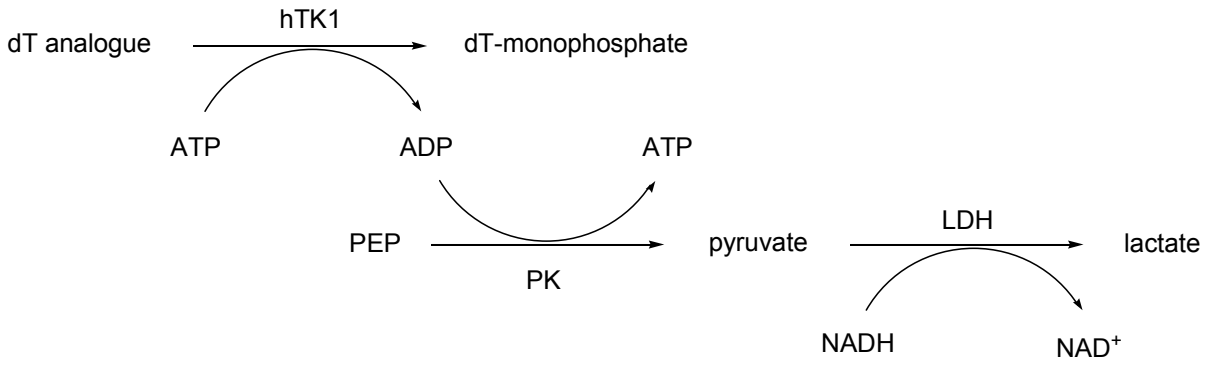

Scheme 1. The formation of ADP as a result of the phosphorylation of thymidine or thymidine analogues is indirectly proportional to the oxidation of NADH.

Thymidine and the organometallic thymidine derivatives were assayed at 25 °C for 15 minutes in 200 µL of a mixture containing 155.38 µL water, 10 µL 1 M HEPES buffer (pH 7.5), 0.2 µL 1 M DTT, 0.42 µL 100 mM PEP, 0.5 µL 1 M $MgCl_2$, 7.2 µL 5 mM NADH, 2 µL 100 mM ATP, 0.6 µL pyruvate kinase (1350 U/mL), 0.7 µL lactate dehydrogenase (1420 U/mL), 5 µL hTK1 (~0.5 mg/mL) and 20 µL of a 10 mM solution of thymidine or $[Re(CO)_3$**7-16**$]^{0/+/-}$.

For each substrate the linear decrease in UV absorption over time was measured from 0 to 15 minutes (Figure 15). The gradients of the regression lines between 6 and 12 minutes were compared to thymidine, the phosphorylation of which was assumed to be 100% (Table 1).

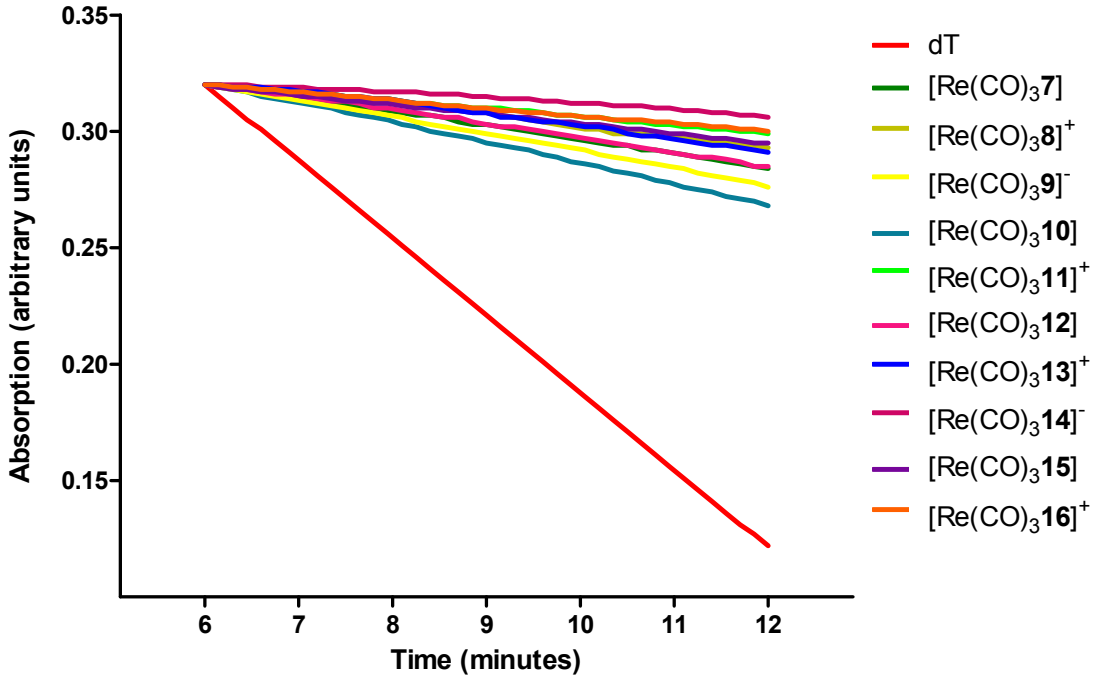

Figure 15. Phosphorylation of thymidine or organometallic thymidine analogue dependent decrease in UV absorption of NADH. Initial UV absorptions have been corrected to the value for thymidine for clarity.

Table 1. Phosphorylation of organometallic thymidine complexes [Re(CO)$_3$**7-16**]$^{0/+/-}$.

Compound	Position of functionalization	Overall charge	Phosphorylation [%][a]
[Re(CO)$_3$**7**]	N3	Neutral	17.9 ± 0.1
[Re(CO)$_3$**10**]	N3	Neutral	14.1 ± 0.2
[Re(CO)$_3$**9**]NEt$_4$	N3	Anionic	9.0 ± 0.4
[Re(CO)$_3$**8**]Br	N3	Cationic	10.9 ± 0.4
[Re(CO)$_3$**11**]Br	N3	Cationic	16.8 ± 0.2
[Re(CO)$_3$**12**]	C3′	Neutral	20.3 ± 0.8
[Re(CO)$_3$**15**]	C3′	Neutral	27.6 ± 1.9
[Re(CO)$_3$**14**]NEt$_4$	C3′	Anionic	23.1 ± 1.8
[Re(CO)$_3$**13**]Br	C3′	Cationic	12.5 ± 0.5
[Re(CO)$_3$**16**]Br	C3′	Cationic	14.2 ± 0.2
Thymidine	-	-	100[a]

[a] The phosphroylation of thymidine was arbitrarily set to 100%.

C3 Time-dependent phosphorylation assay

Organometallic thymdine analogues [$Re(CO)_3$**12**] was assayed at 37 °C in a 200 µL mixture containing 162.3 µL water, 10 µL 1 M HEPES buffer (pH 7.5), 0.2 µL 1 M DTT, 0.5 µL 1 M $MgCl_2$, 2 µL 100 mM ATP, 5 µL hTK1 (~0.5 mg/mL) and 20 µL of a 10 mM solution of the thymidine analogue. The reaction mixtures was analyzed by HPLC after 15 minutes, 1 hour, 2 hours and 3 hours (Figure 17). Reference HPLC traces are shown in Figure 16.

A

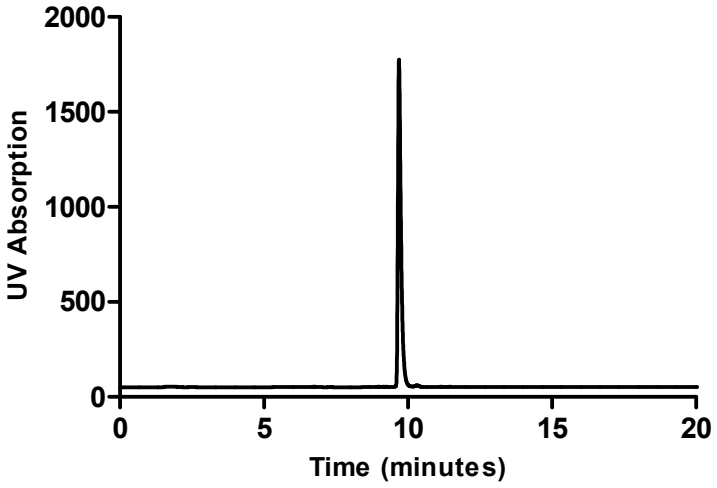

B

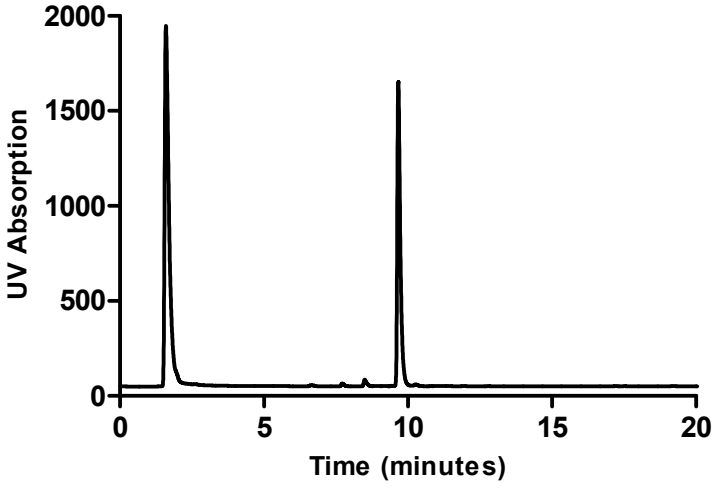

Figure 16. (A) [$Re(CO)_3$**12**] reference HPLC. (B) [$Re(CO)_3$**12**] and phosphorylation assay reaction mixture without enzyme. UV-trace after 1 hour at 37 °C.

A

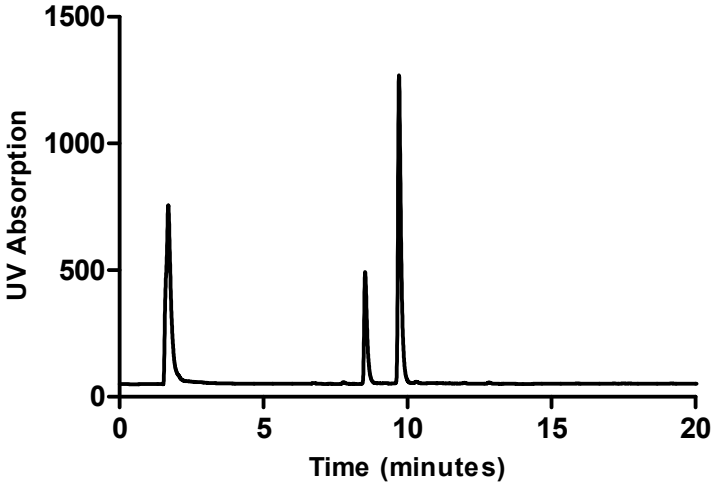
1500
1000
500
0
UV Absorption
0
5
10
15
20
Time (minutes)

B

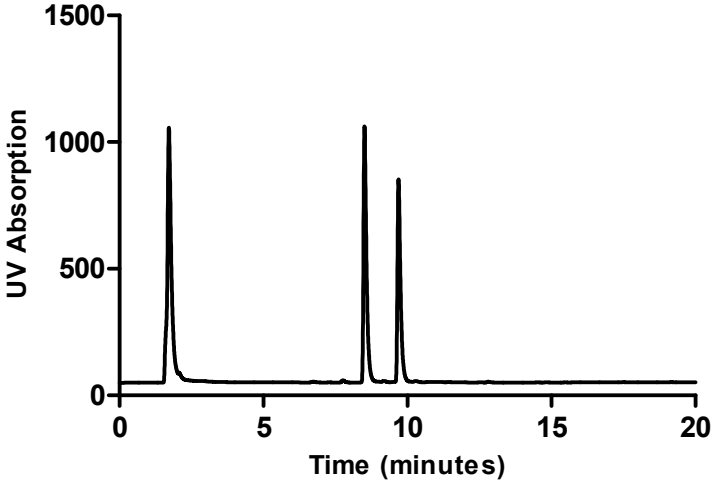
1500
1000
500
0
UV Absorption
0
5
10
15
20
Time (minutes)

C

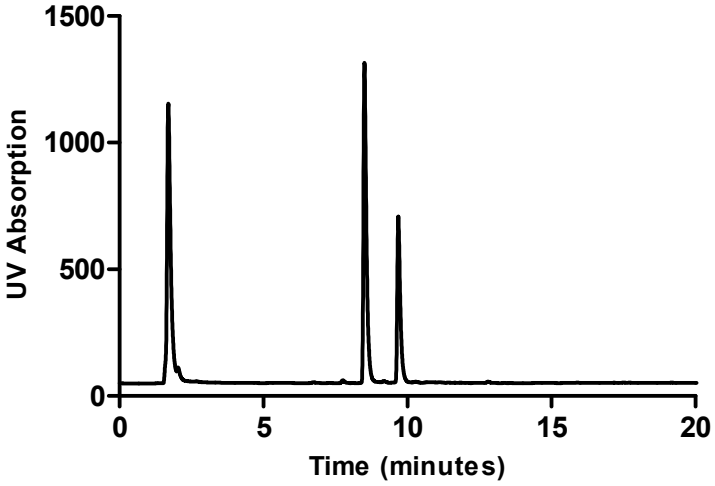
1500
1000
500
0
UV Absorption
0
5
10
15
20
Time (minutes)

D

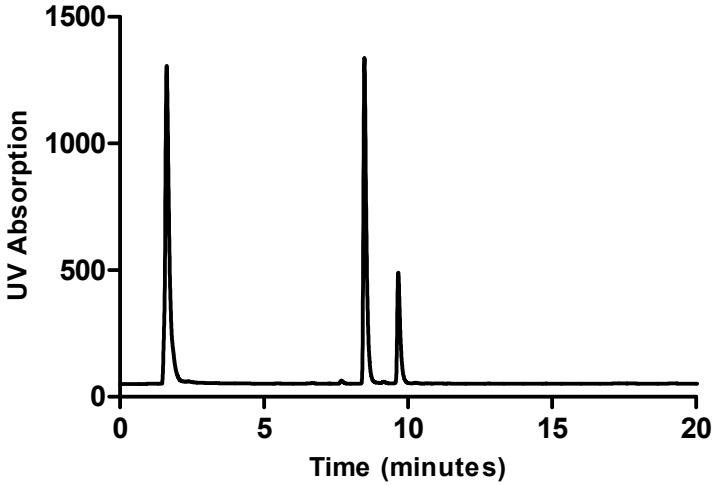

Figure 17. Phosphorylation assay with [Re(CO)$_3$**12**]. Reaction mixture after (A) 15 minutes, (B) 1 hour, (C) 2 hours, (D) 3 hours.

C4 Mass spectroscopy analysis of phosphorylation

[Re(CO)$_3$**12**] was assayed at 37 °C in a 200 µL mixture containing 162.3 µL water, 10 µL 1 M HEPES buffer (pH 7.5), 0.2 µL 1 M DTT, 0.5 µL 1 M $MgCl_2$, 2 µL 100 mM ATP, 5 µL hTK1 (~0.5 mg/mL) and 20 µL of a 10 mM solution of [Re(CO)$_3$**12**]. After 1 hour the reaction mixture was purified by analytical HPLC (see Figure 17 B). MS analysis revealed the first peak corresponded to the phosphorylated complex (Figure 19) and as expected the second peak corresponded to the starting material (Figure 20). The structures of [Re(CO)$_3$**12**] and [Re(CO)$_3$**12**]-phosphate are shown in Figure 18.

A

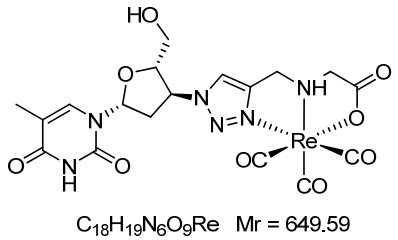

$C_{18}H_{19}N_6O_9Re$ Mr = 649.59

B

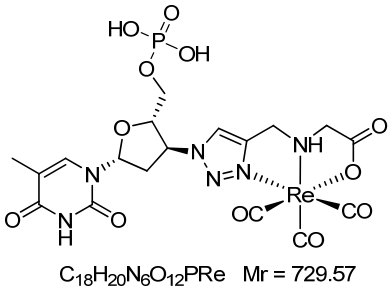

$C_{18}H_{20}N_6O_{12}PRe$ Mr = 729.57

Figure 18. Structures and chemical formulae for (A) [Re(CO)$_3$**12**] and (B) [Re(CO)$_3$**12**]-phosphate.

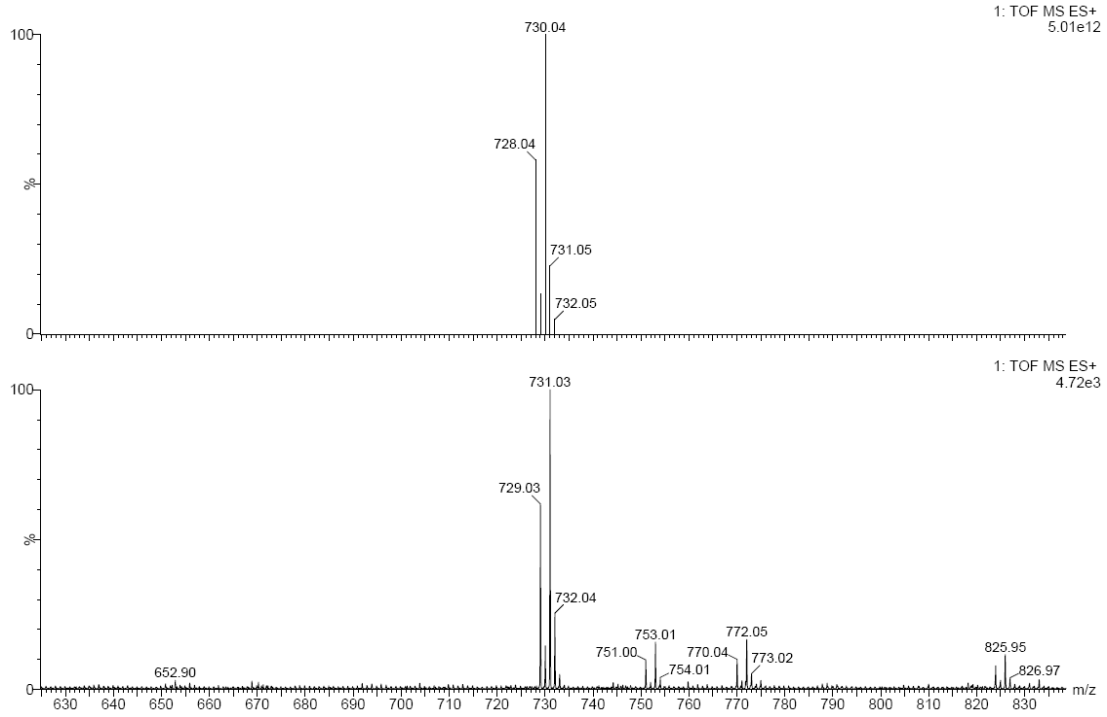

Figure 19. Predicted (above) and experimental mass spectra for the complex [Re(CO)$_3$**12**]-phosphate ($C_{18}H_{20}N_6O_{12}PRe$, Mr = 729.57).

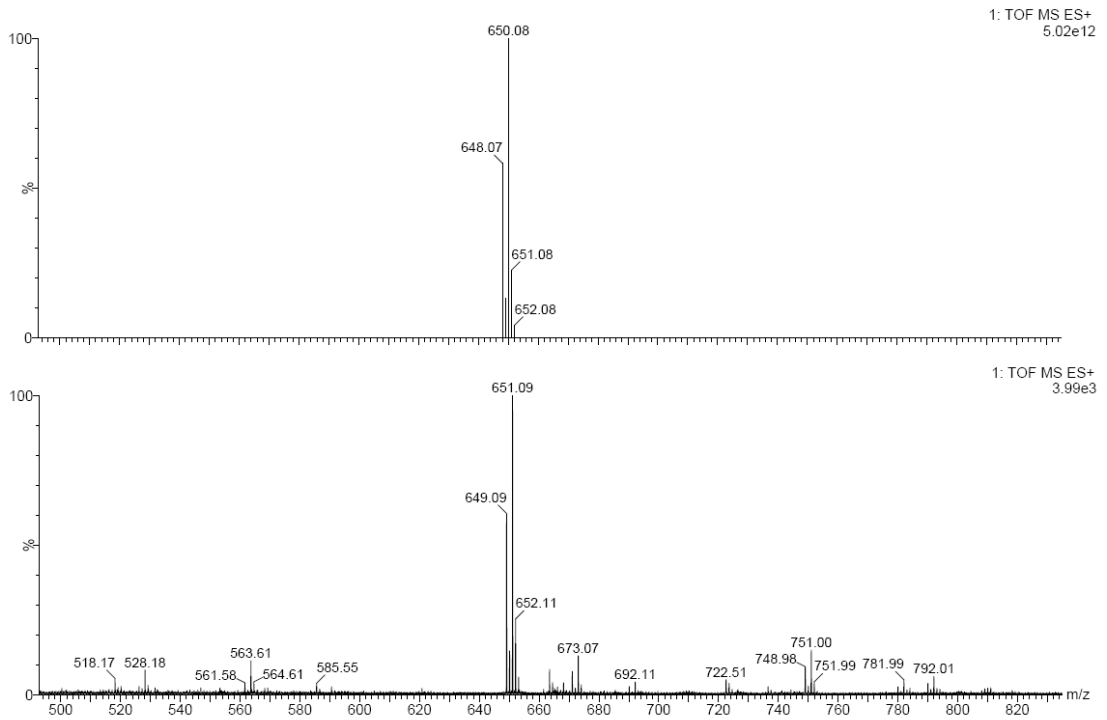

Figure 20. Predicted (above) and experimental mass spectra for the complex [Re(CO)$_3$**12**] ($C_{18}H_{19}N_6O_9Re$, Mr = 649.59).

Supplementary information for chapter 5

D1 Representative NMR analysis of $\{Re(CO)_2(NO)\}^{2+}$ and $\{Re(CO)_3\}^{+}$ labelled compounds

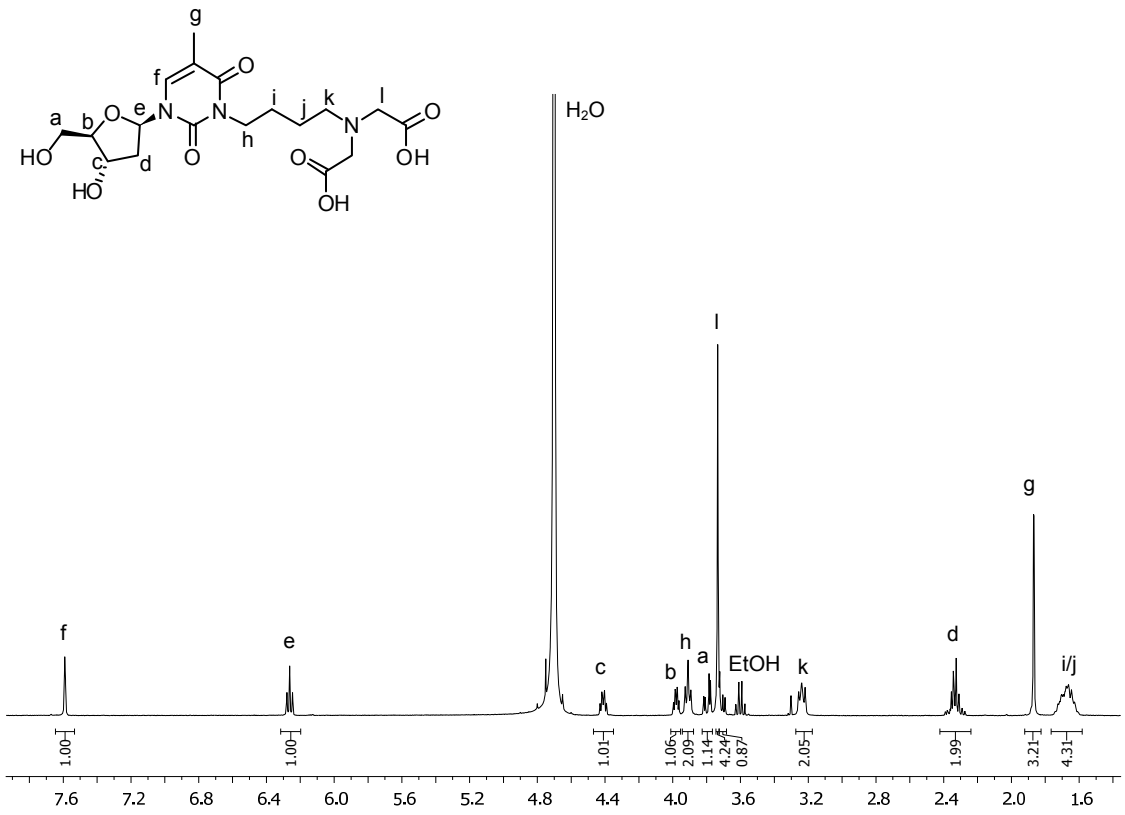

Figure 1. ^{1}H-NMR of **L2**.

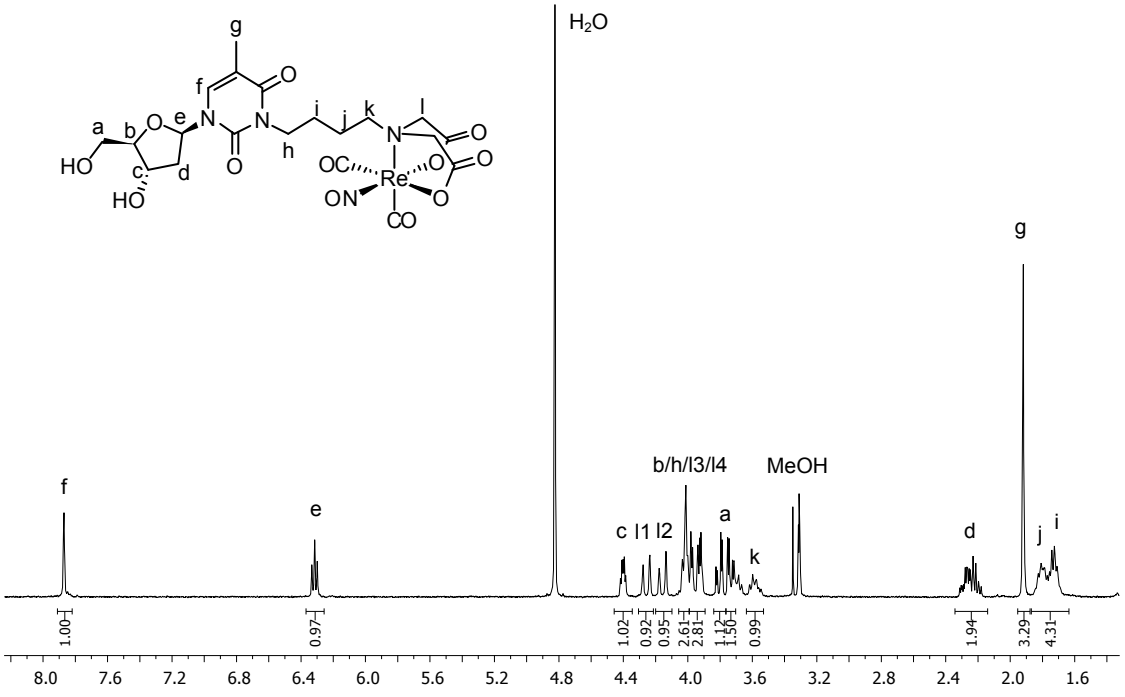

Figure 2. ^{1}H-NMR of [Re(CO)$_2$(NO)**L2**].

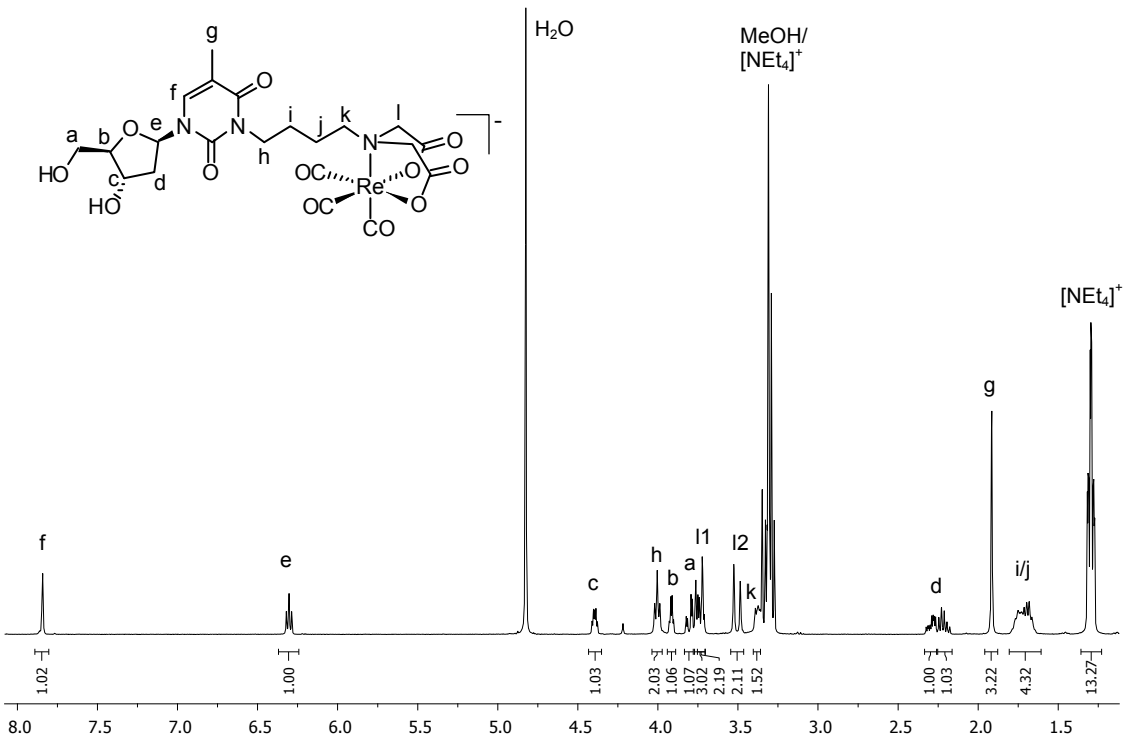

Figure 3. ^{1}H-NMR of [Re(CO)$_3$**L2**]NEt$_4$.

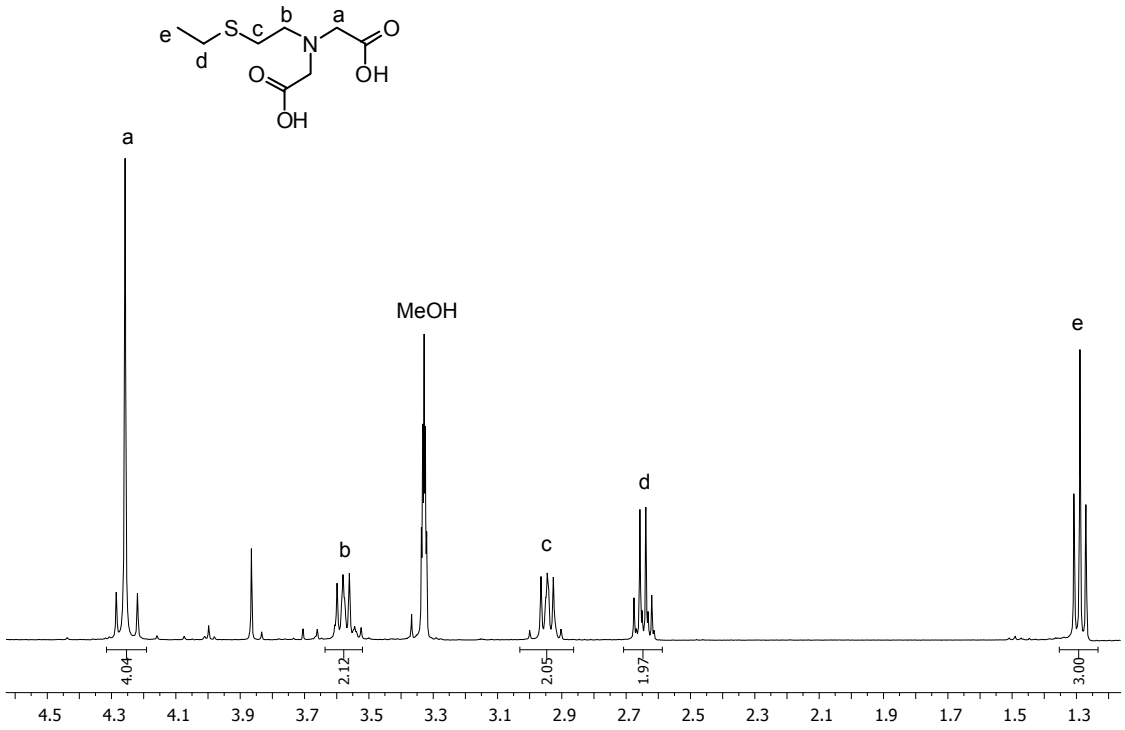

Figure 4. ^{1}H-NMR of **L3**.

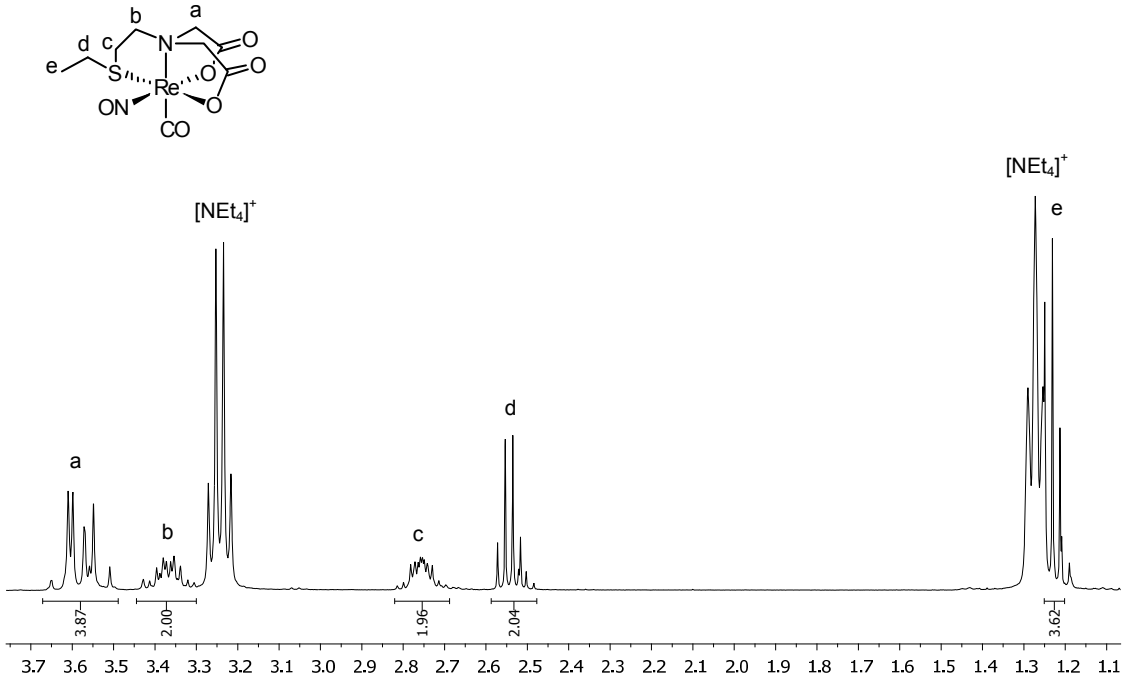

Figure 5. ^{1}H-NMR of [Re(CO)(NO)**L3**].

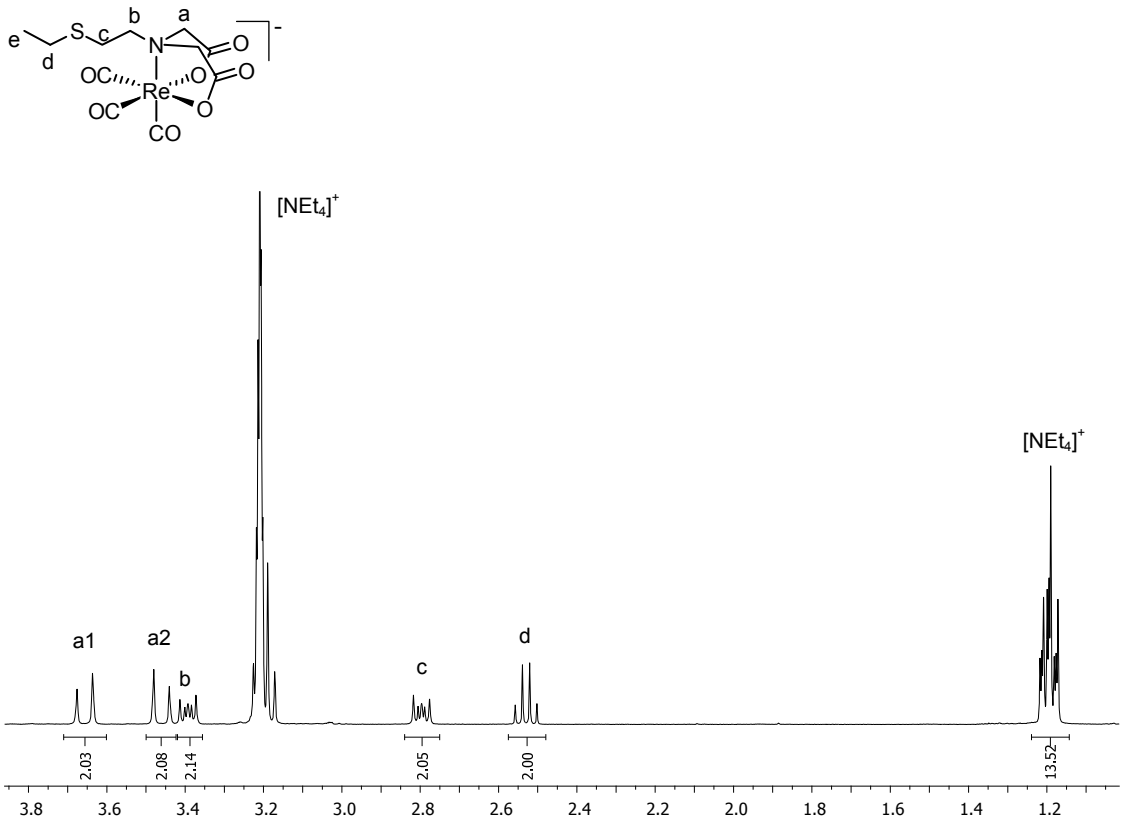

Figure 6. ^{1}H-NMR of [Re(CO)$_3$**L3**]NEt$_4$.

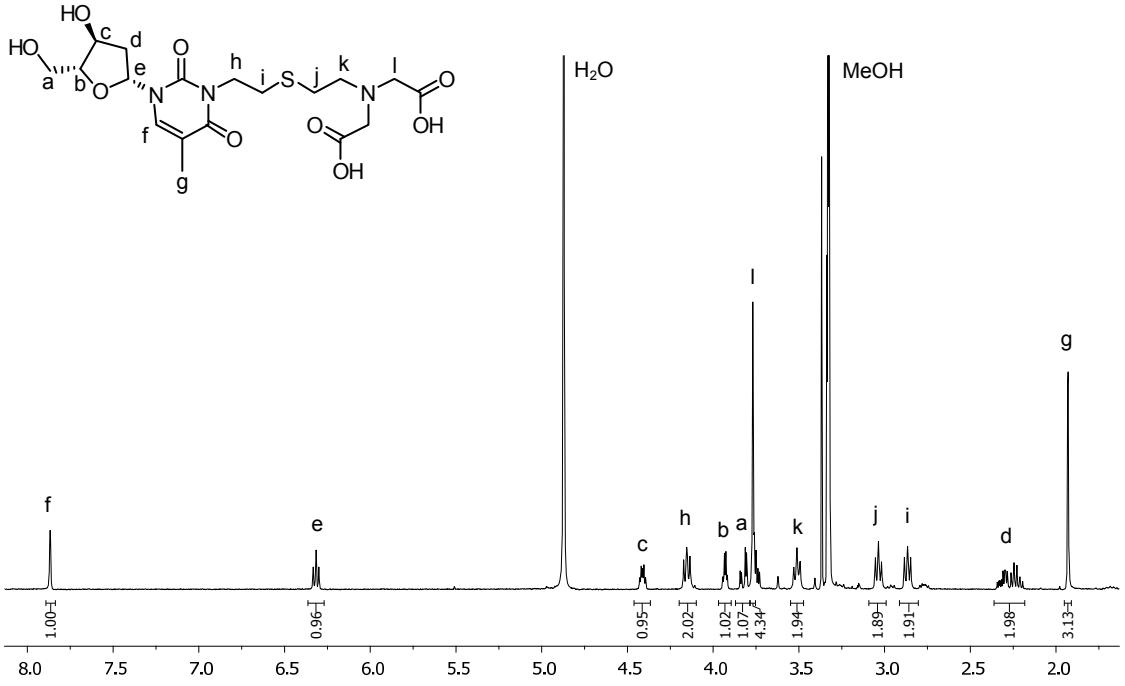

Figure 7. ^{1}H-NMR of **L4**.

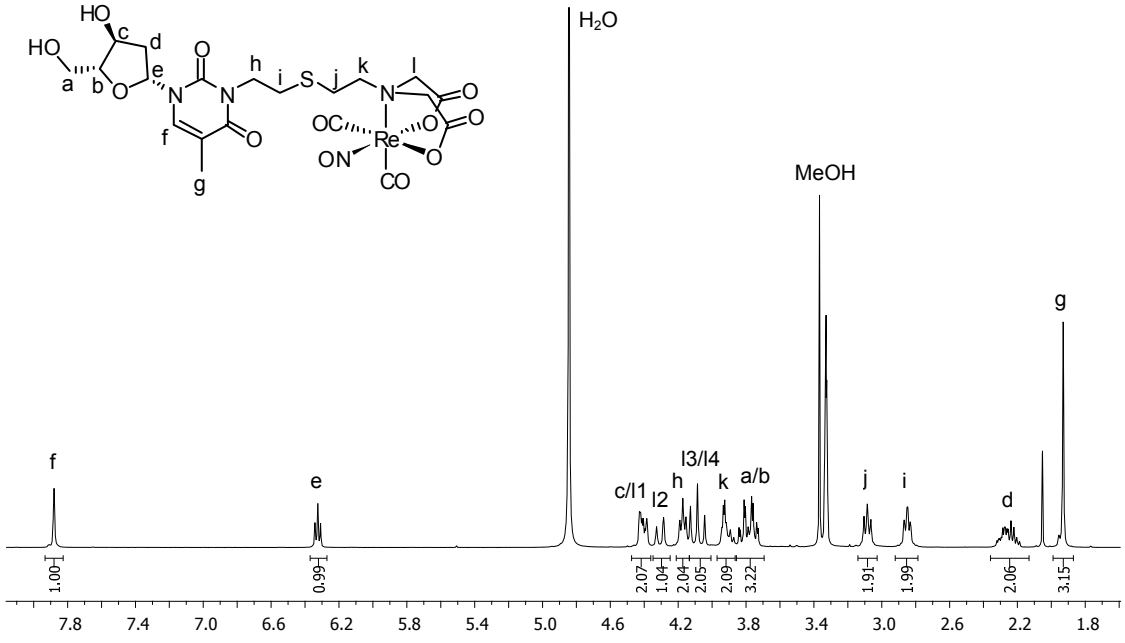

Figure 8. ^{1}H-NMR of [Re(CO)$_2$(NO)**L4**].

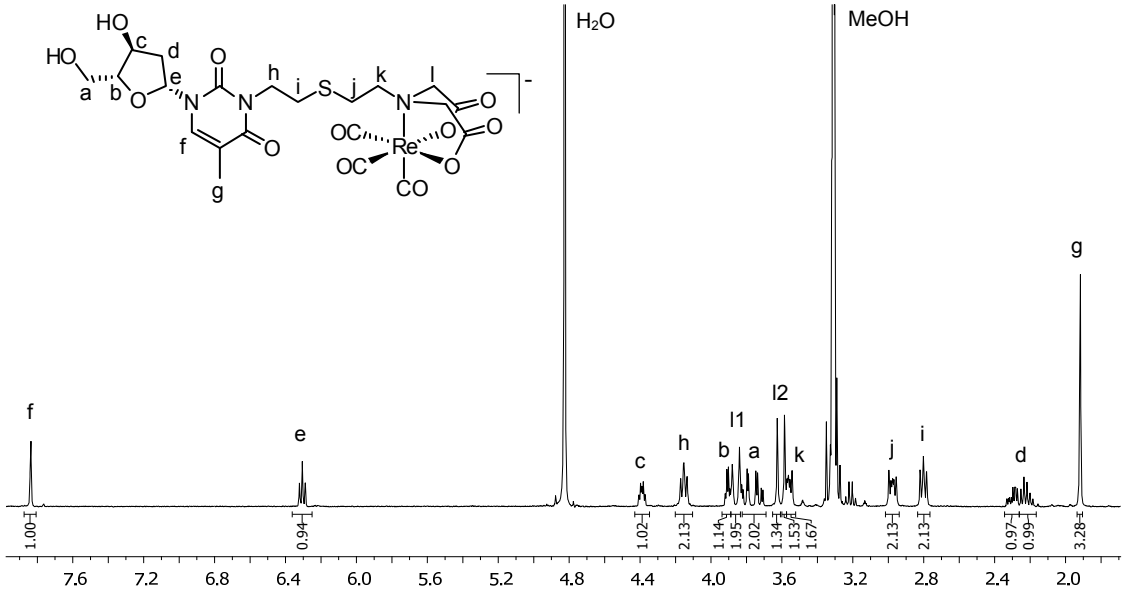

Figure 9. ^{1}H-NMR of [Re(CO)$_3$**L4**]NEt$_4$.

D2 UV analysis of PK/LDH coupled hTK1 phosphorylation assay

Thymidine and the organometallic thymidine derivatives $[Re(CO)_3\mathbf{L^1/L^2/L^4/L^5}][NEt_4]$ and $[Re(CO)_2(NO)\ \mathbf{L^1/L^2/L^4/L^5}]$ were assayed at 25 °C for 15 minutes in 200 µL of a mixture containing 155.38 µL water, 10 µL 1 M HEPES buffer (pH 7.5), 0.2 µL 1 M DTT, 0.42 µL 100 mM PEP, 0.5 µL 1 M $MgCl_2$, 7.2 µL 5 mM NADH, 2 µL 100 mM ATP, 0.6 µL pyruvate kinase (1350 U/mL), 0.7 µL lactate dehydrogenase (1420 U/mL), 5 µL hTK1 (~0.5 mg/mL) and 20 µL of a 10 mM 1:1 DMSO/water solution of thymidine, $[Re(CO)_3\mathbf{L^1/L^2/L^4/L^5}][NEt_4]$ or $[Re(CO)_2(NO)\ \mathbf{L^1/L^2/L^4/L^5}]$.

For each substrate the linear decrease in UV absorption over time was measured from 0 to 15 minutes (Figure 10). The gradients of the regression lines between 6 and 12 minutes were compared to thymidine, the phosphorylation of which was assumed to be 100%.

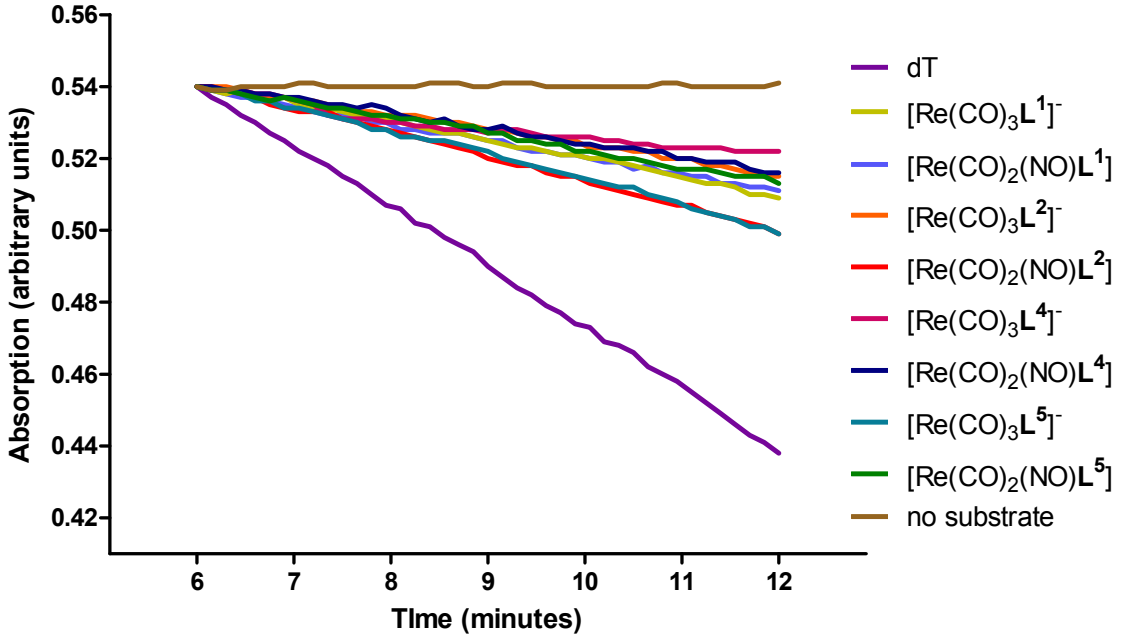

Figure 10. Phosphorylation of thymidine and the organometallic thymidine derivatives $[Re(CO)_3\mathbf{L^1/L^2/L^4/L^5}][NEt_4]$ and $[Re(CO)_2(NO)\ \mathbf{L^1/L^2/L^4/L^5}]$ measured using the coupled decrease in NADH absorption. Thymidine derivatives were dissolved in a mixture of DMSO (5% total volume) and water to give a final substrate concentration of 1 mM. Initial UV absorptions have been corrected to the value for thymidine for clarity.

Curriculum Vitae

Personal Details

Name: **Harriet Sarah Rose Struthers** Date of Birth: 27.05.1983

Address: Rathausgasse 22
5400 Baden
Switzerland

Email: harriet.struthers@pharma.ethz.ch

Education

2005 – 2009 **ETH Zurich, Department of Chemistry and Applied Biosciences**

PhD thesis: "Click-to-Chelate": An Efficient Strategy for the Development of Organometallic Technetium and Rhenium Compounds for Potential Application in Radiopharmacy

2001 – 2005 **University of Oxford, Somerville College**

MChem (Master of Chemistry): First Class
Distinction in Preliminary Examinations
Dukinfield Scholarship for academic achievement

1996 – 2001 **The Cherwell School, Oxford**

A-levels: Maths (Grade A); Chemistry (A); Biology (A); German (A)

Employment

2005 – 2009 PhD student in the group of Professor Roger Schibli, Paul Scherrer Institute, Villigen, Switzerland

2005 Researcher in the group of Professor Jon Dilworth, Chemistry Research Laboratory, Oxford, UK

2002 – 2004 Undergraduate assistant, Admissions Information Centre, Oxford University, Oxford, UK

2000 – 2001 Runner, Le Petit Blanc restaurant, Oxford, UK

Interests

Basketball (Oxford University Blue 2001-2005, Swiss National League 2005-2006), running, swimming, hiking, photography, cooking.

Publications

Organometallic $\{Re(CO)_3\}^+$ and $\{Re(CO)_2(NO)\}^{2+}$ labelled substrates for human thymidine kinase 1: A side by side comparison of their substitution reactions and substrate activity
H. Struthers, A. Hagenbach, U. Abram, R. Schibli
Inorganic Chemistry, **2009**, accepted

Synthesis, in vitro and in silico evaluation of organometallic technetium and rhenium thymidine complexes with retained substrate activity toward human thymidine kinase type 1
D. Desbouis, H. Struthers, V. Spiwok, T. Küster, R. Schibli
Journal of Medicinal Chemistry, **2008**, 51(21), 6689

"Click-to-Chelate": Design and incorporation of triazole containing metal chelating systems into biomolecules of diagnostic and therapeutic interest
H. Struthers, B. Spingler, T. L. Mindt, R. Schibli
Chemistry - A European Journal, **2008**, 14(20), 6173

Strategies for the development of novel tumor targeting technetium and rhenium radiopharmaceuticals
T. L. Mindt, H. Struthers, E. García-Garayoa, D. Desbouis, R. Schibli
Chimia, **2007**, 61(11), 725

The exocyclic functionalisation of bis(thiosemicarbazonate) complexes of zinc and copper: the synthesis of monomeric and dimeric species
M. Christlieb, H. S. R. Struthers, P. D. Bonnitcha, A. R. Cowley, J. R. Dilworth
Dalton Transactions, **2007**(43), 5043

New bimetallic compounds based on the bis(thiosemicarbazonato) motif
M. Christlieb, A. R. Cowley, J. R. Dilworth, P. S. Donnelly, B. M. Paterson, H. S. R. Struthers, J. M. White
Dalton Transactions, **2007**(3), 327

“Click-to-Chelate”: Synthesis and installation of metal chelates into biomolecules in a single step
T. L. Mindt, H. Struthers, L. Brans, T, Anguelov, C. Schweinsberg, V. Maes, D. Tourwé, R. Schibli
Journal of the American Chemical Society, **2006**, 128(47), 15096

Oral Presentations

"Click-to-Chelate": Functionalization of thymidine with chelating systems for Re and ^{99m}Tc and evaluation of the oragonometallic thymidine derivatives as substrates for hTK1

16. Arbeitstagung der AG Radiochemie/Radiopharmazie der DGN, Münster, Germany, 25-27 September 2008

"Click-to-Chelate": Improving the functionalization and radiolabelling of biomolecules with technetium and rhenium

IPW Doktorandentag, ETH Zurich, 19 September 2007

Triazole-containing chelating systems for the ^{99m}Tc and Re tricarbonyl cores, and their incorporation into tumour targeting biomolecules

Fall Meeting of the Swiss Chemical Society, EPF Lausanne, 12 September 2007

Triazole-containing chelating systems for the ^{99m}Tc and Re tricarbonyl cores, and their incorporation into tumor targeting biomolecules

234th American Chemical Society National Meeting and Exposition, Boston, MA, USA, 19-24 August 2007

Poster Presentations

"Click-to-Chelate": Functionalization of thymidine with chelating systems for rhenium and technetium and their evaluation as substrates for human thymidine kinase type 1

Fall Meeting of the Swiss Chemical Society, University of Zurich, 11 September 2008

Triazole-containing metal chelating systems for the $M(CO)_3$-core (M = ^{99m}Tc, Re), and their incorporation into tumour targeting biomolecules

17th International Symposium on Radiopharmaceutical Sciences, Aachen, Germany, 30 April - 4 May 2007

"Click-to-Chelate": Synthesis and installation of metal chelators into biomolecules in a single step

7th International Symposium on Technetium in Chemistry and Nuclear Medicine, Bressanone, Italy, 6-9 September 2006

Investigating the substitution behaviour of $[Re(CO)_2(NO)Br_3]^{2-}$ in the presence of tetradentate ligands

7th International Symposium on Technetium in Chemistry and Nuclear Medicine, Bressanone, Italy, 6-9 September 2006